

INVESTIGATION OF NATURAL PRODUCT SCAFFOLDS FOR THE DEVELOPMENT OF  
OPIOID RECEPTOR LIGANDS

By

Katherine M. Prevatt-Smith

Submitted to the graduate degree program in Medicinal Chemistry and the Graduate Faculty of  
the University of Kansas in partial fulfillment of the requirements for the degree of Doctor of  
Philosophy.

---

Chairperson: Dr. Thomas E. Prisinzano

---

Dr. Brian S. J. Blagg

---

Dr. Michael F. Rafferty

---

Dr. Paul R. Hanson

---

Dr. Susan M. Lunte

Date Defended: July 18, 2012

The Dissertation Committee for Katherine M. Prevatt-Smith certifies that this is the approved version of the following dissertation:

INVESTIGATION OF NATURAL PRODUCT SCAFFOLDS FOR THE DEVELOPMENT OF  
OPIOID RECEPTOR LIGANDS

---

Chairperson: Dr. Thomas E. Prisinzano

Date approved: July 18, 2012

## ABSTRACT

Kappa opioid (KOP) receptors have been suggested as an alternative target to the mu opioid (MOP) receptor for the treatment of pain because KOP activation is associated with fewer negative side-effects (respiratory depression, constipation, tolerance, and dependence). The KOP receptor has also been implicated in several abuse-related effects in the central nervous system (CNS). KOP ligands have been investigated as pharmacotherapies for drug abuse; KOP agonists have been shown to modulate dopamine concentrations in the CNS as well as attenuate the self-administration of cocaine in a variety of species, and KOP antagonists have potential in the treatment of relapse. One drawback of current opioid ligand investigation is that many compounds are based on the morphine scaffold and thus have similar properties, both positive and negative, to the parent molecule. Thus there is increasing need to discover new chemical scaffolds with opioid receptor activity.

The flavonoid class of natural products has been identified as a potential source of novel opioid ligands. In particular, dioclein (**86**) and dioflorin (**87**) have been reported to have an antinociceptive effect in rodent models of pain, although there has been no *in vitro* pharmacological evaluation to date. Dioclein and several simplified analogs of dioflorin were synthesized in order to develop structure activity relationships (SAR) for the flavonoid scaffold at opioid receptors. The analogs were pharmacologically evaluated in several cell-based assays (radioligand binding, fluorescent calcium mobilization, and luminescent PathHunter™  $\beta$ -arrestin) and found to be inactive at both opioid and cannabinoid receptors.

The novel KOP receptor agonist and neoclerodane diterpene salvinorin A was also investigated. Salvinorin A is the main active component of the hallucinogenic plant *Salvia*

*divinorum* and is the first opioid ligand reported that lacks a basic nitrogen atom in the structure. Ether analogs at the C-2 position of salvinorin A have been reported to have improved affinity and potency over the parent molecule. As alkyl chain ethers have a high degree of flexibility and the oxygen atom may allow for extra hydrogen bonding interactions in the receptor, modifications were made at the C-2 position in order to develop analogs to elucidate the molecular basis for this improved affinity and potency. Tetrahydropyranyl ether **220**, ether **223a**, and methyltetrahydropyranyl ether **231** were found to have similar KOP affinity and potency to salvinorin A in radioligand binding, [<sup>35</sup>S]GTP- $\gamma$ -S functional, and fluorescent calcium mobilization assays. Tetrahydropyranyl ether **220** was further evaluated for its effects on the cocaine-primed reinstatement of extinguished cocaine self-administration in rats; **220** (1 mg/kg) was found to attenuate cocaine self-administration comparably to salvinorin A (0.3 mg/kg), previously reported to be effective in this animal model. This represents the first report of a salvinorin A derivative with demonstrated anti-addictive capability.

## ACKNOWLEDGEMENTS

I would like to thank the NIH Dynamic Aspects of Chemical Biology training grant for funding, presentation opportunities at home and abroad, general scientific enrichment, and the opportunity to do a research rotation outside of my expertise. Thanks to Drs. Hernán Navarro, Brian Gilmour, and Scott Runyon – and to the members of their respective groups – at the Research Triangle Institute for allowing me to invade their labs, tamper with their equipment, and teaching me some pharmacology along the way. Because of your influence, I am a better medicinal chemist and a better scientist. Additional thanks to Dr. Navarro and his group for performing the final pharmacological evaluations for this dissertation. Thank you to Christina M. Dersch and Dr. Richard B. Rothman at the National Institute of Drug Abuse for their collaboration with much of the radioligand binding and functional assays mentioned herein. And thank you also to Dr. Bronwyn Kivell and her group at Victoria University of Wellington in New Zealand for their collaboration with the rodent *in vivo* evaluations mentioned herein. Thanks as well to Drs. Victor W. Day and Justin T. Douglas from the KU Molecular Structures Group for their extensive help with X-ray crystallography and NMR. You both found ways to generate precious data from difficult compounds when I had all but given up. Finally, thank you to the University of Kansas Department of Medicinal Chemistry and very special thanks to my committee.

I have always thought that I would spend some time as a graduate student. I ~~blame~~ thank my parents, both Ph.D. scientists, for being astoundingly supportive of my academic pursuits. Mom and Dad, your unconditional love, encouragement, and commiseration allowed me to be successful these past years. I thank my husband Patrick for his perseverance as I went through this program; you have always been there for me, even when I was being a terror. Your indomitable faith in me keeps me afloat. I thank my dog Solomon for keeping me on task during the writing process by not allowing me to easily move my feet out from under my desk. To my friends and lab mates: you have made graduate school one of the strangest and best phases of my life. Nicolette, Kris, Anthony, and Kim, I cannot imagine having gone through the whole graduate school process without you as confidantes and partners in crime; no one else really gets it. Tammi, Mike, and Andrew, you are each of you so peculiar and so entertaining that it is impossible to have a truly bad day in the lab. Eventually one of you says or does something ridiculous and I have to laugh, no matter what kind of horrible mood was afflicting me. Thank you for making the process of “re”-search bearable. Chris and Denise, thank you for your post-doctoral help and wisdom, and for keeping everyone else in line (or at least trying to). To my fellow graduate students not of KU, Topher and Bob, thanks for staying the course with me so that I felt less alone on my journey. Finally, I thank the Prisinzano family for letting me into their home, enlightening me to the joy of buck-eyes and American Idol, and making sure I never left hungry or un-pelted with Nerf darts. Thank you, Tom, for your support, encouragement, inspiration, and reassurance; you always gave me the right kind of push when I needed it. You wrote “confidence” for me on a piece of paper and I kept it. Hooray for the good guys!

## TABLE OF CONTENTS

<b>ABSTRACT</b>	iii
<b>ACKNOWLEDGEMENTS</b>	v
<b>TABLE OF CONTENTS</b>	vi
<b>LIST OF TABLES</b>	viii
<b>LIST OF FIGURES</b>	ix
<b>LIST OF SCHEMES</b>	xi
<b>CHAPTER 1: INTRODUCTION</b>	1
A Historical Perspective on Natural Products and Traditional Medicine	1
Natural Products and Modern Medicine	2
Opioids: Natural Products used in Modern Medicine	8
Identification of the Opioid Receptors	10
SAR of the Endogenous Opioid Peptides	11
SAR of Non-Peptidic Opioid Ligands	13
4,5 $\alpha$ -Epoymorphinans	13
Morphinans	16
Benzomorphans	16
Piperidine Derivatives	17
Other Classes of Opioids	18
G-Protein Coupled Receptors	21
Opioids, Receptors, and the Treatment of Pain	25
Therapeutic Potential of KOP Receptor Selective Agents	27
Interactions between the Opioid and Cannabinoid Receptor Systems	32
Alternative Chemical Scaffolds for Opioid Ligands	33
<b>CHAPTER 2: INVESTIGATION OF FLAVONOIDS AS OPIOID LIGANDS</b>	35
Introduction to Flavonoids	35
The Identification of Flavonoids as Potential Opioid Receptor Ligands	38
<i>Dioclea Grandiflora</i> Background	40
Antinociceptive Effects of <i>Dioclea Grandiflora</i> Extracts	41
Preliminary Pharmacological Studies of <i>Dioclea Grandiflora</i> Flavonoids	42
Rationale and Specific Aims	42
Results and Discussion	46
Synthesis	46
Radioligand Binding Results	48
Calcium Mobilization Results	49
$\beta$ -Arrestin Luminescence Results	51
Conclusions	52
Future Directions	53

<b>CHAPTER 3: EXPERIMENTAL PROCEDURES FOR FLAVONOID ANALOGS</b>	55
<b>CHAPTER 4: FUTURE INVESTIGATION OF THE BINDING MODE OF SALVINORIN A AT KOP RECEPTORS</b>	69
Introduction	69
Terpenes	71
Salvinorin A KOP Receptor <i>In Vitro</i> Pharmacology	75
Salvinorin A KOP Receptor <i>In Vivo</i> Pharmacology	76
Hallucinogenic and other CNS Effects	76
Metabolism	80
Toxicity	83
Drug Discrimination	83
Antinociceptive Effects	85
Mood Regulation	87
Drug Abuse	90
Proposed Salvinorin A and KOP Receptor Binding Interactions	92
SAR Studies of Salvinorin A	100
Introduction	100
Modifications at the C-2 Position	101
Herkinorin and Other Ester Modifications	101
Bioisosteric Replacements for Esters at C-2	106
C-2 Ether, Amine, and Halogen Analogs	109
C-2 Epimer Analogs	112
Rationale and Specific Aims	113
Results and Discussion	117
Introduction	117
Synthesis	118
Radioligand Binding Results	125
[ <sup>35</sup> S]GTP-γ-S Functional Assay Results	128
Calcium Mobilization Results	130
Crystal Structure Considerations	131
Additional Experimental Results in a Rat Model of Relapse	135
Conclusions	137
Future Directions	139
<b>CHAPTER 5: EXPERIMENTAL PROCEDURES FOR SALVINORIN A ANALOGS</b>	140
<b>CHAPTER 6: DISSERTATION CONCLUSIONS</b>	162
<b>REFERENCES</b>	166
<b>APPENDIX A: <sup>1</sup>H NMR SPECTRA</b>	187
<b>APPENDIX B: HPLC CHROMATOGRAMS</b>	226

## LIST OF TABLES

<b>Table 1.</b> Structure, numbering, and selected SAR summary for morphine.	15
<b>Table 2.</b> Summary of selected opioid receptor ligands.	20
<b>Table 3.</b> Opioid receptor binding affinity for compounds dioclein ( <b>86</b> ), <b>102</b> , and <b>105–108</b> .	49
<b>Table 4.</b> Opioid receptor potency for compounds dioclein ( <b>86</b> ) and <b>105–108</b> in the calcium mobilization assay format.	50
<b>Table 5.</b> CB1 receptor potency for compounds dioclein ( <b>86</b> ) and <b>105–108</b> in the calcium mobilization assay format.	51
<b>Table 6.</b> Receptor potency for compounds dioclein ( <b>86</b> ) and <b>105–108</b> in the $\beta$ -arrestin assay format.	52
<b>Table 7.</b> Opioid receptor binding affinity for compounds <b>108</b> , <b>190</b> , <b>191</b> , <b>220</b> , <b>221</b> , <b>222a,b</b> , <b>223a,b</b> , <b>224a,b</b> , <b>225</b> , <b>226</b> , and <b>227</b> .	126
<b>Table 8.</b> Selected [ $^{35}$ S]GTP- $\gamma$ -S KOP receptor potency and efficacy data for compounds <b>108</b> , <b>190</b> , <b>191</b> , <b>220</b> , <b>222a,b</b> , <b>223a</b> , <b>231</b> , and <b>232a</b> .	129
<b>Table 9.</b> Selected opioid receptor potency for compounds <b>108</b> , <b>191</b> , <b>220</b> , <b>231</b> , and <b>232a</b> in the calcium mobilization assay format.	130



## LIST OF FIGURES

<b>Figure 1:</b> Examples of natural product antibacterials.	4
<b>Figure 2:</b> Examples of natural product cancer chemotherapeutics.	5
<b>Figure 3:</b> Examples of natural product antimalarials and NSAIDs.	7
<b>Figure 4:</b> Examples of clinically used opioids.	9
<b>Figure 5:</b> Endogenous opioid ligands and ligands for receptor characterization.	11
<b>Figure 6:</b> Systematic dismantling of morphine.	13
<b>Figure 7:</b> Examples of 4,5 $\alpha$ -epoxymorphinans.	14
<b>Figure 8:</b> Examples of morphinans.	16
<b>Figure 9:</b> Examples of benzomorphans.	17
<b>Figure 10:</b> Other examples of opioid receptor ligands.	19
<b>Figure 11:</b> GPCR signal cascade.	22
<b>Figure 12:</b> GRK/ $\beta$ -arrestin mechanism.	23
<b>Figure 13:</b> Examples of KOP receptor antagonists.	29
<b>Figure 14:</b> Structural classification of flavonoids.	37
<b>Figure 15:</b> Selected flavonoids evaluated in [ <sup>35</sup> S]GTP- $\gamma$ -S functional assay.	39
<b>Figure 16:</b> Structures of dioclein and dioflorin, isolated from <i>D. grandiflora</i> .	41
<b>Figure 17:</b> Design rationale for simplified dioflorin analogs.	44
<b>Figure 18:</b> Examples of KOP ligands and hallucinogens compared to salvinorin A.	70
<b>Figure 19:</b> Mevalonic acid pathway to IPP.	72
<b>Figure 20:</b> Mechanism of terpene chain elongation.	73
<b>Figure 21:</b> Examples of neoclerodane diterpenes.	74
<b>Figure 22:</b> Metabolites of salvinorin A.	81
<b>Figure 23:</b> Proposed salvinorin A–KOP receptor binding model from Roth et al.	93
<b>Figure 24:</b> Proposed salvinorin A–KOP receptor binding model from Yan et al.	94
<b>Figure 25:</b> Proposed salvinorin A–KOP receptor binding model from Kane et al. (2006).	95
<b>Figure 26:</b> Proposed salvinorin A–KOP receptor binding model from Kane et al. (2008).	96
<b>Figure 27:</b> Proposed salvinorin A–KOP receptor binding model from Singh et al.	97
<b>Figure 28:</b> Drawing of the crystal structure of JD <sub>1</sub> Tic bound in the KOP receptor.	99

<b>Figure 29:</b> Proposed RB-64-KOP receptor binding model.	99
<b>Figure 30:</b> General summary of the SAR of salvinorin A analogs.	100
<b>Figure 31:</b> Selected C-2 ester analogs of salvinorin A.	103
<b>Figure 32:</b> Selected C-2 bioisosteric analogs of salvinorin A.	107
<b>Figure 33:</b> Selected C-2 ether, amine, and halogen analogs of salvinorin A.	110
<b>Figure 34:</b> Selected C-2 epimeric analogs of salvinorin A.	113
<b>Figure 35:</b> Eclipsed or extended conformations of the ethoxymethyl ether at C-2 compared to salvinorin A.	114
<b>Figure 36:</b> 1D $^{13}\text{C}$ NMR spectrum with composite pulse $^1\text{H}$ -decoupling and gated decoupling to show $J_{\text{C,H}}$ for the anomeric carbon of <b>220</b> (A) and <b>221</b> (B).	120
<b>Figure 37:</b> X-ray crystallographic structure of <b>220</b> .	120
<b>Figure 38:</b> X-ray crystallographic structure of <b>231</b> .	123
<b>Figure 39:</b> Proposed stereochemical assignments for tetrahydropyran derivatives.	124
<b>Figure 40:</b> X-ray crystal structure of JD <sub>2</sub> Tic in the KOP receptor with relevant residues.	131
<b>Figure 41:</b> A) Overlay of JD <sub>2</sub> Tic from KOP co-crystal structure with poses of salvinorin A. B) Poses of salvinorin A with residues putatively involved in receptor binding.	132
<b>Figure 42:</b> A) Overlay of the crystal structures of salvinorin A, <b>220</b> , and <b>231</b> . B) Overlay of the crystal structures of salvinorin A and <b>220</b> . C) Overlay of the crystal structures of salvinorin A and <b>231</b> . D) Overlay of the crystal structures of <b>220</b> and <b>231</b> .	134
<b>Figure 43:</b> The effect of <b>220</b> on cocaine-induced drug-seeking.	136

## LIST OF SCHEMES

<b>Scheme 1.</b> Biosynthetic pathway of flavonoids.	36
<b>Scheme 2.</b> Synthesis of dioclein.	46
<b>Scheme 3.</b> Synthesis of dioflorin analogs.	47
<b>Scheme 4.</b> Synthesis of salvinorin B and 2-epi-salvinorin B.	102
<b>Scheme 5.</b> Synthesis of amide derivatives.	108
<b>Scheme 6.</b> Synthesis of C-2 derivatives.	119
<b>Scheme 7.</b> Synthesis of C-2 constrained ethers.	122

## CHAPTER 1: INTRODUCTION

### A Historical Perspective on Natural Products and Traditional Medicine

Throughout recorded history, humans have consumed natural products for medicinal, spiritual, and recreational purposes. In fact, several prominent ancient civilizations developed extensive ethnomedicinal traditions. Documents in the form of cuneiform clay tablets that date to 668–626 BC indicate that the ancient Mesopotamian pharmacopeia included approximately 250 medicines of plant origin and 120 of mineral origin.<sup>1</sup> Additionally, many of these cuneiform tablets are actually copies of much older texts from 3000–2000 BC. The Rigveda sacred text from ancient India contains multiple references to a plant derived inebriant called *soma* that was used ritualistically.<sup>2-3</sup> The practice of Chinese traditional medicine began as early as 4,000 years ago with the Shang dynasty.<sup>4</sup> Perhaps the best known Chinese traditional ethnomedicinals are ginseng and ephedra, which have been in use for thousands of years and are still in current use to treat a rather large variety of ailments from incontinence to asthma. A number of ancient Chinese traditional drug formularies still exist, detailing more than 10,000 medicinal substances as well as common drug formulations.<sup>4</sup> In pre-Columbian Central America, the Toltecs recorded their ritualistic use of two mind-altering natural substances known to them as *teonanácatl* and the more familiar *peyote*.<sup>5</sup> Finally, a well-known documented example of medicinal natural products is *De materia medica*, a detailed record of the medicinal uses of hundreds of plants throughout the then “known world,” written in his native Greek by Dioscorides, a military physician under the Roman Empire during the 1st century AD.<sup>6</sup> The five volume codex was one of very few classical works that did not fall out of circulation between the decline of the Roman Empire (5<sup>th</sup> century AD) and the Renaissance (14<sup>th</sup> century AD), and

continued to be the primary authority for pharmacology, medicine, and herbal writing until the 16<sup>th</sup> century AD.

Although modern medicine has changed the face of healthcare for many people, currently the World Health Organization (WHO) estimates that in some developing countries as much as 80% of the population still depends on traditional medicine as the primary form of healthcare.<sup>7</sup> Even in some developed nations, 70% to 80% of the population has used some form of traditional medicine. In a survey conducted by the Centers for Disease Control and Prevention (CDC) in 2007, 17.7% of adult respondents reported using nonvitamin, nonmineral natural products, such as fish oil, glucosamine, echinacea, or ginseng, as part of a complementary/alternative medicine (CAM) regime to promote overall health.<sup>8</sup>

### **Natural Products and Modern Medicine**

Using current terminology and definitions, the phrase “natural products” typically refers to secondary metabolites that are produced by organisms in response to external changes in their environment from nutrient deficiencies, infection, competition, etc.<sup>9</sup> Historically, natural products have been used therapeutically by humans in the form of crude extracts.<sup>10</sup> For example, extracts of willow bark, *Salix alba* L. (Salicaceae), were used by the ancient Egyptians to treat inflammation.<sup>11</sup> However, it was not until 1897 while working for Friedrich Bayer & Co. that Felix Hoffmann synthesized acetylsalicylic acid from the salicylic acid isolated from willow bark, thus creating aspirin.<sup>12-13</sup> Similarly, extracts of the opium poppy, *Papaver somniferum* L. (Papaveraceae), were used to treat pain and induce sleep throughout the 19<sup>th</sup> century and for millennia prior.<sup>14-16</sup> The principle agent responsible for the effects of the opium poppy, morphine, was isolated by Surtürner in the first decade of the 19<sup>th</sup> century. However, the correct

structure for morphine was not proposed until 1925, by Gulland and Robinson,<sup>17-19</sup> and their proposal was not confirmed until 1953 when the total synthesis was published by Gates and Tschudi.<sup>20-21</sup> Although the discoveries of morphine from opium poppies, aspirin from willow bark, and penicillin from mold (1928) occurred during the 19<sup>th</sup> and 20<sup>th</sup> centuries, these dates belie the millennia of ethnomedicinal use that inspired scientific investigation. The use of these natural products as single chemical entities rather than as extracts created the modern pharmaceutical industry.<sup>9, 13</sup> From 2000–2010, natural products or their semi-synthetic derivatives made up approximately one third of all small molecule new chemical entity (NCE) applications filed.<sup>22</sup> In 2010 alone, 50% of the 20 small molecule NCE applications filed were natural products.

Arguably, one of the most important medical advances made in the 20<sup>th</sup> century is the discovery of antibacterial agents that could be systemically administered (Figure 1).<sup>23</sup> The story of the discovery of the antibacterial penicillin by Sir Alexander Flemming in 1928 is well-known.<sup>24</sup> It was over a decade before penicillin was introduced into the clinic in 1941, and following its success, a large number of penicillins (**1**), cephalosporins (**2**), aminoglycosides like streptomycin (**3**)<sup>25</sup>, chloramphenicol (**4**)<sup>25</sup>, tetracycline (**5**)<sup>26</sup>, macrolides like erythromycin (**6**)<sup>27</sup>, and glycopeptides like vancomycin (**7**) (all natural products or natural product derivatives) were introduced into clinical practice.<sup>23</sup> In 1900, pneumonia, tuberculosis, diarrhea/enteritis, and diphtheria caused one third of all deaths in the United States.<sup>28</sup> In 1997, just 4.5% of all deaths could be attributed to infectious diseases, and life-expectancy had increased by 29.2 years. Nearly a century of research has provided a wide variety of natural product antibacterial agents, and new products continue to be produced. Just from 1981 through 2010, 104 new antibacterial agents were introduced, and of these, just under 75% are natural products.<sup>22</sup>

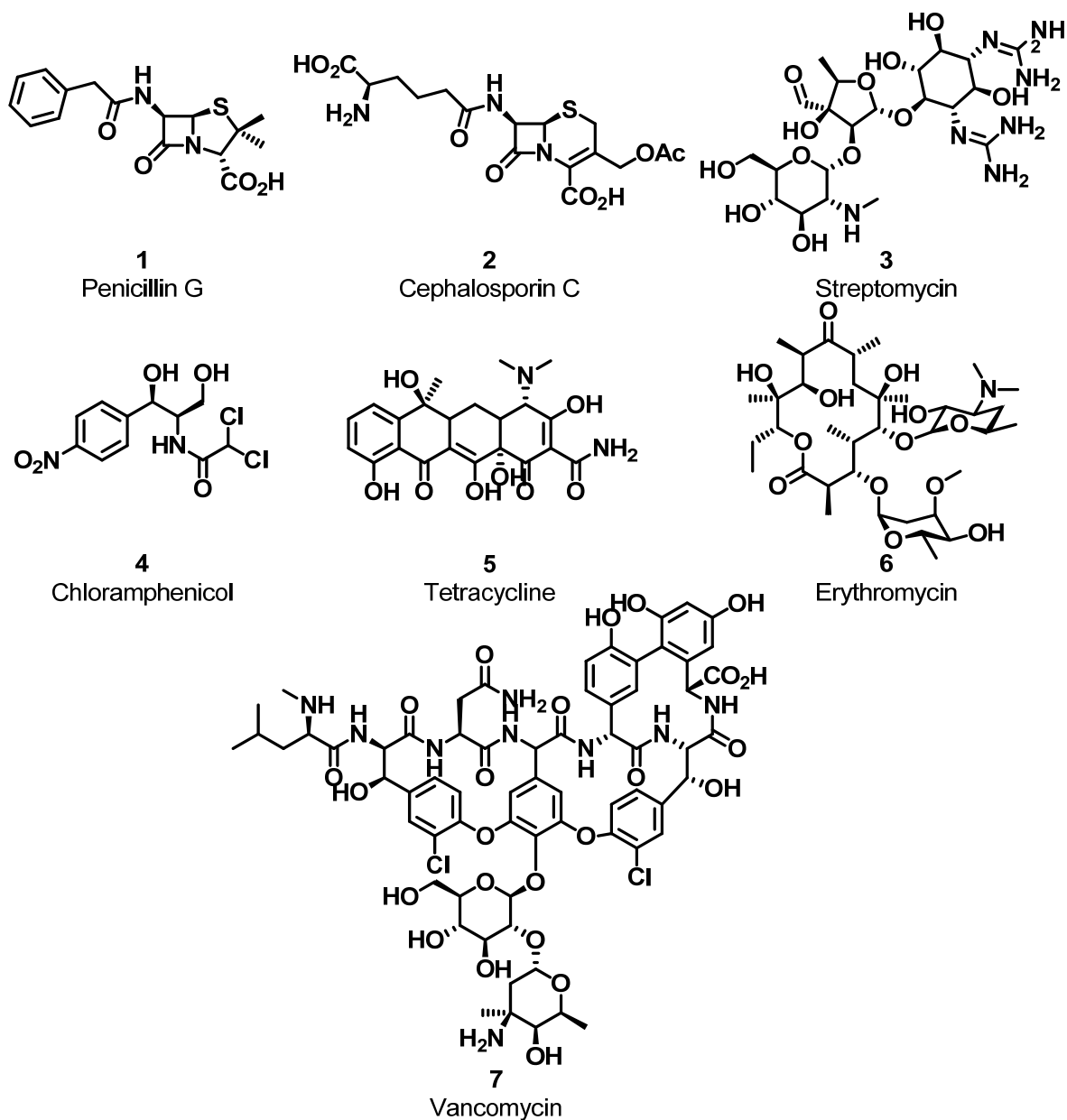


**Figure 1.** Examples of natural product antibacterials.

Another area of medicine for which natural products have been a boon is cancer chemotherapy (Figure 2). Of the 175 approved small molecule anti-cancer agents world-wide, 131 (75%) were derived from research into natural products.<sup>22</sup> The first small molecules to be used clinically against cancer were the vinca alkaloids, the natural products vinblastine (**8**) and

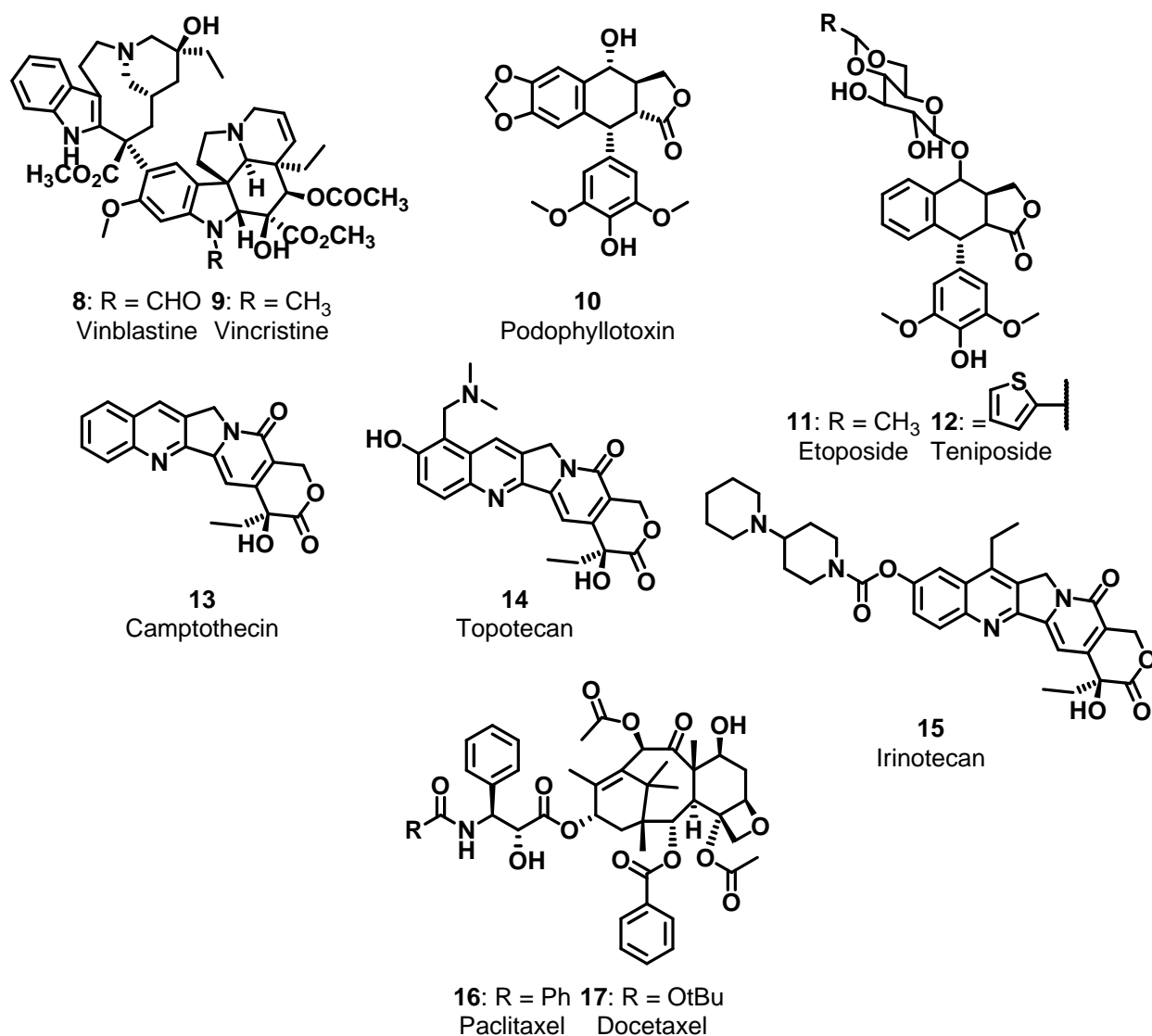


**Figure 2.** Examples of natural product cancer chemotherapeutics.

vincristine (**9**), isolated from the Madagascar periwinkle, *Catharanthus roseus* G. Don (Apocynaceae), in 1958 and 1961, respectively.<sup>29-30</sup> These agents are still in current clinical use, primarily as part of combination therapies to treat a variety of cancers. Podophyllotoxin (**10**) was isolated from the Mayapple, *Podophyllum peltatum* L. (Podophyllaceae) in 1880,<sup>31-32</sup> however the structure was not determined until 1951.<sup>33</sup> Extensive attempts to optimize the efficacy and toxicity profiles of podophyllotoxin led to two clinically useful semisynthetic



derivatives, etoposide (**11**) and teniposide (**12**).<sup>31-32</sup> Another addition to the arsenal of anti-cancer agents is camptothecin (**13**), isolated from the Chinese ornamental tree, *Camptotheca acuminata* Decne (Nyssaceae).<sup>34</sup> This agent was dropped from clinical trials in the 1970s due to unacceptable toxicity,<sup>32</sup> but continued attempts to optimize the scaffold produced topotecan<sup>35</sup> (**14**) and irinotecan<sup>36</sup> (**15**) in the early 1990s. Finally, one of the most important classes of anti-cancer agents is the taxanes. Paclitaxel (**16**), known by the trade name Taxol®, was initially isolated from the bark of the Pacific Yew tree, *Taxus brevifolia* Nutt. (Taxaceae), in 1971.<sup>37</sup> Despite intense interest and promising anti-cancer capabilities, paclitaxel and its semisynthetic derivative docetaxel (**17**) were beset by supply problems and were not able to enter clinical usage until the early 1990s.<sup>31-32</sup> These agents are still in current clinical use against a variety of cancers. Additionally there are currently 23 members of the taxane structural class in preclinical development as potential cancer chemotherapeutics.<sup>32</sup>

Although in the United States rapid progress in medical interventions against bacterial infection has resulted in decreased deaths due to infectious disease and an increase in life expectancy, malaria, a parasitic infection, remains one of the most significant health issues faced worldwide, with 250 million cases and over 800,000 deaths annually.<sup>38</sup> Symptoms of malaria-like disease are found in the *Nei Ching* (The Canon of Medicine), a document from China dated to 2700 BC, as well as in other ancient texts.<sup>39</sup> The history of antimalarial chemotherapy can be traced to herbal medicinal products (Figure 3). Quinine (**18**), a natural product and the first single chemical entity antimalarial treatment, was isolated and purified from cinchona tree bark, *Cinchona succiruba* L. (Rubiaceae), in 1820.<sup>38</sup> The use of the plant source itself against malaria, however, had been known for centuries.<sup>39-40</sup> Attempts to produce quinine synthetically led to the development of the classical 4-aminoquinolines, such as chloroquine (**19**), which have been

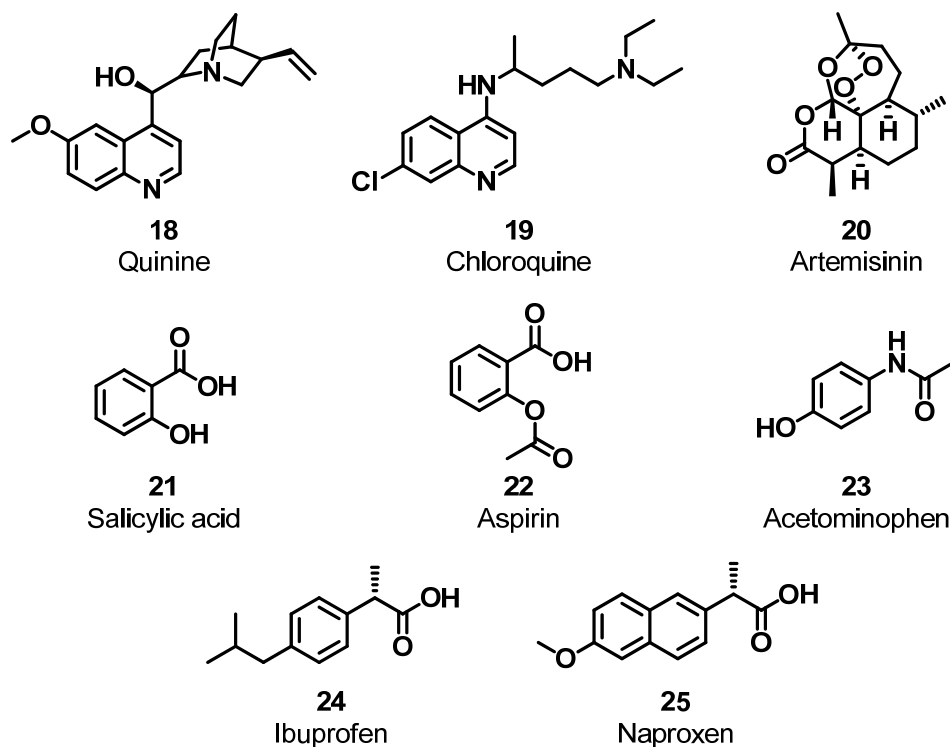


**Figure 3.** Examples of natural product antimalarials and NSAIDs.

mainstays of antimalarial chemotherapy through the last century.<sup>38</sup> In 1972, artemisinin (**20**) was isolated from *Artemisia annua* L. (Asteraceae) as the result of research efforts to find new treatments to combat the malaria parasite's developing resistance to chloroquine and similar drugs.<sup>41</sup> The unusual endoperoxide motif of artemisinin has inspired the production of many fully synthetic analogs with tailored pharmacokinetic and pharmacodynamic properties that are currently in clinical development.<sup>38, 42</sup> However, artemisinin-resistant strains of malaria already exist, and the continual threat of such drug resistance means that it is likely that it will always be necessary to continue the search for new molecular scaffolds.

Finally pain is currently, and likely always has been, one of the most common reasons that individuals seek medical intervention.<sup>43</sup> As previously stated, the use of salicylic acid (**21**), a natural product, can be traced back to ancient Egypt where extracts of willow bark were used to

treat pain and inflammation (Figure 3).<sup>11, 44</sup> Since then, one significant landmark in the history of medicine was the discovery of aspirin (**22**), or acetylsalicylic acid, which alone stimulated the development of an entire family of drugs known as the non-steroidal anti-inflammatory drugs (NSAIDs).<sup>11</sup> Aspirin was first synthesized in the pharmaceutical laboratory of the German dye manufacturer Friedrich Bayer & Co. in 1897 in an effort to produce pain medication that lacked the negative side effects of both morphine and salicylate salts.<sup>12</sup> NSAIDs such as aspirin, acetaminophen (**23**), ibuprofen (**24**), and naproxen (**25**), all three instigated by natural product investigation, have been invaluable drugs for the treatment of pain, inflammation, and fever.

### **Opioids: Natural Products used in Modern Medicine**

Another family of drugs commonly prescribed for the treatment of pain is the opioid analgesics; morphine (**26**) is a member of this family (Figure 4). The term “analgesia” refers to a drug’s ability to diminish pain.<sup>43</sup> Drugs that accomplish this are called analgesics, analgetics, or antinociceptives. In the modern clinical setting, NSAIDs are generally used as an initial treatment for mild to moderate pain, but an opioid analgesic may be added if pain persists; if pain progresses from moderate to severe, an opioid may be used as the sole treatment.<sup>16</sup> However, as previously stated, opioids in the form of extracts from the opium poppy have been used for millennia for the treatment of pain. One of the earliest written references to the medicinal use of such extracts is from the Eber Papyrus dated to 1552 BC, which describes the Egyptian goddess Isis giving the juice of the poppy to the sun god Ra to treat his headache.<sup>45</sup>

Use of opioid analgesics to treat cancer pain and severe, chronic non-cancer pain continues to be a controversial practice in medicine.<sup>16, 45</sup> In the 1960s physicians actually attempted to discontinue opioid use to treat chronic pain.<sup>45</sup> In the 1970s, the work of researchers

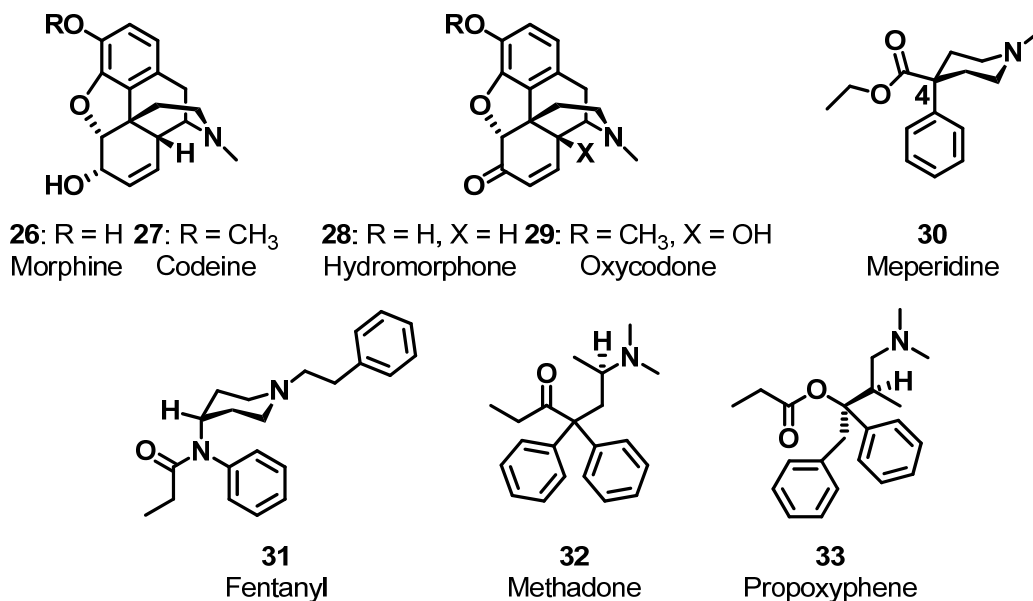


**Figure 4.** Examples of clinically used opioids.

at Sloan-Kettering in New York and St. Christopher's Hospice in London re-established opioid analgesics as an important part of treatment plans for patients suffering from cancer pain.<sup>45</sup> In 2009, the American Geriatric Society (AGS) published clinical practice guidelines recommending that patients with moderate to severe pain and diminished quality of life be considered for chronic opioid therapy.<sup>46</sup> Also in 2009, Chou et al., in conjunction with the American Pain Society and the American Academy of Pain, concluded that opioid therapy should be used for patients with chronic, non-cancer pain under careful supervision.<sup>47</sup>

The controversy over the chronic use of opioids analgesics stems from the fact that their use includes the risk of several clinically important and potentially severe side-effects, namely respiratory depression, constipation, tolerance, and dependence.<sup>14-16</sup> Even so, opioid analgesics are a mainstay of prescription drug therapy for the treatment of pain. The most common clinically used opioids are morphine, codeine (**27**), hydromorphone (**28**), oxycodone (**29**), meperidine (**30**), fentanyl (**31**), methadone (**32**), and until recently, propoxyphene (**33**), which

was withdrawn from the U.S. market in November 2010 due to patient deaths associated with cardiotoxicity (Figure 4).<sup>16, 48</sup>

### **Identification of the Opioid Receptors**

The opioid drugs exert their effects through the opioid receptors of which there are three types:  $\mu$  (MOP), named for its best known agonist, morphine;  $\kappa$  (KOP) named for the agonist first used to characterize it, ketocyclazocine (**34**); and  $\delta$  (DOP), named for the mouse vas deferens tissue preparation.<sup>49</sup> Although it was not until the 1990's that these individual receptor types were cloned and characterized, the concept of specific receptors for opioid compounds was first detailed by Beckett and Casy as early as 1954.<sup>50</sup> In 1971, Goldstein et al. proposed that radiolabeled compounds could be used to interrogate the existence of these receptors as well as characterize them.<sup>51</sup> Following this hypothesis, three different research groups simultaneously and independently demonstrated the existence of stereospecific opioid binding sites in mammalian brain.<sup>52-54</sup> The first convincing evidence of multiple types of opioid receptors came from Martin et al. in 1976.<sup>55</sup> They observed behavioral and neurophysiological differences in the chronic spinal dog model that led them to propose the existence of three different types of opioid receptors. In 1977, Lord et al. observed differences in rank order potency of opioid compounds between electrically induced twitches of guinea pig ileum and mouse vas deferens tissue, bolstering the hypothesis of multiple opioid receptor types.<sup>56</sup>

While researchers were teasing out the pharmacological differences between the opioid receptors, putative endogenous ligands for each receptor were identified (Figure 5). In 1975, the DOP receptor agonists methionine-enkephalin (**35**, Met-enkephalin) and leucine-enkephalin (**36**, Leu-enkephalin) were isolated from pig brains and demonstrated to have activity that could be

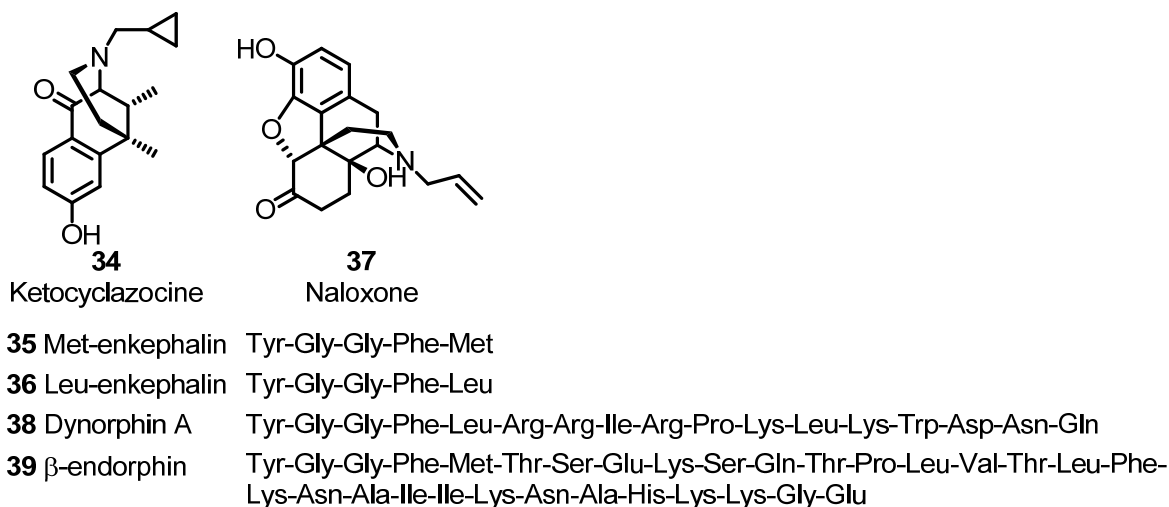


**Figure 5.** Endogenous opioid ligands and ligands for receptor characterization.

inhibited by naloxone (**37**), an opioid antagonist.<sup>57</sup> Also in 1975, the endogenous ligand for KOP receptors, dynorphin A (**38**), was isolated from bovine pituitary glands.<sup>58-59</sup> Finally, in 1976, the endogenous ligand for the MOP receptor,  $\beta$ -endorphin (**39**), was isolated from camel pituitary glands.<sup>60</sup>

The DOP receptors were the first of the three opioid receptors to be cloned and expressed. This was accomplished in 1992 simultaneously and independently by Keiffer et al.<sup>61</sup> at École Supérieure de Biotechnologie in Strasbourg, France and by Evans et al.<sup>62</sup> at the University of California at Los Angeles. Next in 1993, Meng et al.<sup>63</sup> at the University of Michigan isolated and cloned the KOP receptors, and finally in 1994, the MOP receptors were cloned by Wang et al. at the National Institute on Drug Abuse (NIDA).<sup>64</sup>

### SAR of the Endogenous Opioid Peptides

All of the endogenous opioid peptides are derived from one of three precursor peptides; proenkephalin (enkephalins), proopiomelanocortin (endorphins), or prodynorphin

(dynorphins).<sup>65</sup> The cleavage products of these precursor peptides all contain the pentapeptide sequence of either Met-enkephalin or Leu-enkephalin at the *N*-terminus (Tyr-Gly-Gly-Phe-X, where X = Met or Leu), but differ in their *C*-terminal sequence.<sup>16</sup> The differences in *C*-terminal sequences produce differences in preferred receptor interactions. As previously mentioned, the enkephalins exhibit preference for DOP receptors, the dynorphins interact selectively with KOP receptors, and  $\beta$ -endorphin possesses affinity for MOP receptors.

SAR development of the enkephalins produced a peptide with the sequence Tyr-D-Arg-Gly-Phe-D-Leu which came to be known as D-Ala-D-Leu-enkephalin (DADLE) and is a selective DOP receptor agonist.<sup>66</sup> Further changes to the enkephalin sequence led to Tyr-D-Ala-Gly-MePhe-Gly-ol-enkephalin (DAMGO), a selective MOP agonist.<sup>67</sup> Tritiated versions of DADLE and DAMGO are the standard agonists used in radioligand binding studies for DOP and MOP receptors, respectively.<sup>68</sup> From collective studies, the general SAR of the enkephalin peptides is: 1) alteration of either Tyr<sup>1</sup> or Gly<sup>3</sup> results in a loss of opioid activity,<sup>69-70</sup> 2) replacement of Phe<sup>4</sup> is not well tolerated, but the *para* position on the ring may be substituted,<sup>70</sup> 3) adding rigidity to the peptide via a dehydrophenylalanine residue in place of Phe<sup>4</sup> is tolerated.<sup>71</sup> The SAR for  $\beta$ -endorphin is very similar to that of the enkephalins, and replacement or deletion of the *C*-terminal residues is not well tolerated.<sup>72</sup> Finally, in SAR studies of dynorphin it has been published that Arg<sup>7</sup> and Lys<sup>11</sup> are critical for KOP receptor selectivity, while Tyr<sup>1</sup> is required for biological activity.<sup>73</sup> However, relatively recent work has shown that, for opioid peptides in general, modification of Tyr<sup>1</sup> such that the amino-terminus is no longer basic or removal of the phenolic hydroxyl (replacement with Phe residue) can convert opioid agonists to antagonists.<sup>14, 74-75</sup>

## SAR of Non-Peptidic Opioid Ligands

While much research has focused on the development of peptidic ligands for the opioid receptors, there is an even larger body of research concerning the development of morphine-based small molecule ligands. Although compounds with opioid activity appear structurally diverse, ranging from fused multi-cyclic scaffolds to acyclic scaffolds, conceptually these differing molecules can be related to each other by envisioning a systematic dismantling of morphine, the prototypical opioid ligand (Figure 6).<sup>16</sup> With this in mind, non-peptide opioids fall into one of five structural categories: 1) 4,5 $\alpha$ -epoxymorphinans, 2) morphinans, 3) benzomorphans, 4) phenyl piperidines, and 5) acyclic or other opioids.

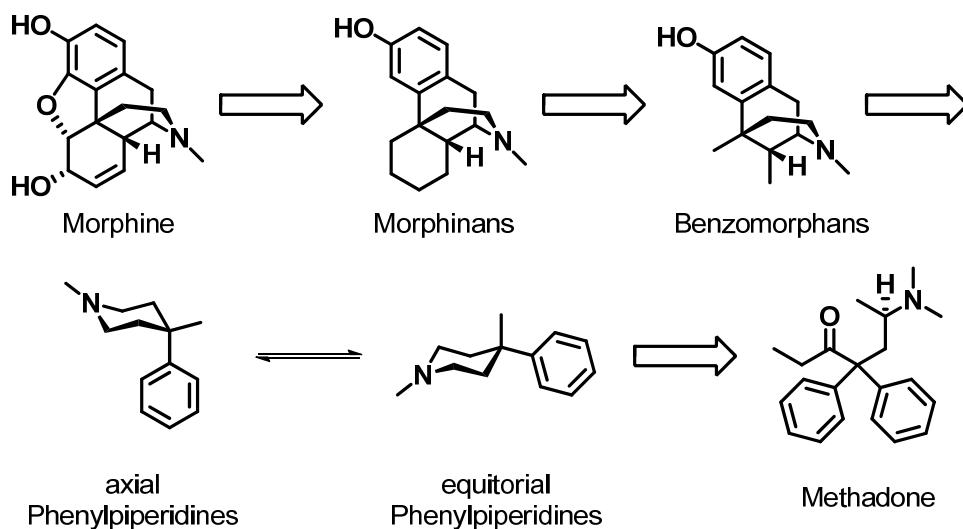
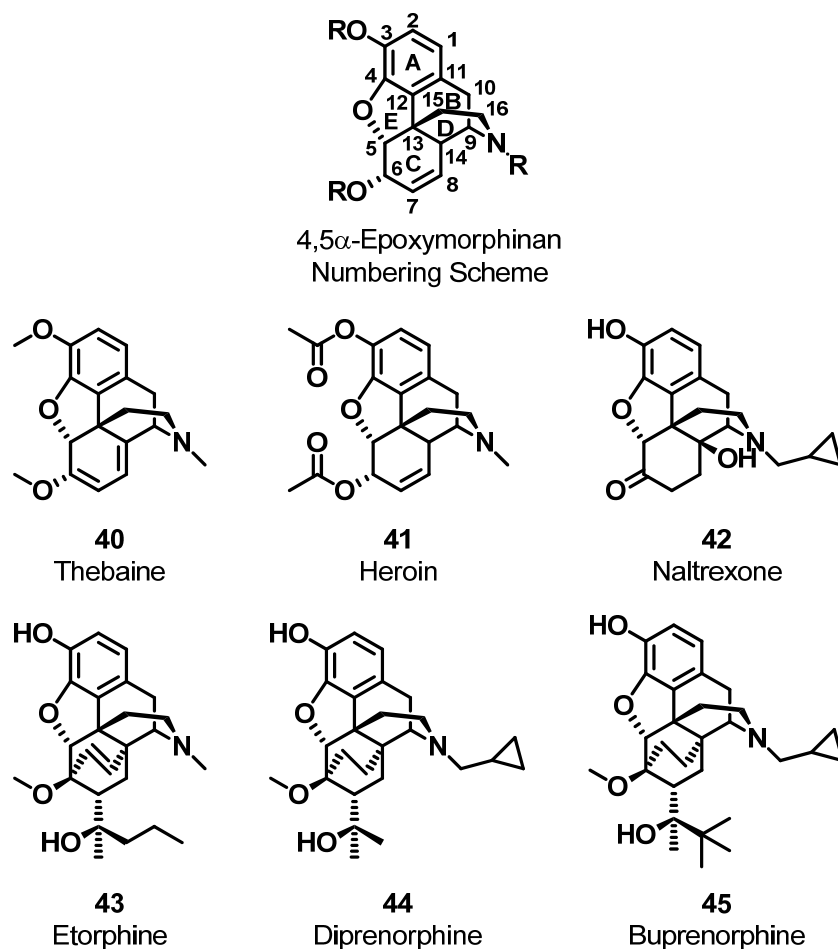


**Figure 6.** Systematic dismantling of morphine.

### *4,5 $\alpha$ -Epoxy-morphinans*

The largest class of opioid ligands is the 4,5 $\alpha$ -epoxy-morphinan class, which includes several natural products found in the opium poppy; morphine (**26**), codeine (**27**), and thebaine



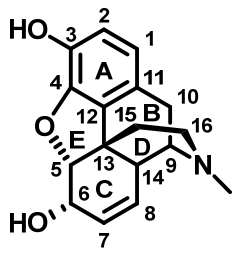


**Figure 7.** Examples of 4,5 $\alpha$ -epoxymorphinans.

(**40**), which is an important precursor for the synthesis of many therapeutically important morphine-based derivatives (Figure 7).<sup>16</sup> The first synthetic derivative of morphine to be produced was 3,6-diacetylmorphine (**41**, heroin) in the late 19<sup>th</sup> century.<sup>76</sup> Masking the 3- and 6-hydroxyl groups of morphine increases the lipophilicity of the molecule, increasing penetration of the blood-brain barrier.<sup>14</sup> Once absorbed, esterases rapidly hydrolyze the 3-acetyl group to produce 6-acetylmorphine, which has MOP agonist activity greater than morphine.<sup>14, 77</sup> Another well-known derivative is codeine, in which the 3-hydroxyl of morphine has been methylated. Codeine has less activity as an analgesic than morphine, but is used as an antitussive due to its

oral bioavailability and low risk of physical dependence.<sup>78-80</sup> The general SAR for 4,5 $\alpha$ -epoxymorphinans is summarized in Table 1.<sup>14</sup> One important feature to note is that alteration of the *N*-alkyl substituent dramatically effects functionality; *N*-Me and *N*-phenethyl are agonists, while *N*-allyl (**37**, naloxone) and *N*-cyclopropylmethyl (**42**, naltrexone) are antagonists.

**Table 1.**<sup>14</sup> Structure, numbering, and selected SAR summary for morphine.

	Substituent Alteration	Analgesic Activity Change
	3-OH to 3-H	10 $\times$ decrease
	6-OH to 6-keto	Decrease or increase with 7,8-dihydro
	6-OH to 6-H	Increase
	7,8-dihydro	Increase
	14- $\beta$ -OH	Increase
	3-OH to 3-OMe	Decrease
	3-OH to 3-OAc	Decrease
	6-OH to 6-OAc	Increase
	<i>N</i> -Me to <i>N</i> -phenethyl	10 $\times$ increase
	<i>N</i> -Me to <i>N</i> -allyl	Becomes MOP antagonist

While thebaine does not produce an analgesic effect, it is a very important precursor in the preparation of codeine as well as the Diels–Alder products etorphine (**43**), diprenorphine (**44**), and buprenorphine (**45**). Etorphine is 8,600 times more potent than morphine as an analgesic and is used for large animal veterinary procedures.<sup>81</sup> Diprenorphine is an antagonist and is used to reverse the effects of etorphine.<sup>16, 72</sup> Interestingly, buprenorphine appears to be a partial MOP agonist, showing a greater analgesic effect than morphine, but with a longer duration of action as well as some KOP antagonist properties.<sup>82</sup> Consequently, buprenorphine has been approved for the treatment of heroin addiction.<sup>83</sup>

## Morphinans

Morphinans differ structurally from the 4,5 $\alpha$ -epoxymorphinans in that they lack the 4,5 $\alpha$ -ether bridge (Figure 8). The best known compounds in the morphinan class are levorphanol (**46**) and dextrorphan (**47**). Levorphanol, the *levo* isomer, has the same configuration as morphine, but is about four times as potent as an analgesic.<sup>84</sup> Dextrorphan, the *dextro* isomer, and particularly its 3-methyl ether dextromethorphan (**48**), are powerful antitussives used in over-the-counter medications.<sup>85</sup> The general SAR for the morphinans is otherwise very similar to the SAR of the 4,5 $\alpha$ -epoxymorphinans.

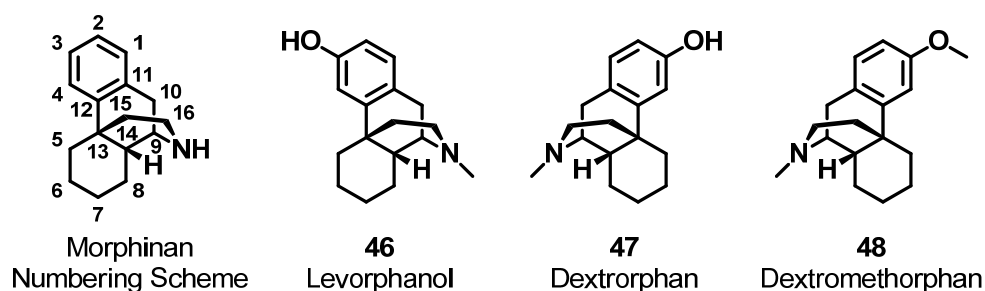


**Figure 8.** Examples of morphinans.

## Benzomorphans

Since the structural simplification of the 4,5 $\alpha$ -epoxymorphinans to the morphinans successfully yielded compounds with biological activity, further simplification was explored through removal of the C-ring, producing the benzomorphan core (Figure 9). Ketocyclazocine (**34**), a selective KOP ligand, is an important member of this class which, as previously described, was used to pharmacologically differentiate the KOP receptor. The majority of analogs made in this structural class are alkyl substitutions at the 5- or 9-positions, as well as at the nitrogen. Substituents at the 9-position that have the  $\beta$ -orientation tend to have higher

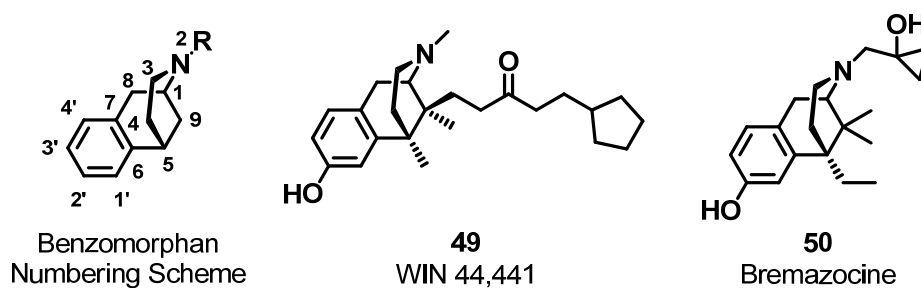


**Figure 9.** Examples of benzomorphan.

analgesic potency than those with the  $\alpha$ -orientation,<sup>86</sup> and compounds with a dual  $\alpha$ -methyl/ $\beta$ -alkanone substitution at this position, such as WIN 44,441 (**49**), tend to be very potent ligands with functionalities ranging from agonist to antagonist.<sup>87</sup> SAR for *N*-substituents is generally similar to that of the 4,5 $\alpha$ -epoxymorphinans and the morphinans; *N*-Me and *N*-phenethyl are agonists however, *N*-allyl or *N*-cyclopropylmethyl can lead to either antagonists or mixed agonist/antagonists.<sup>16</sup> One unique example is bremazocine (**50**), which is a KOP agonist, but a MOP/DOP antagonist.<sup>88</sup>

#### *Piperidine Derivatives*

Further simplification of the benzomorphan scaffold through removal of the B-ring yields the 4-phenylpiperidines. This results in more flexible compounds and therefore more complex SAR, which can be explained through different conformations (e.g. axial or equatorial) of the phenyl ring.<sup>16</sup> The prototypical 4-phenylpiperidine is meperidine (**30**), which is clinically used for the relief of labor pain.<sup>89</sup> A large number of meperidine analogs have been reported; the general SAR is: 1) alterations to the 4-position reduce analgesic activity;<sup>16</sup> 2) incorporation of a *m*-hydroxyl on the phenyl ring enhances activity and can be either an agonist or antagonist depending on the *N*-substituent;<sup>16, 90</sup> 3) while *N*-phenethyl is an agonist, *N*-allyl and *N*-

cyclopropylmethyl do not necessarily produce antagonism;<sup>91</sup> 4) reversed esters of meperidine are more potent.<sup>14</sup>

The 4-anilidopiperdines, fentanyl (**31**) being the best known example, are potent analgesics; fentanyl is 200 times more potent than morphine.<sup>92-94</sup> Because of its rapid onset and short duration of action, fentanyl is used almost exclusively for anesthesia.<sup>16</sup> The SAR for 4-anilidopiperdines and 4-phenylpiperidines is very similar, leading to the hypothesis that the two classes of compounds interact with the opioid receptor in a very similar fashion.<sup>95</sup>

#### *Other Classes of Opioids*

Methadone (**32**) and its derivatives can be considered as “ring-opened” derivatives of the 4-phenylpiperidine class.<sup>16</sup> Currently, methadone is used clinically as replacement therapy for opioid addiction. This is because it has a similar analgesic effect to morphine but a much longer duration of action; methadone can be more easily dosed to achieve steady blood concentrations and alleviate withdrawal symptoms.<sup>96</sup> In general, alteration of the *N*-substituent leads to derivatives with reduced analgesic efficacy.<sup>97</sup>

Discovered in 1982 by the Upjohn Company, the arylacetamides are a relatively recently developed class of opioid ligands (Figure 10).<sup>98</sup> The selective KOP agonists U50,488 (**51**) and U69,593 (**52**) are members of this class and tritiated versions of these are the standard agonists of choice for KOP radioligand binding assays.<sup>99-100</sup> In 1994, SNC 80 (**53**) was reported as a selective DOP receptor agonist; it is a member of the benzhydrylic piperazine class.<sup>101</sup> Another recently developed (2001) class of opioid ligand is the tetrahydroisoquinolines, of which JDTC (**54**) is a member.<sup>102</sup> The development of JDTC was inspired by the 4-phenylpiperidine class, and it is a highly potent and selective KOP antagonist. In 2010, the 8-azabicyclo[3.2.1]octan-3-

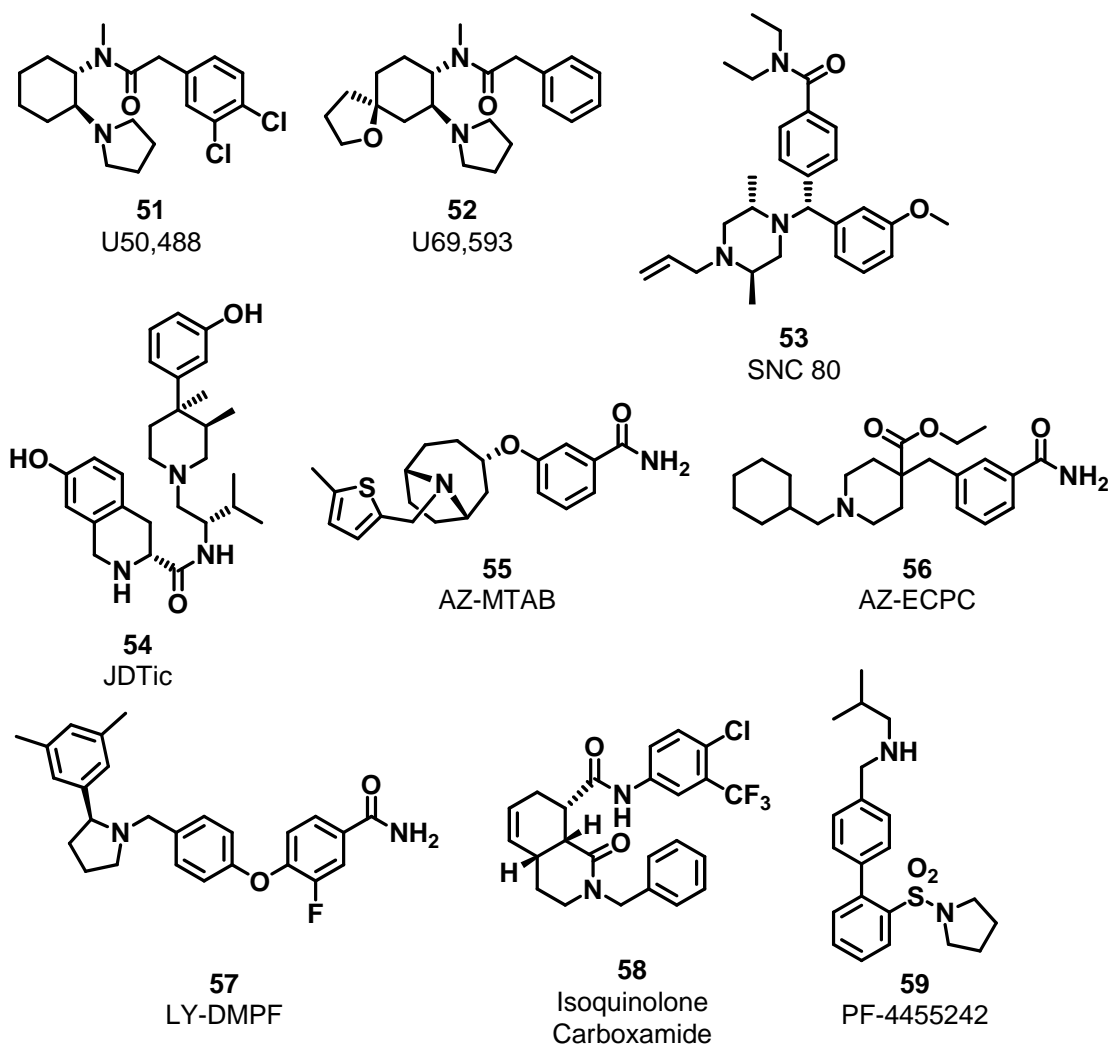


**Figure 10.** Other examples of opioid receptor ligands.

yloxy-benzamide structural class was reported to produce selective KOP antagonists.<sup>103-104</sup> From this initial *in vitro* work, AZ-MTAB (**55**) and AZ-ECPC (**56**) were found to be short acting antagonists *in vivo* compared to standard KOP antagonists.<sup>105</sup> Eli Lilly has reported similar compounds (**57**, LY-DMPF) that have similar activity.<sup>106</sup> Also in 2010 (with a follow-up in 2012), Frankowski et al. reported a high through-put screening (HTS) strategy that identified *N*-alkyl-octahydroisoquinolin-1-one-8-carboxamides (**58**) as nonbasic, selective KOP ligands.<sup>107-108</sup> Finally, in 2011, Pfizer reported PF-4455242 (**59**) as a selective KOP antagonist.<sup>109</sup> This

**Table 2.** Summary of selected opioid receptor ligands.

Structural Class	Ligand	Selective Receptor	Agonist (+) / Antagonist (-)
Peptidic	Met-enkephalin ( <b>35</b> )	DOP	+
	Leu-enkephalin ( <b>36</b> )	DOP	+
	$\beta$ -Endorphin ( <b>39</b> )	MOP	+
	Dynorphin ( <b>38</b> )	KOP	+
	DADLE	DOP	+
	DAMGO	MOP	+
4,5 $\alpha$ -Epoxy-morphinan	Morphine ( <b>26</b> )	MOP	+
	Codeine ( <b>27</b> )	MOP	+
	Heroin ( <b>41</b> )	MOP	+
	Naloxone ( <b>37</b> )	MOP	-
	Naltrexone ( <b>42</b> )	MOP	-
	Etorphine ( <b>43</b> )	MOP	+
	Diprenorphine ( <b>44</b> )	MOP	-
	Buprenorphine ( <b>45</b> )	MOP	+ MOP, - KOP
Morphinan	Levorphanol ( <b>46</b> )	MOP	+
	Dextrorphan( <b>47</b> )	MOP	+
	Dextromethorphan ( <b>48</b> )	MOP	+
Benzomorphan	Ketocyclazocine ( <b>34</b> )	KOP	+
	WIN 44,441 ( <b>49</b> )	KOP	- KOP/MOP
	Bremazocine ( <b>50</b> )	KOP	+ KOP, - MOP/DOP
4-Phenylpiperidine	Meperidine ( <b>30</b> )	MOP	+
4-Anilidopiperidine	Fentanyl ( <b>31</b> )	MOP	+
Acyclic	Methadone ( <b>32</b> )	MOP	+
Arylacetamide	U50,488 ( <b>51</b> )	KOP	+
	U69,593 ( <b>52</b> )	KOP	+
Benzhydryl Piperazine	SNC 80 ( <b>53</b> )	DOP	+
Tetrahydroisoquinoline	JDTic ( <b>54</b> )	KOP	-
Benzamides	AZ-MTAB ( <b>55</b> )	KOP	-
	AZ-ECPC ( <b>56</b> )	KOP	-
	LY-DMPF ( <b>57</b> )	KOP	-
Isoquinolone carboxamide	<b>58</b>	KOP	+
Biphenylsulfonamide	PF-4455242 ( <b>59</b> )	KOP	-

compound is a biphenylsulfonamide, the core structure of which was identified from a HTS campaign, and has entered Phase 1 clinical trials for depression.

Since the 19<sup>th</sup> century the morphine scaffold has been explored as a source of molecules with opioid receptor activity, and there exists a wide variety of derivatives, only a few of which have been mentioned here, that span different potencies, functionalities, and receptor selectivities (Table 2). Even so, the utility of ligands related to the morphine scaffold is limited due to the associated negative side effects that seem to follow through even with simplification and derivatization. Therefore the identification of non-morphine-like scaffolds is important for new ligand development.

### **G-Protein Coupled Receptors**

As previously stated, all of the opioid ligands exert their effects through the opioid receptor system. There is substantial evidence that the opioid receptors are members of the G-protein coupled receptor (GPCR) superfamily, one of the largest and most diverse protein families in the mammalian genome with more than 800 unique receptors.<sup>16, 110-111</sup> In fact, all of the opioid receptor isolation and cloning studies noted that the receptors shared significant sequence homology with known GPCRs. Despite their large array of functional diversity, all GPCRs share a similar structure consisting of 7 transmembrane domains connected by alternating intra- and extra-cellular loops (Figure 11).<sup>110</sup> Extra-cellular loops, which differ among the different types of GPCRs, apparently contribute to ligand recognition and binding, whereas coupling to particular G-proteins is determined by the intra-cellular loops.<sup>112-113</sup> When an agonist binds to the extra-cellular loop of a GPCR, it induces a conformational change in the receptor structure which leads to intra-cellular coupling to and activation of one or more G-proteins.<sup>110</sup>



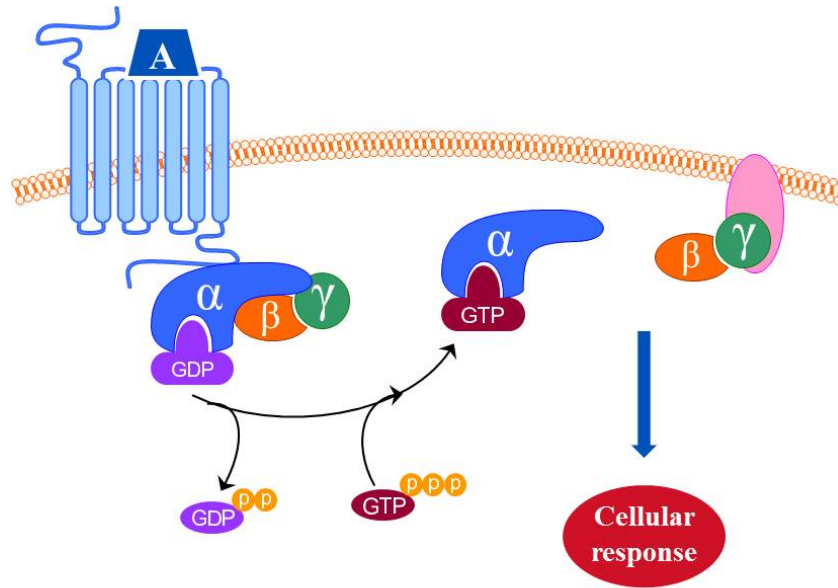


**Figure 11.** GPCR signal cascade.

G-proteins are heterotrimeric, consisting of 3 subunits named  $\alpha$ ,  $\beta$ , and  $\gamma$ , and bind guanine nucleotides to their  $\alpha$ -subunit, catalyzing the hydrolysis of guanosine triphosphate (GTP) to guanosine diphosphate (GDP) upon agonist binding.<sup>16, 110</sup> A variety of different genes have been identified which encode each of these subunits. Coupling of the GPCR to the G-protein results in dissociation of the  $\alpha$ -subunit from the  $\beta\gamma$ -subunit, and the  $\beta\gamma$ -subunit can then activate a number of different effectors, such as enzymes or ion channels.<sup>110, 114-115</sup> The  $\alpha$ -subunit has a role in determining receptor specificity and can also influence the efficiency of interactions of the  $\beta\gamma$ -subunit.<sup>110</sup> On the basis of G-protein coupling preference, GPCRs can be classified into 4 major categories:  $G\alpha_s$ -,  $G\alpha_{i/o}$ -,  $G\alpha_{q/11}$ -, and  $G\alpha_{12/13}$ -coupled receptors.<sup>114</sup> Almost all agonists that have an analgesic action are coupled to  $G\alpha_{i/o}$  proteins.<sup>110</sup> The  $G\alpha_i$  and  $G\alpha_o$  proteins inhibit adenylate cyclase, while  $G\alpha_s$  stimulates production, and of the effectors implicated in signaling mechanisms for opioid receptors, inhibition of adenylate cyclase and

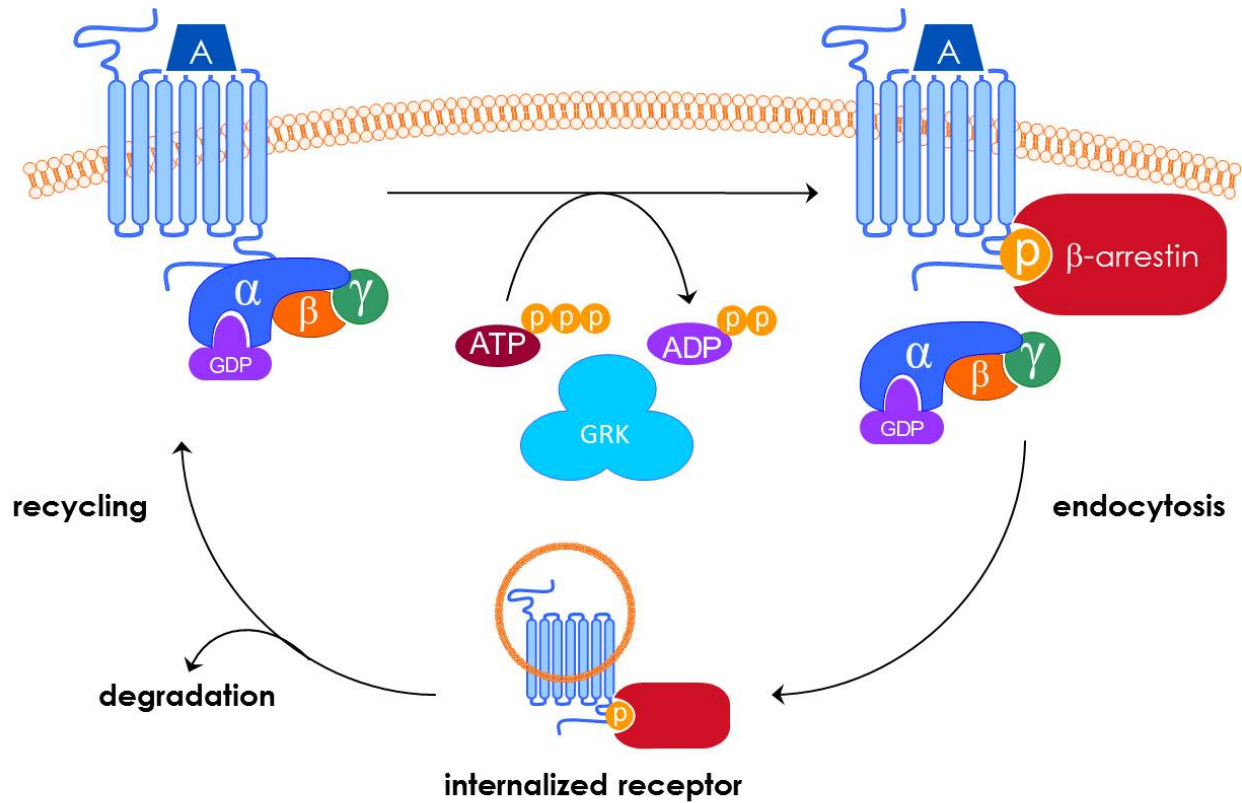


**Figure 12.** GRK/β-arrestin mechanism.

subsequent decrease in intra-cellular cyclic adenosine monophosphate (cAMP) concentrations is the best studied.<sup>16</sup>

GPCRs can also signal through G-protein independent mechanisms, the best characterized of which is the GPCR kinase (GRK)/β-arrestin pathway.<sup>116</sup> Mammals express seven GRK isoforms. Isoforms GRK1 and GRK7 are confined to the retina, GRK4 has limited cellular distribution with high expression localized in the testes, and GRK2, GRK3, GRK5, and GRK6 are ubiquitously expressed.<sup>116-117</sup> In the first step of the pathway, serine and threonine residues of the third intra-cellular loop and the carboxy terminus region of the agonist-bound receptor are phosphorylated by a GRK (Figure 12). For some GPCRs, agonist activation and

phosphorylation by a GRK are enough to cause the G-protein to become decoupled from the receptor itself, leading to receptor desensitization, however many GPCRs require the additional step of recruitment of proteins called arrestins.<sup>116-117</sup>

There are four members in the arrestin family. Arrestin 1 (visual arrestin) and arrestin 4 (cone arrestin) are localized to retinal rods and cones, whereas arrestin 2 ( $\beta$ -arrestin 1) and arrestin 3 ( $\beta$ -arrestin 2) are ubiquitous.<sup>117</sup> Recruitment of a  $\beta$ -arrestin protein to an agonist-activated, GRK-phosphorylated receptor sterically hinders further G-protein coupling of the receptor, causing desensitization.<sup>118</sup> Further,  $\beta$ -arrestins are known to interact with and serve as adaptors for components of the endocytotic machinery, thus their recruitment to the receptor promotes receptor internalization from the cell surface and sequestration from G-proteins, followed by either eventual degradation or recycling back to the cell surface.<sup>116-117, 119</sup> In order to signal through the GRK/ $\beta$ -arrestin pathway,  $\beta$ -arrestin that has been recruited to an agonist-activated, GRK-phosphorylated receptor also promotes association of the receptor with other signaling proteins, such as kinases, furthering intracellular signal cascades completely independently of the G-protein.<sup>117</sup> Thus, even as  $\beta$ -arrestin interferes with G-protein signaling, it also promotes a second, parallel signaling pathway.

Until recently, a ligand's efficacy for  $\beta$ -arrestin recruitment/signaling was thought to be proportional to its efficacy for G-protein signaling; the signaling paradigm for receptors and their ligands was completely linear in nature. However, it is now known that "biased ligands" can selectively activate either the  $\beta$ -arrestin or the G-protein signaling pathway, indicating a more complicated, non-linear paradigm for ligand-GPCR signaling.<sup>119</sup> This also implies that there are novel biological consequences to be discovered, even for well-studied GPCRs. Furthermore, this

suggests that molecules can be discovered or even designed to selectively activate either pathway, possibly resulting in either novel biological probes or more therapeutically beneficial drugs.

### **Opioids, Receptors, and the Treatment of Pain**

One area of medicine that would benefit greatly from the elucidation of novel biological mechanisms or the development of improved therapeutics is the area of pain management. Acute pain, postoperative pain, and types of chronic pain are initiated by the activation of a nociceptor, a peripheral sensory receptor that responds to noxious stimuli.<sup>43, 120</sup> Nociceptors are present in all tissues and can respond to different stimuli such as thermal, mechanical, or chemical mediators released from surrounding tissues (e.g. histamine or lactic acid).<sup>120</sup> The manifestation of pain, however, is a complex experience that is not only governed by the central nervous system (CNS), but is informed by such cognitive input as environment (e.g. society and culture), life experience, and gender.<sup>43</sup> As previously stated, pain is one of the most common reasons that individuals seek medical intervention. This phenomenon results in around 40 million physician visits annually and is estimated to cost \$100 billion each year in health care and lost productivity.<sup>43</sup> The opium alkaloids, such as morphine and its derivatives, are among the most potent analgesics used in the clinic. Clinically used opioid analgesics are a popular choice for the treatment of severe pain, however their negative side effects—respiratory depression, constipation, tolerance, and dependence—decrease their appeal.<sup>16</sup> The opium alkaloids and many of their synthetic derivatives are selective agonists at MOP receptors, and it is MOP receptor activation that is linked to these agents' negative effects.

The most common side effect of opioid use is constipation in addition to a collection of other gastrointestinal (GI) effects termed opioid bowel dysfunction.<sup>16</sup> The frequency of opioid-related GI effects is quite high, 40-50% or more in patients receiving opioid therapy.<sup>121-123</sup> The constipation is mediated by MOP receptors in the bowel; delayed food digestion and a decrease in peristaltic waves in the intestines results in retention of contents.<sup>89</sup> Tolerance does not usually develop to this side effect, and patients receiving chronic opioid therapy are chronically constipated. Fortunately, this side effect can be diminished with prophylactic administration of a laxative and/or a stool softener.<sup>124-125</sup>

The slowed breathing associated with opioid analgesics is termed respiratory depression, and constitutes the most severe side effect of opioid use.<sup>124</sup> The interaction of opioid analgesics with the respiratory center in the brain causes a decreased response to carbon dioxide concentration in the blood and thus a decrease in breathing rate.<sup>89</sup> Such an effect occurs at drug doses much lower than those that affect consciousness and increases in a dose-dependent manner. Death from opioid overdose is nearly always a result of respiratory depression. The severity of this side effect can be diminished by careful titration of opioid drug dose.<sup>124</sup>

Chronic use of opioids often results in tolerance and physical dependence.<sup>16</sup> Tolerance is a phenomenon that results when continuous drug exposure leads to decreased effectiveness, and larger doses are required to achieve the previous therapeutic effect.<sup>126</sup> It is hypothesized that tolerance to opioid analgesics may be caused physiologically by the receptor desensitization and internalization processes described previously that take place in the GRK/ $\beta$ -arrestin signaling pathway. Physical dependence is a physiologically adaptive state that is characterized by the appearance of withdrawal symptoms specific to the opioid family of drugs upon abrupt cessation

or significant reduction in dose, or upon administration of an opioid antagonist.<sup>126</sup> It is important to note that physical dependence is distinct from addiction. Physical dependence is defined only by the appearance of withdrawal symptoms at decreased drug concentrations in blood (or when an antagonist is administered). Addiction is defined by chronic, uncontrolled and/or compulsive drug use, and continued drug use despite grievous harm to health and well-being.<sup>126</sup>

### **Therapeutic Potential of KOP Receptor Selective Agents**

In part because of the side effect liabilities of MOP receptor ligands, opioid ligands that are selective for other types of opioid receptors show promise as clinical agents to treat a variety of conditions. One example is KOP receptor selective ligands; selective KOP agonists are capable of producing clinically useful analgesia, but lack the constipation, respiratory depression, and tolerance and physical dependence properties associated with MOP agonists.<sup>14-16</sup> Still, there is an important negative side effect associated with KOP receptor activation in the CNS, and that is dysphoria, a hallucinogenic-like, aversive effect that is the opposite of euphoria.<sup>127</sup> In spite of this, KOP agonists are targets for pain relief absent the negative side effects of MOP agonists. Although some KOP agonists are known to produce a dysphoric effect, there is still some hope that a clinically useful analgesic may be found. KOP agonists whose action is restricted to the peripheral nervous system (PNS) have been shown to be effective in relieving inflammatory and visceral pain, and due to the PNS restriction, this analgesia occurs without dysphoria.<sup>16, 120</sup>

Another important indication for KOP-selective ligands is mood regulation. The endogenous opioid systems in the brain are certainly involved in the regulation of mood, although they have received far less research interest than the monoamine systems such as dopamine, norepinephrine, and serotonin.<sup>128</sup> Work focused on the effects of stimulant drugs on

cAMP response element binding protein (CREB), a transcription factor, found that repeated administration of stimulants such as amphetamine increased the function of CREB in the nucleus accumbens (NAc) region of rodent brains.<sup>129</sup> Stress was also found to activate CREB in the rodent NAc.<sup>130</sup> Continued study of these phenomena lead to the observation that elevated CREB function in the NAc, whether by drug administration or stress, produces the rodent equivalent of symptoms of major depression: dysphoria, anhedonia, and despair.<sup>130</sup> Further, disruption of CREB function in the NAc leads to opposite effects and has anti-depressant-like qualities.

Because CREB is a transcription factor that regulates gene expression, it is logical that the effects of elevated CREB function are caused by target genes, and recent work indicates that the same stress that activates CREB in the NAc also increases the expression of prodynorphin (PDYN), the precursor to the endogenous KOP agonist, dynorphin (DYN).<sup>131</sup> In fact, elevations in CREB function in the NAc increase PDYN expression, whereas disruptions in CREB function reduce expression.<sup>132</sup> Taken together, these observations suggest the idea that depression could be attributed in part to increased DYN and subsequent elevations in KOP receptor activation in the NAc.<sup>128</sup> Therefore, a KOP antagonist, whose action would decrease KOP receptor activation, could be a useful target for the treatment of depression.

The KOP receptor antagonists nor-binaltorphimine (norBNI, **60**), GNTI (**61**), ANTI (**62**), and JDITic have all been investigated for anti-depressant effects in various rodent behavioral models and found to be effective (Figure 13).<sup>130, 133-134</sup> However, study of the effects of selective KOP antagonists in rodents, non-human primates, and humans is hindered by the abnormally long half-life of these agents: a single injection can block the effects of a KOP agonist for as long as 56 days.<sup>135</sup> The cause of this extremely long duration of action is not fully understood,

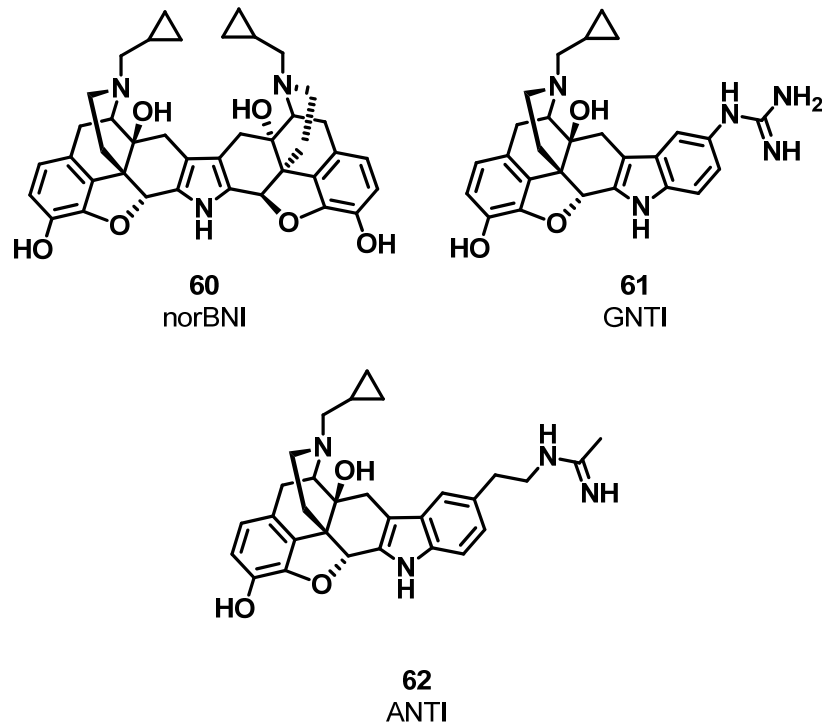


**Figure 13.** Examples of KOP receptor antagonists.

although it does not seem to be an inevitable consequence of KOP receptor inactivation; non-selective opioid antagonists do not produce this complication.<sup>136</sup> Work from the Chavkin group indicates that the long duration of selective KOP antagonists is not caused by antagonist deposition in lipid membranes, or by antagonist-mediated changes in the KOP receptor population, or by the antagonist covalently binding to the receptor. The Chavkin group did find that the long duration of selective antagonist action is positively correlated to activation of c-Jun N-terminal kinase (JNK), although how JNK activation leads to long-term KOP receptor inactivation remains unclear.<sup>136-137</sup> Thus, the search for selective KOP antagonists with improved pharmacokinetic and pharmacodynamic properties continues.

Despite their documented dysphoric effect, selective KOP agonists have been suggested as anti-manic agents based on studies that found that clinically used anti-manic agents increase



the activity of dynorphinergic neurons, implying that these drugs may increase DYN and therefore KOP receptor activation, eliciting a mood lowering effect.<sup>128, 138</sup> This idea is bolstered by the fact that known selective KOP agonists such as U69,593 and U50,488 produce pro-depressive-like behaviors in rodent models, identical to behavior caused by CREB elevation in the NAc.<sup>130, 133</sup> While many selective KOP agonists reported in the literature are full agonists, partial agonists may have a decreased propensity to cause dysphoria while retaining mood lowering capabilities, and this type of effect might be useful in the treatment of mania or bi-polar disorder.<sup>128</sup>

Finally, KOP-selective ligands have also been implicated as pharmacotherapies for drug addiction.<sup>139-142</sup> Addiction is a chronic, relapsing disease characterized by compulsive drug-seeking and drug-taking behavior that persists despite severe adverse consequences.<sup>143</sup> Addicts typically demonstrate diminished motivation for the natural rewards that drive behavior (e.g. food, sex), and the abrupt cessation of drug use produces withdrawal symptoms.<sup>144-146</sup> While there are currently FDA-approved treatments for opioid (methadone), nicotine (varenicline), and alcohol (naltrexone) abuse, at present there are no FDA-approved therapies for the abuse of stimulants such as cocaine and methamphetamine.<sup>139</sup>

A wealth of research has established that the DYN/KOP receptor system has an inhibitory influence on brain reward function by suppressing dopamine (DA) release from the mesolimbic and nigrostriatal pathways.<sup>147-151</sup> These brain regions are intimately associated with the development of drug dependence.<sup>142</sup> Additionally, several studies in both rodents and non-human primates have demonstrated that selective KOP agonists functionally attenuate many behavioral effects of cocaine including locomotor activity,<sup>152</sup> sensitization and place

preference,<sup>152-154</sup> and self-administration.<sup>155-158</sup> Place preference studies in animals provide a measurement of the conditioned, reinforcing effects of drugs on behavior; in rodents, conditioned place aversions are observed upon systemic administration of KOP receptor agonists.<sup>140, 159</sup> KOP selective agonists also attenuate the reinstatement of extinguished drug-taking behavior in animal models of relapse.<sup>158, 160</sup> This collection of inhibitory effects on cocaine-induced, abuse-related behavior is possibly accomplished through direct inhibition of DA release from dopaminergic neurons,<sup>150-151, 161</sup> modulation of DA uptake in the NAc,<sup>162</sup> and alterations in the synaptic concentration of the dopamine transporter (DAT).<sup>163-164</sup> Frustratingly, while consistent data are produced that find that KOP stimulation antagonizes the rewarding and reinforcing effects of drugs of abuse, KOP antagonists show no consistent results.<sup>141</sup> Still, these observations implicate selective KOP agonists as candidates for pharmacotherapies for drug abuse in that such therapies could diminish the rewarding effects associated with stimulant use and thus the resultant negative behavioral changes.

Despite these seemingly positive effects, KOP agonists are still known still precipitate pro-depression-like behaviors (dysphoria) in rodents, which is not an ideal side-effect for a potential pharmacotherapy for drug addiction.<sup>133</sup> Paradoxically, KOP agonists can themselves also potentiate the rewarding effects of cocaine under stress conditions and stress-induced reinstatement.<sup>149, 165-166</sup> Previously mentioned behavioral studies were performed with animals otherwise naive to KOP ligands (drug administered  $\leq 15$  min before challenge), but animals with a history of exposure to KOP agonists (continuous exposure or drug administered 60 min before challenge) demonstrated this phenomenon.<sup>141, 166</sup> In these animals, KOP receptor antagonists were found to be effective in decreasing the increased intake of cocaine.<sup>167</sup> This observation is likely due to persistent KOP receptor activation producing a stress-like effect in the animal.<sup>141</sup>

Consequently, in a state of addiction/drug-dependence, KOP receptor antagonists, which would suppress the KOP receptor system, may be a potential target for diminishing compulsive drug use and relapse.

Finally, while several selective full KOP receptor agonists have been evaluated for their usefulness in treating addiction in animal models, no such data have been reported for selective partial KOP receptor agonists. This type of compound has the potential to block the rewarding effects of CNS stimulants such as cocaine as a full KOP agonist does, but without the dysphoric effect and such persistent KOP receptor activation that it produces a stress-like effect and then subsequently promotes relapse.<sup>139</sup>

### **Interactions between the Opioid and Cannabinoid Receptor Systems**

An alternative way in which selective KOP ligands could be of use both as clinical agents and as biological probes is in conjunction with the cannabinoid receptor system. The cannabinoid receptor system is another type of GPCR system, and compounds from the cannabis plant, *Cannabis sativa* L. (Cannabaceae), have been ingested for centuries for medicinal, spiritual, and recreational purposes. SAR development of known cannabinoid ligands and research into their biological targets eventually resulted in the isolation and cloning of the cannabinoid receptors, CB1 in 1988 and CB2 in 1993.<sup>168-170</sup>

Cannabinoids and opioids share many pharmacological properties including antinociception and sedation.<sup>171</sup> In fact, there is a known synergistic antinociceptive effect upon activation of both cannabinoid and opioid receptor systems.<sup>172-175</sup> A plausible hypothesis for this observation is that drugs that activate these receptors reciprocally influence the synthesis and/or release of the endogenous ligands.<sup>171</sup> In the spinal cord, cannabinoid induced antinociception

can be reversed by KOP antagonists.<sup>176-177</sup> Also, an increase in extra-cellular levels of endogenous DYN can be measured after acute administration of cannabinoid agonists.<sup>176-178</sup> These findings suggest that the DYN/KOP receptor system is involved in the mechanism of cannabinoid induced antinociception.

The benefits of simultaneous opioid and cannabinoid receptor activation have not been fully exploited or investigated for use in the clinic. Since the KOP receptor system has been implicated in a variety of conditions as described previously, study of the interactions between the cannabinoid and opioid receptor systems would provide a clearer view of the underlying neurobiology and possibly offer new therapeutic targets. In order to conduct these studies, existing KOP and cannabinoid ligands need to be characterized at the reciprocal receptors, and new ligands need to be developed.

### **Alternative Chemical Scaffolds for Opioid Ligands**

In summary, since the 19<sup>th</sup> century the morphine scaffold has been intensively explored as a source of molecules with opioid receptor activity. However, the utility of ligands related to the morphine scaffold is limited due to the associated negative side effects that seem to follow through, despite extensive scaffold simplification and derivatization. The identification of novel, diverse, non-morphine-like chemical scaffolds with opioid receptor activity is important because scaffolds different from known opioids have the potential to have different side effect profiles and different and useful pharmacological profiles. Recent research has shown that flavonoids possess some opioid activity, making them a novel class of non-nitrogenous opioid receptor ligands.<sup>179</sup> Another non-nitrogenous structural class that bears investigation is the neoclerodane

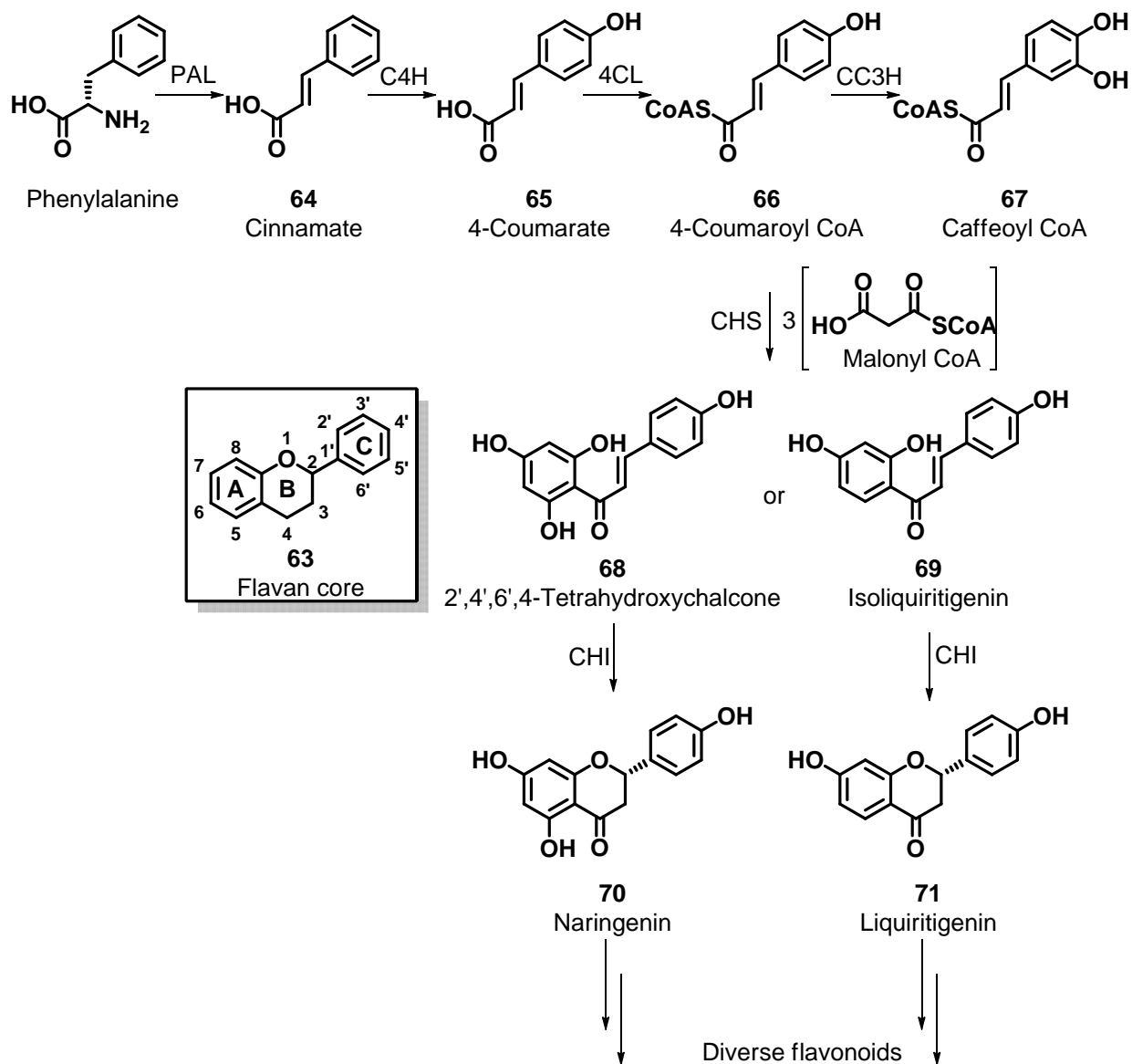
diterpenes, a subclass of the terpene class of natural products. The neoclerodane diterpene salvinorin A has been identified as a selective KOP receptor agonist.<sup>180</sup>

## CHAPTER 2: INVESTIGATION OF FLAVONOIDS AS OPIOID LIGANDS

### Introduction to Flavonoids

The flavonoids are part of a family of polyphenolic natural products that are produced in high quantities by a variety of plants.<sup>181-183</sup> They are recognized for their anti-cancer, anti-oxidant, anti-inflammatory, and free-radical scavenging activities. The flavonoid class is known to chelate bivalent metals and prevent redox cycling, inhibit enzymes involved in prostaglandin biosynthesis (e.g. lipoxygenase, phospholipase, and cyclooxygenase), inhibit a variety of kinases, inhibit topoisomerase I and II, and bind to the estrogen receptor.<sup>182</sup> The major source of flavonoids is fruits and fruit products, vegetables, tea leaves, soybeans, and herbs.<sup>182</sup> Because they are produced by so many plants, flavonoids are widely distributed in foods and other consumable plant products, and are thus more likely than other scaffolds to have acceptable side effect and toxicity profiles.<sup>184</sup> This makes them an attractive investigational target for molecules with biological activity.

The basic structure of a flavonoid is the flavan core (**63**) which consists of 15 carbon atoms arranged in three rings, called A, B, and C.<sup>185</sup> The biosynthesis of flavonoids begins with the condensation of one molecule of 4-coumaroyl CoA (**66**) with three molecules of malonyl CoA to yield a chalcone, a precursor for all flavonoids (Scheme 1).<sup>182</sup> To produce 4-coumaroyl CoA, phenylalanine is deaminated by phenylalanine ammonia-lyase (PAL), and the *trans*-cinnamate (**64**) product is then hydroxylated to 4-coumarate (**65**) by cinnamate 4-hydroxylase (C4H), a cytochrome P450 (CYP450) enzyme.<sup>186</sup> Activation of 4-coumarate to the CoA thioester is catalyzed by 4-coumarate:CoA ligase (4CL), giving the necessary precursor 4-coumaroyl CoA. This precursor can be further hydroxylated at the 3 position by 4-coumaroyl



**Scheme 1.** Biosynthetic pathway of flavonoids.

CoA 3-hydroxylase (CC3H) to give caffeoyl CoA (**67**), an alternative flavonoid precursor in some plant species. Malonyl CoA is derived from the condensation of acetyl CoA and CO<sub>2</sub>, facilitated by acetyl CoA carboxylase. Next, the step-wise condensation of 4-coumaroyl CoA and three molecules of malonyl CoA is catalyzed by the enzyme chalcone synthase (CHS) to produce 2',4',6',4'-tetrahydroxychalcone (**68**). An alternative chalcone precursor in some plant

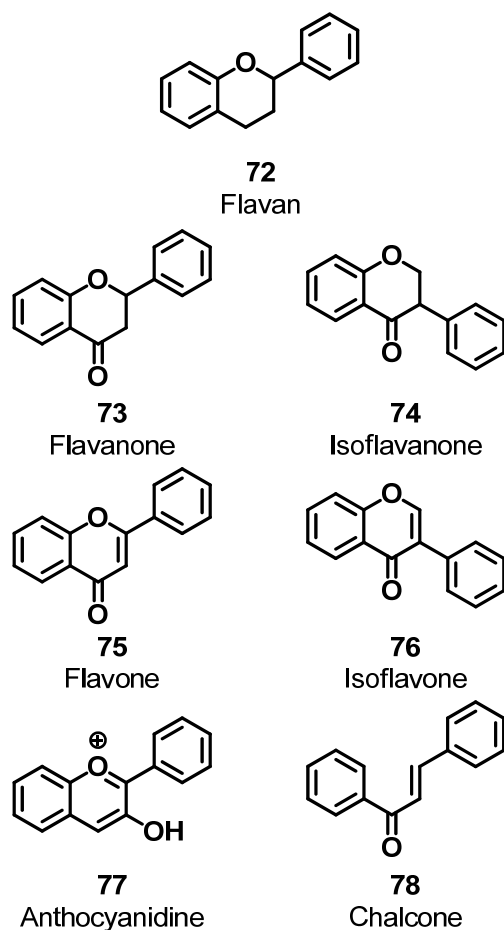


**Figure 14.** Structural classification of flavonoids.

species is isoliquiritigenin (**69**), also synthesized from 4-coumaroyl CoA and malonyl CoA, but in conjunction with a NADPH-dependent reductase. The stereospecific cyclization of the chalcone precursor, catalyzed by chalcone isomerase (CHI), yields a 2*S*-flavonone (e.g. naringenin (**70**), liquiritigenin (**71**)), which has the typical flavonoid skeletal core. These relatively simple scaffolds can then be extensively modified by many different types of enzymes, producing an overwhelming diversity of unique structures with a wide array of biological activities.



Based on structural details of their carbon skeletons, flavonoids are classified into eight groups (Figure 14): flavans (**72**), flavanones (**73**), isoflavanones (**74**), flavones (**75**), isoflavones (**76**), anthocyanidines (**77**), chalcones (**78**), and flavonolignans (part flavonoid, part lignan).<sup>182</sup> Since the chemical structures and sometimes also the biological activities of several flavonoids are similar to those of naturally occurring estrogens, flavonoids are frequently assigned as phytoestrogens.<sup>187</sup> More than 8,000 compounds that conform to the flavonoid structural definition have been discovered.<sup>185</sup> Because of their ubiquity, wide range of biological activity, and relative ease of synthesis, flavonoids as a structural class continue to be an investigational target for new disease pharmacotherapies.

### **The Identification of Flavonoids as Potential Opioid Receptor Ligands**

Flavonoids from *Hypericum perforatum* L. (Hypericaceae), commonly called St. John's Wort, have been recently investigated for their biological activities. Published work indicates that *H. perforatum* may have antiaddictive potential.<sup>179</sup> In rat models of alcohol dependence, extracts of *H. perforatum* have been observed to attenuate alcohol self-administration.<sup>188-189</sup> They have also been shown to work synergistically with opioid antagonists in the attenuation of rodent alcohol intake.<sup>190</sup> As opioid antagonists such as naltrexone are used clinically to treat alcohol abuse, these findings indicate that the attenuation of alcohol self-administration in rats caused by *H. perforatum* extracts may be opioid receptor mediated.<sup>179</sup> Extracts of *H. perforatum* have also been evaluated for anti-inflammatory and antinociceptive potential in different rodent models and found to be effective.<sup>191-194</sup> Such effects are mediated in part by opioid receptors.<sup>195-196</sup> Furthermore, *in vitro* receptor screens have shown that *H. perforatum* extracts inhibited the binding of [<sup>3</sup>H]naloxone and [<sup>3</sup>H]deltorphin to opioid receptors.<sup>197-198</sup> Finally, amentoflavone

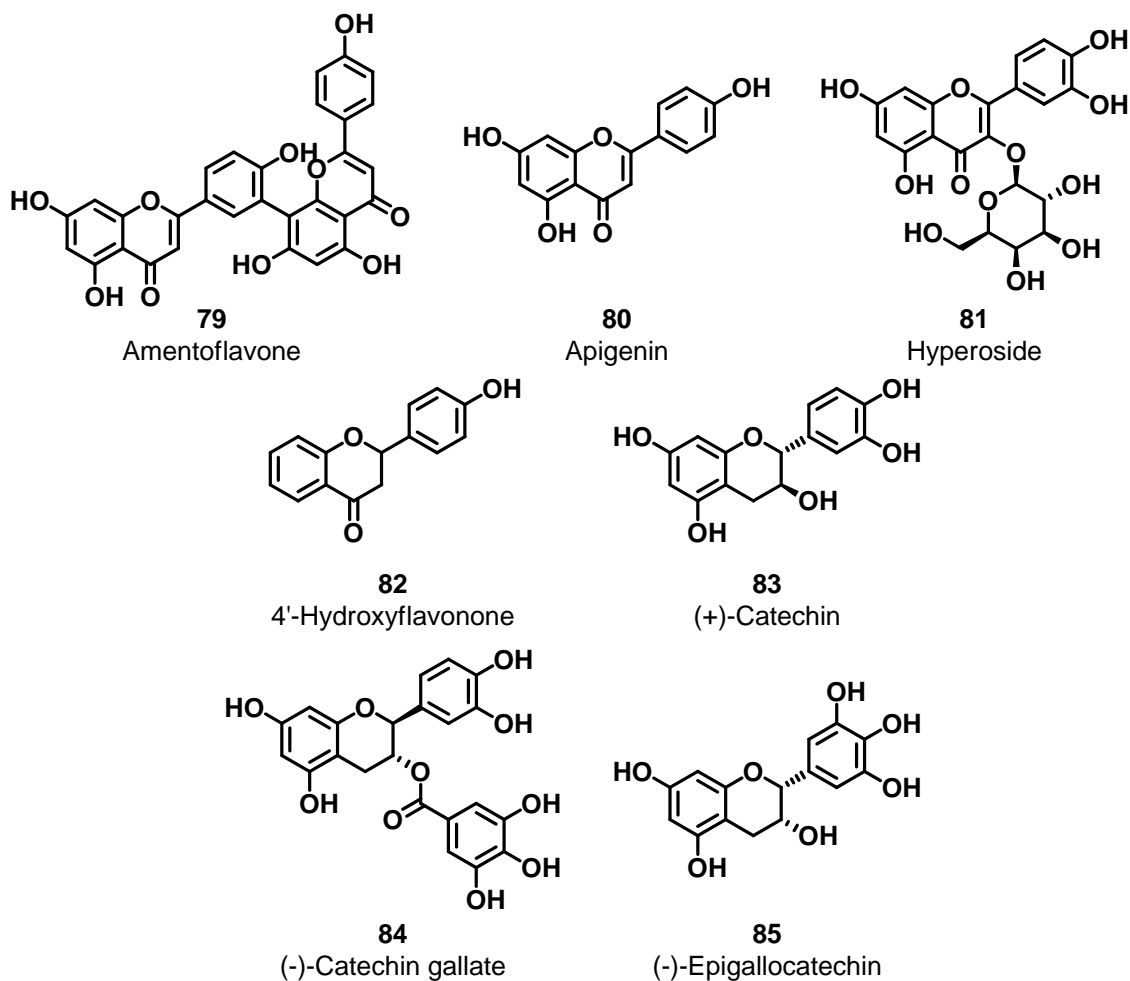


**Figure 15.** Selected flavonoids evaluated in  $[^{35}\text{S}]\text{GTP-}\gamma\text{-S}$  functional assay.

(79), a biflavone found in *H. perforatum* extracts is known to compete for binding to opioid receptors and in fact has relatively high affinity for the DOP receptor ( $K_i = 36 \text{ nM}$ )<sup>199</sup> and is an antagonist at both DOP (weak,  $K_e = 6000 \text{ nM}$ ) and KOP receptors ( $K_e = 490 \pm 150 \text{ nM}$ ).<sup>179</sup> These findings further support the hypothesis that the actions of *H. perforatum* extracts are opioid receptor mediated. Amentoflavone is the first reported flavonoid with KOP receptor antagonist activity, opening the possibility of a new structural scaffold for the development of opioid antagonists, and opioid ligands in general.

Following the success with amentoflavone, efforts began to investigate structural modification of its flavonoid core.<sup>179</sup> A small library of flavonoid natural products (Figure 15) was submitted to screening in the [<sup>35</sup>S]GTP- $\gamma$ -S functional assay, including apigenin (**80**), hyperoside (**81**), 4'-hydroxyflavonone (**82**), (+)-catechin (**83**), (-)-catechin gallate (**84**), and (-)-epigallocatechin (**85**). All of these flavonoids had potency at KOP receptors in the range of  $K_e = 220\text{--}550$  nM, with potencies at the MOP receptor ranging from  $K_e = 210\text{--}10,000$  nM; their DOP receptor potencies were negligible.<sup>179</sup> These findings indicate that flavonoids are a potential source of molecules with both opioid receptor activity and low structural similarity to known opioid ligands. Furthermore, given the range of potencies between the different opioid receptor subtypes, these findings also suggest that flavonoid ligands may be designed and manipulated for optimal receptor selectivity.

### ***Dioclea Grandiflora* Background**

*Dioclea grandiflora* Mart. ex Benth. (Leguminosae) is a vine that is native to northeastern Brazil.<sup>200</sup> Commonly called “Mucunã”, the plant is well known locally for its medicinal value, and an infusion of the roots is used in traditional medicine to treat kidney stones and prostate gland disorders.<sup>200-201</sup> Prior to 1995, *D. grandiflora* had never been screened pharmacologically. Subsequently, observations of the antinociceptive actions of extracts of this plant were undertaken by collaborating groups at Universidade Federal da Paraíba, Brazil and University of Georgia, Athens, GA. The flavonoid natural products dioclein (**86**)<sup>202</sup> and dioflorin (**87**),<sup>203</sup> obtained from the chloroform fraction of the ethanolic extract of *D. grandiflora* root bark, are two minor constituents that have been isolated and characterized from this plant and found to have antinociceptive properties (Figure 16).

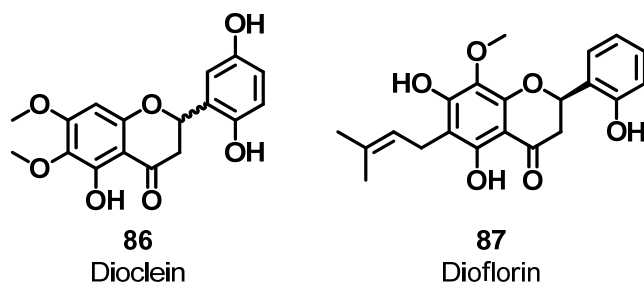


**Figure 16.** Structures of dioclein and dioflorin, isolated from *D. grandiflora*.

### **Antinociceptive Effects of *Dioclea Grandiflora* Extracts**

The crude, 90% ethanolic extract of *D. grandiflora* root bark was found to dose dependently reduce the number of writhes in the acetic acid induced writhing test in mice; this effect was naloxone reversible.<sup>200</sup> The same extract was also found to significantly increase reaction time in the tail-flick assay in rats.<sup>200</sup> The crude, 70% ethanolic extract of *D. grandiflora* seeds significantly increased reaction time in the tail-flick test in rats, as well as in the hot-plate test in mice; the increased reaction times in the hot-plate were reversed by pre-treatment with naloxone.<sup>204</sup> In the same study, a daily dose of 500 mg/kg of seed extract not only failed to produce any signs of toxicity, but also maintained an antinociceptive effect through 30 days, whereas morphine (6 mg/kg daily) lost effectiveness after 21 days. In a recent study, the crude, 70% ethanolic extract of *D. grandiflora* seed pods was found to significantly decrease the number of writhes in the acetic acid induced writhing test in mice.<sup>205</sup> However, the seed pod extract had only a numerical, but not statistically significant effect in the hot plate test. In the formalin test, treatment with the seed pod extract significantly reduced formalin-induced licking in both the neurogenic (first phase) and inflammatory (second phase) phases; interestingly, this attenuation was actually enhanced in both phases by naloxone pretreatment.<sup>205</sup> These collective findings suggest that the antinociceptive effects of *D. grandiflora* extracts may in part be opioid receptor mediated.

## **Preliminary Pharmacological Studies of *Dioclea Grandiflora* Flavonoids**

The antinociceptive effects of dioclein were assessed by the acetic acid induced writhing test in male Swiss mice and by the tail-flick assay in male Wistar rats.<sup>200</sup> In the acetic acid induced writhing test, 50 and 100 mg/kg dioclein significantly, although not dose dependently, reduced the number of writhes. This effect was reversed by pretreatment with naloxone. In the tail-flick test, a single dose (50 mg/kg) of dioclein produced a significant increase in reaction time and had a longer duration of action than morphine (6 mg/kg), maintaining significant antinociceptive activity through 2 h post administration. These results indicate that dioclein may act centrally, involving an opioid-like mechanism.

The antinociceptive effects of dioflorin were assessed by the acetic acid induced writhing test and by the tail-immersion test, both in male Swiss mice.<sup>201</sup> A single dose of 10 mg/kg of dioflorin was found to produce near maximal reduction of the writhing response, very similar to morphine (6 mg/kg). In the tail immersion test, the same single dose of dioflorin significantly increased reaction times. The effects of naxolone pretreatment were not reported for this particular study. However, these results still demonstrate that dioflorin exhibits a central antinociceptive effect in mice.

### **Rationale and Specific Aims**

Dioclein and dioflorin are flavonoid natural products that demonstrate antinociceptive properties in rodent models of pain that are reversible by pretreatment with an opioid antagonist. Although these observations indicate that the mechanism of action of these flavonoids proceeds through opioid receptors, this information has not been investigated *in vitro* and no SAR studies of these molecules have been published. This is significant because the flavonoid structural class

represents a novel chemical scaffold for the discovery of new opioid receptor ligands. Furthermore, the opioid receptors themselves have been linked to a variety of conditions including pain, mood disorders, and drug abuse. Exploration of the SAR of dioclein and dioflorin has the potential to yield novel opioid ligands with altered pharmacological profiles that may be of use both in the clinic and as probes for biological evaluation.

**Specific Aim 1: Prepare dioclein and simplified dioflorin analogs for biological evaluation through total synthesis.**

Dioclein and dioflorin are not commercially available, nor are there any published reports of large-scale, high-yielding extractions of these constituents from *D. grandiflora* plant material. Furthermore, even with the advent of the Convention on Biological Diversity,<sup>206</sup> since *D. grandiflora* is not native to the United States it is likely to be difficult and very expensive to obtain the significant quantities of plant material that would be required to investigate and accomplish a successful extraction procedure. Since flavonoids as a structural class are relatively simple molecules, the most reliable and economical way to produce analogs for biological evaluation is through total synthesis.

There is a previously published total synthesis of dioclein that obtains the desired product in three steps from commercially available material and 43% over all yield.<sup>207</sup> Simplified analogs of dioflorin may be made racemically from commercially available starting materials using well known synthetic organic methods.<sup>208-212</sup> The initial hypothesis in the design of these simplified analogs of dioflorin is that the 8-methoxy group of the A-ring is not required for opioid activity of the flavonoid scaffold as dioclein itself lacks a methoxy in the analogous position (Figure 17). Removal of this moiety from the structural scaffold of dioflorin is also

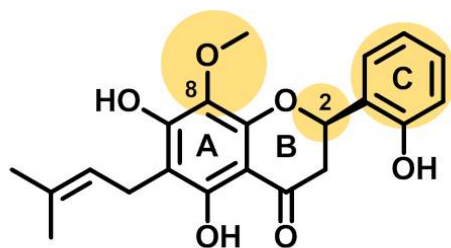


**Figure 17.** Design rationale for simplified dioflorin analogs.

desirable as the 8-methoxy group is difficult to install relative to the other synthetic steps required to build the flavonoid core. To this end, a series of dioflorin analogs were synthesized in which the 8-methoxy group has been removed from the A-ring. Additionally, the tolerance of the C-ring to changes in the position of the hydroxyl group will be investigated. Finally, these analogs will first be synthesized and evaluated in a racemic fashion as the absolute configuration of dioclein is not reported,<sup>202</sup> making comparison to dioflorin for initial determinations of the stereochemical preferences of the target receptors difficult. These modifications are intended to develop preliminary SAR for these flavonoids at opioid receptors and demonstrate that these scaffolds may be manipulated and retain or improve opioid receptor affinity and efficacy.

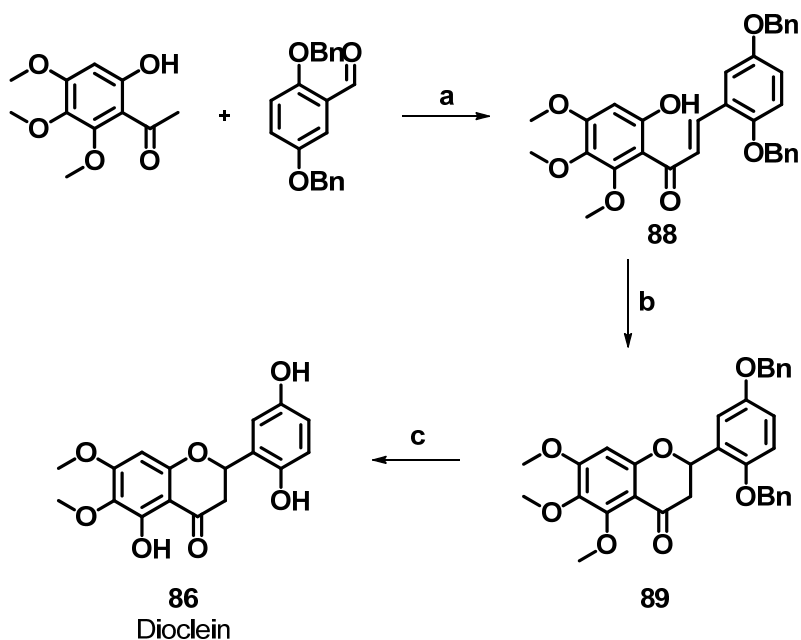
**Specific Aim 2: Evaluate dioclein and simplified dioflorin analog opioid receptor affinity through radioligand binding assays, and opioid and cannabinoid receptor efficacy through calcium mobilization fluorescent and  $\beta$ -arrestin luminescent assays.**

Using known methodology, compounds generated from Specific Aim 1 will be evaluated *in vitro* for affinity at MOP and KOP receptors through displacement of the radioligands [<sup>3</sup>H]DAMGO (MOP) and [<sup>3</sup>H]U69,593 (KOP).<sup>213</sup> In order to determine the efficacy of these compounds at all three subtypes of opioid receptors, they will also be evaluated in a fluorescent calcium mobilization assay using a known protocol.<sup>214</sup> This assay uses chimeric G-proteins

coupled to opioid receptors in order to measure changes in intracellular calcium concentration using a fluorescent, calcium-sensitive dye.<sup>215</sup> The calcium assay format as an efficacy evaluation has an advantage over the [<sup>35</sup>S]GTP- $\gamma$ -S assay format as it requires less time and special training because it excludes the use of radiolabeled ligands. Further, the compounds generated from Specific Aim 1 will also be evaluated for efficacy at CB1 cannabinoid receptors using the same calcium mobilization assay format. As previously described, cannabinoid ligands are able to produce an antinociceptive effect that is reversed by opioid antagonists and can upregulate endogenous opioids. Thus, the purpose of this assay is to determine if these compounds are exerting their opioid-like antinociceptive effect through cannabinoid receptors.

Finally, the compounds will also be evaluated for both opioid receptor and GPR-55 (a GPCR and novel, putative cannabinoid receptor<sup>216-217</sup>) efficacy in the PathHunter™  $\beta$ -arrestin luminescence assay format. As previously mentioned, some GPCR signaling can be accomplished through the G-protein independent GRK/ $\beta$ -arrestin pathway. If the ligands being tested do not operate through a G-protein mediated pathway, they will not be detected in either the [<sup>35</sup>S]GTP- $\gamma$ -S assay or the calcium mobilization assay. Thus, the PathHunter™  $\beta$ -arrestin assay format will investigate if the antinociceptive effects previously seen in animal models are operating through the GRK/ $\beta$ -arrestin signaling pathway. These proposed assays are intended to thoroughly investigate mechanism of action behind the observed antinociceptive effects of dioclein and dioflorin. Identification of a specific mechanism of action will be a boon to further SAR development, and speed the eventual discovery of a new ligand for the clinic or biological probe.





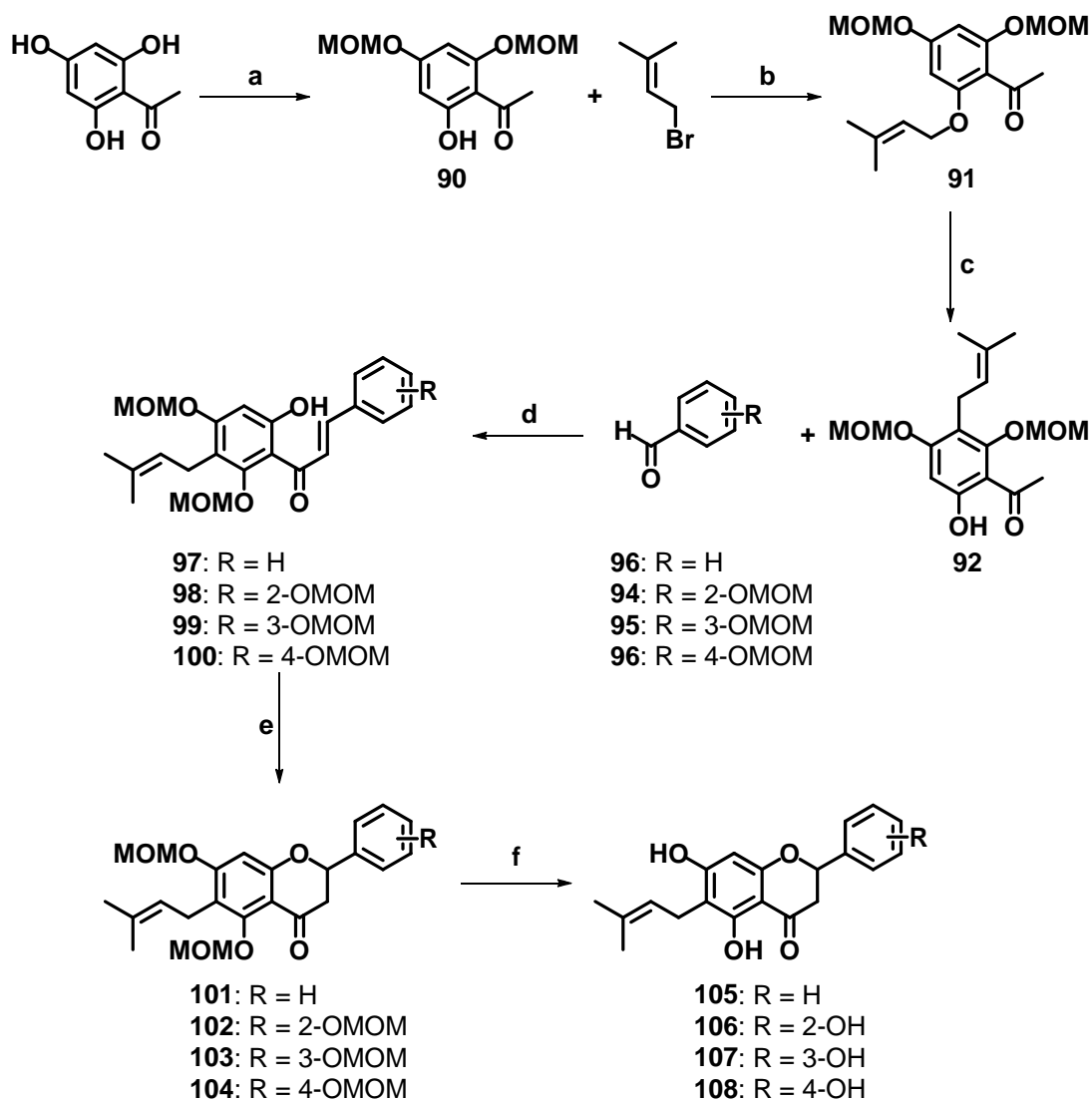
**Scheme 2.** Synthesis of dioclein. *Reagents and conditions:* a) 50% aq. KOH; b) KF/MeOH, reflux; c) BCl<sub>3</sub>/CH<sub>2</sub>Cl<sub>2</sub>, -60 °C.

These specific aims are intended to investigate the hypothesis that dioclein and dioflorin can be simplified and/or altered and that these derivatives will serve as novel opioid receptor ligands. The ability to synthesize novel opioid analogues inspired by these molecules would further demonstrate the utility of flavonoids as lead molecules as well as provide evidence that they can be employed as structural scaffolds for the construction of biologically relevant compounds that interact at opioid receptors. The results of these studies will be presented and discussed.

## Results and Discussion

### *Synthesis*

In an effort to generate SAR and elucidate the pharmacophore of flavonoids at opioid receptors, dioclein and several simplified analogs of dioflorin were synthesized. The racemic synthesis of dioclein from commercially available materials was accomplished following the published procedure of Spearing et al. (Scheme 2).<sup>207</sup> First, 2-hydroxy-4,5,6-



**Scheme 3.** Synthesis of dioflorin analogs. *Reagents and conditions:* a) DIPEA, MOM-Cl, CH<sub>2</sub>Cl<sub>2</sub>; b) K<sub>2</sub>CO<sub>3</sub>, acetone, reflux; c) *N,N*-DMA, reflux; d) NaOH, H<sub>2</sub>O/EtOH; e) NaOAc, EtOH, reflux; f) HCl, MeOH, reflux.

trimethoxyacetophenone was condensed with 2,5-bis(benzyloxy)benzaldehyde in the presence of 50% aqueous KOH to give chalcone **88**. Treatment of chalcone **88** with KF in methanol at reflux afforded flavonone **89**, which was globally deprotected with BCl<sub>3</sub> to reveal the desired product, dioclein (**86**).

The racemic synthesis of simplified dioflorin analogs (Scheme 3) began with the partial protection of commercially available 2',4',6'-trihydroxyacetophenone monohydrate as the

methoxymethyl (MOM) ether **90** in 66% yield using *N,N*-diisopropylethylamine (DIPEA) and chloromethyl methyl ether (MOM-Cl).<sup>208</sup> A prenyl group was installed by refluxing **90** and 3,3-dimethylallyl bromide in acetone/K<sub>2</sub>CO<sub>3</sub> to afford **91** in 92% yield.<sup>210</sup> A thermal Claisen rearrangement of **91** in *N,N*-dimethylaniline (*N,N*-DMA) produced the desired prenylated acetophenone **92** in 46% yield.<sup>208, 210</sup> Chalcones **97–100** were generated in 52–83% yield via coupling to the appropriately protected benzaldehydes (**93–96**, prepared in 92–95% yield from commercially available hydroxybenzaldehydes<sup>208-209</sup>) in the presence of NaOH in a mixture of water and ethanol.<sup>211</sup> Chalcones **97–100** were then cyclized to afford flavonones **101–104** in 73–78% yield using NaOAc in refluxing ethanol.<sup>212</sup> Finally, flavonones **101–104** were subjected to acidic conditions in a global deprotection of the MOM-ether groups to afford flavonoids **105–108** in 24–47% yield.<sup>212</sup>

#### *Radioligand Binding Results*

Compounds **86**, **102**, and **105–108** were evaluated for affinity at human opioid receptors using methodology previously described (Table 3).<sup>213</sup> The results of this assay revealed that these flavonoid compounds have very little affinity for opioid receptors. This was unexpected given that preliminary work in rodent models showed that the antinociceptive effect of dioclein (**86**) could be attenuated with the antagonist naloxone, suggesting a mechanism of action directly involving opioid receptors.<sup>200</sup> However, our finding is consistent with a recent report in which it was found that naloxone was unable to reverse to antinociceptive effects of *D. grandiflora* seed pod extract in the formalin test in mice.<sup>205</sup>

The flat SAR suggests that the initial hypothesis in the design of compounds **102** and **105–108** may have been incorrect, and that the 8-methoxy group present in the parent compound dioflorin may be required for affinity at opioid receptors. Also, these flavonoid compounds were

**Table 3.** Opioid receptor binding affinity for compounds dioclein (**86**), **102**, and **105–108**.

Compound	K <sub>i</sub> nM <sup>a</sup>	
	[ <sup>3</sup> H]DAMGO (MOP)	[ <sup>3</sup> H]U69,593 (KOP)
<b>86</b>	>2,500	>8,700
<b>102</b>	>2,500	>8,700
<b>105</b>	>2,500	>8,700
<b>106</b>	>2,500	>3,200
<b>107</b>	>2,500	>8,700
<b>108</b>	>2,500	>8,700

<sup>a</sup>Receptor binding was performed in CHO cells expressing the human MOP or KOP receptors.

synthesized in a racemic fashion, while dioflorin is a chiral molecule. The racemic nature of the compounds evaluated may contribute to their apparent lack of opioid receptor affinity. Finally, it is possible that the reported flavonoids dioclein and dioflorin are exerting their effects through a mechanism that only indirectly involves opioid receptors; this would account for both the apparent lack of opioid receptor affinity of dioclein, as well as the previously observed naloxone-reversible, antinociceptive effects. This means that the mechanism of action of the antinociceptive effects of the flavonoid scaffold requires further study.

#### *Calcium Mobilization Results*

One drawback of the radioligand binding assay format is that it assumes that the compounds being scrutinized bind in such a way that would compete with or displace the radioligand. However, since flavonoids are structurally distinct from other known opioid ligands, it may be the case that they bind to opioid receptors in an entirely different manner that does not lead to the displacement of the radioligand being used in the assay. In order to determine this, flavonoids **86** and **105–108** were screened at all three opioid receptor subtypes in the calcium mobilization assay format.<sup>214</sup> This assay format is not binding-and-displacement,

**Table 4.** Opioid receptor potency for compounds dioclein (**86**) and **105–108** in the calcium mobilization assay format.

Compound	EC <sub>50</sub> ± SEM nM <sup>a</sup>		
	MOP	KOP	DOP
<b>DAMGO</b>	22.6 ± 1.8		
<b>U69,593</b>		6.4 ± 1.4	
<b>DPDPE</b>			5.2 ± 3.8
<b>86</b>	>10,000	>10,000	>10,000
<b>105</b>	>10,000	>10,000	>10,000
<b>106</b>	>10,000	>10,000	>10,000
<b>107</b>	>10,000	>10,000	>10,000
<b>108</b>	>10,000	>10,000	>10,000

<sup>a</sup>Receptor binding was performed in CHO cells expressing the human MOP, KOP, or DOP receptors.

but functional. Thus, no matter how the ligands being investigated bind to the receptor, as long as they lead to activation of the traditional GPCR signal cascade, they will be detected. Human G<sub>αq16</sub> is a relatively promiscuous G-protein with regards to the number of GPCR interactions it is known to have. Opioid receptors are intrinsically G<sub>αi</sub>-coupled, so for these assays each receptor is cotransfected with G<sub>αq16</sub> in order to stimulate the G<sub>αq</sub> pathway.<sup>215</sup> When an agonist binds to the chimeric G<sub>αq16</sub>-opioid receptor and activates the G<sub>αq</sub> GPCR signal cascade, intracellular calcium is mobilized and changes in calcium concentration can be detected with a calcium-sensitive fluorescent dye and a fluorimetric plate reader.

Unfortunately, while the standard agonists behaved as expected, none of the flavonoid ligands generated a dose-response curve to indicate that the EC<sub>50</sub> would be less than 10 μM (Table 4). The same possibilities to explain the lack of affinity of these ligands in the radioligand binding assays apply to these opioid receptor calcium mobilization assays as well.

In an attempt to determine if flavonoids **86** and **105–108** were interacting indirectly with opioid receptors via the stimulation of cannabinoid receptors, these compounds were screened at

CB1 cannabinoid receptors in the calcium mobilization assay format. And again, unfortunately, while the standard agonist behaved as expected, none of the flavonoid ligands generated a dose-response curve to indicate that the EC<sub>50</sub> would be less than 10 μM (Table 5).

**Table 5.** CB1 receptor potency for compounds dioclein (**86**) and **105–108** in the calcium mobilization assay format.

Compound	CB1 EC <sub>50</sub> nM <sup>a</sup> ± SEM
<b>CP55,940</b>	26.3 ± 14
<b>86</b>	>10,000
<b>105</b>	>10,000
<b>106</b>	>10,000
<b>107</b>	>10,000
<b>108</b>	>10,000

<sup>a</sup>Receptor binding was performed in CHO cells expressing the human CB1 receptor.

#### *β-Arrestin Luminescence Results*

Finally, in an attempt to determine if flavonoids **86** and **105–108** were interacting with opioid receptors in a G-protein independent manner, these compounds were screened at both KOP receptors and GPR-55 receptors in the PathHunter™ β-arrestin luminescence assay format. This assay platform uses an enzyme fragment complementation technique in which complementing fragments of the β-galactosidase enzyme are expressed in different compartments of a stably transfected cell; one enzyme fragment is localized within the cell and the other fragment is fused to an extra-cellular portion of the GPCR of interest.<sup>218</sup> When an agonist binds to the GPCR and activates signaling, β-arrestin is recruited and the fused receptor is internalized. Upon receptor internalization, the two fragments of the enzyme meet, forming a functional β-galactosidase enzyme that hydrolyzes a proprietary substrate and generates a chemiluminescent signal that can be detected with a microplate reader.

**Table 6.** Receptor potency for compounds dioclein (**86**) and **105–108** in the  $\beta$ -arrestin assay format.

Compound	EC <sub>50</sub> nM <sup>a</sup> $\pm$ SEM	
	KOP	GPR-55
<b>U69,593</b>	152 $\pm$ 79	
<b>LPI</b>		2.1 $\pm$ 1.1 ( $\mu$ M)
<b>86</b>	>10,000	>10,000
<b>105</b>	>10,000	>10,000
<b>106</b>	>10,000	>10,000
<b>107</b>	>10,000	>10,000
<b>108</b>	>10,000	>10,000

<sup>a</sup>Receptor binding was performed in CHO cells expressing the human KOP or GPR-55 receptors.

Unfortunately, not only did the test ligands once again fail to generate a dose-response curve to indicate that the EC<sub>50</sub> would be less than 10  $\mu$ M while the standard agonist ligands behaved as expected (Table 6), but in the GPR-55 assay, the test compounds appeared to be toxic to the cells at concentrations above 100 nM. Additionally, the flavonoid ligands were screened at KOP receptors at 10  $\mu$ M for antagonist ability against 1  $\mu$ M U69,593, and at GPR-55 receptors at 10  $\mu$ M for antagonist ability against 3  $\mu$ M LPI. While 10  $\mu$ M naltrexone completely knocked down U69,593 receptor activation, none of the test ligands appeared to have any effect. Similarly, none of the test ligands were able to knock down LPI receptor activation either. Once again, these results mean that the mechanism of action of the antinociceptive effects of the flavonoid scaffold requires further study.

## Conclusions

Given the collective findings, it is apparent that the mechanism of action that underlies the antinociceptive effects of dioclein and dioflorin is more complex than simple opioid receptor activation. While dioclein itself and five simplified analogs of dioflorin were successfully

generated through organic synthetic methods, none of the tested flavonoids appeared to activate opioid receptors through the traditional G-protein coupled pathway or through the GRK/ $\beta$ -arrestin pathway. Further, none of the tested flavonoids appeared to activate CB1 cannabinoid receptors either, which would indicate an indirect opioid-activation mechanism. The reasons for these failures may be because the initial hypothesis was incorrect, and that the 8-methoxy group present in the parent compound dioflorin may be required for affinity at opioid receptors. Also, these flavonoid compounds were synthesized in a racemic fashion, while dioflorin is a chiral molecule. The racemic nature of the compounds evaluated may contribute to their apparent lack of activity. Additionally, in the rodent studies reported in the literature, the flavonoids being tested were isolated from *D. grandiflora* plant material, not generated synthetically. It is possible that the molecules identified as the constituents responsible for antinociceptive activity were inactive, yet the samples contained a small amount of unidentified impurity that was the active compound. Finally, it is also possible that these compounds exert their effects through a receptor system not examined in this report.

### **Future Directions**

One *in vitro* experiment that may be worth performing is an assay to determine if these flavonoids have any effect on the dopamine transporter (DAT). In the synapse, dopamine is inactivated mainly by reuptake into the neuron by DAT.<sup>219</sup> Because changes in dopamine concentration have been linked to many CNS disorders, a compound that modulates the activity of DAT (and therefore dopamine concentration) is potentially useful as both a drug and an experimental probe. Flavonoids that modulate the DAT have been reported.<sup>219</sup>

Finally, in order to make progress in determining the mechanism, if any, of the antinociceptive effects of the flavonoid scaffold, the previously reported rodent studies need to



be repeated. Confirming that these flavonoids have antinociceptive effects in rodents would make it more worthwhile to keep performing *in vitro* experiments to determine the mechanism of action behind such activity. Furthermore, these rodent studies should ideally be revisited with both plant-extracted and synthetic compound, especially for dioclein, whose antinociceptive effects were found to be naloxone-reversible. This would determine whether or not the reported flavonoids are actually responsible for the observed effects, or if the responsible constituent is an unidentified impurity in the plant extract.

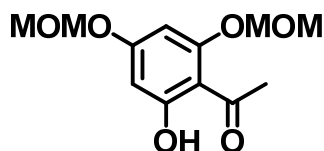
## CHAPTER 3: EXPERIMENTAL PROCEDURES FOR FLAVONOID ANALOGS

### *Chemistry*

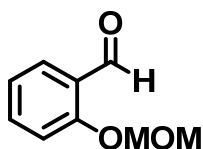
**General Procedures.** Unless otherwise indicated, all reagents were purchased from commercial suppliers and are used without further purification. All melting points were determined on a Thomas–Hoover capillary melting apparatus and are uncorrected. NMR spectra were recorded on a Bruker Avance-300 spectrometer, Bruker DRX-400 with qnp probe or a Bruker AV-500 with cryoprobe using  $\delta$  values in ppm (TMS as internal standard) and  $J$  (Hz) assignments of  $^1\text{H}$  resonance coupling. High resolution mass spectrometry data was collected on a LCT Premier (Waters Corp., Milford, MA) time of flight mass spectrometer or an Agilent 6890 N gas chromatograph in conjunction with a Quatro Micro GC mass spectrometer (Micromass Ltd, Manchester UK). Thin-layer chromatography (TLC) was performed on 0.25 mm plates Analtech GHLF silica gel plates using mixtures of EtOAc/*n*-hexanes as the solvent system. Spots on TLC were visualized when appropriate with 254 nm UV light, phosphomolybdic acid in ethanol, or vanillin in ethanol. Column chromatography was performed with Silica Gel (32–63  $\mu$  particle size) from MP Biomedicals (Solon, OH). Analytical HPLC was carried out on an Agilent 1100 Series Capillary HPLC system with diode array detection at 209 nm, 214 nm, and 235 nm on a Phenomenex Luna C18 column (250  $\times$  10.0 mm, 5  $\mu\text{m}$ ) with isocratic elution in mixtures of  $\text{CH}_3\text{CN}/\text{H}_2\text{O}$  as noted at a flow rate of 5.0 mL/min.

**General Procedure A: MOM Protection.**<sup>208-209</sup> Chloromethyl methyl ether (3.0 equiv.) was added in a dropwise manner to a solution of the appropriate substrate (1.0 equiv.) and *N,N*-diisopropylethylamine (3.0 equiv.) in anhydrous methylene chloride at 0 °C under an argon atmosphere. The reaction mixture was allowed to reach room temperature and stirred for 4 h – 6 h, until complete or no additional progress as observed by TLC. The reaction was quenched by

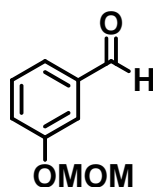
the addition of a solution of saturated aqueous  $\text{NH}_4\text{Cl}$ . This mixture was then extracted three times with 1:1 DCM/ $\text{H}_2\text{O}$ . The organic layers were combined, dried over  $\text{Na}_2\text{SO}_4$ , filtered, and the solvent removed *in vacuo*. The resulting residue was purified by flash column chromatography using EtOAc/*n*-hexanes (1:5) to yield the known MOM protected products.



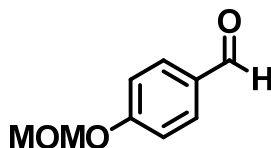
**1-(2-hydroxy-4,6-bis(methoxymethoxy)phenyl)ethanone (90).** Synthesized following general procedure A to afford 4.4393 g (66% yield) as a colorless oil that solidified upon standing overnight at room temperature,  $R_f = 0.45$  (EtOAc/*n*-hexanes 1:5). Spectral data in agreement with reported.<sup>208</sup>



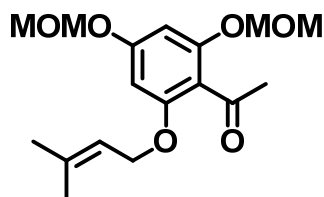
**2-(Methoxymethoxy)benzaldehyde (94).** Synthesized following general procedure A to afford 1.5024 g (92% yield) as a light red-brown oil,  $R_f = 0.47$  (EtOAc/*n*-hexanes 1:5). Spectral data in agreement with reported.<sup>209</sup>



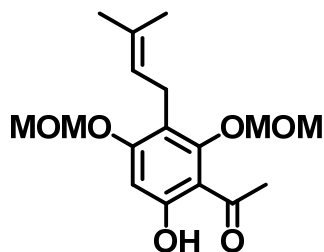
**3-(Methoxymethoxy)benzaldehyde (95).** Synthesized following general procedure A to afford 1.5100 g (91% yield) as a light yellow oil,  $R_f = 0.42$  (EtOAc/*n*-hexanes 1:5). Spectral data in agreement with reported.<sup>209</sup>



**4-(Methoxymethoxy)benzaldehyde (96).** Synthesized following general procedure A to afford 1.5867 g (95% yield) as a light yellow oil,  $R_f = 0.40$  (EtOAc/*n*-hexanes 1:5). Spectral data in agreement with reported.<sup>209</sup>



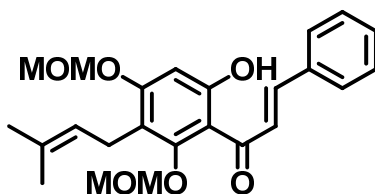
**1-(2,4-bis(methoxymethoxy)-6-((3-methylbut-2-en-1-yl)oxy)phenyl)ethanone (91).** Synthesized following the procedures of Vogel et al.<sup>210</sup> 3,3-dimethylallyl bromide (1.47 mL, 11.7 mmol, 1.5 equiv.),  $K_2CO_3$  (4.31 g, 31.2 mmol, 4 equiv.), and acetophenone **90** (2.00 g, 37.8 mmol) were refluxed in acetone (30 mL) for 24 h. The reaction mixture was allowed to cool to room temperature and the solids were filtered off and the filtrate evaporated. The resulting residue was purified by flash column chromatography using EtOAc/*n*-hexanes (1:5) to afford 2.3504 g (92% yield) of the known prenylated product as a colorless oil,  $R_f = 0.37$  (EtOAc/*n*-hexanes 1:5). Spectral data in agreement with reported.<sup>210</sup>



**1-(6-hydroxy-2,4-bis(methoxymethoxy)-3-(3-methylbut-2-en-1-yl)phenyl)ethanone (92).** Synthesized following the procedures of Vogel et al.<sup>210</sup> Acetophenone **91** was refluxed in

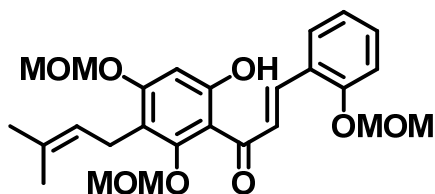
*N,N*-dimethylaniline (10 mL) for 4 h. The reaction mixture was allowed to cool to room temperature and diluted with 50 mL of EtOAc. The organic layer was washed with 1 N HCl (3 × 50 mL), dried over Na<sub>2</sub>SO<sub>4</sub>, filtered, and the solvent removed *in vacuo*. The resulting residue was purified by flash column chromatography using a gradient of EtOAc/*n*-hexanes (1:20 to 1:5) to afford 0.2103 g (46 % yield) of the rearranged product as a yellow-orange oil, *R<sub>f</sub>* = 0.60 (EtOAc/*n*-hexanes 1:5). Spectral data in agreement with reported.<sup>210</sup>

**General Procedure B: Synthesis of Chalcones (97–100).**<sup>211</sup> The appropriate MOM protected benzaldehyde (**93–96**, 1.1 equiv.) was added in a dropwise manner to a solution of acetophenone **92** (1 equiv.) in 2 mL of absolute EtOH and 3.25 mL of 2.75 M NaOH. The mixture was allowed to warm to room temperature and stirred overnight. The reaction was quenched by the addition of saturated aqueous NH<sub>4</sub>Cl (10 mL), and extracted into diethyl ether (3 × 10 mL). The combined organic layers were dried over Na<sub>2</sub>SO<sub>4</sub>, filtered, and the solvent removed *in vacuo*. The resulting residue was purified by flash column chromatography using a gradient of EtOAc/*n*-hexanes (1:20 to 1:10) to yield the chalcones as yellow-orange oils.

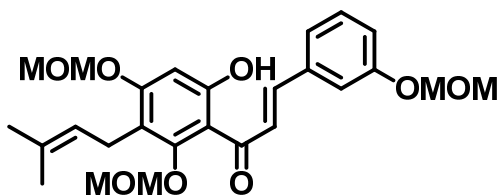


**(E)-1-(6-Hydroxy-2,4-bis(methoxymethoxy)-3-(3-methylbut-2-enyl)phenyl)-3-phenylprop-2-en-1-one (97).** Synthesized using general procedure B to afford 0.3507 g (83% yield) as a yellow oil, *R<sub>f</sub>* = 0.35 (EtOAc/*n*-hexanes 1:20). <sup>1</sup>H NMR (500 MHz, CDCl<sub>3</sub>) δ 12.82 (s, 1H), 7.84 (s, 2H), 7.68 – 7.62 (m, 2H), 7.46 – 7.38 (m, 3H), 6.51 (s, 1H), 5.23 (s, 2H), 5.21 – 5.16 (m, 1H), 4.89 (s, 2H), 3.46 (d, 6H), 3.37 (d, 2H), 1.79 (s, 3H), 1.70 (s, 3H). <sup>13</sup>C NMR (126 MHz, CDCl<sub>3</sub>) δ 193.00, 163.79, 161.65, 156.96, 143.03, 135.10, 131.50, 130.40, 128.96, 128.56,

126.60, 123.03, 116.66, 111.01, 101.82, 98.80, 93.92, 58.41, 56.34, 25.76, 22.95, 17.92. HRMS ( $m/z$ ): [M-H] calcd for C<sub>24</sub>H<sub>27</sub>O<sub>6</sub>, 411.1808; found 411.1639.

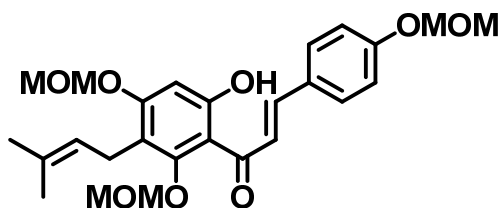


**(E)-1-(6-Hydroxy-2,4-bis(methoxymethoxy)-3-(3-methylbut-2-enyl)phenyl)-3-(2-(methoxymethoxy)phenyl)prop-2-en-1-one (98).** Synthesized using general procedure B to afford 0.3440 g (52% yield) as a yellow oil,  $R_f = 0.27$  (EtOAc/*n*-hexanes 1:10). <sup>1</sup>H NMR (500 MHz, CDCl<sub>3</sub>)  $\delta$  12.86 (s, 1H), 8.24 (d, 1H), 7.86 (d, 1H), 7.70 (dd, 1H), 7.37 – 7.32 (m, 1H), 7.20 – 7.16 (m, 1H), 7.04 (t, 1H), 6.50 (s, 1H), 5.28 (s, 2H), 5.23 (s, 2H), 5.21 – 5.17 (m, 1H), 4.90 (s, 2H), 3.52 (s, 3H), 3.46 (d, 6H), 3.37 (d, 2H), 1.79 (s, 3H), 1.69 (s, 3H). <sup>13</sup>C NMR (126 MHz, CDCl<sub>3</sub>)  $\delta$  193.32, 163.72, 161.49, 157.07, 156.46, 138.05, 131.70, 131.43, 128.30, 126.92, 124.71, 123.09, 121.94, 116.57, 114.80, 111.06, 101.86, 98.75, 94.55, 93.92, 58.36, 56.37, 56.33, 25.77, 22.95, 17.91. HRMS ( $m/z$ ): [M-H] calcd for C<sub>26</sub>H<sub>31</sub>O<sub>8</sub>, 471.2019; found 471.1839.



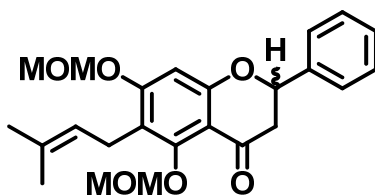
**(E)-1-(6-Hydroxy-2,4-bis(methoxymethoxy)-3-(3-methylbut-2-enyl)phenyl)-3-(3-(methoxymethoxy)phenyl)prop-2-en-1-one (99).** Synthesized using general procedure B to afford 0.3278 g (71% yield) as a yellow oil,  $R_f = 0.33$  (EtOAc/*n*-hexanes 1:10). <sup>1</sup>H NMR (500 MHz, CDCl<sub>3</sub>)  $\delta$  12.83 (s, 1H), 7.84 – 7.77 (m, 2H), 7.36 – 7.28 (m, 3H), 7.11 – 7.07 (m, 1H), 6.51 (s, 1H), 5.23 (s, 2H), 5.22 (s, 2H), 5.21 – 5.16 (m, 1H), 4.89 (s, 2H), 3.50 (s, 3H), 3.48 (s, 3H), 3.46 (s, 3H), 3.37 (d, 2H), 1.79 (s, 3H), 1.70 (s, 3H). <sup>13</sup>C NMR (126 MHz, CDCl<sub>3</sub>)  $\delta$

192.94, 163.83, 161.68, 157.65, 156.95, 142.76, 136.60, 131.51, 129.97, 127.01, 123.03, 122.25, 118.19, 116.67, 116.14, 111.00, 101.78, 98.80, 94.47, 93.93, 58.39, 56.34, 56.10, 25.76, 22.96, 17.92. HRMS ( $m/z$ ):  $[M-H]$  calcd for  $C_{26}H_{31}O_8$ , 471.2019; found 471.1840.



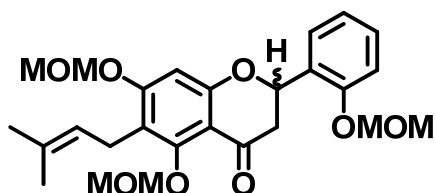
**(E)-1-(6-Hydroxy-2,4-bis(methoxymethoxy)-3-(3-methylbut-2-enyl)phenyl)-3-(4-(methoxymethoxy)phenyl)prop-2-en-1-one (100).** Synthesized using general procedure B to afford 0.3030 g (77% yield) as a yellow oil,  $R_f = 0.34$  (EtOAc/*n*-hexanes 1:10). Spectral data in agreement with reported.<sup>220</sup>

**General Procedure C: Synthesis of Flavonones (101–104).**<sup>221</sup> A mixture of the appropriate chalcone (**97–100**, 1 equiv.) and NaOAc (5 equiv.) in 5 mL of EtOH with 3 drops of water was refluxed for 24 hours. The mixture was poured into 10 mL of ice-cold water and extracted with EtOAc ( $3 \times 15$  mL). The combined organic layers were dried over  $Na_2SO_4$ , filtered, and the solvent removed *in vacuo*. The resulting residue was purified by flash column chromatography using EtOAc/*n*-hexanes (1:10) to yield the flavonones as yellow oils.

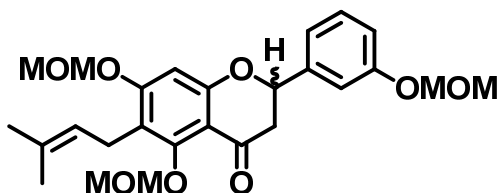


**5,7-bis(methoxymethoxy)-6-(3-methylbut-2-enyl)-2-phenylchroman-4-one (101).** Synthesized using general procedure C to afford 0.2116 g (73% yield) as a light yellow oil.  $R_f = 0.20$  (EtOAc/*n*-hexanes 1:10).  $^1H$  NMR (500 MHz,  $CDCl_3$ )  $\delta$  7.48 – 7.35 (m, 5H), 6.56 (s, 1H), 5.41 (dd,  $J = 2.8, 13.4$ , 1H), 5.24 – 5.17 (m, 4H), 5.07 (d,  $J = 6.7$ , 1H), 3.61 (s, 3H), 3.45 (s, 3H),

3.39 (d,  $J = 6.7$ , 2H), 3.00 (dd,  $J = 13.4$ , 16.8, 1H), 2.77 (dd,  $J = 2.8$ , 16.8, 1H), 1.78 (s, 3H), 1.66 (d,  $J = 1.0$ , 3H).  $^{13}\text{C}$  NMR (126 MHz,  $\text{CDCl}_3$ )  $\delta$  189.33, 162.68, 161.57, 156.91, 138.62, 131.34, 128.80, 128.71, 126.11, 122.80, 118.93, 108.82, 101.66, 98.39, 93.85, 78.86, 57.69, 56.31, 45.42, 25.75, 22.70, 17.89. HRMS ( $m/z$ ):  $[\text{M}+\text{Na}]$  calcd for  $\text{C}_{24}\text{H}_{28}\text{O}_6\text{Na}$ , 435.1748; found 435.1776.



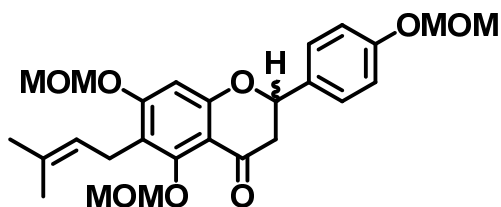
**5,7-bis(methoxymethoxy)-2-(2-(methoxymethoxy)phenyl)-6-(3-methylbut-2-enyl)chroman-4-one (102).** Synthesized using general procedure C to afford 0.2925 g (73% yield) as a yellow oil.  $R_f = 0.17$  (EtOAc/*n*-hexanes 1:10).  $^1\text{H}$  NMR (500 MHz,  $\text{CDCl}_3$ )  $\delta$  7.63 – 7.59 (m, 1H), 7.33 – 7.28 (m, 1H), 7.18 – 7.13 (m, 1H), 7.12 – 7.07 (m, 1H), 6.57 (s, 1H), 5.79 (dd, 1H), 5.25 – 5.18 (m, 6H), 5.09 (d, 1H), 3.63 (s, 3H), 3.47 (s, 3H), 3.45 (s, 3H), 3.42 – 3.38 (m, 2H), 2.87 – 2.83 (m, 2H), 1.78 (s, 3H), 1.67 (s, 3H).  $^{13}\text{C}$  NMR (126 MHz,  $\text{CDCl}_3$ )  $\delta$  189.95, 163.10, 161.45, 156.95, 153.55, 131.31, 129.41, 127.88, 126.45, 122.86, 122.03, 118.78, 113.88, 108.84, 101.65, 98.37, 94.27, 93.85, 73.90, 57.68, 56.31, 56.24, 44.65, 25.75, 22.70, 17.89. HRMS ( $m/z$ ):  $[\text{M}+\text{Na}]$  calcd for  $\text{C}_{26}\text{H}_{32}\text{O}_8\text{Na}$ , 495.1995; found 495.1937. HPLC in 60% MeCN/40%  $\text{H}_2\text{O}$ ,  $t_R = 28.902$  min; purity = 99.1%.



**5,7-bis(methoxymethoxy)-2-(3-(methoxymethoxy)phenyl)-6-(3-methylbut-2-enyl)chroman-4-one (103).** Synthesized using general procedure C to afford 0.2975 g (78% yield) as a yellow oil.  $R_f = 0.13$  (EtOAc/*n*-hexanes 1:10).  $^1\text{H}$  NMR (400 MHz,  $\text{CDCl}_3$ )  $\delta$  7.34 (t,

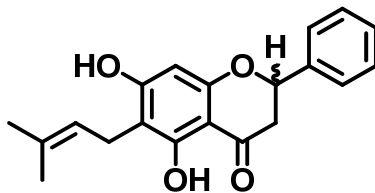


1H), 7.15 – 7.12 (m, 1H), 7.10 – 7.02 (m, 2H), 6.56 (s, 1H), 5.38 (dd, 1H), 5.25 – 5.16 (m, 6H), 5.06 (d, 1H), 3.62 (s, 3H), 3.50 (s, 3H), 3.45 (s, 3H), 3.40 (d, 2H), 2.98 (dd, 1H), 2.77 (dd, 1H), 1.78 (s, 3H), 1.66 (s, 3H). <sup>13</sup>C NMR (126 MHz, CDCl<sub>3</sub>) δ 189.24, 162.61, 161.59, 157.63, 156.91, 140.27, 131.32, 129.93, 122.83, 119.48, 118.99, 116.33, 114.16, 108.87, 101.65, 98.43, 94.48, 93.89, 78.68, 57.68, 56.31, 56.09, 45.45, 25.73, 22.71, 17.88. HRMS (*m/z*): [M+Na] calcd for C<sub>26</sub>H<sub>32</sub>O<sub>8</sub>Na, 495.1995; found 495.1713.

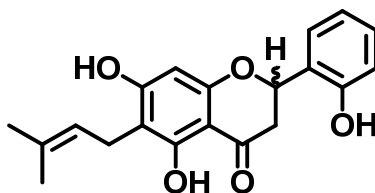


**5,7-bis(methoxymethoxy)-2-(4-(methoxymethoxy)phenyl)-6-(3-methylbut-2-enyl)chroman-4-one (104).** Synthesized using general procedure C to afford 0.2800 g (74% yield) as a yellow oil. *R<sub>f</sub>* = 0.14 (EtOAc/*n*-hexanes 1:10). Spectral data in agreement with reported.<sup>220</sup>

**General Procedure D: Synthesis of Flavonoids (105–108).**<sup>221</sup> 3N HCl (2 mL) was added to a solution of the appropriate flavonone (**101–104**) in MeOH (10 mL). The mixture was refluxed for 45 min then poured into 10 mL of ice-cold water and extracted with EtOAc (3 × 20 mL). The combined organic layers were dried over Na<sub>2</sub>SO<sub>4</sub>, filtered, and the solvent removed *in vacuo*. The resulting residue was purified by flash column chromatography using EtOAc/*n*-hexanes (1:4) to yield the flavonoids as off-white to yellow powders.

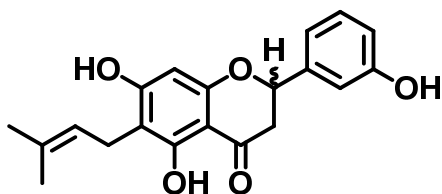


**5,7-dihydroxy-6-(3-methylbut-2-enyl)-2-phenylchroman-4-one (105).** Synthesized using general procedure D to afford 0.0171 g (24% yield) as off-white powder, mp 196–198 °C.  $R_f = 0.68$  (EtOAc/*n*-hexanes 1:3).  $^1\text{H}$  NMR (500 MHz,  $\text{CDCl}_3$ )  $\delta$  12.40 (s, 1H), 7.42 (m,  $J = 7.5$ , 15.9, 5H), 6.20 (s, 1H), 6.01 (s, 1H), 5.40 (dd,  $J = 3.0, 13.0$ , 1H), 5.26 (m, 1H), 3.36 (d,  $J = 7.1$ , 2H), 3.08 (dd,  $J = 13.0, 17.1$ , 1H), 2.83 (dd,  $J = 3.1, 17.2$ , 1H), 1.82 (s, 3H), 1.77 (s, 3H).  $^{13}\text{C}$  NMR (126 MHz,  $\text{CDCl}_3$ )  $\delta$  196.05, 163.93, 161.39, 161.16, 138.64, 135.95, 129.00, 128.97, 126.27, 121.51, 107.06, 103.10, 95.72, 79.23, 43.61, 26.00, 21.28, 18.04. HRMS ( $m/z$ ): [M-H] calcd for  $\text{C}_{20}\text{H}_{19}\text{O}_4$ , 323.1283; found 323.1167. HPLC in 65% MeCN/35%  $\text{H}_2\text{O}$ ,  $t_R = 12.207$  min; purity = 95.5%.



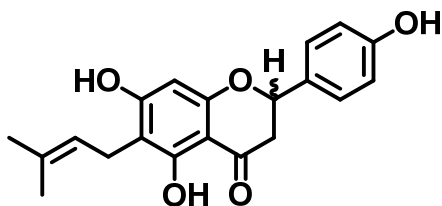
**5,7-dihydroxy-2-(2-hydroxyphenyl)-6-(3-methylbut-2-enyl)chroman-4-one (106).** Synthesized using general procedure D to afford 0.0277 g (37% yield) as light yellow powder, mp. 178–180 °C.  $R_f = 0.30$  (EtOAc/*n*-hexanes 1:3).  $^1\text{H}$  NMR (500 MHz, Acetone)  $\delta$  12.48 (s, 1H), 7.55 – 7.51 (m, 1H), 7.24 – 7.19 (m, 1H), 6.97 – 6.91 (m, 2H), 6.09 (s, 1H), 5.78 (dd, 1H), 5.27 – 5.22 (m, 1H), 3.26 (d, 2H), 3.09 (dd, 1H), 2.83 (dd, 1H), 1.75 (s, 3H), 1.64 (s, 3H).  $^{13}\text{C}$  NMR (126 MHz, Acetone)  $\delta$  197.95, 165.30, 162.84, 162.73, 155.30, 131.77, 130.68, 128.21, 127.01, 124.10, 121.21, 116.80, 109.60, 103.61, 95.85, 75.83, 43.13, 26.39, 22.16, 18.36.

HRMS ( $m/z$ ): [M-H] calcd for  $C_{20}H_{19}O_5$ , 339.1233; found 339.1140. HPLC in 50% MeCN/50%  $H_2O$ ,  $t_R$  = 20.062 min; purity = 96.7%.



**5,7-dihydroxy-2-(3-hydroxyphenyl)-6-(3-methylbut-2-enyl)chroman-4-one (107).**

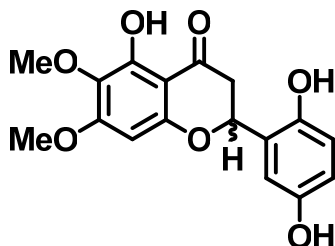
Synthesized using general procedure D to afford 0.0471 g (47% yield) as light yellow powder, mp. 185–187 °C.  $R_f$  = 0.28 (EtOAc/*n*-hexanes 1:3).  $^1H$  NMR (500 MHz, Acetone)  $\delta$  12.45 (s, 1H), 7.25 (t, 1H), 7.05 – 6.97 (m, 2H), 6.88 – 6.82 (m, 1H), 6.06 (s, 1H), 5.47 (dd, 1H), 5.26 – 5.20 (m, 1H), 3.25 (d, 2H), 3.11 (dd, 1H), 2.78 (dd, 1H), 1.75 (s, 3H), 1.64 (s, 3H).  $^{13}C$  NMR (126 MHz, Acetone)  $\delta$  197.47, 165.30, 162.77, 162.27, 158.97, 142.23, 131.79, 131.08, 124.03, 118.76, 116.72, 114.62, 109.62, 103.64, 95.82, 80.26, 44.24, 26.36, 22.12, 18.34. HRMS ( $m/z$ ): [M-H] calcd for  $C_{20}H_{19}O_5$ , 339.1233; found 339.1027. HPLC in 50% MeCN/50%  $H_2O$ ,  $t_R$  = 16.271 min; purity = 96.3%.



**5,7-dihydroxy-2-(4-hydroxyphenyl)-6-(3-methylbut-2-enyl)chroman-4-one (108).<sup>220</sup>**

Synthesized using general procedure D to afford 0.0396 g (36% yield) as yellow powder, mp. 188–190 °C.  $R_f$  = 0.23 (EtOAc/*n*-hexanes 1:3).  $^1H$  NMR (500 MHz, Acetone)  $\delta$  12.34 (s, 1H), 7.29 – 7.20 (m, 2H), 6.79 – 6.73 (m, 2H), 5.90 (s, 1H), 5.29 (dd, 1H), 5.14 – 5.06 (m, 1H), 3.12 (d, 2H), 3.03 (dd, 1H), 2.58 (dd, 1H), 1.62 (s, 3H), 1.50 (s, 3H).  $^{13}C$  NMR (126 MHz, Acetone)

$\delta$  197.86, 165.31, 162.77, 162.51, 159.16, 131.74, 131.44, 129.52, 124.08, 116.64, 109.51, 103.60, 95.79, 80.38, 44.11, 26.36, 22.12, 18.33. HRMS ( $m/z$ ): [M-H] calcd for C<sub>20</sub>H<sub>19</sub>O<sub>5</sub>, 339.1233; found 339.1169. HPLC in 50% MeCN/50% H<sub>2</sub>O,  $t_R$  = 16.136 min; purity = 96.6%.



**Dioclein (86).**<sup>207</sup> Synthesized following the procedures of Spearing et al.<sup>207</sup> to afford 0.0245 g (23% yield over 3 steps) as a yellow powder.  $R_f$  = 0.33 (EtOAc/*n*-hexanes 1:1). <sup>1</sup>H NMR (500 MHz, Acetone)  $\delta$  11.99 (s, 1H), 8.20 (s, 1H), 7.91 (s, 1H), 7.03 (d, 1H), 6.78 (d, 1H), 6.70 (dd, 1H), 6.24 (s, 1H), 5.75 (dd, 1H), 3.92 (s, 3H), 3.72 (s, 3H), 3.08 (dd, 1H), 2.85 (dd, 1H). <sup>13</sup>C NMR (126 MHz, Acetone)  $\delta$  198.83, 162.53, 160.55, 156.45, 152.00, 147.97, 131.75, 127.45, 117.59, 117.10, 114.59, 104.24, 93.09, 76.20, 61.03, 57.14, 43.12. HRMS ( $m/z$ ): [M-H] calcd for C<sub>17</sub>H<sub>15</sub>O<sub>7</sub>, 331.0818; found 331.0627. HPLC in 40% MeCN/60% H<sub>2</sub>O,  $t_R$  = 5.480 min; purity = 97.6%.

### *Binding and Efficacy Studies*

**Radioligand Binding Studies.**<sup>213</sup> MOP receptor binding sites were labeled using [<sup>3</sup>H]D-Ala<sup>2</sup>-MePhe<sup>4</sup>,Gly-ol<sup>5</sup>]-enkephalin ([<sup>3</sup>H]DAMGO, SA = 44 – 48 Ci/mmol) while DOP receptor binding sites were labeled using [<sup>3</sup>H][D-Ala<sup>2</sup>, D-Leu<sup>5</sup>]-enkephalin ([<sup>3</sup>H]DADLE, SA = 40 – 50 Ci/mmol) in rat brain homogenates. KOP receptor binding sites were labeled using [<sup>3</sup>H]*N*-methyl-2-phenyl-*N*-[(5*R*,7*S*,8*S*)-7-(pyrrolidin-1-yl)-1-oxaspiro[4.5]dec-8-yl]acetamide ([<sup>3</sup>H]U69,593, SA = 50 Ci/mmol). On the day of the assay, Cell pellets were thawed on ice for 15 minutes followed by homogenization with a polytron in 10 mL/pellet of ice-cold 10mM Tris-

HCl, pH 7.4. The membranes were centrifuged at  $30,000 \times g$  for 10 minutes, then resuspended in 10 mL/pellet ice-cold 10mM Tris-HCl, pH 7.4 followed again by centrifugation at  $30,000 \times g$  for 10 minutes. Membranes were then resuspended in 25°C 50 mM Tris-HCl, pH 7.4 (~100 mL/pellet hMOP-CHO, 50 mL/pellet hDOP-CHO, and 120 mL/pellet hKOP-CHO). All assays were performed in 50 mM Tris-HCl, pH 7.4 in a final assay volume of 1.0 mL, with a protease inhibitor cocktail: bacitracin (100  $\mu\text{g}/\text{mL}$ ), bestatin (10  $\mu\text{g}/\text{mL}$ ), leupeptin (4  $\mu\text{g}/\text{mL}$ ) and chymostatin (2  $\mu\text{g}/\text{mL}$ ). Drug dilution curves were determined with buffer containing 1 mg/mL BSA. 20  $\mu\text{M}$  levallorphan ( $[^3\text{H}]\text{DAMGO}$  and  $[^3\text{H}]\text{DADLE}$ ) or 10  $\mu\text{M}$  (-)-U69,593 (for  $[^3\text{H}]\text{U69,593}$  binding) was used to account for nonspecific binding.  $[^3\text{H}]\text{Radioligands}$  were used at concentrations of approximately 2 nM. After 2 hours of incubation at 25°C, triplicate samples were filtered with Brandell Cell Harvesters (Biomedical Research & Development Inc., Gaithersburg, MD), over Whatman GF/B filters. The filters were punched into 24-well plates in which 0.6 mL of LSC-cocktail (Cytoscint) was added. After an overnight extraction, the samples were counted in a Trilux liquid scintillation counter at 44% efficiency. Approximately 30  $\mu\text{g}$  protein was in each assay tube for the opioid binding assays. The inhibition curves were determined by displacing a single concentration of radioligand by 10 concentrations of drug.

**Calcium Mobilization Assay.**<sup>214</sup> All cells were maintained in F-12 nutrient medium (Ham), supplemented with 10% fetal bovine serum (FBS), 1% penicillin and streptomycin (p/s), and 0.2% normocin. Cell culture supplies were from Invitrogen (Carlsbad, CA) unless otherwise specified. Chinese hamster ovary (CHO) cells stably expressing MOR-, KOR-, DOR-, or CB1-Gaq16 were removed from their flasks using Versene and quenched with the Ham media, centrifuged and re-suspended in media. Cells were counted with a Cellometer Auto T4

(Nexcelom Bioscience, Lawrence, MA) and 30,000 cells were transferred to each well of a black Costar 96-well optical bottom plate (Corning Corporation, Corning, NY). Each plate was incubated at 37°C/5% CO<sub>2</sub> overnight to confluence. The culture media was removed from the plates and cells were subsequently loaded with a fluorescent calcium probe (Calcium 5 dye, Molecular Devices, Sunnyvale, CA) in an HBSS-based buffer containing 20 mM HEPES, 0.25% BSA, 1% DMSO (or 0.5% DMSO + 0.5% EtOH for CB1-expressing cells), and 10 μM probenecid (Sigma) in a total volume of 225 μL. Cells were incubated at 37°C/5% CO<sub>2</sub> for 1 h and then stimulated with DMSO solutions of DAMGO, U69,593, DPDPE, ethanol solutions of CP55,940 or DMSO solutions of test compounds at various concentrations using a Flexstation 3 plate-reader, which automatically added 25 μL of the compounds at 10X concentration to each well after reading baseline values for ~17 sec. Agonist-mediated change in fluorescence (485 nm excitation, 525 nm emission) was monitored in each well at 1.52 sec intervals for 60 sec and reported for each well. Data were collected using Softmax version 4.8 (MDS Analytical Technologies) and analyzed using Prism software (GraphPad, La Jolla, CA). Nonlinear regression analysis was performed to fit data and obtain maximum response ( $E_{max}$ ),  $EC_{50}$ , correlation coefficient ( $r^2$ ) and other parameters. All experiments were performed at least 2 times to ensure reproducibility and data reported as mean ± standard error, unless noted otherwise.

**PathHunter™ β-Arrestin Assay.**<sup>218</sup> All cells were maintained in F-12 nutrient medium (Ham), supplemented with 10% fetal bovine serum (FBS), 1% penicillin and streptomycin (p/s), and 0.2% normocin. Cell culture supplies were from Invitrogen (Carlsbad, CA) unless otherwise specified. Chinese hamster ovary (CHO) cells stably expressing KOP or GPR-55 were removed from their flasks using Cell Dissociation Buffer and quenched with the Ham media, centrifuged

and re-suspended in media. Cells were counted with a Cellometer Auto T4 (Nexcelom Bioscience, Lawrence, MA) and a volume of cell suspension to equal 30,000 cells/well was centrifuged and re-suspended in PathHunter™ Cell Plating 2 Reagent. 90  $\mu$ L of the cell suspension was transferred to each well of white Costar 96-well optical bottom plates (Corning Corporation, Corning, NY). Each plate was incubated at 37°C/5% CO<sub>2</sub> overnight to confluence. U69,593, LPI, or test compounds at various concentrations were dissolved in a PBS-based buffer containing 10% DMSO. 10  $\mu$ L of the compound solutions were transferred to the assay plates, making a total well volume of 100  $\mu$ L and 1% DMSO concentration. Cells were incubated at 37°C/5% CO<sub>2</sub> for 90 min, and then 50  $\mu$ L of detection reagents (prepared from the assay kit as a working solution the day of the assay: 1 part Galacton Star® + 5 parts Emerald II™ + 19 parts PathHunter™ Cell Assay Buffer) were transferred to each well. The cells were incubated at room temperature in the dark for 1 h, and then the luminescence read using a Flexstation 3 plate reader. Data were collected using Softmax version 4.8 (MDS Analytical Technologies) and analyzed using Prism software (GraphPad, La Jolla, CA). Nonlinear regression analysis was performed to fit data and obtain maximum response ( $E_{\max}$ ),  $EC_{50}$ , correlation coefficient ( $r^2$ ) and other parameters. All experiments were performed at least 2 times to ensure reproducibility and data reported as mean  $\pm$  standard error, unless noted otherwise.

## CHAPTER 4: FUTURE INVESTIGATION OF THE BINDING MODE OF SALVINORIN A AT KOP RECEPTORS

### Introduction

Salvinorin A (**108**), structurally classified as a neoclerodane diterpene, is the principle constituent responsible for the psychoactivity of the widely available plant *Salvia divinorum* Epling & Jativa (Lamiaceae).<sup>222</sup> The structure and absolute configuration of salvinorin A were determined through NMR and X-ray crystallography studies.<sup>223-224</sup> *S. divinorum* is indigenous to Oaxaca, Mexico and an infusion of the leaves is used traditionally by native shamans for divination ceremonies, to treat the magical curse *panzón de borrego*, as well as to treat mundane ailments such as anemia, diarrhea, headache, and rheumatism.<sup>222, 225</sup> Salvinorin A is a potent hallucinogen and rivals classical hallucinogens such as lysergic acid diethylamide (**109**, LSD) and 4-bromo-2,5-dimethoxyamphetamine (**110**, DOB).<sup>226-227</sup> Because of the intense experience it produces, *S. divinorum* has become popular as a recreational drug.<sup>228-229</sup> This has caused *S. divinorum* to be labeled as a “drug of concern” by the Drug Enforcement Administration (DEA), and several states in the U. S. have enacted legislation to criminalize its use and sale.<sup>230-231</sup>

Interestingly, unlike the classical hallucinogens, salvinorin A does not exert its effects through the 5-HT<sub>2A</sub> (serotonin) receptor.<sup>180</sup> Rather, it was found to be a selective agonist at KOP receptors.<sup>180</sup> Salvinorin A is the first non-nitrogenous compound to have high affinity and selectivity for the KOP receptor, and its structure is unique among known KOP ligands, such as bremazocine, U69,593, JDTic, norBNI, and GNTI, as well as known hallucinogens, such as LSD, DOB, and phencyclidine (**111**, PCP) (Figure 18). Previous hypotheses proposed that a basic nitrogen atom was required for opioid receptor affinity; at physiological pH, the positively



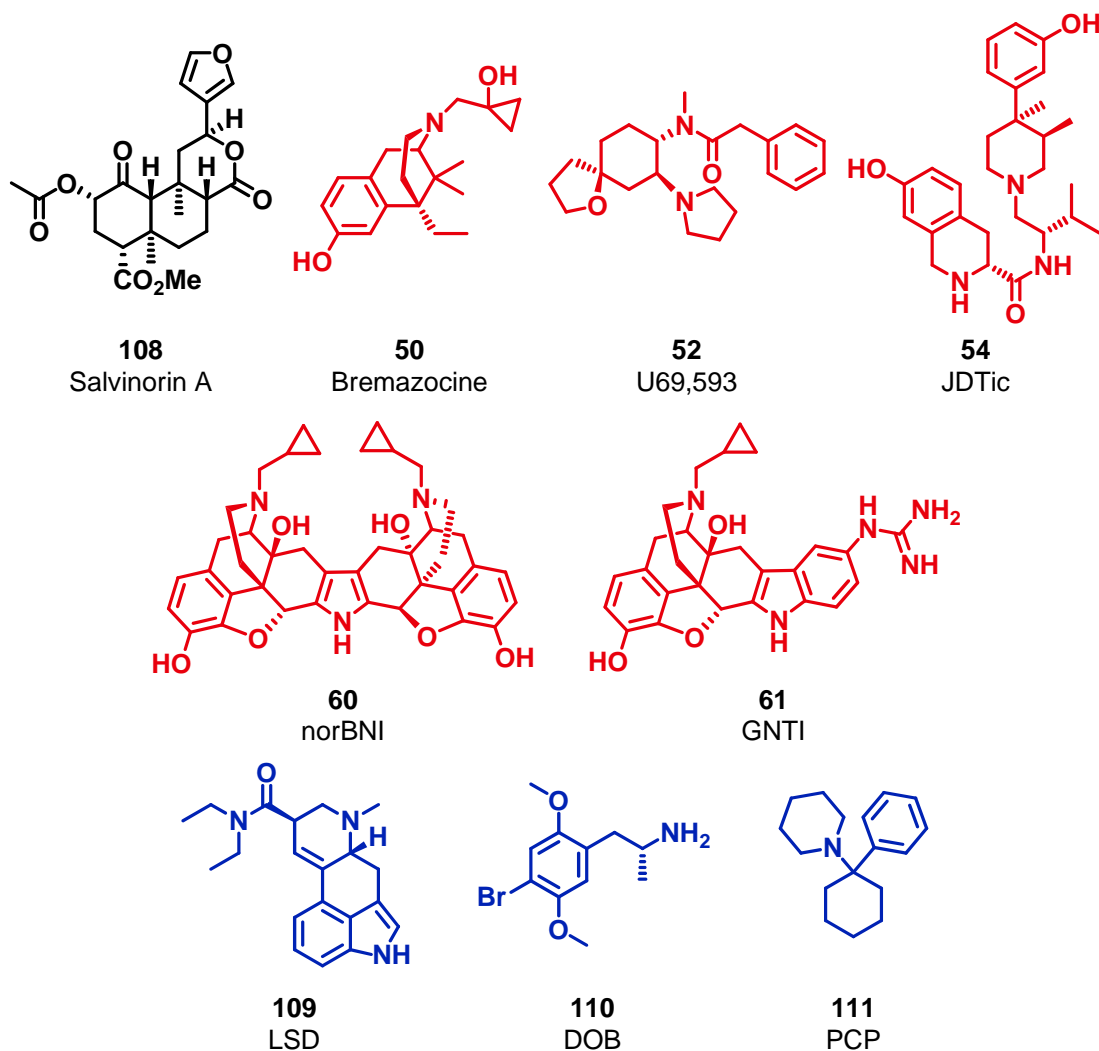


**Figure 18.** Examples of KOP ligands (red) and hallucinogens (blue) compared to salvinorin A (black).

charged nitrogen atom in the ligand would interact with an aspartic acid residue in the third transmembrane region of the GPCR.<sup>232-234</sup> However, salvinorin A lacks a nitrogen atom, indicating that hypotheses for opioid receptor-ligand binding interactions merit re-evaluation.<sup>235</sup> Given the molecule's unique features, salvinorin A is a target for pharmacological exploration and SAR development.

## Terpenes

As previously stated, salvinorin A is structurally classified as a neoclerodane diterpene. Neoclerodane diterpenes are a subclass of the terpene class of natural products. Terpenes provide interesting investigational targets for organic chemists and pharmacologists because of their structural complexity, diversity, and unique pharmacological profiles.<sup>236</sup> Many clinically used medications, such as taxol (anti-cancer) and artemisinin (anti-malarial), are members of the terpene class. Because they are secondary metabolites, terpenes are found in very low concentrations in living organisms.<sup>237</sup>

Biosynthetically, terpenes are constructed from chemically activated isoprene units, 3-isopentenyl pyrophosphate (**115**, IPP) and dimethylallyl pyrophosphate (**116**, DMAPP), which are produced from the mevalonic acid pathway (Figure 19).<sup>238-242</sup> In the mevalonic acid pathway, two units of acetyl CoA condense, facilitated by acetyl CoA transferase (ACT), to yield acetoacetyl CoA. This then condenses with another unit of acetyl CoA to produce 3-hydroxy-3-methylglutaryl CoA (**112**, HMG CoA) via the help of HMG CoA synthase (HMGCS). HMG CoA is then reduced to mevalonate (**113**) by HMG CoA reductase (HMGCR), which is NADPH dependent. Mevalonate is subsequently phosphorylated first by mevalonate kinase (MVK), then by phosphomevalonate kinase (PMVK), yielding mevalonate-5-pyrophosphate (**114**). The actions of a decarboxylase enzyme then afford IPP, which itself can be enzymatically isomerized to DMAPP.<sup>243</sup> In order to build terpenes, chain elongation of DMAPP and/or IPP units occurs through a series of electrophilic alkylations that consist of three steps: 1) removal of the carbon-oxygen bond of DMAPP/IPP to form a carbocation;<sup>244</sup> 2) alkylation of the double bond of another IPP unit, generating a second carbocation;<sup>245</sup> and 3) stereoselective elimination to

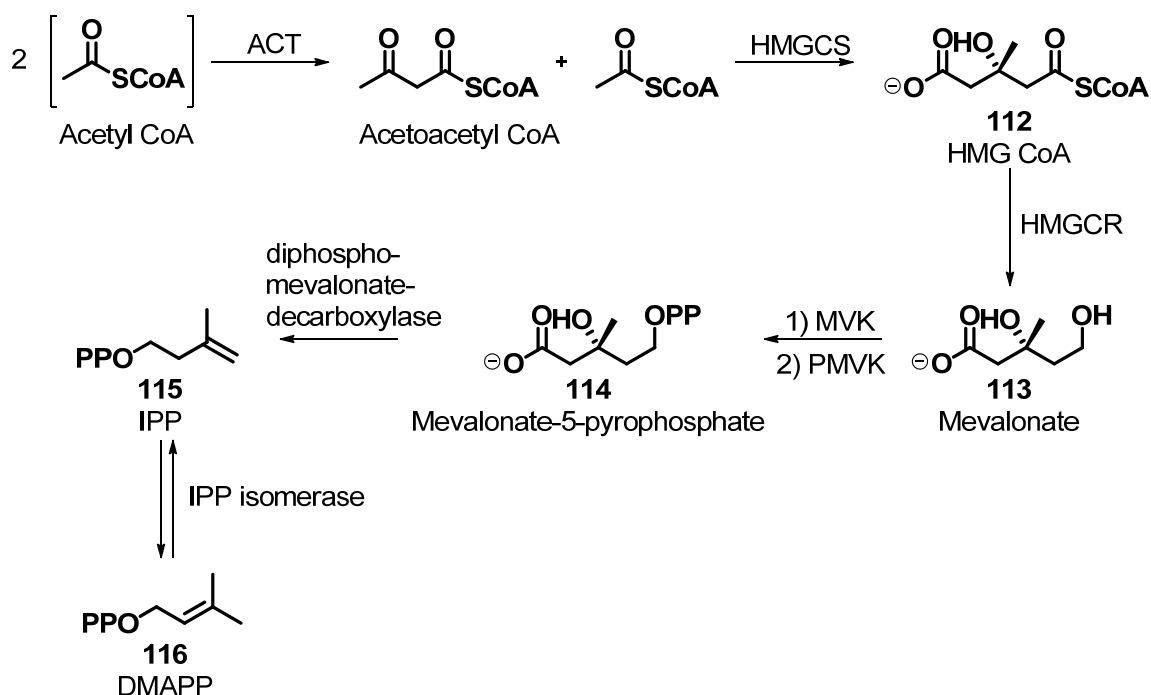


**Figure 19.** Mevalonic acid pathway to IPP.

quench the carbocation and produce a new allylic diphosphate which has been elongated by one isoprene unit (Figure 20).<sup>245</sup> Successive elongations in a head-to-tail manner yield a 10 carbon chain called geranyl diphosphate (**117**, GPP).<sup>244</sup> Further chain elongation iterations yield farnesyl diphosphate (**118**, FPP), containing 15 carbons, and geranylgeranyl diphosphate (**119**, GGPP), containing 20 carbons, and even longer chain products.<sup>246</sup> Chain elongation, rearrangement, and cyclization of GPP, FPP, and GGPP, all performed enzymatically, leads to the construction of all terpenes.

Terpenes are classified by the number of isoprene units present in the carbon skeleton.<sup>237</sup> The chemical formula of isoprene is  $\text{C}_5\text{H}_8$ , meaning that each isoprene unit equates to five carbons present in the terpene skeleton.<sup>237</sup> Using this definition, types of terpenes include: hemiterpenes, monoterpenes, sesquiterpenes, diterpenes, sesterterpenes, and triterpenes, and

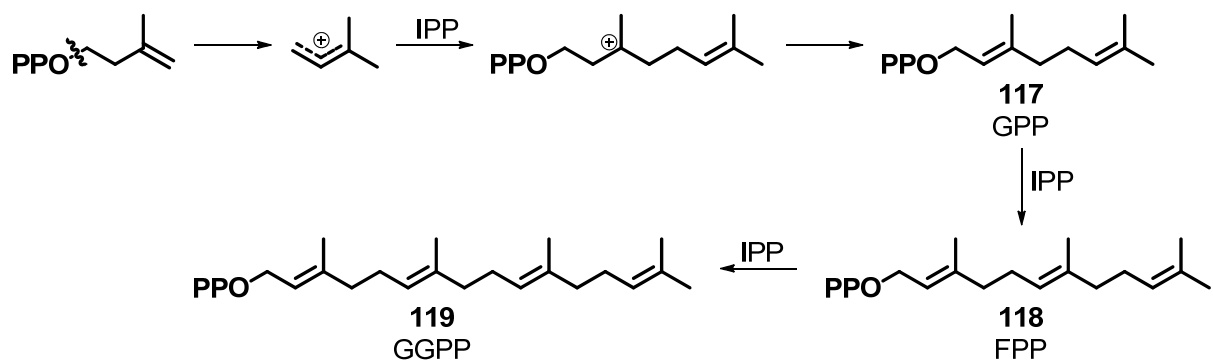


**Figure 20.** Mechanism of terpene chain elongation.

these consist of one through six isoprene units, respectively.<sup>246</sup> Additional terpenes include tetraterpenes, with eight isoprene units, and polyterpenes, which include isoprene chains. Each type of terpene in the classification system is further divided into subclasses.<sup>237</sup>

There are over 50 different subclasses of diterpene skeletons and many of these subclasses include compounds with biological activity.<sup>246</sup> Some of the best-studied are labdanes, kauranes, gibberlins, beyeranes, aphidicolins, cembranes and abietanes. The clerodanes—ubiquitous in nature and found in a variety of plants, fungi, and microorganisms—are another subclass of diterpenes that are known to have biological activity.<sup>247</sup> A diterpene is classified as a clerodane (**120**) if it contains four isoprene units and four contiguous stereocenters on a *cis* or *trans* decalin ring system (Figure 21).<sup>247</sup> Approximately 25% of clerodanes contain the *cis* ring fusion, columbin (**121**) being one example. Columbin is a diterpenoid furanolactone, isolated from several plants including *Sphenocentrum jollyanum* Pierre (Menispermaceae) and *Jateorhiza Columba* Miers (Menispermaceae).<sup>248-249</sup> Columbin has been shown to have both anti-inflammatory activity and chemopreventative activity against colorectal cancer,<sup>248-250</sup> and is sold as a crude drug preparation called *Calumbae Radix* or *Tinosporae Radix*.<sup>248</sup> The rest of the clerodanes contain the *trans* ring fusion exemplified by clerodin (**122**). Clerodin, isolated from

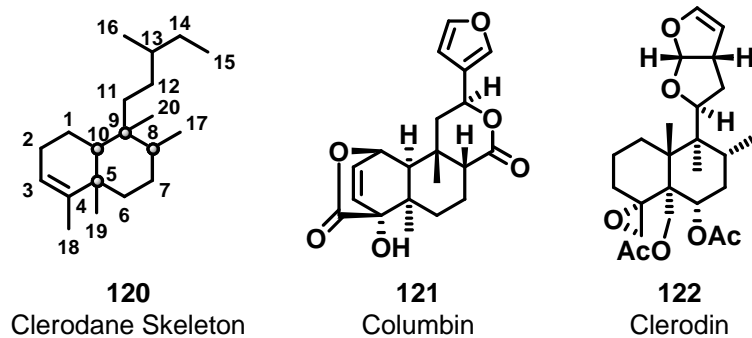


**Figure 21.** Examples of neoclerodane diterpenes.

*Clerodendrum infortunatum* L. (Lamiaceae), is an insect anti-feedant and potential natural pesticide.<sup>251-253</sup> In addition to the relative configuration of the *trans* or *cis* junctions of the fused rings, clerodanes are further classified by their relative configuration at C-8 and C-9.<sup>247</sup> This additional clarification gives four types of clerodane skeletons defined with respect to configuration of ring fusion and substitution pattern at C-8 and C-9: *trans-cis* (TC), *trans-trans* (TT), *cis-cis* (CC) and *cis-trans* (CT).<sup>247</sup> Clerodanes are even further classified by their absolute stereochemistry. Structures that have the same absolute stereochemistry as clerodin are termed neoclerodanes and enantiomers of clerodin are referred to as *ent*-neoclerodanes.<sup>254-255</sup>

Because of their structural complexity, neoclerodane diterpenes have been investigated for structure-activity relationships (SAR) through synthetic organic means as well as pharmacological studies. However, such studies have been rather difficult to conduct because the neoclerodane diterpene class in general has sensitivity to the conditions of many typical organic reactions. This sensitivity complicates and lengthens the analog design and development process as new synthetic methodologies often need to be explored and established. Despite this difficulty, one particular neoclerodane diterpene that has attracted relatively recent interest is salvinorin A.

## Salvinorin A KOP Receptor *In Vitro* Pharmacology

In 2002, Roth et al. identified that salvinorin A was a potent and selective agonist at KOP receptors.<sup>180</sup> For this study, salvinorin A (10  $\mu$ M) and LSD (10  $\mu$ M) were screened against a panel of 50 GPCRs, transporters, and ligand-gated ion channels. Salvinorin A inhibited only [<sup>3</sup>H]bremazocine-labeled KOP receptors, and neither MOP receptors, nor DOP receptors, nor any of the other targets in the screen. Further evaluation found that for salvinorin A at KOP receptors  $K_i \leq 16$  nM, whereas at both MOP and DOP receptors  $K_i \geq 5,000$  nM. Studies of agonist/antagonist properties revealed that, for the inhibition of adenylate cyclase, salvinorin A was a potent agonist ( $EC_{50} = 1.05$  nM), comparable to the known KOP agonist U69,593 ( $EC_{50} = 1.2$  nM). Salvinorin A was also found to be a potent agonist in the [<sup>35</sup>S]GTP- $\gamma$ -S assay ( $EC_{50} = 235$  nM), again comparable to U69,593 ( $EC_{50} = 377$  nM).

In 2004, Chavkin et al. independently reproduced and confirmed findings that salvinorin A was a KOP receptor agonist via displacement of [<sup>3</sup>H]bremazocine and inhibition of adenylate cyclase.<sup>256</sup> They further showed that salvinorin A also behaved as a full KOP agonist in the fluorescent calcium mobilization assay, where salvinorin A ( $EC_{50} = 7$  nM) was comparable to or better than the known KOP agonists U69,593 ( $EC_{50} = 13$  nM), U50,488 ( $EC_{50} = 24$  nM), and dynorphin A ( $EC_{50} = 83$  nM). Wang et al. found that while salvinorin A ( $EC_{50} = 4.6$  nM) and U50,488 ( $EC_{50} = 2.2$  nM) had very similar potencies as measured by the [<sup>35</sup>S]GTP- $\gamma$ -S functional assay, salvinorin A was 40-fold less potent than U50,488 at promoting KOP receptor internalization.<sup>257</sup>

## Salvinorin A KOP Receptor *In Vivo* Pharmacology

### *Hallucinogenic and other CNS Effects*

For traditional spiritual uses, *S. divinorum* is ingested by one of three routes: 1) chewing and swallowing the leaves, 2) crushing the leaves to extract the juices and swallowing the extract, and 3) smoking the leaves.<sup>258</sup> In 1994, Siebert reported that salvinorin A is inactivated in the gastrointestinal tract before entering the bloodstream; when encapsulated doses of salvinorin A were swallowed by human volunteers, no effect was detected.<sup>226</sup> Thus absorption through the oral mucosa and inhalation are the most efficient routes to achieve efficacy. Initial studies of the psychoactive effects of salvinorin A reported that a smoked dose of 200–500 µg produced intense hallucinations with peak effects lasting 5–10 min and lingering, diminishing effects lasting approximately 1 h.<sup>226-227</sup>

In 2011, Johnson et al. reported a double-blind, placebo controlled study in which 16 doses of salvinorin A were evaluated in four human volunteers.<sup>259</sup> Drug doses of 0.375–21 µg/kg or placebo were administered via vaporization and inhalation, and participants' blood pressure and heart rate were monitored at 2 min intervals for 1 h post administration. Participants were also verbally cued to rate perceived drug strength at 2 min intervals for 1 h post administration, as well as retrospectively after the session was completed. In order further characterize the subjective aspects of the salvinorin A experience in comparison to classical hallucinogens, approximately 1 h after the session, participants filled out two questionnaires: the Hallucinogen Rating Scale (HRS) and the Mysticism Scale (M Scale). The study found that the participant-rated drug strength peaked at 2 min post administration, the first time point measured, and decreased such that, at 20 min post administration mean ratings only indicated a “possible

mild” drug effect. Study participants rated salvinorin A doses in the 4.5–21 µg/kg range as significantly stronger than placebo, and this dose range was also reflected in their answers on the HRS and M Scale questionnaires. The study found no dose-related physiological changes in heart rate or blood pressure, nor any observable resting or kinetic tremors. Furthermore, no study participants refused to receive the same or higher dose of drug at the end of any session. These results indicate that inhaled salvinorin A has hallucinogenic effects comparable to classical hallucinogens and is physiologically safe and psychologically tolerated at the doses tested.

In 2012, Addy reported a larger (30 participants) double-blind, placebo controlled study of the psychological effects of salvinorin A in humans.<sup>260</sup> Participants in the study smoked a dose of 1,017 µg of salvinorin A deposited on 25 mg of dried *S. divinorum* leaf material or placebo; the unaltered leaf material was presumed to be non-psychoactive and was used as the placebo for the study. Prior to and 1 h after administration, participants’ blood pressure and heart rate were measured, as well as body temperature and respiration rate. In order to measure salvinorin A inebriation, during experimental sessions, researchers recorded participants’ behavior using a standardized scale. Behaviors recorded during the first 20 min post drug administration were used for analysis, and 1 h after administration study participants filled out the HRS. The researchers also conducted follow-up interviews with all study participants approximately 8 weeks after their final experimental session. In agreement with the previously described study, this study also found no dose-related physiological changes during experimental sessions, and both doses of salvinorin A were tolerated by the study participants. After inhaling a dose of salvinorin A, participants displayed increased talking, laughing, and movement in comparison to placebo, as well as physical contact with the experimental monitor and paranoid



ideation. In HRS scores, the active dose of salvinorin A produced an experience significantly different from placebo with 43% of study participants reporting their experience as similar to dreaming and 50% reporting it as unlike any previous experience. In the follow-up interviews, 87% of study participants reported salvinorin A use after-effects lasting fewer than 24 h, and 70% reported after-effects lasting more than 24 h, persisting for up to 3 days post use. However, no participant reported that they would refuse to use salvinorin A or *S. divinorum* again. Finally, in agreement with the previous study, this study's findings indicate that inhaled salvinorin A has hallucinogenic effects comparable to classical hallucinogens and is physiologically safe and psychologically tolerated at the doses tested.

In 2007, Butelman et al. reported that salvinorin A produced dose- and time-dependent neuroendocrine effects in non-human primates.<sup>261</sup> Serum prolactin concentration has been used in non-human primates to evaluate the potency, receptor selectivity, and efficacy of opioid agonists *in vivo*.<sup>262-263</sup> Rhesus monkeys were given vehicle, salvinorin A, or U69,593 (all drug concentrations 0.0032–0.056 mg/kg i.v.) and serum samples were taken at certain time points through 2 h. For antagonist experiments, monkeys were given a single dose of antagonist 30 min before agonist challenge and subsequent serum sample collection. The study found that i.v. salvinorin A caused a robust dose- and time- dependent increase in prolactin concentrations that were observable 5 min after injection, peaked at 15 min, and gradually declined over 2 h. The effects of U69,593 were similar to those of salvinorin A, except that elevated prolactin levels persisted through the 2 h end point of the study indicating a longer duration of action. The study also evaluated the differences between i.v. and s.c. injection of salvinorin A and found that s.c. injection produced a slower on-set and overall smaller release of prolactin. In both the i.v. and s.c. studies, the effects of salvinorin A were more robust in female monkeys than in male

monkeys. For antagonist experiments, 0.1 mg/kg nalmefene, a universal opioid antagonist, was found to strongly attenuate the effects of 0.032 mg/kg salvinorin A. The non-selective 5-HT<sub>2</sub> antagonist ketanserin (0.1 mg/kg) demonstrated no attenuation of the effects of salvinorin A (0.032 mg/kg). These findings support previous conclusions that salvinorin A produces its effects through KOP receptors and not 5-HT<sub>2</sub>. Finally, the study reported that the rhesus monkey OPRK1 gene had 98.4% sequence homology to the human OPRK1 gene.

In a following study in 2009, Butelman et al. investigated the fast on-set and entry into the CNS and the unconditioned behavioral effects of salvinorin A in non-human primates.<sup>264</sup> Salvinorin A (0.032 or 0.1 mg/kg i.v.) or U69,593 (0.01, 0.032, or 0.056 mg/kg i.v.) was administered to rhesus monkeys as a bolus dose and behavior was observed at certain time points through an end point of 90 min. For antagonist experiments, a single dose of antagonist was administered 30 min prior to agonist challenge. Behavioral effects were characterized with two rating scales measuring sedation and posture, which are known to be sensitive to centrally-acting KOP agonists as well as non-opioids that have sedative effects, and less sensitive to peripherally restricted KOP agonists.<sup>265-266</sup> Facial relaxation and ptosis were also monitored. In order to study on-set and CNS entry, salvinorin A (0.032 mg/kg i.v.) was given and cerebrospinal fluid (CSF) samples were collected at certain time points through 30 minutes, with a final sample collected at approximately 3 h post injection. These studies found salvinorin A produced dose-dependent increases in sedation and postural scores with peak effects observed 5 min post administration and declining by 30 min. This was comparable to the effects of U69,593 which also produced dose-dependent increases in behavior scores with a fast on-set, but had a longer duration of action through 60 min. Salvinorin A also caused facial relaxation and ptosis with a very rapid onset (1–2 min post administration) and short duration of action (15 min), similar to

U69,593, although the timing of the effects of U69,593 were less well defined due to apparent intersubject variability. Pretreatment with the universal opioid antagonist nalmefene (0.1 mg/kg) nearly completely attenuated all behavioral effects of salvinorin A (0.032 mg/kg). Further, nalmefene (administered 11 min post salvinorin A) was able to completely reverse on-going salvinorin A facial relaxation and ptosis. This finding suggests that the effects of salvinorin A are both initiated and maintained by KOP receptors. In contrast, pretreatment with either the CB1 antagonist rimonabant (1 mg/kg) or the 5-HT<sub>2</sub> antagonist ketanserin (0.1 mg/kg) was no different than pretreatment with vehicle. In the CSF studies, salvinorin A was found to enter the CNS almost immediately; it was detectable at time 0 after injection and concentration peaked at 2 min, decreasing through the end-point of the experiment. This result is in agreement with a study by Hooker et al. which traced [<sup>11</sup>C]salvinorin A in live baboon brains using non-invasive positron emission tomography (PET); the drug was found to rapidly enter the brain, reaching peak concentration in 40 s, as well as rapidly clear the brain, having a half-life of 8 min and diminishing to below 25% of maximum in less than 30 min.<sup>267</sup> Collectively, these findings are consistent with descriptive information from humans and support that salvinorin A is a centrally acting KOP agonist with fast on-set and short duration of action.

### *Metabolism*

Schmidt et al. reported that the principal metabolite of salvinorin A *ex vivo* in both human and rhesus monkey plasma is the C-2 deacetylated derivative, salvinorin B (**123**), which they observed to accumulate as the quantity of salvinorin A decreased (Figure 22).<sup>268</sup> Kutrzeba et al. confirmed that salvinorin B is the major metabolite of salvinorin A; using a variety of live fungal species as well as rat brain and liver homogenate, they were unable to observe any metabolic

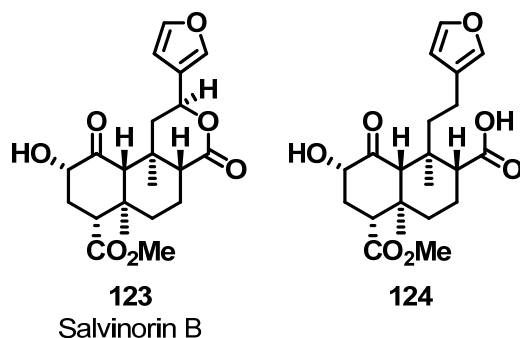


**Figure 22.** Metabolites of salvinorin A.

products other than salvinorin B.<sup>269</sup> In a follow up study, Schmidt et al. reported that for *in vivo* experiments with rhesus monkeys, the plasma concentration of salvinorin B did not increase, and was below the lower limits of detection over the course of study.<sup>270</sup> These results likely indicate that salvinorin B is rapidly cleared from the body, or that it accumulates in other tissues and organs that were not examined. A study in human volunteers by Pichini et al. found that 0.4–1.2% of a total theoretically administered smoked dose of salvinorin A (0.58 mg) is excreted in urine.

Tsujikawa et al. attempted to characterize the esterase enzymes responsible for salvinorin A metabolism in rat plasma via incubation with selective inhibitors.<sup>271</sup> They confirmed through a control study that the degradation of salvinorin A was not due to inherent chemical instability, but to metabolizing enzymes; incubating salvinorin A in buffer at 37 °C for 24 h produced no observable degradation products. Further, the degradation of salvinorin A to salvinorin B in rat plasma could be inhibited by the addition of NaF, a general esterase inhibitor. The study found that the metabolism of salvinorin A in rat plasma could be inhibited by sodium *bis-p*-nitrophenyl phosphate (BNPP), which is selective for carboxylesterase (CES), in a concentration-dependent manner. Salvinorin A metabolism could also be inhibited by phenylmethylsulfonyl fluoride

(PMSF), which is selective for the class of serine esterases. This particular finding supports the involvement of CES in the plasma metabolism of salvinorin A to salvinorin B because CES is a serine esterase. Selective inhibitors for other enzymes—butyrylcholinesterase, acetylcholinesterase, and arylesterase—did not inhibit the metabolism of salvinorin A, further implicating CES. In rat plasma in the presence of the esterase inhibitor NaF, the study also observed another major metabolite of the salvinorin A scaffold, the lactone-ring open form of salvinorin B (**124**). The appearance of this metabolite could be reduced by the addition of EDTA, a calcium chelating agent. Considering that rats have calcium-dependent lactonase enzymes in their serum,<sup>272</sup> this suggests that a such a lactonase is involved in the metabolism of salvinorin B.

Teksin et al. investigated the *in vitro* metabolism of salvinorin A with ten CYP450 isoforms and UGT2B7, the major enzyme involved in drug metabolism via glucuronidation.<sup>273</sup> When concentrations of 5 and 50  $\mu\text{M}$  salvinorin A were incubated with CYP2D6, CYP1A1, CYP2C18, and CYP2E1 for 1 h, statistically significant reductions in remaining concentration were observed. In order to further characterize *in vitro* metabolism, salvinorin A (5, 10, and 50  $\mu\text{M}$ ) was incubated with UGT2B7. Similar to the CYP450 experiments, statistically significant reductions in remaining concentration were observed for all concentrations of salvinorin A. Additionally, the study observed that for CYP1A1, CYP2C18, CYP2E1, and UGT2B7 metabolism of salvinorin A appeared saturable at high concentrations; that is, lower concentrations of salvinorin A were metabolized more efficiently than higher concentrations. These findings suggest that CYP2D6, CYP1A1, CYP2C18, CYP2E1, and UGT2B7 are involved in the metabolism of salvinorin A.

### *Toxicity*

Mowry et al. published the first study of the toxicity of pure salvinorin A using rats and mice.<sup>274</sup> Acute exposure to salvinorin A (1,600 µg/kg) showed no statistically significant effect on rat heart rate and there were no apparent effects on cardiac conduction. Acute exposure also did not produce changes in body temperature or galvanic skin response (an indication of sympathetic nervous system activity). Pulse pressure did appear to increase between 20–40 min post exposure, however this increase was only numerical and not statistically significant. No histological differences were observed between experimental and control populations in mouse liver, spleen, kidney, bone marrow, or brain tissue after 14 days of chronic exposure to salvinorin A (400, 800, 1,600, 3,200, or 6,400 µg/kg). Based on their findings, the researchers concluded that salvinorin A had very little physiological effect, consistent with literature and anecdotal reports.

### *Drug Discrimination*

Butelman et al. published the first investigation of the KOP discriminative effects of salvinorin A in rhesus monkeys.<sup>275</sup> Monkeys were trained to discriminate the KOP agonist U69,593 from vehicle. U69,593 (0.001–0.01 mg/kg) produced dose- and time-dependent generalization, and when tested under identical conditions, salvinorin A (0.001–0.032 mg/kg) also dose-dependently generalized. In a control experiment, the psychoactive NMDA antagonist ketamine (0.1–3.2 mg/kg) was not generalized, indicating that not all hallucinogenic or psychotomimetic compounds are generalized by monkeys trained to discriminate U69,593. Pretreatment with the opioid antagonist quadazocine (0.32 mg/kg) fully blocked the discriminative effects of both U69,593 and salvinorin A. Interestingly, the long-acting, KOP

selective antagonist GNTI only blocked the discriminative effects of salvinorin A in two of the three subjects.

Willmore–Fordham et al. expanded experimentation into rats and also found that salvinorin A fully substituted for U69,593.<sup>276</sup> These effects could be completely blocked by pre-administration of the KOP antagonist norBNI. Baker et al. went further and compared salvinorin A, and two derivatives of salvinorin B (2-methoxymethyl- and 2-ethoxymethylsalvinorin B) to U69,593 and U50,488.<sup>277</sup> The study found that in rats trained to distinguish U69,593 from vehicle, salvinorin A and both salvinorin B derivatives fully substituted for U69,593. Further, they also found that in rats trained to distinguish salvinorin A from vehicle, both U69,593 and U50,488 produced full generalization. This cross-generalization further supports that salvinorin A acts as a KOP agonist. In a follow up study, Killinger et al. found that in rats trained to discriminate the 5-HT<sub>2</sub> agonist LSD from vehicle, salvinorin A did not generalize.<sup>278</sup> Neither did salvinorin A generalize in rats trained to distinguish ketamine from vehicle, further supporting that salvinorin A does not act in the same manner as other known hallucinogens. Finally, Walentiny et al. reported that salvinorin A did not substitute for  $\Delta^9$ -tetrahydrocannabinol ( $\Delta^9$ -THC) in mice trained to discriminate  $\Delta^9$ -THC from vehicle, indicating that salvinorin A does not direct its effects through the cannabinoid receptor system.

In a follow up study to their earlier work, Butelman et al. further expanded their investigation and characterized the discriminative effects of salvinorin A in rhesus monkeys in comparison to an array of structurally diverse KOP agonists, as well as MOP and DOP agonists, a 5-HT<sub>2</sub> agonist, and a NMDA antagonist.<sup>279</sup> In this study, monkeys were trained to discriminate salvinorin A from vehicle. The centrally acting KOP agonists bremazocine, U69,593, and

U50,488 were found to generalize, but the peripherally restricted KOP agonist ICI204,488 was only generalized in one of the three subjects. This result seems to indicate that the effects of salvinorin A are predominantly centrally mediated. Further, the MOP agonist fentanyl, the DOP agonist SNC80, the 5-HT<sub>2</sub> agonist psilocybin, and the NMDA antagonist ketamine were not generalized by any subjects. As before, the opioid antagonist quadazocine fully blocked discriminative stimulus effects of salvinorin A. In contrast, the 5-HT<sub>2</sub> antagonist ketanserin did not cause any blockade. These findings are supported by a study by Li et al. in which U50,488 and salvinorin A did not generalize in rhesus monkeys trained to distinguish the hallucinogenic 5-HT<sub>2</sub> agonist DOM from vehicle (LSD did generalize).<sup>280</sup> Collectively, the results of these studies support that salvinorin A exerts its effects centrally as a KOP receptor agonist and underscore its uniqueness as a hallucinogen.

#### *Antinociceptive Effects*

Since documented ethnomedicinal uses for *S. divinorum* include relief from headaches and rheumatism, several studies have been conducted in animal models regarding the antinociceptive effects of salvinorin A. Wang et al. reported that salvinorin A (30 mg/kg s.c) showed very low and inconsistent activity in the compound 48/80-induced scratching test in mice, which pretreatment with norBNI (20 mg/kg) was able to reverse.<sup>257</sup> They also found salvinorin A (15–50 mg/kg, administered 20 min prior to acetic acid challenge) was similarly inactive in the acetic acid abdominal constriction test in the same species. However, Harding et al. reported the ED<sub>50</sub> of salvinorin A in the *p*-phenylquinone writhing and tail-flick assays in mice to be 0.59 mg/kg and 1.98 mg/kg s.c., respectively, comparable to morphine.<sup>281</sup> They also tested salvinorin A in the hotplate assay, but did not observe any antinociceptive activity. No



time course for these experiments was reported. In a subsequent study, McCurdy et al. confirmed the activity of salvinorin A in the tail-flick assay in mice, observing dose- and time-dependent antinociceptive effects at doses of 1.0, 2.0, and 4.0 mg/kg that could be reversed by pre-treatment with norBNI (10 mg/kg).<sup>282</sup> They also found that salvinorin A (1.0 mg/kg) showed antinociceptive effects in the hotplate test in the same species. Further, they observed robust dose- and time-dependent antinociceptive effects from salvinorin A in the mouse acetic acid abdominal constriction assay. In all of their experiments, McCurdy et al. note the short duration of action of salvinorin A with peak effects being observed at the 10-min time point and diminishing after that. They posit that experimental time course could explain the lack of antinociception in the acetic acid abdominal constriction assay reported by Wang et al.; 20 min after administration the effects of salvinorin A are no longer present. John et al. also confirmed the dose- and time-dependent antinociceptive effects of salvinorin A in the mouse tail-flick assay, and further demonstrated that while the effects of salvinorin A could be reversed by pre-treatment with KOP antagonist norBNI, pre-treatment with the MOP antagonist  $\beta$ FNA or the DOP antagonist naltrindole did not diminish antinociception.<sup>283</sup> Fichna et al. characterized the antinociceptive effects of salvinorin A in a mouse model of inflammatory bowel disease and found that it could attenuate the pain-related behaviors associated with injection of mustard oil; further, the antinociception could be inhibited by both norBNI and the CB1 antagonist AM251, but not the CB2 antagonist AM630.<sup>284</sup> Finally, Ansonoff et al. evaluated the antinociceptive effects of salvinorin A in KOP receptor knockout mice.<sup>285</sup> They found that a dose of 7.5  $\mu$ g injected i.c.v. showed antinociceptive effects in the tail flick assay using wild type mice; in the KOP receptor knockout mice the same dose produced no antinociception. This indicates that the antinociceptive actions of salvinorin A are KOP receptor dependent.

### *Mood Regulation*

Given the previously discussed body of evidence that activation of the KOP receptor system can produce pro-depressive-like behaviors in laboratory animals, several studies investigating the effects of salvinorin A in this area have been published. Carlezon et al. examined the effects of salvinorin A in two rat models of depressive-like behavior, the forced swim test (FST) and the intracranial self-stimulation (ICSS) test.<sup>286</sup> They found that in the FST, salvinorin A produced behaviors that were opposite to those typically elicited by selective serotonin reuptake inhibitors (SSRIs); salvinorin A (0.25–2.0 mg/kg) dose-dependently increased occurrences of immobility, and simultaneously dose-dependently decreased occurrences of swimming behavior. Importantly, the doses of salvinorin A tested were not found to effect locomotor activity in an open field, confirming that the effects of the drug are not due to general, non-specific behavioral depression. The ICSS assay electrically stimulates areas of the brain (in this study, the medial forebrain bundle) associated with reward via an implanted electrode. Rats are then trained to self-stimulate by pushing a lever, and the effects of different drugs can be measured by observing the change in lever-pressing behavior. Addictive drugs lower the electrical threshold required to maintain ICSS, presumably because they enhance the effects of stimulation. Aversive drugs increase the threshold required to maintain ICSS. Salvinorin A (0.5–2.0 mg/kg) was found to dose-dependently increase ICSS thresholds, suggesting that it was able to reduce the rewarding of effects medial forebrain bundle stimulation. This type of observation in rodents reflects anhedonia (a hallmark of clinical depression), therefore providing additional evidence that salvinorin A has pro-depressive like effects. Finally, microdialysis experiments found that 1.0 mg/kg salvinorin A produced a rapid decrease in extracellular

concentrations of DA in the NAc with no effect on 5-HT concentrations. This provides evidence that the effects of salvinorin A in the FST are not due to reduction in 5-HT activity.

Braida et al. expanded the evaluation of the effects of salvinorin A in rodent models of emotional behavior to the elevated plus maze paradigm and the tail suspension test, as well as the FST.<sup>287</sup> The elevated plus maze is used as a rodent model of anxiety. The apparatus includes an open-arm and a closed-arm; a greater number of entries into or a greater percentage of experimental time spent in the open-arm indicates an anxiolytic effect. The study found that in this model, pretreatment with salvinorin A (0.1–160 µg/kg) 20 min prior to maze testing produced an increase in the number of entries into the open-arm similar to the clinically used anxiolytic diazepam. Salvinorin A also increased the percentage of experimental time spent in the open-arm, although to only half the amount of time observed upon treatment with diazepam. Additionally, no dose-related increase in effect was observed. Still, these findings indicate that salvinorin A has some anxiolytic effect. The KOP antagonist norBNI given in combination with the CB1 antagonist AM251 was able to completely block the effects of salvinorin A. In the tail suspension test, salvinorin A (0.001–1.0 µg/kg) produced a significant decrease in the amount of time spent immobile, and this was reversed by both norBNI and AM251, alone or in combination. The reduction in immobility was comparable to treatment with the antidepressant imipramine, suggesting an antidepressant-like effect from salvinorin A. This observation was echoed in the FST, where it was found that salvinorin A (0.001–10 µg/kg) dose-dependently decreased the occurrence of immobility and simultaneously increased swimming. The antagonists norBNI and AM251, alone or in combination, were able to block this effect. These findings appear to be in direct conflict with the findings of Carlezon et al. The authors suggest that the differences between the studies can be explained by dosing. Carlezon et al. administered

relatively large doses of salvinorin A in triple-administration; Braida et al. administered relatively small doses acutely. Although the data were not reported, they state that the highest dose of salvinorin A they used (1 mg/kg) given in triple-administration produced pro-depressant-like effects, indicating that salvinorin A has anxiolytic effects at very low or acute doses, and is a pro-depressant at higher, repeated doses.

Ebner et al. extended the observations of Carlezon et al. regarding the effects of salvinorin A on extracellular DA levels in rats.<sup>288</sup> They found that salvinorin A (2.0 mg/kg) significantly decreased DA release in both the NAc core and NAc shell, in agreement with Carlezon et al. Further, salvinorin A had no impact on the rate of DA reuptake in either brain region. In parallel, through ICSS testing, it was found that salvinorin A dose- and time-dependently increased thresholds, again in agreement with Carlezon et al. A third assay used in the study was operant responding for sucrose reward. In this model, animals are trained to press a lever to obtain a sucrose pellet; the training schedule assesses motivation to respond by progressively increasing the number of lever-presses required to receive the sucrose pellet reward. Alterations in lever-pressing behavior after drug administration can be attributed to changes in motivation or motor deficits. The study found that salvinorin A (2.0 mg/kg) significantly lowered the breakpoint in responding, the point in the schedule where the animals stop lever-pressing behavior, indicative of a decrease in motivation. Salvinorin A also suppressed the rate of lever-pressing. Collectively, these findings confirm the idea that salvinorin A can alter mood states by simultaneously decreasing DA release as well as reward function and motivation.

## *Drug Abuse*

Because the KOP receptor agonists U50,488 and U69,593 were reported to decrease cocaine self-administration in rodents,<sup>155, 158</sup> and because previous literature has shown that cocaine-induced reinstatement of extinguished cocaine self-administration behavior in rodents can be attenuated by pre-treatment with KOP receptor agonists, several groups have undertaken investigations into whether or not salvinorin A has similar effects. Morani et al. reported that KOP agonists salvinorin A, U69,593, U50,488, and spiradoline produced a dose-dependent reduction in cocaine-induced reinstatement in rats.<sup>289</sup> Additionally, Zhang et al. found that salvinorin A (1.0 and 3.2 mg/kg) dose-dependently decreased DA levels in the caudate putamen of mice, and that the decrease was reversible by pretreatment with norBNI, suggesting KOP receptor system involvement.<sup>290</sup> Further, the study found that salvinorin A (1.0 and 3.2 mg/kg) produced conditioned place aversion, which was blocked by pretreatment with norBNI, similar to findings published about other KOP agonists. Gehrke et al. expanded upon these findings and reported that the same doses of salvinorin A also decreased DA in the NAc of rats (in agreement with previously described findings from Carlezon et al.), and that the effect was norBNI-reversible.<sup>291</sup>

Interestingly, Gehrke et al. also found that while acute administration of salvinorin A led to a decrease in DA levels, DA dynamics after repeated administration were unaltered. Additionally, repeated administration of salvinorin A (3.2 mg/kg) appeared to enhance cocaine-induced increases in extracellular DA, but not locomotor activity. This is in contrast to reports in the literature on KOP agonists such as U69,593 that show that repeated administration reduces cocaine-induced locomotor activity. A study by Chartoff et al. investigated whether acute KOP

receptor activation would attenuate the effects of cocaine, whereas prior, repeated KOP receptor activation would potentiate the effects of cocaine.<sup>149</sup> In rats, they found that acute administration of salvinorin A 5 min prior to cocaine challenge blocked cocaine-induced locomotor activity. These conditions also led to increased c-Fos expression (indicative of cAMP or Ca<sup>2+</sup> second messenger system activation) in the NAc, dorsal striatum, and other brain regions. In rats that had been previously repeatedly administered salvinorin A, cocaine-induced locomotor activity was enhanced. This was paired with no change in c-Fos expression in the dorsal striatum. In a follow-up study, Potter et al. found that in rapid response to repeated treatment with salvinorin A, ICSS thresholds in rats increased (decreased reward), whereas in a delayed response (24 h post administration), ICSS thresholds decreased (increased reward).<sup>292</sup> Further, they found that prior, repeated exposure to salvinorin A blunted the ability of cocaine to decrease ICSS thresholds, indicating a reduction in reward-related effects. Treatment with norBNI was able to normalize these effects. Collectively, these findings further underscore that salvinorin A is able to modulate reward-related effects and is unique among KOP receptor agonists.

Given the relatively high doses of salvinorin A used by other studies, Braida et al. characterized the effects of relatively low doses of salvinorin A on DA concentration, conditioned place preference, and self-administration in rats.<sup>293</sup> They found that salvinorin A (40 µg/kg) increased extracellular DA levels in the shell of the NAc. Further, they report that salvinorin A (0.1–40 µg/kg) produced a conditioned place preference. In contrast, a dose of 80 µg/kg had no apparent effect, and a dose of 160 µg/kg provoked aversion. The effects of salvinorin A could be blocked by co-administration of the KOP antagonist norBNI and CB1 antagonist rimonabant, but not by either antagonist alone. Additionally, the study found that at the low doses used (0.1–0.5 µg/2 µL saline), the animals would self-administer salvinorin A; if

the dose was increased to 1  $\mu\text{g}/2 \mu\text{L}$ , self-administration would significantly decrease. The authors suggest that these observations explain salvinorin A use by humans as well as suggest abuse potential. Very low doses are obtained from smoking the leaves, which would account for the reinforcing effect that is modeled by place preference and self-administration in rodents. At the relatively high doses used in other studies, salvinorin A then becomes aversive. Beerepoot et al. reported similar observations; co-administration of U69,593 or 2mg/kg salvinorin A and the  $\text{D}_2/\text{D}_3$  agonist quinpirole potentiated locomotor sensitization to quinpirole, whereas 0.04 mg/kg salvinorin A attenuated quinpirole locomotor sensitization.<sup>294</sup> These findings suggest that the actions of salvinorin A *in vivo* are more complex than previously appreciated.

### **Proposed Salvinorin A and KOP Receptor Binding Interactions**

Since salvinorin A was identified as the first non-nitrogenous opioid ligand, it has challenged previous hypotheses as to the binding epitope of ligands at opioid receptors. Previous hypotheses proposed that a basic nitrogen atom was required for opioid receptor affinity; at physiological pH, the positively charged nitrogen atom in the ligand would interact with an aspartic acid residue (Asp138) in the third transmembrane region of the GPCR.<sup>232-234</sup> However, salvinorin A lacks a nitrogen atom, so it is unlikely that the molecule ionically binds to the receptor in this manner. In support of this, in a study reported by Singh et al., a ligand-based pharmacophore model generated from KOP selective arylacetamide agonists failed to identify salvinorin A as a KOP ligand, suggesting that it binds to the receptor through a unique recognition site.<sup>295</sup> Several studies have been devoted to elucidating the binding interactions between salvinorin A and the KOP receptor, including the development of chimeric opioid receptors, site-directed mutagenesis, as well as computational models. In 2012, both the MOP

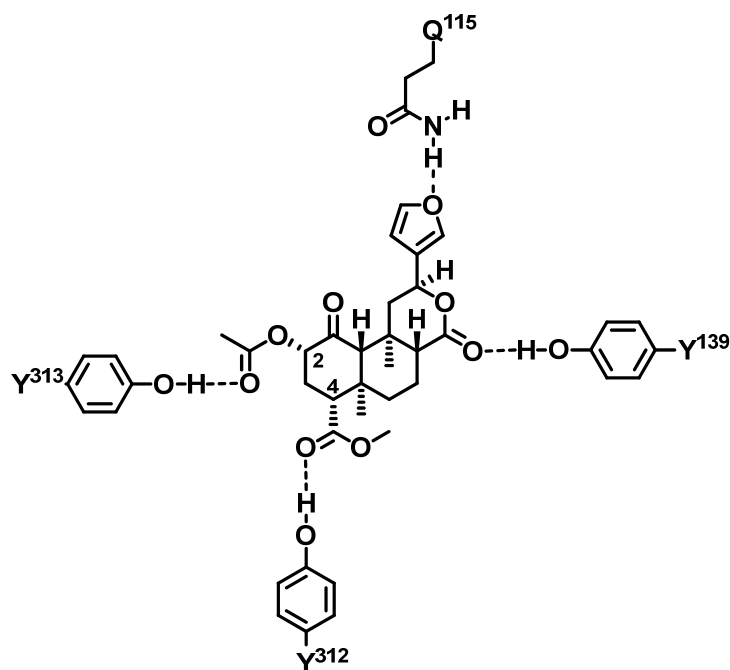


**Figure 23.** Proposed salvinorin A-KOP receptor binding model from Roth et al.

and KOP receptor crystal structures were reported, co-crystallized with the selective antagonists  $\beta$ FNA and JDTe, respectively.<sup>296-297</sup>

In 2002, after they identified salvinorin A as a selective KOP receptor agonist, Roth et al. also attempted to predict ligand–receptor binding interactions via molecular modeling using a previously reported computational model of the KOP receptor and U69,593 as a starting point.<sup>180, 298</sup> In their best ligand–receptor complex, the furan ring of salvinorin A is oriented towards TM1 and TM2, with a proposed hydrogen bonding interaction between Gln115 and the oxygen of the furan (Figure 23). The 4-methoxycarbonyl is oriented towards TM5 and TM6, with a proposed hydrogen bonding interaction between Tyr312 and the carbonyl oxygen. Finally, the carbonyl oxygen of the lactone is proposed to hydrogen bond with Tyr139 and the carbonyl oxygen of the C-2 acetate is proposed to hydrogen bond with Tyr313. They also identified several variable residues in their proposed salvinorin A–KOP receptor binding region



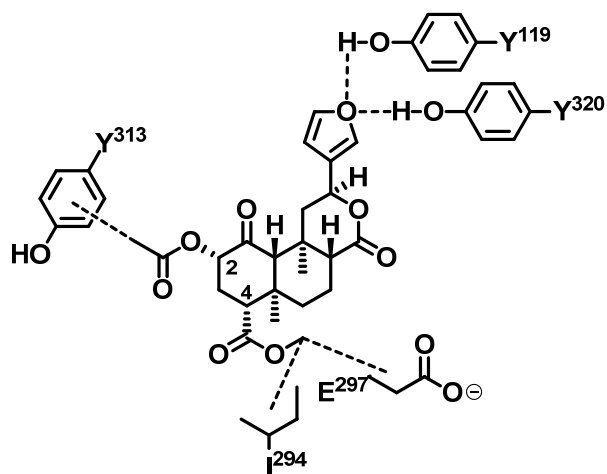


**Figure 24.** Proposed salvinorin A-KOP receptor binding model from Yan et al.

that are not conserved in the MOP and DOP receptors; these residues produce significant electronic and steric alterations that could explain the KOP selectivity of salvinorin A.

In 2005, Yan et al. used site-directed mutagenesis in combination with molecular modeling to attempt to elucidate binding interactions between salvinorin A and the KOP receptor.<sup>299</sup> They observed a dramatic decrease (22-fold) in the binding affinity of salvinorin A to the Y313A mutant; when the mutation was changed to Y313F, no loss in affinity was observed indicating a hydrophobic interaction between Tyr313 and salvinorin A. They also found that mutations to Tyr119, Tyr320, and Tyr139 resulted in loss of affinity; in the cases of Tyr119 and Tyr320, mutation to Phe accounted for the loss of affinity, indicating hydrogen bonding interactions with salvinorin A. The study then translated the mutagenesis observations into a proposed binding model in which the oxygen of the furan ring hydrogen bonds with Tyr119 and Tyr320, the C-2 acetate has hydrophobic interactions with Tyr313, and the C-4 ester interacts with Ile294 and Glu297 (Figure 24).

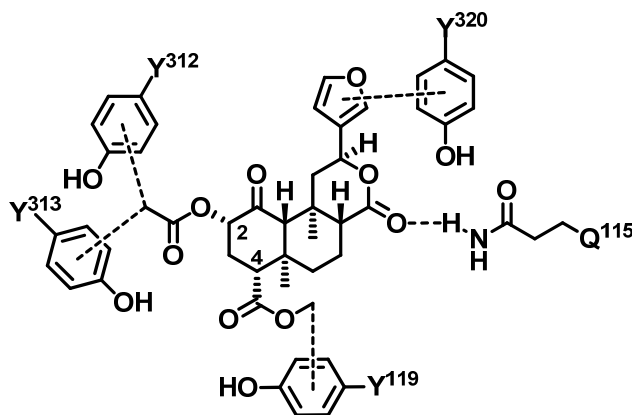


**Figure 25.** Proposed salvinorin A-KOP receptor binding model from Kane et al. (2006).

In 2006, Kane et al. investigated the binding and selectivity of salvinorin A using a combination of chimeric and single-point mutant opioid receptors.<sup>300</sup> Chimeric receptors can probe various receptor regions in order to determine which are required for binding. For this study, chimeric receptors were designed around the *Bgl*III and *Afl*III restriction sites, which are located in TMV and TMIII, respectively. From *Bgl*III chimera, the study found that a combination of KOP(1–227)/DOP(215–372) bound salvinorin A with approximately 10-fold higher affinity ( $2.5 \text{ nM} \pm 0.4$ ) than the wild type receptor ( $17.5 \text{ nM} \pm 1.5$ ). The converse chimera, DOP(1–214)/KOP(228–380) did not bind salvinorin A at all. Additionally, from *Afl*III chimera, it was found that KOP(1–141)/DOP(132–372) showed a considerable loss of affinity ( $910 \text{ nM} \pm 245$ ) compared to the analogous KOP/DOP *Bgl*III chimera ( $2.5 \text{ nM} \pm 0.4$ ). Collectively, these results imply that the KOP region between the *Bgl*III and *Afl*III restriction sites (the latter half of TMIII, IL2, TMIV, EL2, and the beginning of TMV) may play a role in salvinorin A binding. Of these regions, TMIII and IL2 are unlikely due to their depth in the membrane-bound receptor, however EL2 has been implicated in past studies if KOP ligand–receptor interactions. From site-directed mutagenesis the study confirmed the previously

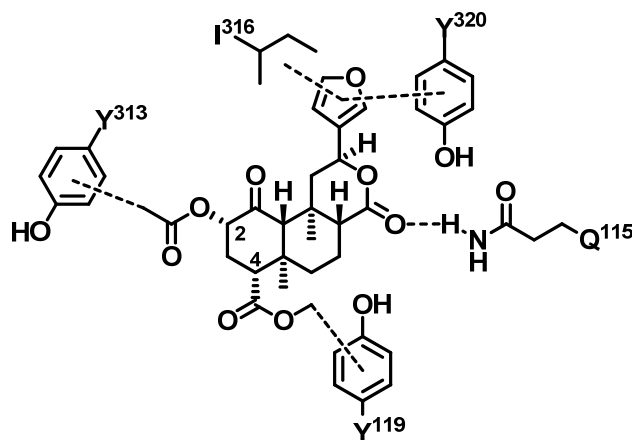


**Figure 26.** Proposed salvinorin A-KOP receptor binding model from Kane et al. (2008).

reported importance of Gln115, Tyr313, and Tyr320 to salvinorin A binding, although other residues were found to have less significant effects on binding than previously observed (Figure 25). Vortherms et al. expanded this research, creating more detailed chimeric receptors in which single TM or loop regions were exchanged between receptor subtypes.<sup>301</sup> They found that substituting the TMII and EL2 regions of the KOP receptor into the MOP or DOP receptors resulted in binding affinity for salvinorin A; conversely, substituting TMII and EL2 from DOP into the KOP receptor markedly reduced salvinorin A binding. Further, through site-directed mutagenesis, the study found that V108A and V118K (both in TMII of KOP receptor) significantly decreased affinity for salvinorin A. Since Val118 does not face into the putative binding pocket of rhodopsin-based KOP receptor models, this finding seems to indicate that the subtype selectivity of salvinorin A for KOP receptors is due to helical rotations of TMII. In a 2008 follow-up study to their 2006 work, Kane et al. further identified Ile316 as an important residue through site-directed mutagenesis; the I316A mutant abolished salvinorin A affinity for the receptor.<sup>302</sup> In the putative binding pocket, Ile316 is located in space between Tyr313 and Tyr320, residues previously identified as having important interactions with salvinorin A (Figure

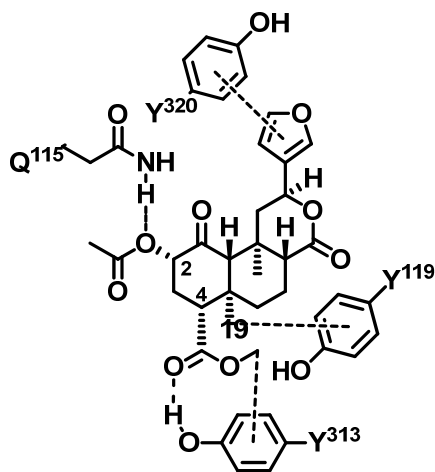


**Figure 27.** Proposed salvinorin A-KOP receptor binding model from Singh et al.

26). This is consistent with the general hypothesis that salvinorin A-KOP receptor binding interactions are primarily hydrophobic.

In 2006, Singh et al. used an integrated approach to develop a model for salvinorin A-KOP receptor binding; they developed quantitative, ligand-based pharmacophores simultaneously refined with target-based methods.<sup>303</sup> First, a training set of 15 previously reported salvinorin A derivatives was used to develop a ligand-based pharmacophore that was validated against a different test set of 12 previously reported derivatives, as well as a set of negative controls (known inactive molecules). The pharmacophore model was successfully able to distinguish between ligands with moderate to low affinity for KOP receptors and did not predict any affinity for the negative control molecules. Some important features of the pharmacophore are hydrophobic regions, corresponding to the furan ring and the C-4 ester, which are 8.38 Å apart, and hydrogen bonding regions around the C-2 acetate and C-4 ester. Next, a target-based model was then created from induced-fit docking of salvinorin A into a binding site guided by previous site-directed mutagenesis studies. In accordance with previously reported data, the salvinorin A binding pocket was formed primarily between TMII and TMVII

and was largely hydrophobic. In accordance with previous reports, the model predicted hydrophobic interactions between the furan ring of salvinorin A and Tyr320 and between the C-19 methyl group and Tyr119. Interestingly, the model also predicted a hydrogen bonding interaction between the ester oxygen of the C-2 acetate and Gln115, and a hydrogen bonding interaction between the C-4 ester carbonyl oxygen and Tyr313, as well as a hydrophobic interaction between the methyl of the ester and the aromatic ring of the residue (Figure 27). Overall, it was found that the hydrophobic and hydrogen bonding regions from the pharmacophore model coincided well with the residues identified from the receptor docked model.

More recently in 2010, McGovern et al. used comparative molecular field analysis (CoMFA) to describe three dimensional quantitative SARs of salvinorin A derivatives.<sup>304</sup> A training set of derivatives modified at the C-2 acetate moiety was correlated with published binding affinity data. This model suggested a region of steric bulk tolerance around the C-2 position that could accommodate alkyl ester chains up to four carbons in length. This region also fell within a hydrophobic pocket formed by Tyr312, Tyr313, and Ile316, residues previously reported to be important to salvinorin A binding.

Finally, in 2012 the co-crystal structure of the human KOP receptor with the antagonist JDtic was published.<sup>297</sup> In the co-crystal structure, the protonated amines in both the piperidine and isoquinoline moieties of JDtic form salt bridges with Asp138, and Tyr312 has a hydrogen bonding interaction with the oxygen of the amide (Figure 28). JDtic also appears to have interactions with Val108, Val118, and Ile294, residues which, along with Tyr312, are different in the KOP receptor vs. the MOP and DOP receptors. Also of note, the isopropyl group of JDtic

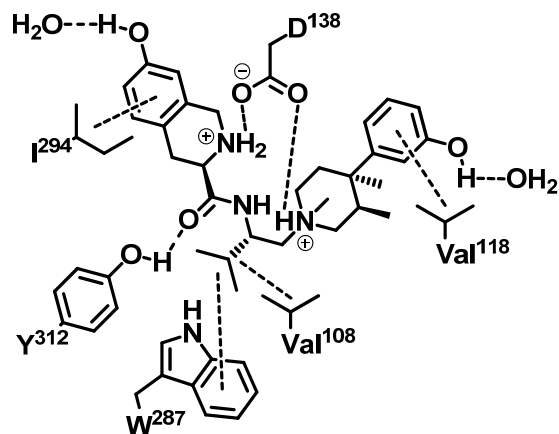


**Figure 28.** Drawing of the crystal structure of JDtic bound in the KOP receptor.

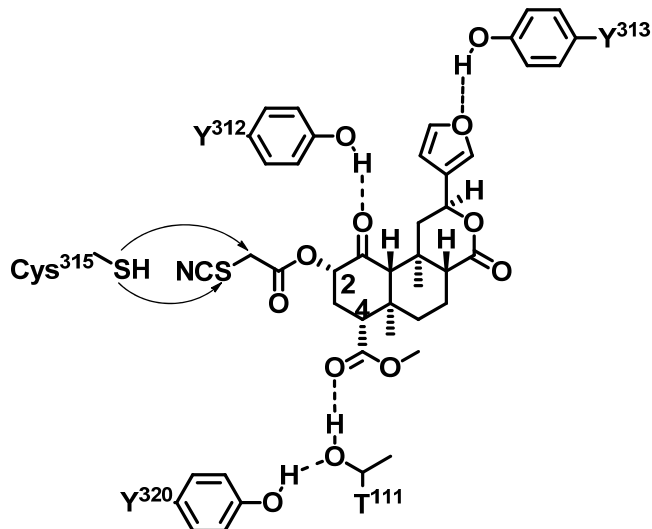


**Figure 29.** Proposed RB-64-KOP receptor binding model.

was observed to form a hydrophobic interaction with a conserved Trp287, a residue thought to be a key part of the GPCR receptor activation mechanism. This finding indicates that this particular residue may have a critical role in the pharmacological properties of JDtic. Using the JDtic–KOP receptor co-crystal structure as a model, the authors attempted to dock 22-thiocyanatosalvinorin A (RB-64, an irreversible KOP agonist that reportedly binds to Cys315 in

the KOP receptor)<sup>305</sup> into the same binding pocket used by JD1c. This study predicted that the 2-position of the salvinorin A scaffold would be able to access Cys315 while maintaining many of the binding interactions implicated by site-directed mutagenesis (Figure 29). Even so, additional studies, such as the co-crystallization of the KOP receptor with a selective agonist or, ideally, with salvinorin A, are still required for the binding interactions of salvinorin A and the KOP receptor to be fully elucidated and understood.

## SAR Studies of Salvinorin A

### Introduction

A wide variety of semi-synthetic modifications have been made to salvinorin A in order to develop SAR at the KOP receptor, and there are published reviews that cover these derivatives.<sup>236, 306-308</sup> The general SAR of the salvinorin A scaffold known presently is summarized in Figure 30. Reduction or removal of the C-1 carbonyl is tolerated, and when removed, the introduction of a 1,10-alkene is likely to be an antagonist. Reduction or hydrolysis of the C-4 ester reduces affinity; replacement with small alkyl groups is tolerated, but larger

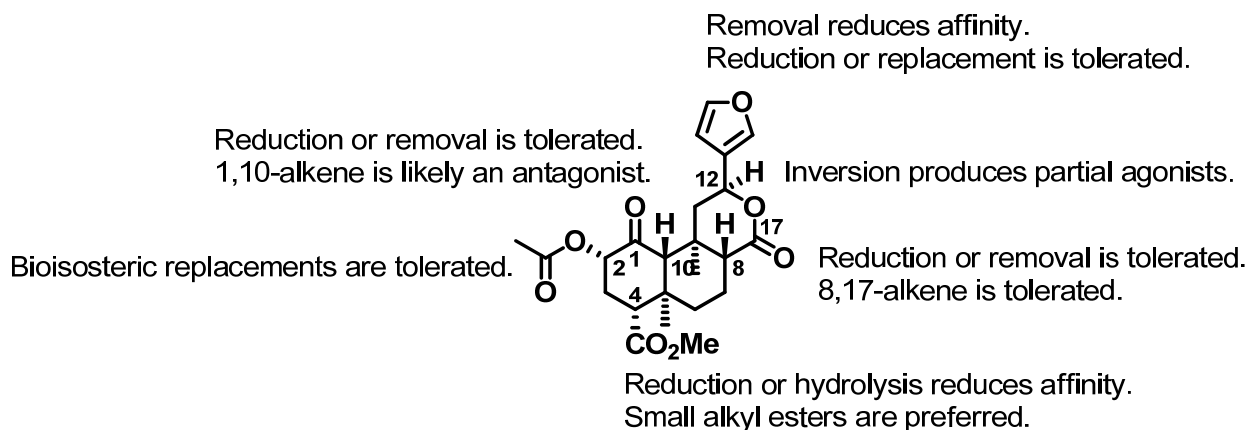


**Figure 30.** General summary of the SAR of salvinorin A analogs.

groups reduce affinity. Reduction of the C-17 lactone is tolerated, as is introduction of a 8,17-alkene. Removal of the furan ring reduces affinity; however, reduction or replacement with other heterocycles is tolerated. Inversion of the stereochemistry at C-12 produces partial KOP agonists. Bioisosteric replacements of the C-2 acetate are tolerated and can modulate receptor selectivity, and these modifications will be discussed in depth.

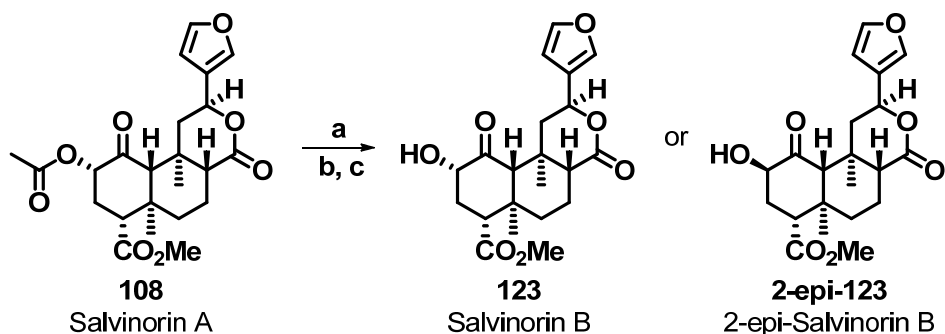
### *Modifications at the C-2 Position*

The most extensively investigated position on the salvinorin A core is the C-2 acetate moiety. This is likely due to relatively easy methodology to selectively hydrolyze the acetate to produce the C-2 free hydroxyl, salvinorin B. In this methodology, salvinorin A is treated with  $\text{Na}_2\text{CO}_3$  in MeOH at room temperature, yielding salvinorin B (**123**) in 77% yield after trituration (Scheme 4).<sup>309</sup> No chromatography is involved. Salvinorin A can also be converted to 2-epi-salvinorin B (**2-epi-123**) through Mitsunobu conditions (DIAD,  $\text{PPh}_3$ ) using 4-nitrobenzoic acid as the nucleophile; the intermediate is subsequently hydrolyzed with  $\text{K}_2\text{CO}_3$  in MeOH to afford **2-epi-123** in 64% yield over the two steps (Scheme 4).<sup>310</sup> From salvinorin B and 2-epi-salvinorin B, modifications have been made to the C-2 position in order to study 1) esters other than acetate, 2) bioisosteric replacements for esters (amides, carbamates, carbonates, sulfonates, and thioesters), and 3) ethers and amines.

### *Herkinorin and Other Ester Modifications*

Because of the relatively straightforward chemistry involved, initial attempts to probe the role of the C-2 carbonyl substituent involved the synthesis of various aliphatic esters. These esters are typically generated using standard acylating conditions; salvinorin B and catalytic 4-(dimethylamino)pyridine (DMAP) are dissolved in  $\text{CH}_2\text{Cl}_2$  and treated with the appropriate acid





**Scheme 4.** Synthesis of salvinorin B and 2-epi-salvinorin B. *Reagents and conditions:*

a)  $\text{Na}_2\text{CO}_3$ , MeOH; b) 4-nitrobenzoic acid,  $\text{PPh}_3$ , DIAD,  $\text{CH}_2\text{Cl}_2$ ; c)  $\text{K}_2\text{CO}_3$ , MeOH

chloride or anhydride in the presence of a weak base (pyridine,  $\text{Et}_3\text{N}$ , or DIPEA), or salvinorin B, EDCI or DCC, and HOBT are dissolved in  $\text{CH}_2\text{Cl}_2$  and treated with the appropriate carboxylic acid in the presence of a weak base ( $\text{Et}_3\text{N}$  or DIPEA) (Figure 31).<sup>256, 311</sup> Modification at the C-2 position has generated analogs with differing activities, from full agonists to partial agonists in the inhibition of cAMP production. Of particular interest, while salvinorin A was found to be a full agonist, propionate **126** ( $K_i = 32.63$  nM,  $\text{EC}_{50} = 4.7$  nM) and heptanoate **130** ( $K_i = 3199$  nM,  $\text{EC}_{50} = 40$  nM) were found to be partial agonists with lower affinity compared to salvinorin A.<sup>256</sup> Salvinorin B, had no affinity at opioid receptors. Subjecting salvinorin B to a mixture of formic acid and acetic acid produced the C-2 formate (**125**), which had decreased affinity and potency at KOP receptors by approximately 5-fold ( $K_i = 18$  nM,  $\text{EC}_{50} = 315$  nM) relative to salvinorin A.<sup>312</sup> Increasing the ester chain to a butyl group (**127**) decreased KOP affinity and potency at KOP receptors approximately 2-fold ( $K_i = 4.9$  nM,  $\text{EC}_{50} = 9.9$  nM) relative to salvinorin A,<sup>311</sup> while adding some MOP receptor affinity ( $K_i = 520$  nM).<sup>313</sup> KOP receptor binding affinity was reported to decrease with increasing ester chain length ( $\text{C}_3$ - $\text{C}_5$ ; **127**, **128**:  $K_i = 15$  nM, **129**:  $K_i = 70$  nM), but no such effect was observed for MOP receptor affinity.

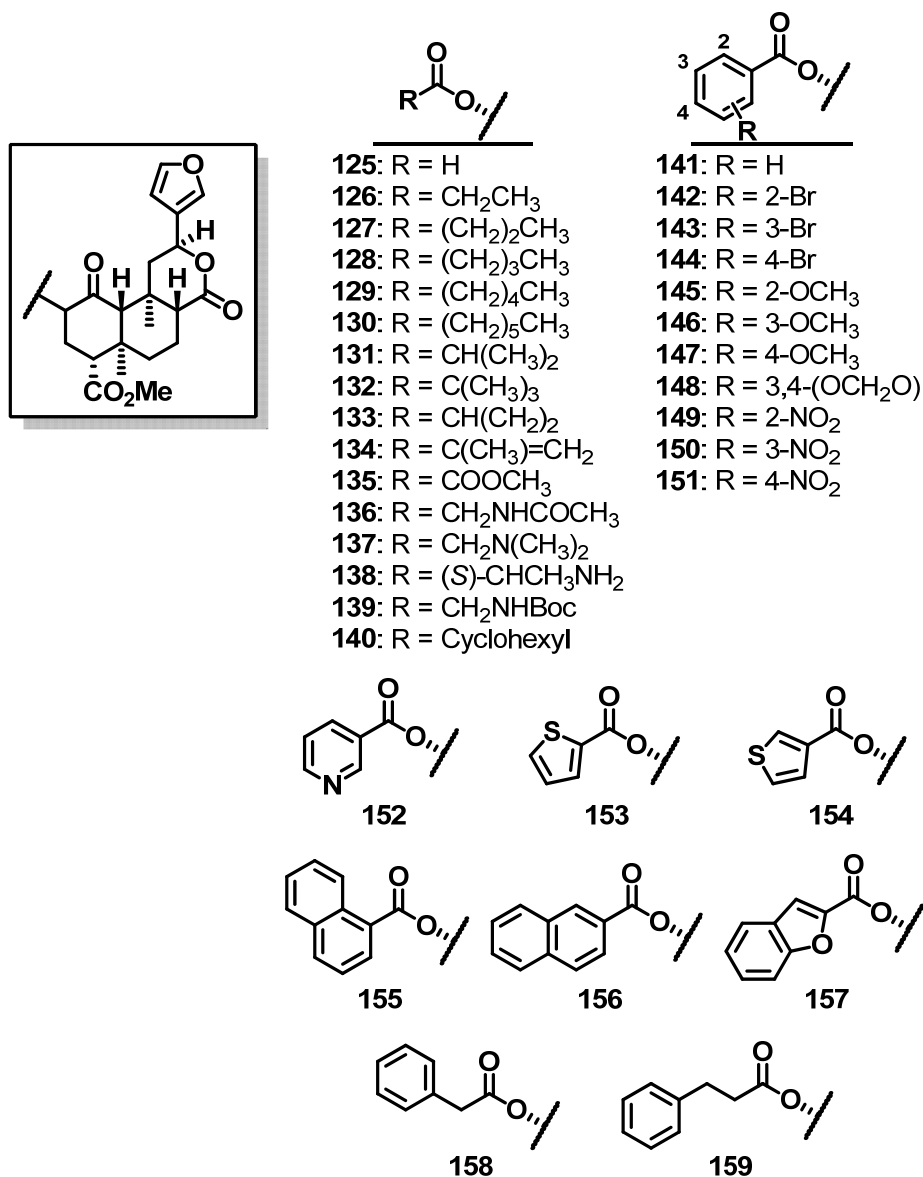


**Figure 31.** Selected C-2 ester analogs of salvinorin A.

Branching is generally poorly tolerated at the KOP receptor; isopropyl **131** had 10-fold decreased affinity ( $K_i = 19$  nM) compared to salvinorin A,<sup>281</sup> and *tert*-butyl **132** and cyclopropyl **133** abolished affinity ( $K_i > 10,000$  nM).<sup>256</sup> Introduction of an alkene to the isopropyl (**134**) resulted in a 20-fold decrease in KOP receptor affinity ( $K_i = 42$  nM) relative to salvinorin A (2-fold decrease relative to **131**) and a 4-fold increase in MOP receptor affinity ( $K_i = 260$  nM) (11-

fold increase relative to **131**).<sup>281</sup> Substitution of the 2-methylacroyl group in **134** with a methyl glyoxyl group (**135**) led to a 10-fold loss in KOP receptor affinity ( $K_i = 430$  nM).<sup>281</sup>

Introduction of nitrogen containing substituents generally has detrimental effects on KOP receptor affinity. KOP affinity was abolished ( $K_i > 10,000$  nM) for acetamido **136**, as well as for derivatives **137** and **138**, both of which contain basic amino substituents.<sup>311</sup> Introduction of a *tert*-butoxycarbonylamino (Boc) group (**139**) reduced affinity for KOP receptors by 47-fold ( $K_i = 90$  nM) relative to salvinorin A.<sup>313</sup>

Incorporation of aromaticity at the C-2 position has produced one of the most interesting salvinorin A analogs to date. A benzoyl substitution at C-2 (**141**, herkinorin) reduced affinity for KOP receptors 47-fold ( $K_i = 90$  nM), but increased MOP receptor affinity 83-fold ( $K_i = 12$  nM) compared to salvinorin A ( $K_{iKOP} = 1.9$  nM,  $K_{iMOP} > 1,000$  nM).<sup>281</sup> The [<sup>35</sup>S]GTP- $\gamma$ -S functional assay revealed herkinorin to be a selective, full agonist at MOP receptors ( $EC_{50MOP} = 500$  nM,  $EC_{50KOP} = 1320$  nM), signifying the first example of a non-nitrogenous MOP agonist. Pharmacological evaluation has found that, unlike morphine and DAMGO, herkinorin does not promote the recruitment of  $\beta$ -arrestin-2 to the MOP receptor, nor does it promote receptor internalization, even in cells engineered to overexpress GRK.<sup>314</sup> This makes herkinorin a striking example of functional selectivity/biased agonism at opioid receptors and a useful tool for the study of opioid tolerance and dependence. It has been hypothesized that  $\beta$ -arrestin mediated receptor desensitization and internalization are responsible for the development of tolerance to and dependence upon opioid agonists. However, *in vitro* studies comparing herkinorin (non-internalizing) and DAMGO (internalizing) revealed that chronic treatment with either drug resulted in cellular signs of tolerance and dependence, indicating that internalization is perhaps

not a critical factor in these phenomena.<sup>315</sup> Studies of prolactin levels in non-human primates have provided neuroendocrine evidence that herkinorin has both MOP and partial KOP agonist effects *in vivo*.<sup>316</sup> In a recent study, it was found that not only did herkinorin produce dose-dependent, naloxone-reversible antinociceptive effects in rats in the formalin test, but chronic herkinorin treatment (5-day) did not diminish efficacy, and herkinorin produced antinociceptive effects in rats made opioid tolerant through chronic morphine treatment.<sup>317</sup> Collectively, all these studies highlight the uniqueness of herkinorin and its potential as a biological probe as well as a pharmacotherapy, and underscore the value of the salvinorin A scaffold for opioid ligand research.

After the identification of herkinorin, the structural features responsible for MOP/KOP receptor selectivity were investigated. Aromaticity plays an important role, as the cyclohexyl analog **140** showed greatly reduced affinity at all opioid receptors ( $K_i > 1,000$  nM).<sup>318</sup> Incorporation of a 2-Br (**142**) or 3-Br (**143**) substituent to the aromatic ring had no effect on KOP affinity, but decreased MOP affinity 9-fold (for both,  $K_i = 110$  nM) compared to herkinorin.<sup>313</sup> The 4-Br substituent (**144**) caused an 8-fold decrease in KOP affinity ( $K_i = 740$  nM) relative to herkinorin, while maintaining MOP affinity,<sup>313</sup> in contrast to a previous study indicating that **144** had no MOP affinity.<sup>256</sup> Incorporation of electron-donating and electron-withdrawing substituents on the aromatic ring was also examined. Addition of a 2-substituent (**145**, **149**), regardless of the electronic nature, decreased both MOP and KOP affinity, implying that steric interactions may hinder the binding of these ligands.<sup>318</sup> In comparison to herkinorin, introduction of a 3-OMe (**146**:  $K_i = 30$  nM) or 4-OMe (**147**:  $K_i = 70$  nM) substituent decreased MOP affinity approximately 3-fold and 6-fold, respectively, however KOP affinity was decreased 6-fold (for both  $K_i = 550$  nM), resulting in a net increase in receptor selectivity for

MOP.<sup>318</sup> Piperonylate **148** showed no affinity for opioid receptors.<sup>256</sup> Addition of a 3-NO<sub>2</sub> substituent (**149**) completely abolished MOP receptor affinity and reduced KOP receptor affinity 10-fold compared to herkinorin, and the addition of a 4-NO<sub>2</sub> substituent (**151**) reduced MOP affinity 22-fold ( $K_i = 260$  nM) and KOP affinity 6-fold ( $K_i = 570$  nM).<sup>318</sup> Additionally, 4-position derivatives **144**, **147**, and **151**, similarly to herkinorin, did not promote  $\beta$ -arrestin-2 recruitment or MOP receptor internalization.<sup>318</sup>

Heteroaromatic and extended chain aromatic esters at the C-2 position have also been investigated. Nicotinoyl ester (**152**) showed a 6-fold loss in MOP affinity ( $K_i = 73$  nM) relative to herkinorin, and a 21-fold loss in KOP affinity ( $K_i = 1930$  nM).<sup>281</sup> Replacement of the benzoyl group in herkinorin with a 2-thiophene (**153**) reduced KOP affinity 3-fold ( $K_i = 260$  nM) with little effect on MOP affinity, and the 3-thiophene analog (**154**) was essentially indistinguishable from herkinorin.<sup>318</sup> The 1-naphthoyl derivative (**155**) abolished MOP affinity,<sup>256, 318</sup> however, the 2-naphthoyl derivative (**156**) showed a 15-fold ( $K_i = 180$  nM) decrease in MOP receptor affinity relative to herkinorin and a 61-fold decrease ( $K_i = 5490$  nM) in KOP receptor affinity.<sup>318</sup> Similar to 3-thiophene **154**, benzofuran **157** was essentially indistinguishable from herkinorin.<sup>318</sup> However, extension of the aromatic ring by one (**158**) or two (**159**) carbons reduced binding affinity over all, and in the case of **159** also abolished MOP/KOP receptor selectivity (**158**:  $K_{iMOP} = 1090$  nM,  $K_{iKOP} = 290$  nM; **159**:  $K_{iMOP} = 280$  nM,  $K_{iKOP} = 180$  nM).<sup>313</sup>

#### *Bioisosteric Replacements for Esters at C-2*

Amide substituents as bioisosteric replacements for the C-2 acetate have been investigated (Figure 32). These analogs are generated by first converting salvinorin B to the  $\beta$ -halogen (**160**) with either SOCl<sub>2</sub> or CBr<sub>4</sub>/PPh<sub>3</sub>, followed by SN<sub>2</sub> displacement with NaN<sub>3</sub> to yield

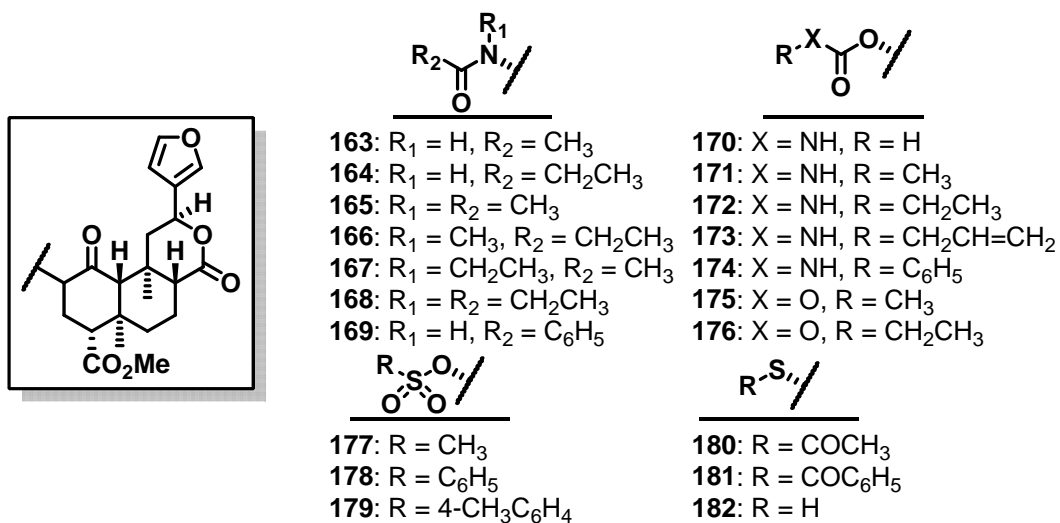
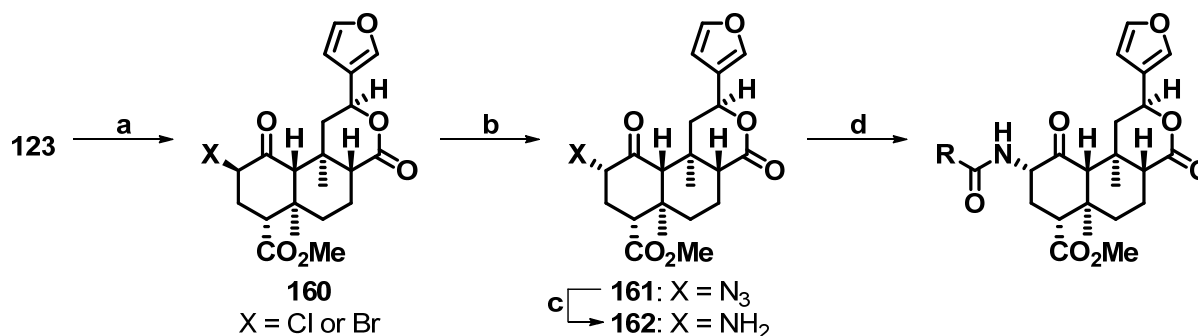


**Figure 32.** Selected C-2 bioisosteric analogs of salvinorin A.

the C-2 azide (**161**, Scheme 5).<sup>310, 318</sup> Azide **161** can then be reduced to the primary amine (**162**) with either TMSCI/NaI in  $CH_3CN$  or zinc metal and  $NH_4Cl$ , and amides produced using standard coupling conditions of the appropriate acyl chloride or anhydride and catalytic DMAP in the presence of weak base. Substitution of an acetamido group (**163**) decreases affinity and potency at KOP receptors, and extension to a propionamido (**164**) continues the trend.<sup>310, 318</sup> The *N*-methyl analogs of **163** (**165**) and **164** (**166**) showed similar affinity and potency to salvinorin A ( $K_i = 1.3$  nM,  $EC_{50} = 4.5$  nM), although **166** did exhibit increased potency ( $EC_{50} = 0.75$  nM).<sup>310</sup> A similar trend is observed with *N*-ethyl substituents of **163** (**167**) and **164** (**168**), however, **167** and **168** have lower affinity and potency than **165** and **166**.<sup>310</sup> Similar to herkinorin, the *N*-benzamide analog **169** had increased affinity and selectivity for MOP over KOP receptors ( $K_i = 3.1$  nM), making it the most potent ( $EC_{50} = 360$  nM) MOP agonist ever derived from salvinorin A.<sup>318</sup> Unlike herkinorin, benzamide **169** was found to promote MOP receptor desensitization and internalization.<sup>318</sup>



**Scheme 5.** Synthesis of amide derivatives. *Reagents and conditions:* a) SOCl<sub>2</sub>, NEt<sub>3</sub>, ClCH<sub>2</sub>CH<sub>2</sub>Cl or CBr<sub>4</sub>, PPh<sub>3</sub>, CH<sub>2</sub>Cl<sub>2</sub>; b) Na<sub>3</sub>N, DMF, AcOH; c) TMSCl, NaI, CH<sub>3</sub>CN or Zn, NH<sub>4</sub>Cl, MeOH, CH<sub>2</sub>Cl<sub>2</sub>; d) appropriate acyl chloride or anhydride, DMAP (cat.), NEt<sub>3</sub>, CH<sub>2</sub>Cl<sub>2</sub>.

Carbamoyl derivatives at the C-2 position were synthesized by exposing salvinorin B to the appropriate isocyanate in the presence of catalytic DMAP or TMSCl.<sup>281, 311</sup> Replacement of the acetyl group with a carbamate (**170**) was well tolerated and had very similar in affinity and potency to salvinorin A.<sup>311</sup> Extension to a *N*-methyl- (**171**) or *N*-ethyl carbamate (**172**) produced a trend of decreasing KOP affinity and potency.<sup>311</sup> Incorporation of an allyl carbamoyl group (**173**) decreased affinity at KOP receptors 63-fold ( $K_i = 120$  nM) relative to salvinorin A, but showed moderate MOP affinity ( $K_i = 640$  nM).<sup>281</sup> Phenylcarbamoyl **174** maintained similar KOP affinity to **173**, but increased MOP affinity ( $K_i = 16$  nM) similar to herkinorin.<sup>281</sup> Initially, carbonates (produced using the appropriate chloroformate and catalytic DMAP) appeared to be poorly tolerated at KOP receptors; carbonates **175** and **176** completely abolished affinity.<sup>319</sup> However, in a more recent study, carbonate **176** was found to have modest KOP affinity ( $K_i = 171$  nM).<sup>320</sup> This difference may be attributed to choice of radioligand for the binding assay; [<sup>3</sup>H]bremazocine and [<sup>3</sup>H]diprenorphine in the earlier study, and [<sup>3</sup>H]U69,593 in the more recent study.

Sulfonate esters (synthesized by treating salvinorin B with the appropriate sulfonyl chloride in the presence of catalytic DMAP) have also been targeted as replacements for the C-2 acetate.<sup>281, 313</sup> Substitution of a mesylate group (**177**) produced KOP receptor affinity and potency very similar to that of salvinorin A.<sup>281</sup> Benzenesulfonate **178** had 32-fold reduced affinity at KOP receptors ( $K_i = 60$  nM) compared to salvinorin A, and surprisingly, unlike the aromatic ester (herkinorin), amide, and carbamoyl derivatives, had no affinity for MOP receptors.<sup>313</sup> Incorporation of a 4-methyl group to **178** (**179**) showed little change in KOP affinity, but increased MOP affinity ( $K_i = 220$  nM).<sup>313</sup> Collectively, the SAR for sulfonate esters does not parallel the SAR for standard esters, implying that these “bioisosteres” are not actually binding to the receptor identically.

Thioester bioisosteric analogs at the C-2 position are synthesized in very similar fashion to the amide analogs: salvinorin B is converted to the  $\beta$ -halogen (**160**) at C-2 (Scheme 5).<sup>318, 321</sup> Replacement of the C-2 acetate with a thioacetate (**180**) decreased both affinity and potency at KOP receptors.<sup>318, 321</sup> As with the ester and the amide derivatives, incorporation of a benzene ring in the C-2 position (**181**) increased MOP affinity ( $K_i = 290$  nM).<sup>318</sup> Removal of the acetyl group to the free thiol (**182**) decreased KOP affinity and potency.<sup>321</sup>

#### *C-2 Ether, Amine, and Halogen Analogs*

The conversion of salvinorin A to various ethers has generated a large number of analogs (Figure 33). Generally, simple alkyl ethers at the C-2 position are synthesized by treating salvinorin B with the appropriate alkyl halide in the presence of  $Ag_2O$  or DMAP and weak base.<sup>310-311, 319, 322</sup> Methyl ether derivative (**183**) was very similar to salvinorin B and had 169-fold reduced KOP affinity ( $K_i = 220$  nM) and 82-fold reduced KOP potency ( $EC_{50} = 389$  nM)



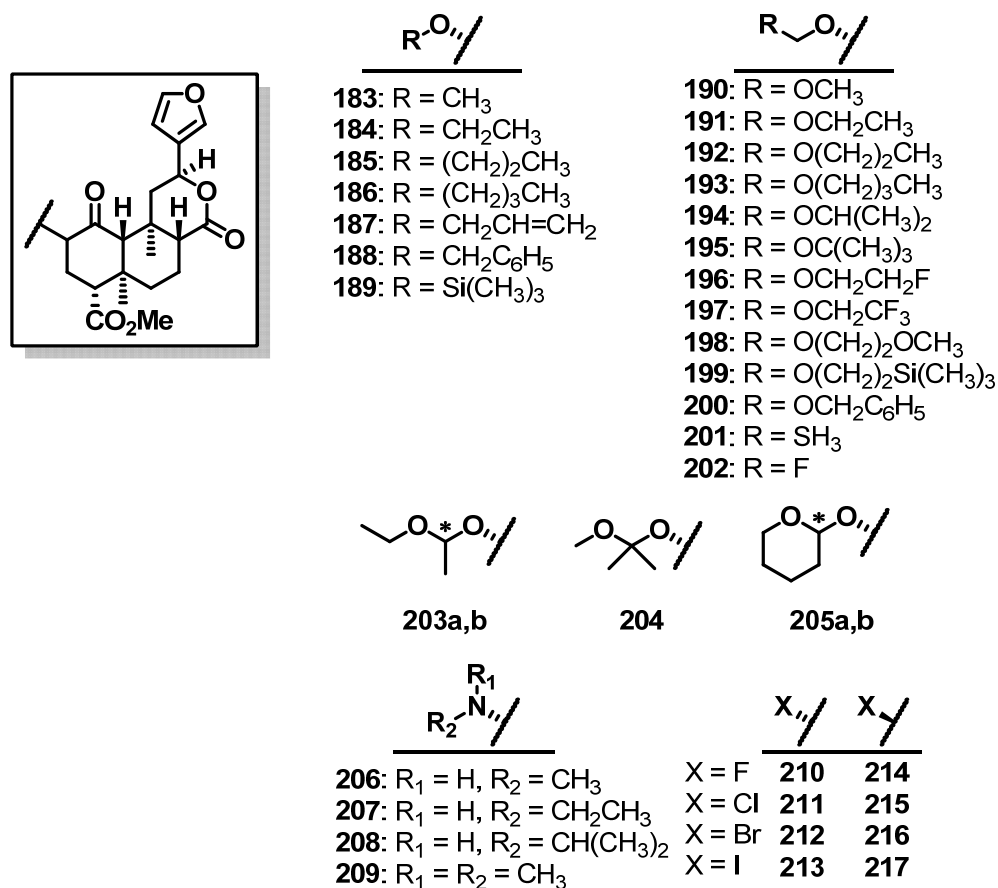


**Figure 33.** Selected C-2 ether, amine, and halogen analogs of salvinorin A.

compared to salvinorin A.<sup>311</sup> Extension of the chain to ethyl (**184**) increases KOP affinity and potency ( $K_i = 7.9$  nM,  $EC_{50} = 18.6$  nM), but further chain extension beyond that (**185**, **186**), including allyl (**187**) and benzyl (**188**), returns to a trend of increasingly diminished affinity and potency.<sup>311</sup> Trimethylsilyl ether (**189**) had essentially no affinity for opioid receptors.<sup>281</sup>

Introduction of a methoxymethyl ether (**190**) at the C-2 position was found to increase affinity and potency at KOP receptors ( $K_i = 0.4$  nM,  $EC_{50} = 0.6$  nM) greater than that of salvinorin A.<sup>319</sup> One possible explanation for this is that the additional oxygen substituent could be involved in synergistic binding interactions with the KOP receptor.<sup>322</sup> This finding prompted investigation into a large series of oxygenated, halogenated, and silylated C-2 methyl ether

derivatives. Aliphatic straight-chain (**192**, **193**) and branched (**194**, **195**) derivatives showed similar affinity and potency compared to salvinorin A.<sup>322</sup> Ethoxymethyl ether derivative **191** demonstrated the highest KOP affinity and potency ( $K_i = 0.32$  nM,  $EC_{50} = 0.14$  nM) of all salvinorin A derivatives known to date.<sup>322</sup> The incorporation of halogen atoms (**196**, **197**, **202**) and additional oxygen atoms (**198**) had the effect of reducing KOP affinity and potency compared to **191**.<sup>322</sup> Silyl **199** and benzyl **200** also showed a loss of affinity and potency compared to both **191** and salvinorin A.<sup>322</sup> Conversion of **190** to the methyl thiomethyl analog (**201**) caused a 22-fold drop in KOP affinity ( $K_i = 13$  nM) and a 78-fold drop in potency ( $EC_{50} = 31$  nM).<sup>322</sup> Alkylation of the acetal carbon had a negative effect on KOP affinity and potency relative to **191**. These ether derivatives are produced by treating salvinorin B with the appropriate alkene in the presence of catalytic *p*-TsOH or PPTS.<sup>322</sup> Epimers **203a** and **203b** were partially separated from each other (absolute configuration undetermined) had found to have reduced affinities and potencies (**203a**:  $K_i = 11$  nM,  $EC_{50} = 10$  nM; **203b**:  $K_i = 6.6$  nM,  $EC_{50} = 5.7$  nM) in comparison to **191**, but were comparable to salvinorin A.<sup>322</sup> Dimethyl analog **204** showed even further reduced affinity and potency ( $K_i = 72$  nM,  $EC_{50} = 72$  nM).<sup>322</sup> The epimeric mixture of tetrahydropyran **205** had similar affinity and potency ( $K_i = 4$  nM,  $EC_{50} = 2.8$  nM) to salvinorin A, however as they were not separated, the effects of the individual epimers remains to be determined.<sup>322</sup>

Amines can be installed at the C-2 position by converting 2-epi-salvinorin B to the triflate and then displacing with the appropriate alkyl amine.<sup>310-311</sup> The conversion of the methoxy group in **183** to a methylamino (**206**) decreased both affinity and efficacy at KOP receptors.<sup>310</sup> Increasing the chain length to ethyl (**207**) or isopropylamino (**208**), or adding an *N*-methyl (**209**),

increased KOP affinity and potency relative to **206**, but was still less compared to salvinorin A.<sup>310</sup>

Although halogenation of the C-2 position has been reported for intermediates in the synthesis of other analogs,<sup>318, 323</sup> a full series of C-2 halogenated analogs was not described until very recently.<sup>324</sup> Pharmacological evaluation revealed that C-2- $\beta$  analogs (**214**, **215**, **216**) generally displayed higher affinity and efficacy than their C-2- $\alpha$  counterparts (**210**, **211**, **212**), with the exception of iodo analogs **213** and **217** which had approximately equal affinity and potency.<sup>324</sup> Overall, installation of a halogen atom in place of the C-2 acetate diminished affinity and potency at KOP receptors.

#### *C-2 Epimer Analogs*

Finally, the stereochemical requirements of the C-2 position have been examined (Figure 34). C-2 inverted analogs of salvinorin A can be synthesized using previously described synthetic methods, but simply starting from 2-epi-salvinorin B (or by starting from salvinorin B in the case of C-2 amine derivatives). Inversion of the C-2 acetate of salvinorin A (**218**) resulted in decreased affinity at KOP receptors, but was also the first neoclerodane diterpene reported to have DOP antagonist activity.<sup>325</sup> Additionally, amine **219** was the most potent amine analog reported, approximately equal to salvinorin A at KOP receptors.<sup>310</sup> In spite of these two interesting analogs, epimerization at the C-2 position was generally found to be detrimental for opioid binding affinity and potency of esters, ethers, thiols, amides, and amines.<sup>310, 321</sup>

Even though a large number of C-2 analogs of salvinorin A have already been made, there is still opportunity for further investigation. This is especially true regarding the stereochemical preferences of C-2 ligands with additional stereocenters. Continued investigation

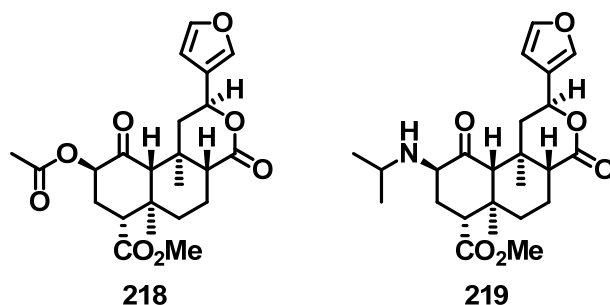


**Figure 34.** Selected C-2 epimeric analogs of salvinorin A.

of such ligands will inevitably lead to deeper understanding of the SAR of the salvinorin A scaffold, and will potentially provide new biological probes for the study of opioid receptors or new pharmacotherapies to treat disease.

### Rationale and Specific Aims

Salvinorin A is a selective KOP receptor agonist that is structurally unique from other known opioid ligands. This is important because a novel structural motif grants the possibility that compounds may be developed with altered pharmacological and side effect profiles at opioid receptors. The development of herkinorin, a potent MOP agonist, shows that the opioid receptor selectivity of the salvinorin A scaffold can be modulated through synthetic changes. Relatively recent research has also revealed that modifications to the salvinorin A scaffold are tolerated at the KOP receptor, and even improve affinity and potency (e. g. ethers **190** and **191**). However, as alkoxy ethers **190** and **191** have a relatively high degree of conformational flexibility, the structural basis underlying their improved profiles is not currently known. Because opioid receptors themselves have been linked to a variety of conditions from pain to mood disorders and drug abuse, further development of salvinorin A SAR promises to yield novel opioid ligands that may be used as biological probes and/or eventually as clinical therapies. Since the endogenous opioid system has also been linked to other endogenous systems, such as the cannabinoid system

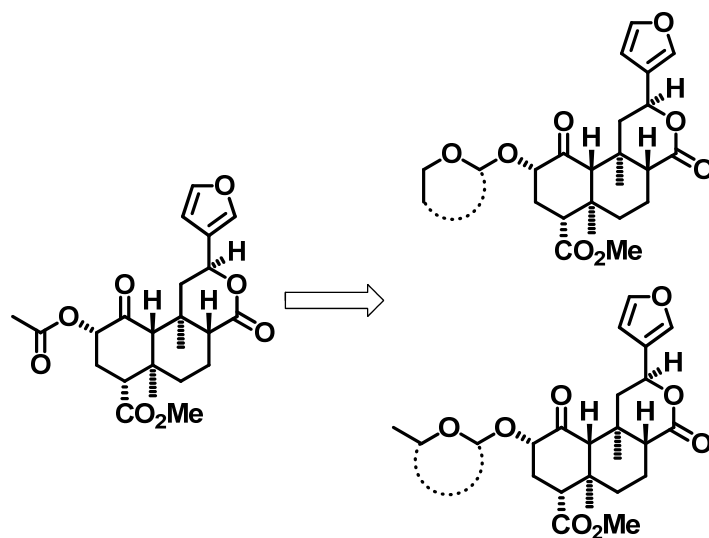


**Figure 35.** Eclipsed (upper) or extended (lower) conformations of the ethoxymethyl ether at C-2 compared to salvinorin A.

as well as the physiological stress response, investigation into salvinorin A SAR also has the potential to uncover new pharmacological targets for CNS disease treatment.

**Specific Aim 1: Prepare selected analogs of salvinorin A at the C-2 position through semi-synthesis in order to elucidate the binding mode of alkoxy ethers at C-2.**

Research has shown that modifications made to replace the acetate off the C-2 position in the salvinorin A scaffold are tolerated at opioid receptors. Specifically, converting the acetate to a benzoyl to make herkinorin (**141**) alters the receptor selectivity of the scaffold from KOP to MOP.<sup>281</sup> Converting the acetate to a methoxy- (**190**) or ethoxymethyl (**191**) ether improves both KOP affinity and potency.<sup>322</sup> However, the structural basis that underlies this improvement is unknown. One hypothesis is that the alkoxy ether moieties at C-2 are rather flexible and can adopt different conformations when interacting with the KOP receptor; for example an eclipsed or an extended conformation (Figure 35). Another possibility is that the oxygen atom in the alkoxy ether moieties could participate in hydrogen bonding interactions with the receptor that

are not exploited by salvinorin A. Thus C-2 modified derivatives of salvinorin A will be synthesized in order to further describe the SAR of salvinorin A while identifying analogs with more desirable pharmacological profiles than the parent molecule. The concept of conformational constraint will be applied in order to design ligands in which the flexible portions have been pre-organized. Cyclic ligands such as tetrahydropyrans and tetrahydrofurans will directly mimic both the eclipsed and extended conformations and probe steric tolerances. Acyclic ligands such as a formate, a carbonate, and a carbamate will also probe steric tolerances as well as the effects of electronic changes on affinity and potency. Analogs at the C-2 position will have improved or comparable receptor affinity, selectivity, and efficacy compared to the parent ligands. They will also aid in the investigation and elucidation of the structural basis for the observed improvements in affinity and potency of alkoxy ether ligands over salvinorin A.

**Specific Aim 2: Evaluate C-2 analogs of salvinorin A for opioid receptor affinity and efficacy through radioligand binding, [<sup>35</sup>S]GTP- $\gamma$ -S, and fluorescent calcium mobilization assays.**

Using known methodology, compounds generated from Specific Aim 1 will be evaluated for *in vitro* affinity at opioid receptors through the displacement of the ligands [<sup>3</sup>H]DAMGO (MOP), [<sup>3</sup>H]DADLE (DOP), and [<sup>3</sup>H]U69,593 (KOP).<sup>213</sup> Selected compounds having receptor affinity of  $K_i \leq 100$  nM will be further evaluated for efficacy in the [<sup>35</sup>S]GTP- $\gamma$ -S functional assay using a known protocol.<sup>68</sup> Other selected compounds will be evaluated in the fluorescent calcium mobilization assay using a known protocol.<sup>214</sup> A second functional assay was selected in order to confirm rank-order potencies among the compounds tested. Since the fluorescent calcium mobilization assay is a different format from the [<sup>35</sup>S]GTP- $\gamma$ -S assay, preservation of

rank-order potencies of compounds between the two assays supports that the data being generated is not an artifact of the particular assay system. These proposed assays are intended to characterize the opioid receptor behavior of C-2 analogs of salvinorin A.

**Specific Aim 3: Use molecular modeling in order to further examine the possible binding mode of C-2 alkoxy ethers in the KOP receptor crystal structure.**

With the very recent publication of the co-crystal structure of the KOP receptor and JDTic, it may be possible to explain binding and functional data through docking studies with the ligands of interest.<sup>297</sup> Additionally, a model of salvinorin A in the KOP crystal structure would aid in elucidating which of the several proposed residues are actually important for receptor binding interactions. Further, the development of a reliable salvinorin A–KOP receptor model would allow for *in silico* design and testing of ligands and enhance the SAR development process. To this end, compounds generated from Specific Aim 1 will be evaluated in receptor docking studies based on the KOP–JDTic co-crystal structure, and their docking scores will be compared with binding and potency data generated from Specific Aim 2. If the model is viable, the calculated docking scores will correlate with the *in vitro* binding affinity and/or potency data from Specific Aim 2, and the model may be used in the future for *in silico* ligand design and evaluation.

The purpose of these specific aims is to provide greater insight into the role the C-2 position plays in opioid affinity and potency. Generating and evaluating such compounds also provides further support that the salvinorin A scaffold can be amended to produce ligands with altered opioid receptor interactions. These ligands will serve as novel opioid receptor probes and may lead to the development of new therapies for clinical use. The ability to develop novel

opioid ligands based on the structure of salvinorin A demonstrates its value as a lead molecule, and suggests that the neoclerodane diterpene structural class may be useful as a generic scaffold for the construction of molecules with opioid receptor activity. The results of these studies will be presented and discussed.

## **Results and Discussion**

### *Introduction*

In an effort to elucidate the binding conformation of C-2 ether analogs of salvinorin A in hopes of explaining the improved affinity and potency, a series of derivatives was generated. These compounds were meant to mimic either the eclipsed or extended conformation that may be adopted by alkoxy ether **191** (Figure 35). In order to mimic the eclipsed conformation, unsubstituted tetrahydrofuran and tetrahydropyran derivatives were designed and produced; tetrahydropyrans would directly mirror the eclipsed conformation and tetrahydrofurans would probe the size requirements of the binding pocket. In order to mimic the extended conformation, acyclic, branched ethers were synthesized in which the carbon between the oxygen atoms was alkylated. Analogs in which the alkylation was a methyl group tested flexibility requirements; they are less conformationally flexible than the unbranched alkoxy ethers, but more flexible than the ring-constrained derivatives. Analogs in which the alkylation was a methyl-bromo moiety probed flexibility requirements as well as steric tolerances. In order to directly mirror the extended conformation, methylated tetrahydropyran derivatives were produced. A formate at C-2 investigated size requirements for binding, having only one additional carbon atom and one additional oxygen atom compared to salvinorin B. Extending the C-2 moiety to an ethyl carbonate once again was a model for the extended conformation, but with the additional

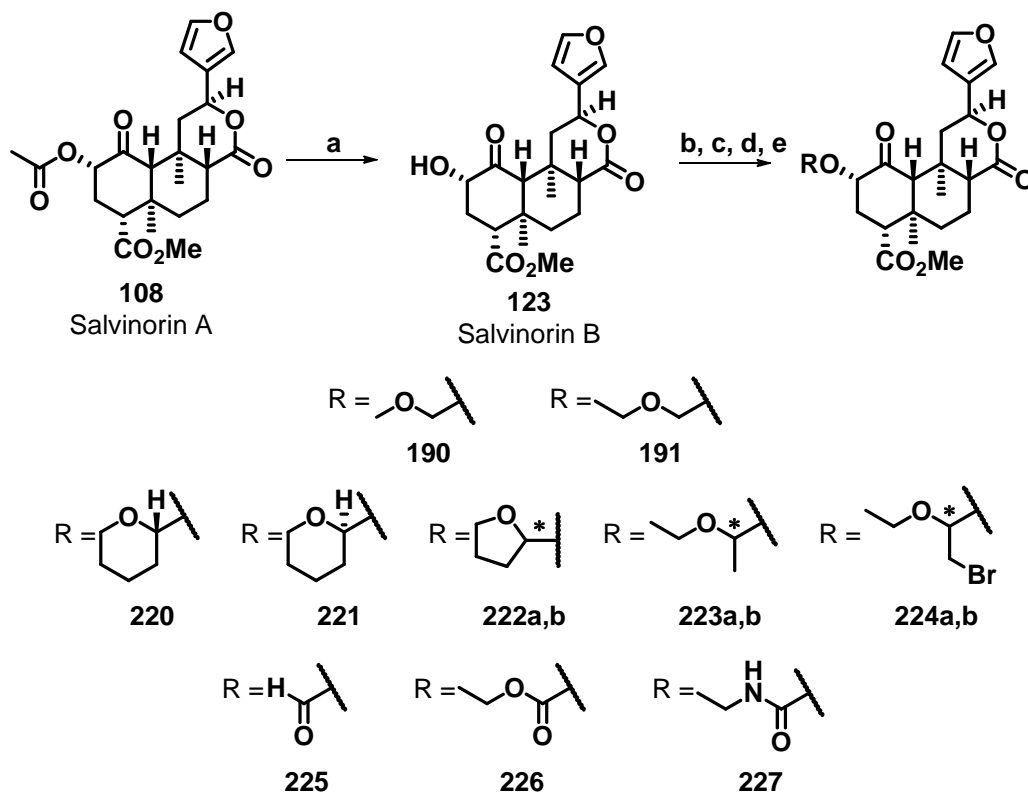


carbonyl oxygen also tested for the possibility of an additional interaction with residues in the binding pocket. An ethyl carbamate C-2 derivative probed whether or not electronic changes at this position would follow previously reported SAR trends for receptor subtype selectivity; the incorporation of allyl- and benzylcarbamates diminished KOP affinity and increased MOP affinity.<sup>281</sup>

### *Synthesis*

For comparison purposes, compounds **190** and **191** were synthesized according to Scheme 6. Salvinorin A (**108**) was extracted from commercially available dried *S. divinorum* leaves and converted to salvinorin B (**123**) as previously described.<sup>309</sup> Treatment of **123** with the appropriate chloromethyl ether in the presence of DIPEA yielded the desired ether products **190** and **191** in 41% and 54% yield, respectively.<sup>319</sup>

Compounds **220**, **221**, and **222a,b** were synthesized according to Scheme 6. To a solution of **123** in CH<sub>2</sub>Cl<sub>2</sub> was added 3,4-dihydro-2*H*-pyran or 2,3-dihydrofuran, followed by a catalytic amount of PPTS. This afforded the previously reported tetrahydropyran (**220** and **221**)<sup>322</sup> in 41% combined yield, and novel tetrahydrofuran (**222a,b**) C-2 derivatives in 68% combined yield. Under these synthetic conditions, epimers were formed and, in the case of tetrahydropyrans **220** and **221**, were separated from each other through flash column chromatography, and characterized by NMR studies and X-ray crystallography. The epimers **222a,b** were separated from each other by flash column chromatography and characterized by NMR only.



**Scheme 6.** Synthesis of C-2 derivatives. *Reagents and conditions:* a)  $\text{Na}_2\text{CO}_3$ , MeOH; b) appropriate chloromethyl ether, DIPEA,  $\text{CH}_2\text{Cl}_2$ ; c) 3,4-dihydro-2H-pyran or 2,3-dihydrofuran, PPTS,  $\text{CH}_2\text{Cl}_2$ ; d) PPTS, ethyl vinyl ether, reflux e)  $\text{Br}_2$ , ethyl vinyl ether, DIPEA,  $\text{CH}_2\text{Cl}_2$ ; f)  $\text{Ac}_2\text{O}/\text{HCO}_2\text{H}$ , pyridine; g) ethyl chloroformate, DMAP,  $\text{Et}_3\text{N}$ ,  $\text{CH}_2\text{Cl}_2$ ; f) ethyl isocyanate, DMAP, pyridine.

NMR spectroscopy studies and X-ray crystallography were used to assign the stereochemistry of the new stereocenter in compounds **220** and **221**. For carbohydrates, anomeric  $^1\text{J}_{\text{C,H}}$  values are useful for the assignment of configuration at that position because pyranoses with an axial proton have a  $^1\text{J}_{\text{C,H}}$  value that is approximately 10 Hz lower than the corresponding value in pyranoses with an equatorial anomeric proton.<sup>326-328</sup> For compounds **220** and **221** it was determined that the anomeric  $^1\text{J}_{\text{C,H}}$  values were 168.55 Hz and 159.36 Hz respectively, which are consistent with published reported of substituted pyranoses. These data indicate that **220** contains an equatorial,  $\beta$ -H (*R*) and **221** contains an axial,  $\alpha$ -H (*S*) (Figure 36).

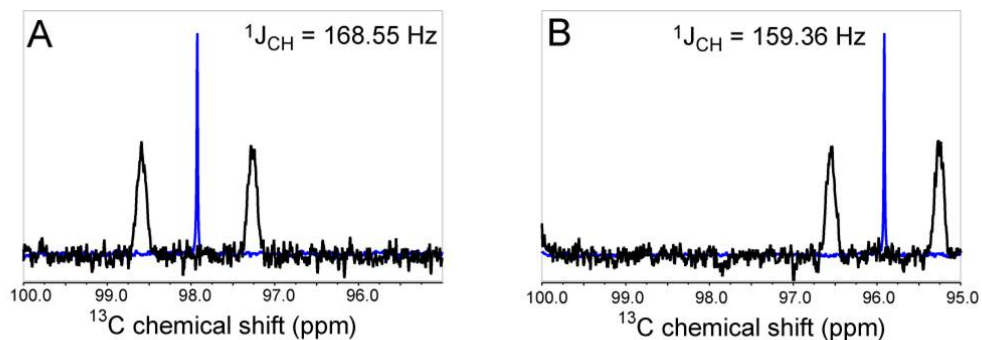


**Figure 36.** 1D  $^{13}\text{C}$  NMR spectrum with composite pulse  $^1\text{H}$ -decoupling (blue) and gated decoupling to show  $J_{\text{C,H}}$  (black) for the anomeric carbon of **220** (A) and **221** (B).

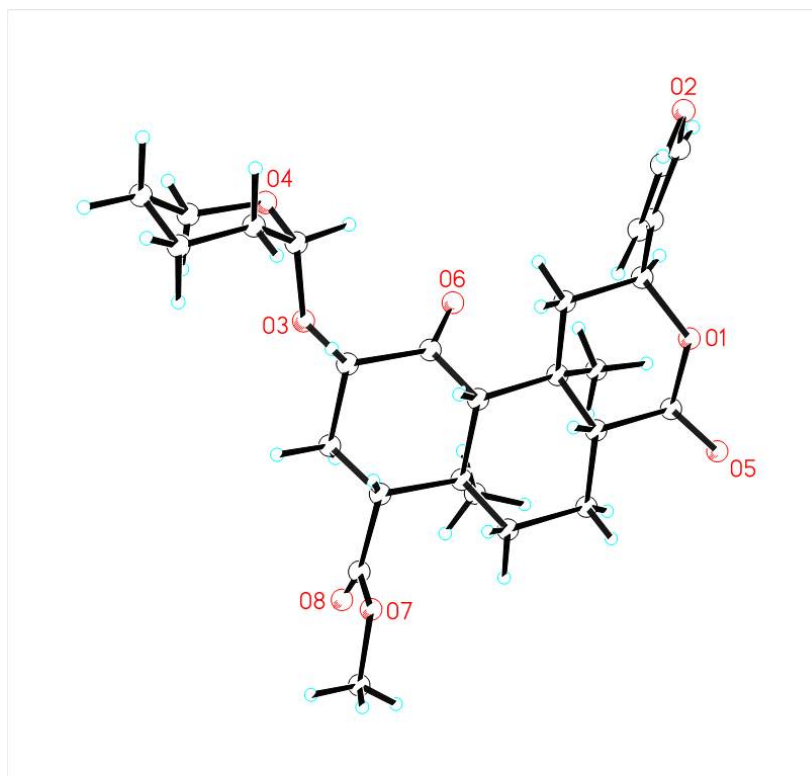


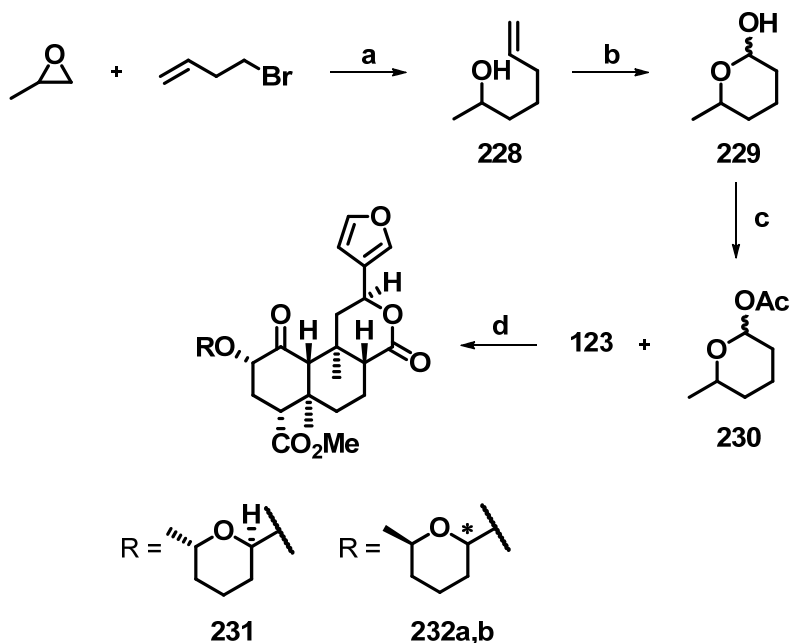
**Figure 37.** X-ray crystallographic structure of **220**.

Tetrahydropyran **220**, the less polar epimer, crystallized and the structure was determined using X-ray crystallography (Figure 37). This confirmed the orientation of the hydrogen that was predicted by NMR analysis. In the crystal structure, the tetrahydropyran moiety forms an  $\alpha$ -

glycosidic bond with the salvinorin A core in an axial position and the anomeric hydrogen in an equatorial,  $\beta$  position. Subsequently, tetrahydropyran **221** must be the other epimer.

Compounds **223a,b** and **224a,b** were synthesized according to Scheme 6. A suspension of **123** in ethyl vinyl ether with a catalytic amount of PPTS was refluxed for 2 h, yielding an epimeric mixture of the previously reported ethers **223a,b** in 21% combined yield.<sup>322</sup> The epimers were separated from each other by flash column chromatography and the less polar epimer (**223a**) was isolated. The more polar epimer (**223b**) appeared to degrade during purification and could not be completely purified (purity = 81.9%) through trituration, additional flash column chromatography, or HPLC. The impurity was not determined, although there were no traces of either **123** or the other epimer **223a** as detectable by HPLC. Both **223a** and **223b** were characterized by NMR. In order to produce novel ethers **224a,b** (11% combined yield), ethyl vinyl ether was added in a dropwise fashion to a solution of Br<sub>2</sub> in CH<sub>2</sub>Cl<sub>2</sub>, and the reaction mixture was stirred until the solution turned colorless (~15 min). DIPEA was then added, followed by the dropwise addition of a suspension of **123** in CH<sub>2</sub>Cl<sub>2</sub>. These synthetic conditions yielded a mixture of epimers which were separated from each other by HPLC and characterized by NMR.

Compounds **225**, **226**, and **227** were synthesized according to Scheme 6. Following a literature procedure, a mixture of acetic anhydride and acetic acid was added to a mixture of **123** in pyridine at 0 °C.<sup>312</sup> The mixture was allowed to warm to room temperature and stirred for 30 min, affording formate **225**. Carbonate **226** was produced by treating a solution of **123** in CH<sub>2</sub>Cl<sub>2</sub> with ethyl chloroformate in the presence of DMAP and Et<sub>3</sub>N at room temperature for 24



**Scheme 7.** Synthesis of C-2 constrained ethers. *Reagents and conditions:* a) Mg turnings, I<sub>2</sub>, CuI, THF, -10 °C; b) RuCl<sub>3</sub>·3H<sub>2</sub>O, NaIO<sub>4</sub>, CH<sub>3</sub>CN/H<sub>2</sub>O (6:1); c) acetic anhydride, DMAP, Et<sub>3</sub>N, CH<sub>2</sub>Cl<sub>2</sub>, 0 °C; d) PPTS (cat.), 1,2-DCE, 80 °C.

h.<sup>256, 319</sup> Following a literature procedure, carbamate **227** was produced by treating a mixture of **123** in pyridine with ethyl isocyanate at 35 °C overnight.<sup>311</sup>

The synthesis of compounds **231** and **232a,b** followed Scheme 7. For *in situ* generation of the Grignard reagent, a solution of commercially available 4-bromo-1-butene in THF was added via dropping funnel to a suspension of Mg turnings and catalytic I<sub>2</sub> in THF at reflux.<sup>329</sup> When the reaction was complete (~20 min), the mixture was cooled to -78 °C and CuI was added, and the reaction mixture was allowed to stir for 30 min at that temperature. Commercially available *R*-(+)-propylene oxide or *S*-(-)-propylene oxide was then added in a drop wise manner. The reaction mixture warmed to -10 °C and was allowed to stir overnight, yielding alcohol intermediate **228**, which could be purified by flash column chromatography, in 71% yield. The olefin of alcohol **228** was subsequently oxidatively cleaved using RuCl<sub>3</sub>·3H<sub>2</sub>O and

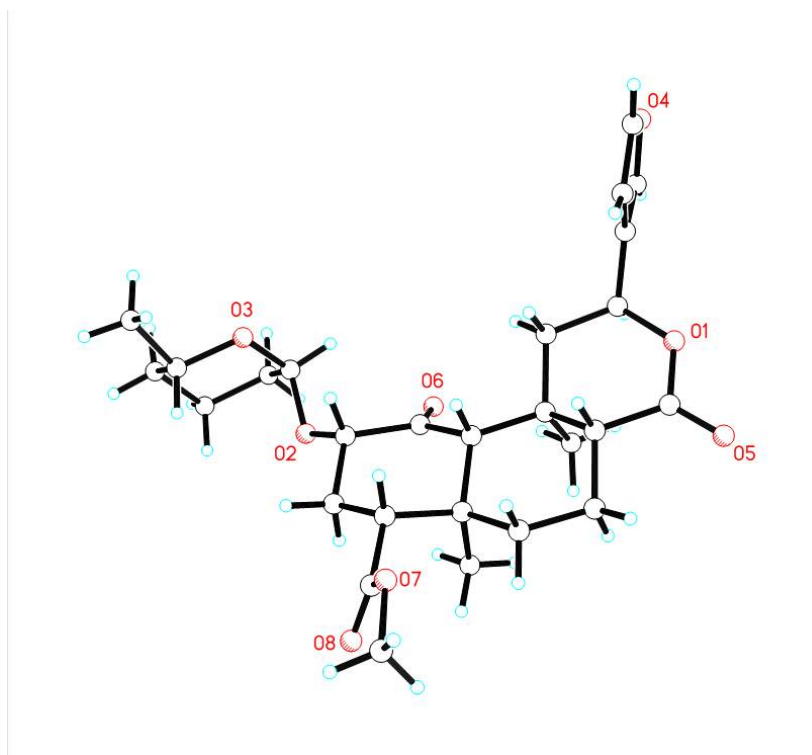


**Figure 38.** X-ray crystallographic structure of **231**.

$\text{NaIO}_4$  in  $\text{CH}_3\text{CN}/\text{H}_2\text{O}$  (6:1), and the resultant aldehyde cyclized *in situ* to afford intermediate **229** with no additional purification.<sup>330</sup> Acetylation of crude **229** was immediately performed by treatment with acetic anhydride and catalytic DMAP in the presence of  $\text{Et}_3\text{N}$  to give intermediate **230** with no additional purification.<sup>331</sup> Finally, catalytic PPTS and crude pyran **230** were added to a solution of **123** in 1,2-dichloroethane (1,2-DCE) and the mixture was heated to  $80\text{ }^\circ\text{C}$  for 24 h.<sup>332</sup> These synthetic conditions afforded methyltetrahydropyran **231** (9% yield) as a single isomer that could be purified from starting materials by flash column chromatography, and methyltetrahydropyrans **232a,b** (15% combined yield) as a mixture of epimers that could be separated from each other by HPLC. Methyltetrahydropyrans **231** and **232a,b** were characterized by NMR. Methyltetrahydropyran **231** also crystallized and the structure was determined using X-ray crystallography (Figure 38).

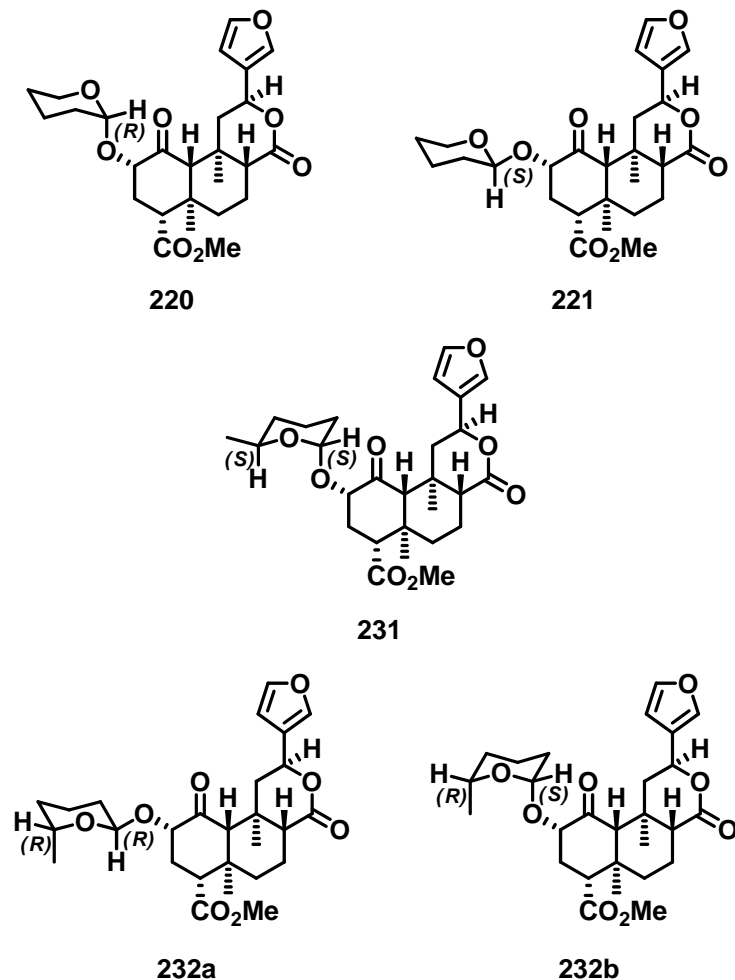


**Figure 39.** Proposed stereochemical assignments for tetrahydropyran derivatives.

Similar to the structure of **220**, in the structure of **231** the methyltetrahydropyran moiety forms an  $\alpha$ -glycosidic bond with the salvinorin A core in the axial position and the anomeric hydrogen in a equatorial,  $\beta$  position. The *S*-methyl group and the anomeric hydrogen are also on the same side of the tetrahydropyran ring making the absolute configuration of the anomeric center  $\beta$ -H (*S*) (compared to  $\beta$ -H (*R*) as in **220**). The oxygen of the tetrahydropyran ring in **231** is also oriented in the opposite direction of the tetrahydropyran oxygen of **220**. The anomeric  $^1J_{C,H}$  values of methyltetrahydropyrans **232a,b** were examined during NMR characterization; using the same reasoning as previously described, the less polar epimer (**232a**) had a  $^1J_{C,H}$  value

of 158.73 Hz and the more polar epimer (**232b**) had a  $^1J_{C,H}$  value of 170.73 Hz. These data indicate that the anomeric proton in **232a** is in the axial,  $\alpha$ -H position making the absolute configuration of the stereocenter *R*, and that the anomeric proton in **232b** is in the equatorial,  $\beta$ -H position making the absolute configuration of the stereocenter *S* (Figure 39). However, these proposed assignments need to be confirmed through X-ray crystallography.

### *Radioligand Binding Results*

Compounds **190**, **191**, **220**, **221**, **222a,b**, **223a,b**, **224a,b**, **225**, **226**, and **227** were evaluated for affinity at human opioid receptors using methodology previously described (Table 7).<sup>213</sup> For previously reported ethers **190** and **191**, the results of the radioligand binding assay were in agreement with published data.<sup>322</sup> From previous literature, tetrahydropyran epimers **220** and **221** were not completely separated from each other before pharmacological evaluation. For a mixture of predominantly one of the epimers, absolute configuration undetermined, the reported KOP binding affinity and potency were  $K_i = 4.0$  nM and  $EC_{50} = 2.8$  nM.<sup>322</sup> Tetrahydropyrans **220** and **221** have now been separated and isolated from each other, and the observed binding affinities reveal an eutomer (**220**) and distomer (**221**), indicating a preference for the hydrogen of the new stereocenter to be in the  $\beta$  (*R*) configuration.<sup>320</sup> Interestingly, the related tetrahydrofuran derivatives **222a,b** have only modest binding affinities at KOP receptors that are very similar to each other and show no preference for stereochemistry. One possible explanation for this is that by reducing the ring size by one carbon, a binding interaction within the receptor is eliminated or weakened, negating the influence of the configuration of the new stereocenter. Additionally, the  $^1J_{C,H}$  values at the new stereocenter in these derivatives were obtained during NMR characterization, and although they followed the accepted trend for



**Table 7.** Opioid receptor binding affinity for compounds **108**, **190**, **191**, **220**, **221**, **222a,b**, **223a,b**, **224a,b**, **225**, **226**, and **227**.

Compound	K <sub>i</sub> nM <sup>a</sup> ± SD		
	[ <sup>3</sup> H]DAMGO (MOP)	[ <sup>3</sup> H]DADLE (DOP)	[ <sup>3</sup> H]U69,593 (KOP)
<b>108</b> <sup>b</sup>			7.4 ± 0.7
<b>190</b>	390 ± 20	2,840 ± 180	1.9 ± 0.2
<b>191</b>	41 ± 3	1,017 ± 99	3.13 ± 0.40
<b>220</b>	> 10,000	> 10,000	6.21 ± 0.40
<b>221</b>	> 10,000	> 10,000	300 ± 23
<b>222a</b>	> 10,000	> 10,000	75 ± 3
<b>222b</b>	> 10,000	> 10,000	81 ± 6
<b>223a</b>	777 ± 40	> 5,000	6.7 ± 0.32
<b>223b</b>	> 5,800	> 5,000	1,233 ± 33
<b>224a</b>	> 3,000	> 5,000	5,621 ± 680
<b>224b</b>	3,523 ± 389	> 5,000	7,438 ± 764
<b>225</b>	ND	ND	41 ± 1
<b>226</b>	ND	ND	171 ± 7
<b>227</b>	1,540 ± 140	ND	ND

<sup>a</sup>Receptor binding was performed in CHO cells expressing the human MOP, DOP, or KOP receptors. All results are N = 3.

<sup>b</sup>Data from Lozama, A. et al. *J. Nat. Prod.* **2011**, *74*, 718–726.

ND indicates that K<sub>i</sub> was found to be >10,000 nM in a range finding study.

pyranoses as previously described, the difference was less pronounced (174.18 Hz and 171.85 Hz), so configuration was not assigned.

Like the tetrahydropyran derivatives ethers **223a,b** were also previously reported but were not completely separated from each other before pharmacological evaluation. The literature reports both epimers to have very similar binding affinities (K<sub>i</sub> = 11 nM and K<sub>i</sub> = 6.6 nM) and potencies (EC<sub>50</sub> = 10 nM and EC<sub>50</sub> = 5.7 nM).<sup>322</sup> The less polar epimer (**223a**) has now been isolated and separated.<sup>320</sup> Observed by HPLC, the more polar epimer (**223b**) appeared to degrade during purification and was not completely purified (purity = 81.9 %), although there was no detectable starting material or **223a** contamination. Like tetrahydropyrans **220** and **221**,

ethers **223a,b** also reveal an eutomer (**223a**) and distomer (**223b**), indicating a preference for configuration of the new stereocenter. The  $^1J_{C,H}$  values at the new stereocenter in these derivatives were obtained during NMR characterization, and although they followed the accepted trend for pyranoses as previously described, the difference was less pronounced (165.60 Hz and 163.82 Hz). However, given this observation and the trend in the radioligand binding data in which the less polar epimers (**220** and **223a**) had the highest affinity, it is likely that the absolute configuration of the new stereocenter in **223a** is the same as that of **220**. This hypothesis needs to be confirmed through X-ray crystallography. The related brominated ethers **224a,b** had very poor binding affinities at the KOP receptor and show no preference for stereochemistry. One explanation for this is that the brominated moiety was too bulky and precluded binding to the receptor altogether.

Formate **225** produced KOP radioligand binding data that was well in agreement with published reports<sup>312, 324</sup> and was 6-fold lower than that of salvinorin A. This would seem to indicate that the slightly smaller C-2 substituent was missing a binding interaction in the receptor that salvinorin A and C-2 ligands with larger substituents are able to exploit. Carbonate **226** and carbamate **227** behaved differently than previously reported. In two previously published radioligand binding studies, carbonate **226** showed no appreciable affinity at the KOP receptor vs. [ $^3H$ ]bremazocine<sup>256</sup> or [ $^3H$ ]diprenorphine.<sup>319</sup> The data generated in this report showed that carbonate **226** displaces [ $^3H$ ]U69,593 at the KOP receptor at  $K_i = 171 \pm 7$  nM,<sup>320</sup> 23-fold lower than salvinorin A and 55-fold lower than ether **191**. Moderate KOP receptor affinity for carbonate **226** is actually unsurprising considering how similar it appears to ether **191**; the lower KOP binding affinity implies that the additional carbonyl moiety is not particularly favorable. Additionally, carbamate **227** was reported to have a KOP receptor binding affinity (vs.

[<sup>3</sup>H]diprenorphine) and potency of  $K_i = 462 \pm 20$  nM and  $EC_{50} = >1,000$  nM.<sup>311</sup> This report found that while carbamate **227** has no appreciable affinity at the other opioid receptors, it does displace [<sup>3</sup>H]DAMGO at the MOP receptor at  $K_i = 1540 \pm 140$  nM.<sup>320</sup> While this particular  $K_i$  is unimpressive, it does agree with previously published reports in which alkyl carbamates at the C-2 position of salvinorin A were found to lose KOP affinity and gain MOP affinity relative to the parent compound.<sup>281</sup>

#### *[<sup>35</sup>S]GTP- $\gamma$ -S Functional Assay Results*

Compounds **190**, **191**, **220**, **222a,b**, **223a**, **231**, and **232a**, were also evaluated for functional activity at KOP receptors using the [<sup>35</sup>S]GTP- $\gamma$ -S functional assay (Table 8).<sup>68</sup> Compounds **190**, **191**, and **220** were found to have potencies comparable to or better than salvinorin A (**108**), in agreement with literature reports.<sup>322</sup> Compounds **222a,b** were observed to be 30- and 17-fold less potent than salvinorin A as agonists, respectively.<sup>320</sup> Similar to the radioligand binding results, this may be due to the smaller ring size eliminating the possibility of or weakening certain binding interactions with the receptor. Ether **223a**, which had binding affinity identical to tetrahydropyran **220**, was found to be 2.5-fold less potent than **220** and 4-fold less potent than salvinorin A. One explanation for this could be that in order to avoid steric interactions, **223a** would adopt an extended conformation (review Figure 35), implying that such a conformation is not favored by the KOP receptor. Methyltetrahydropyran **231** was approximately 3-fold less potent than tetrahydropyran **220** and 7-fold less potent than salvinorin A. This result further supports the hypothesis that the KOP receptor does not favor an extended conformation; the addition of a methyl group to a structure otherwise comparable in activity to salvinorin A resulted in reduced potency at KOP receptors. Methyltetrahydropyran **232a** had

**Table 8.** Selected [<sup>35</sup>S]GTP-γ-S KOP receptor potency and efficacy data for compounds **108**, **190**, **191**, **220**, **222a,b**, **223a**, **231**, and **232a**.

Compound	EC <sub>50</sub> nM <sup>a</sup> ± SD	E <sub>max</sub> ± SD
<b>108</b> <sup>d</sup>	40 ± 10	120 ± 2
<b>190</b> <sup>b</sup>	6 ± 1	118 ± 2
<b>191</b> <sup>b</sup>	0.65 ± 1	127 ± 5
<b>220</b> <sup>b</sup>	60 ± 6	109 ± 3
<b>222a</b> <sup>b</sup>	1220 ± 230	112 ± 8
<b>222b</b> <sup>b</sup>	690 ± 80	103 ± 4
<b>223a</b> <sup>b</sup>	150 ± 14	101 ± 3
<b>231</b> <sup>c</sup>	202 ± 60	90 ± 6
<b>232a</b> <sup>c</sup>	5100 ± 980	80 ± 9

<sup>a</sup>Receptor binding was performed in CHO cells expressing the human KOP receptor. All results are at least N = 3.

<sup>b</sup>E<sub>max</sub> is % at which compound stimulates binding compared to U50,488 (500 nM).

<sup>c</sup>E<sub>max</sub> is % at which compound stimulates binding compared to U69,593.

<sup>d</sup>Data from Lozama, A. et al. *J. Nat. Prod.* **2011**, *74*, 718–726.

very poor potency (176-fold lower) compared to salvinorin A, and its epimer **232b** was completely inactive at concentrations up to 10 μM.

Interestingly, when compounds **191**, **220**, **231**, and **232a,b** were screened at 10 μM at DOP and MOP receptors in this assay format, **191** appeared to be a full DOP agonist (E<sub>max</sub> = 100% vs. DPDPE) as well as a partial MOP agonist (E<sub>max</sub> = 67% vs. DAMGO). Methyltetrahydropyran **232b**, which was found to be completely inactive at KOP receptors, appeared to be a potential DOP partial agonist, showing E<sub>max</sub> = 49% vs. DPDPE. Tetrahydropyran **220** was less active than **191** and **232b**, having E<sub>max</sub> = 33% vs. DPDPE and E<sub>max</sub> = 16% vs. DAMGO. Compounds **231** and **232a** showed negligible (≤ 30%) activity at DOP

and MOP receptors. These preliminary results will need to be further explored with additional *in vitro* screening.

### Calcium Mobilization Results

In order to examine whether or not the rank-order potencies from the [<sup>35</sup>S]GTP- $\gamma$ -S assay were preserved across different assay formats, compounds **191**, **220**, **231**, and **232a** were evaluated in a second functional assay format, the fluorescent calcium mobilization assay (Table 9).<sup>214</sup> The rank-order potencies were preserved between the different functional assays, and as expected and in agreement with published literature,<sup>322</sup> **191** and **220** were full agonists and had potency comparable to or better than salvinorin A. Methyltetrahydropyran **231** was approximately 19-fold less potent than tetrahydropyran **220** and 8-fold less potent than salvinorin A and a full agonist, continuing the trend observed in the [<sup>35</sup>S]GTP- $\gamma$ -S functional assay results. Methyltetrahydropyran **232a** also appeared to have much worse potency (762-fold lower) compared to **220** and salvinorin A (332-fold lower) in this assay format, and the epimer **232b** was inactive at concentrations up to 10  $\mu$ M.

**Table 9.** Selected opioid receptor potency for compounds **108**, **191**, **220**, **231**, and **232a** in the calcium mobilization assay format.

Compound	EC <sub>50</sub> $\pm$ SEM nM <sup>a</sup>	E <sub>max</sub> $\pm$ SEM <sup>b</sup>
<b>108</b>	1.7 $\pm$ 0.6	103 $\pm$ 2
<b>191</b>	0.36 $\pm$ 0.03	110 $\pm$ 6
<b>220</b>	0.74 $\pm$ 0.06	108 $\pm$ 5
<b>231</b>	14.4 $\pm$ 5	101 $\pm$ 2
<b>232a</b>	564 $\pm$ 80	91 $\pm$ 2

<sup>a</sup>Receptor binding was performed in CHO cells expressing the human KOP receptors. All results are at least N = 3.

<sup>b</sup>E<sub>max</sub> is % at which compound stimulates binding compared to U69,593.

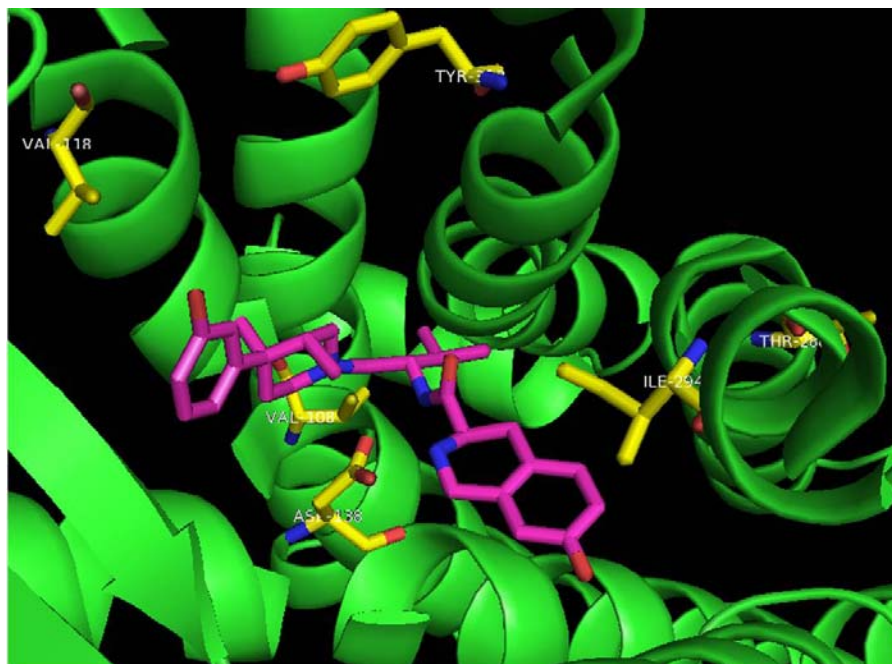


**Figure 40.** X-ray crystal structure of JDtic (magenta) in the KOP receptor (green) with relevant residues (yellow).

### *Crystal Structure Considerations*

Using the published KOP–JDtic co-crystal structure as a starting point (Figure 40), attempts were made to model the C-2 ligands in this report in the KOP receptor binding site, in hopes of correlating docking scores with affinity and potency data. Docking runs into the KOP–JDtic co-crystal structure (PDB ascension code 4DJH) were performed using SYBYL 8.0 (Tripos) and Suflex–Dock (Tripos). Default parameters were used except where noted. The KOP–JDtic co-crystal structure was used as a monomer instead of a dimer. The structures of salvinorin A (CSD code BUJJIZ) and C-2 analogs were energy minimized using the Tripos Force Field (Gasteiger–Hückel charges), and the coordinates of JDtic were used to generate the protomol (the putative binding pocket for docking ligands). Unfortunately, the docking scores

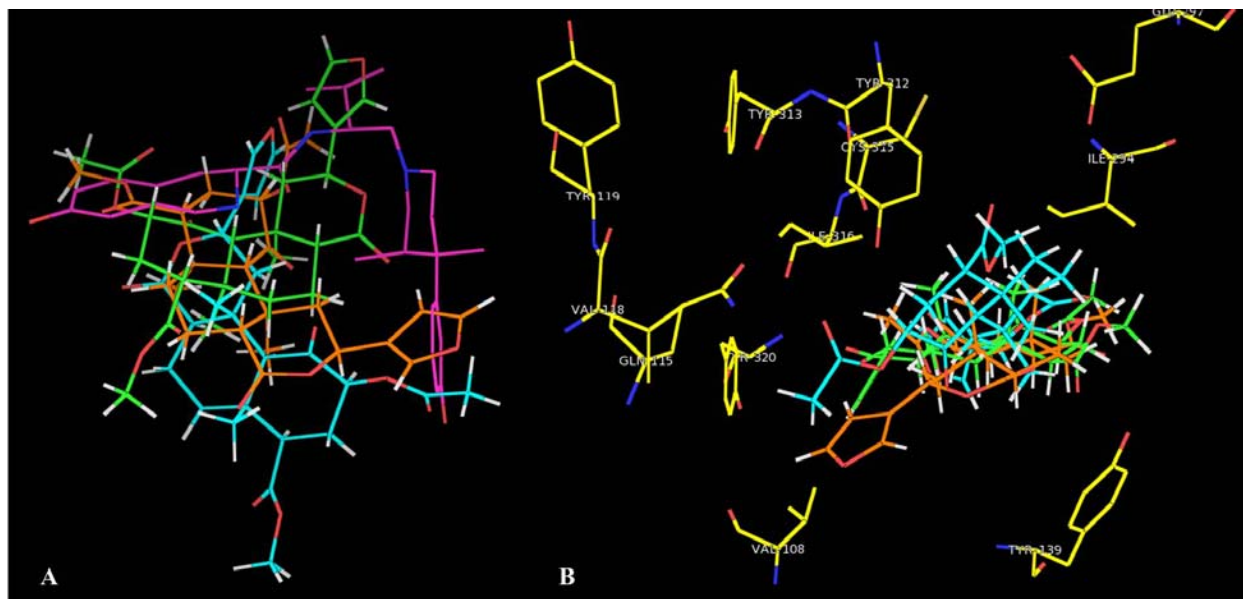


**Figure 41.** A) Overlay of JDtic (magenta) from KOP crystal structure with poses of salvinorin A (cyan, green, orange). Poses of salvinorin A (cyan, green, orange) with residues (yellow) putatively involved in receptor binding.

did not correlate with the binding affinity data (data not shown). On closer inspection of the docking run, it seemed that while salvinorin A was able to fit into a binding pocket near JDtic, it did not overlap very well with the antagonist and could take several very different poses itself (Figure 41A). Extracting the proposed important binding residues from the crystal structure, it is apparent that all of the residues do form a sort of binding pocket within the receptor, but salvinorin A is not interacting with them in a way that resembles the models previously proposed through mutagenesis studies,<sup>180, 299-304</sup> and in fact seems to be shunted off to one side of the pocket, too far away from most of the residues (Figure 41B). One possible explanation for the failure of the docking run is that the crystal structure is of an unfavorable conformation of the KOP receptor. JDtic is a KOP antagonist, whereas salvinorin A and the ligands herein are KOP agonists; it is possible that JDtic binds to an inactive receptor conformation that would otherwise preclude the binding of the salvinorin A scaffold. This hypothesis is supported by the fact that in the original co-crystal structure report, in order to model the covalently binding

ligand RB-64 (22-thiocyanatosalvinorin A) in the receptor, the torsion angle of the Cys315 residue it supposedly binds to had to be modified by  $+60.0^\circ$  in order for the sulfhydryl sidechain to point into the binding pocket and be accessible to the C-2 position of the salvinorin A scaffold.<sup>297</sup> Further, in order to allow room for RB-64 to fit, Gln115, Asp138, Ile290, Ile294, Tyr313, and Ile316 were allowed to flex via a “rotamer library,” which is not further defined. In attempting to repeat this work and manually draw the structure of RB-64 bound to Cys315 in the KOP receptor to use as a starting point for further C-2 docking studies, it became clear that the rotamer library allowed for a very large amount of flexibility in the receptor structure. It was impossible to draw the ligand in the receptor as depicted in the report without making large changes to the orientations of Tyr312 and Tyr313. Since the rotamer library (which includes Tyr313) was not clearly defined, it was not possible to reliably reproduce a model of RB-64 in the KOP receptor, calling into question the usefulness of this particular model. This clearly indicates that conformational changes in the receptor need to take place in order for salvinorin A to bind. What these changes are exactly will likely not be unambiguously elucidated until salvinorin A (or a derivative) is co-crystallized with the KOP receptor.

Another way to explain the binding and functional data is to examine the crystal structures of the molecules themselves. When the crystal structures of salvinorin A (CSD code BUJJIZ), tetrahydropyran **220**, and methyltetrahydropyran **231** are overlaid, the differences in the C-2 appendages seem to indicate that the three molecules are binding the KOP receptor differently from each other (Figure 42A). When salvinorin A and **220** are compared, the oxygen of the tetrahydropyran ring occupies the same space as the methyl of the acetate, while the anomeric hydrogen occupies the same space as the acetate carbonyl oxygen (Figure 42B). This implies that **220** takes advantage of a different hydrogen bonding interaction than salvinorin A



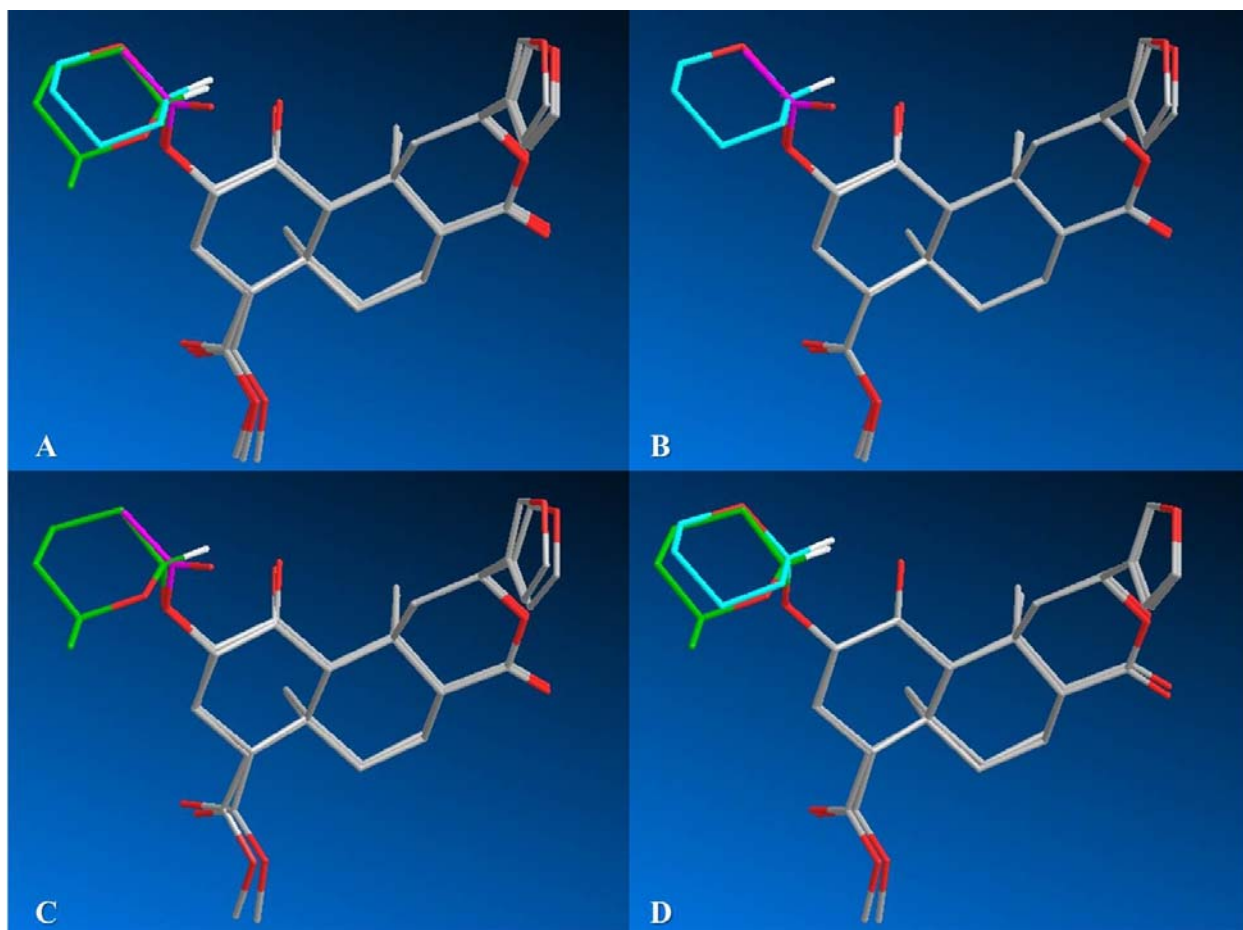


**Figure 42.** A) Overlay of the crystal structures of salvinorin A (magenta), **220** (cyan), and **231** (green). B) Overlay of the crystal structures of salvinorin A (magenta) and **220** (cyan). C) Overlay of the crystal structures of salvinorin A (magenta) and **231** (green). D) Overlay of the crystal structures of **220** (cyan) and **231** (green).

does. When salvinorin A and **231** are compared, the oxygen is flipped, occupying space left empty by salvinorin A, but in the general vicinity of the acetate carbonyl oxygen (Figure 42C). This may indicate that **231** and salvinorin A are able to take advantage of the same hydrogen bonding interaction, but **231** may be able to participate in some lipophilic interactions with its greater bulk compared to the acetate moiety. When the structures of **220** and **231** are compared, the most apparent feature is that the anomeric hydrogen of both derivatives occupies the same space (Figure 42D). This explains the stereochemical preference in the receptor binding affinity data; the anomeric hydrogen of **221**, the epimer of **220**, would not be in the same space,

potentially physically interfering with binding and leading to the comparatively poor affinity. This also seems to explain the lower potency of **231** relative to **220**; in order for the anomeric hydrogen of **231** to be in the same space as **220** for binding, the pyran ring itself is flipped, orienting the oxygen in a different position than in **220** and extending the additional methyl group into a region in space occupied by neither salvinorin A nor **220**. In short, in examining the overlaid crystal structures of salvinorin A, **220**, and **231**, it appears as if the KOP receptor prefers an eclipsed conformation (like **220**) over an extended conformation (like **231**), especially in regards to potency.

#### *Additional Experimental Results in a Rat Model of Relapse*

Finally, among the compounds in the series, tetrahydropyran **220** had binding affinity and potency comparable to salvinorin A and also lacked a hydrolyzable ester at C-2. It has been reported that ether **190**, another derivative with this same structural feature, has a longer duration of action *in vivo* than salvinorin A.<sup>333</sup> Therefore, in combination with its comparatively simpler synthesis and purification, **220** seemed the best candidate for further evaluation *in vivo*. Using established methodology,<sup>289</sup> tetrahydropyran **220** was evaluated for its effect on cocaine-induced drug-seeking in rats at doses of 0.3 mg/kg and 1 mg/kg (Figure 43).<sup>320</sup> Drug self-administration studies in animals can be used as a model of addiction relapse phenomena in humans;<sup>334-335</sup> if a compound is able to reduce or prevent reinstatement of extinguished cocaine self-administration in rats, it may be a useful pharmacotherapy for the treatment of drug abuse.

Briefly, the rats were trained on a fixed ratio 5 schedule of reinforcement for cocaine self-administration where a single cocaine infusion was given (0.5 mg/kg/infusion, paired with light cue) for every 5 correct lever presses. The first phase involved 2 h sessions until responding

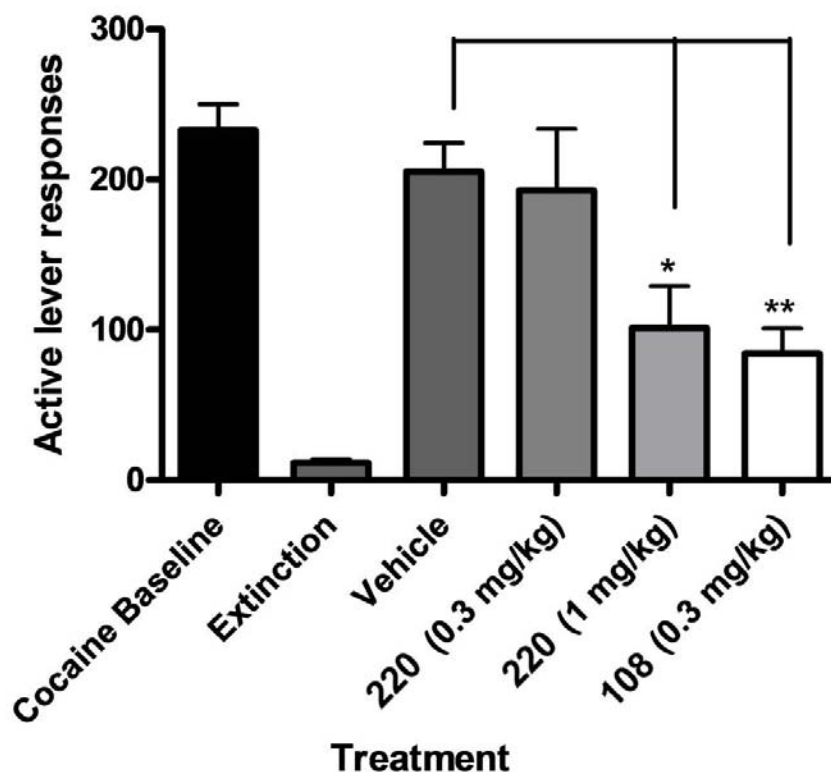


**Figure 43.** The effect of **220** on cocaine-induced drug-seeking. In the first phase (cocaine baseline), the active lever delivered an infusion of cocaine. Recorded active lever responses consisted of access to cocaine (0.5 mg/kg/infusion) for a period of 2 h in operant chambers. At the beginning of the second phase (extinction), cocaine was replaced with sterile heparinized saline and responses were recorded for 2 h, until active lever responses were < 20 for a 2 h daily session. At the beginning of the third phase, animals received an i.p. injection of vehicle (75% DMSO, N = 7), **220** (0.3 mg/kg, N = 3), **220** (1 mg/kg, N = 6), or salvinorin A (**108**) (0.3 mg/kg, N = 7) 5–10 min prior to a priming injection of cocaine (20 mg/kg). Responding in phase 3 was measured for 2 h ( $\pm$ SEM).

showed less than 20% variation across three consecutive days (cocaine baseline). In phase 2, cocaine was replaced with heparinized saline and daily 2 h sessions continued in the same operant chambers until active lever presses were < 20 for a session (typically 2–3 days). When the extinction criteria were met, reinstatement of cocaine-induced cocaine-seeking was tested the following day. Rats received i.p. injections of vehicle (75% DMSO), tetrahydropyran **220** (0.3 mg/kg or 1 mg/kg), or salvinorin A (**108**, 0.3 mg/kg) 5–10 min prior to a priming injection of cocaine (20 mg/kg i.p.). Immediately following the cocaine injection, rats were placed into the

operant chamber and responding was recorded for a further 2 h. The results show a statistically significant reduction in responding between vehicle and the 1 mg/kg dose of **220**. In fact, the 1 mg/kg dose of **220** attenuated responding comparably to 0.3 mg/kg salvinorin A, the positive control, which has previously been shown to attenuate cocaine-induced reinstatement of drug-seeking at a dose of 0.3 mg/kg or greater.<sup>289</sup> This finding represents the first example of a salvinorin A analog that has demonstrated anti-addictive capabilities.

### Conclusions

C-2 modified derivatives of salvinorin A were synthesized in order to further describe the SAR of salvinorin A while identifying analogs with more desirable pharmacological profiles than the parent molecule. Alkyl chain ethers at the C-2 position have been reported to have improved KOP receptor affinity and potency compared to salvinorin A. However, such derivatives are rotationally flexible and may adopt different conformations when bound with the KOP receptor, and the oxygen atom may be able to participate in new hydrogen bonding interactions. Thus, the focus of the series of compounds synthesized was to examine the molecular basis for the reported improved KOP receptor affinity and potency of C-2 alkoxy ethers.

Pharmacological evaluation of the C-2 analog series revealed some preferences inherent in the KOP receptor binding pocket. First, there was a stereochemical preference observed. Compounds **220**, **223a**, and **232a** had consistently much better affinity and/or potency than their epimers **221**, **223b**, and **232b** (which was actually completely inactive). Further, compounds **222a,b**, the tetrahydrofurans and smallest cyclic analogs, showed no preference for configuration, implying that their smaller size might have eliminated a binding interaction in the

receptor, negating the influence of stereochemistry. Additionally, through examination of the crystal structures of tetrahydropyran **220** and methyltetrahydropyran **231**, related cyclic derivatives with differing potencies, it was revealed their anomeric hydrogens occupied the same space, indicating that a different orientation might be unfavorable for KOP affinity. Further, the oxygen atoms of the pyran rings were oriented differently from each other, resulting in the additional methyl of **231** extending into space beyond **220**; since **231** had the lesser potency this implies that an extended conformation is not favorable for KOP receptor potency. Second, there were steric limitations observed in the binding pocket. Compounds **224a,b**, the brominated analogs, had no affinity for the KOP receptor while their related, non-brominated analogs (**223a,b**) did have affinity. This implies that the brominated derivatives **224a,b** were too large to bind to the receptor or other factors were involved. Finally, the possibility of hydrogen bonding interactions not used by salvinorin A was uncovered. In examining overlaid crystal structures of salvinorin A and tetrahydropyran **220**, it was revealed that the pyran oxygen atom of **220** reaches a region of space not occupied by heteroatoms from salvinorin A. Since **220** has similar affinity and potency to salvinorin A, this implies that it is able to interact with features in the receptor binding pocket that are different than those used by salvinorin A. In an interesting twist, when compounds **191** and **232b** were screened at 10  $\mu\text{M}$  at DOP and MOP receptors in the [ $^{35}\text{S}$ ]GTP- $\gamma\text{-S}$  functional assay format, **191** appeared to be a full DOP and partial MOP agonist, and **232b** appeared to be a partial DOP agonist. These results need to be further investigated and confirmed with additional *in vitro* pharmacological evaluation, but they do indicate a need for further SAR development of the salvinorin A scaffold, especially in regard to C-2 position modifications.

Further evaluation of tetrahydropyran **220** for its effects on cocaine-induced drug-seeking in rats revealed that **220** was able to significantly attenuate cocaine-induced drug-seeking behavior at a dose of 1 mg/kg. The effects were very comparable to the effects of 0.3 mg/kg salvinorin A, a dose previously reported to attenuate the same drug-seeking behavior in the same assay. Thus, tetrahydropyran **220** represents the first example of a salvinorin A analog that has experimentally demonstrated anti-addictive capabilities.

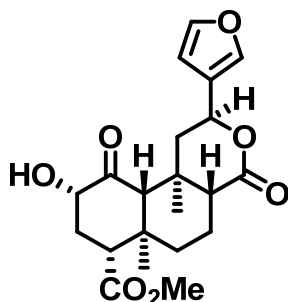
### **Future Directions**

It is vital that the SAR exploration of salvinorin A at opioid receptors continue, especially since pharmacological evaluation of C-2 constrained derivatives of salvinorin A has revealed that there may be features within the KOP receptor binding pocket that are available for binding interactions not used by salvinorin A. Given the recent publication of the KOP receptor co-crystal structure, further structure-based development of neoclerodane diterpenes promises to yield additional useful analogs with opioid activity and potential anti-addictive properties.

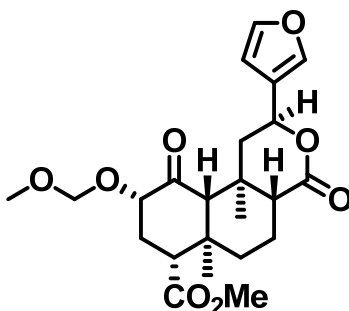
## CHAPTER 5: EXPERIMENTAL PROCEDURES FOR SALVINORIN A ANALOGS

### *Chemistry*

**General Procedures.** Unless otherwise indicated, all reagents were purchased from commercial suppliers and are used without further purification. All melting points were determined on a Thomas–Hoover capillary melting apparatus and are uncorrected. NMR spectra were recorded on a Bruker Avance-300 spectrometer, Bruker DRX-400 with qnp probe or a Bruker AV-500 with cryoprobe using  $\delta$  values in ppm (TMS as internal standard) and  $J$  (Hz) assignments of  $^1\text{H}$  resonance coupling. High resolution mass spectrometry data was collected on either a LCT Premier (Waters Corp., Milford, MA) time of flight mass spectrometer or an Agilent 6890 N gas chromatograph in conjunction with a Quatro Micro GC mass spectrometer (Micromass Ltd, Manchester UK). Thin-layer chromatography (TLC) was performed on 0.25 mm plates Analtech GHLF silica gel plates using mixtures of EtOAc/*n*-hexanes as the solvent system. Spots on TLC were visualized when appropriate with 254 nm UV light, phosphomolybdic acid in ethanol, or vanillin in ethanol. Column chromatography was performed with Silica Gel (32–63  $\mu$  particle size) from MP Biomedicals (Solon, OH). Analytical HPLC was carried out on an Agilent 1100 Series Capillary HPLC system with diode array detection at 209 nm, 214 nm, and 235 nm on a Phenomenex Luna C18 column (250  $\times$  10.0 mm, 5  $\mu\text{m}$ ) with isocratic elution in mixtures of  $\text{CH}_3\text{CN}/\text{H}_2\text{O}$  as noted at a flow rate of 5.0 mL/min.



**Salvinorin B (123).** Salvinorin A (**108**) was extracted from commercially available dried *S. divinorum* leaves and converted to salvinorin B (**123**) as previously described by Tidgewell et al.<sup>309</sup> Na<sub>2</sub>CO<sub>3</sub> (1.96 g, 18.5 mmol, 4 equiv.) was added to a suspension of salvinorin A (2.00 g, 4.62 mmol) in methanol (100 mL). The reaction mixture was stirred at room temperature for 4 h, after which time the solvent was removed *in vacuo*. The residue was dissolved in methylene chloride (100 mL) and washed with 2 N HCl (2 × 60 mL), H<sub>2</sub>O (50 mL), and brine (50 mL). The organic layer was dried over Na<sub>2</sub>SO<sub>4</sub>, filtered, and the solvent removed *in vacuo*. The residue was triturated from EtOAc/*n*-hexanes to afford 1.4607 g of salvinorin B (81% yield) as a light green to off-white powder. Spectral data in agreement with reported.<sup>309</sup>

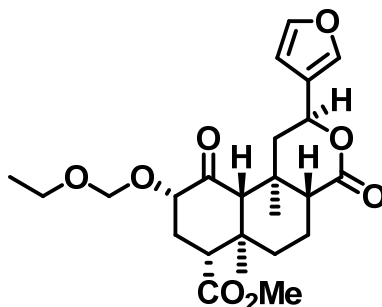


**(2S,4aR,6aR,7R,9S,10aS,10bR)-Methyl 2-(furan-3-yl)-9-(methoxymethoxy)-6a,10b-dimethyl-4,10-dioxododecahydro-1H-benzo[f]isochromene-7-carboxylate (190).**

Chloromethyl methyl ether (0.195 mL, 2.56 mmol, 5 equiv.) was added in a drop wise manner to a solution of **123** (0.200g, 0.512 mmol, 1 equiv.) and *N,N*-diisopropylethylamine (0.446 mL, 2.56 mmol, 5 equiv.) in anhydrous methylene chloride (20 mL) under an argon atmosphere. The mixture was stirred at room temperature overnight. The reaction mixture was washed with

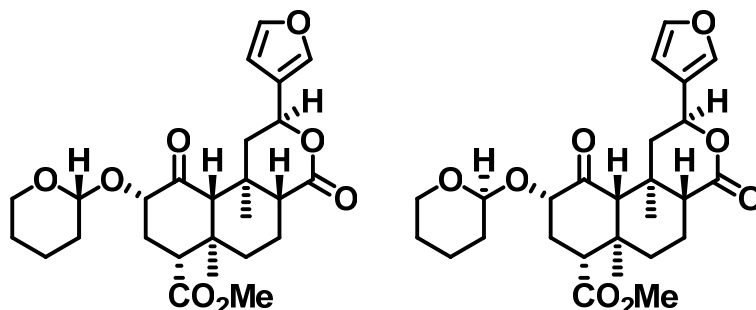


saturated aqueous NaHCO<sub>3</sub> (3 × 10 mL), brine (10 mL), dried over Na<sub>2</sub>SO<sub>4</sub>, filtered, and the solvent removed *in vacuo*. The remaining residue was purified by flash column chromatography using EtOAC/*n*-hexanes (1:3) to afford 0.0894 g (41% yield) as a white powder. HPLC in 60% MeCN/40% H<sub>2</sub>O, t<sub>R</sub> = 4.778 min; purity = 99.1%. Spectroscopic information was in agreement with published data.<sup>311, 319</sup>



**(2S,4aR,6aR,7R,9S,10aS,10bR)-methyl 9-(ethoxymethoxy)-2-(furan-3-yl)-6a,10b-dimethyl-4,10-dioxododecahydro-1H-benzo[f]isochromene-7-carboxylate (191).**

Chloromethyl ethyl ether (0.475 mL, 5.12 mmol, 5 equiv.) was added in a drop wise manner to a solution of **123** (0.400 g, 1.02 mmol, 1 equiv.) and *N,N*-diisopropylethylamine (0.890 mL, 5.12 mmol, 5 equiv.) in anhydrous methylene chloride (40 mL) under an argon atmosphere. The mixture was stirred at room temperature overnight. TLC indicated that starting material was still present after 16 h, thus an additional 5 equiv. (0.475 mL, 5.12 mmol) of chloromethyl ethyl ether was added and the mixture stirred for an additional 24 h. The reaction mixture was washed with saturated aqueous NaHCO<sub>3</sub> (3 × 40 mL), brine (40 mL), dried over Na<sub>2</sub>SO<sub>4</sub>, filtered, and the solvent removed *in vacuo*. The remaining residue was purified by flash column chromatography using EtOAC/*n*-hexanes (2:3) to afford a brown oil, which was subsequently triturated from DCM/*n*-hexanes to give 0.2487 g (54% yield) as a white powder. HPLC in 60% MeCN/40% H<sub>2</sub>O, t<sub>R</sub> = 7.151 min; purity = 98.1%. Spectroscopic information was in agreement with published data.<sup>319</sup>



(2S,4aR,6aR,7R,9S,10aS,10bR)-methyl 2-(furan-3-yl)-6a,10b-dimethyl-4,10-dioxo-9-

((R)-tetrahydro-2H-pyran-2-yloxy)dodecahydro-1H-benzo[f]isochromene-7-carboxylate

(**220**) and (2S,4aR,6aR,7R,9S,10aS,10bR)-methyl 2-(furan-3-yl)-6a,10b-dimethyl-4,10-

dioxo-9-((S)-tetrahydro-2H-pyran-2-yloxy)dodecahydro-1H-benzo[f]isochromene-7-

carboxylate (**220**). 3,4-dihydro-2H-pyran (0.579 mL, 6.16 mmol, 8 equiv.) was added to a

solution of **123** (0.300 g, 0.768 mmol, 1 equiv.) and pyridinium *p*-toluene sulfonate (60 mg, cat.)

in anhydrous methylene chloride (30 mL) at 0 °C under an argon atmosphere. The mixture was

allowed to warm to room temperature and stirred for 5 h. The reaction was quenched with

triethylamine (100  $\mu$ L) and the solvent was removed *in vacuo*. The remaining residue was

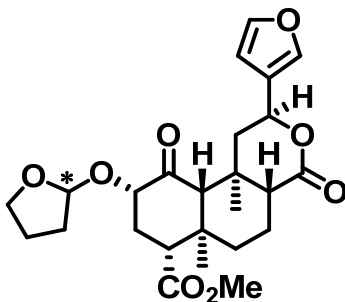
purified by flash column chromatography using EtOAc/*n*-hexanes (3:7) to give 0.0939 g (**220**)

$R_f = 0.56$  (EtOAc/*n*-hexanes 1:1) and 0.0560 g (**220**)  $R_f = 0.48$  (EtOAc/*n*-hexanes 1:1) as white

powders (41% combined yield). HPLC in 60% MeCN/40% H<sub>2</sub>O,  $t_R = 7.902$  min; purity =

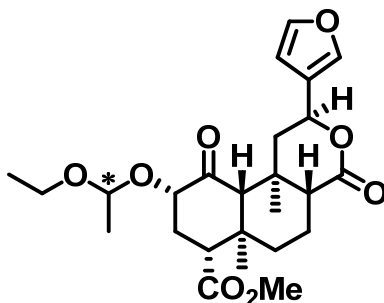
99.2% (**220**) and HPLC in 60% MeCN/40% H<sub>2</sub>O,  $t_R = 7.200$  min; purity = 98.5% (**220**).

Spectroscopic information was in agreement with reported data.<sup>319</sup>



(2S,4aR,6aR,7R,9S,10aS,10bR)-methyl 2-(furan-3-yl)-6a,10b-dimethyl-4,10-dioxo-9-((R)-tetrahydrofuran-2-yloxy)dodecahydro-1H-benzo[f]isochromene-7-carboxylate and (2S,4aR,6aR,7R,9S,10aS,10bR)-methyl 2-(furan-3-yl)-6a,10b-dimethyl-4,10-dioxo-9-((S)-tetrahydrofuran-2-yloxy)dodecahydro-1H-benzo[f]isochromene-7-carboxylate (**222a** and **222b**). 2,3-dihydrofuran (0.465 mL, 6.15 mmol 8 equiv.) was added to a solution of **123** (0.300 g, 0.768 mmol, 1 equiv.) and pyridinium *p*-toluene sulfonate (60 mg, cat.) in anhydrous methylene chloride (30 mL) at 0 °C under an argon atmosphere. The mixture was allowed to warm to room temperature and stirred overnight. The reaction was quenched with triethylamine (100  $\mu$ L) and the solvent was removed *in vacuo*. The remaining residue was purified by flash column chromatography using EtOAc/*n*-hexanes (3:7) to give 0.1497 g (**222a**)  $R_f$  = 0.44 (EtOAc/*n*-hexanes 2:5) and 0.0888 g (**222b**)  $R_f$  = 0.31 (EtOAc/*n*-hexanes 2:5) as white powders (68% combined yield). **222a**:  $^1\text{H}$  NMR (500 MHz,  $\text{CDCl}_3$ )  $\delta$  7.42 (dt,  $J$  = 0.8, 1.6, 1H), 7.40 (t,  $J$  = 1.7, 1H), 6.38 (dd,  $J$  = 0.8, 1.8, 1H), 5.54 (dd,  $J$  = 5.0, 11.7, 1H), 5.26 (d,  $J$  = 4.1, 1H), 4.21 (dd,  $J$  = 7.8, 12.1, 1H), 3.86 (dd,  $J$  = 6.3, 7.5, 2H), 3.71 (s, 3H), 2.70 (dd,  $J$  = 3.4, 13.4, 1H), 2.55 (dd,  $J$  = 5.1, 13.3, 1H), 2.29 (ddd,  $J$  = 3.4, 7.4, 13.4, 1H), 2.20 – 2.08 (m, 3H), 2.06 – 1.92 (m, 3H), 1.88 – 1.80 (m, 1H), 1.77 (dt,  $J$  = 3.0, 13.3, 1H), 1.69 – 1.59 (m, 2H), 1.54 (dd,  $J$  = 8.3, 21.1, 2H), 1.46 (s, 3H), 1.10 (s, 3H).  $^{13}\text{C}$  NMR (126 MHz,  $\text{CDCl}_3$ )  $\delta$  206.90, 171.97, 171.29, 143.74, 139.36, 125.34, 108.35, 103.43, 77.19, 71.99, 67.28, 64.25, 53.99, 51.83, 51.52, 43.58, 41.99, 38.19, 35.51, 33.10, 32.29, 23.19, 18.15, 16.44, 15.20. HRMS ( $m/z$ ):  $[\text{M}+\text{Na}]$  calcd for

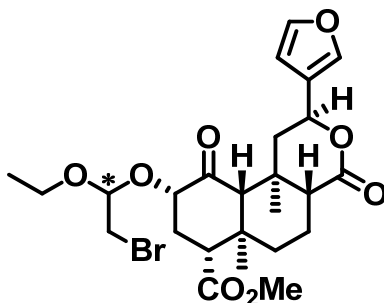
$C_{25}H_{32}O_8Na$ , 483.1995; found 483.1997 0.4 ppm. HPLC in 60% MeCN/40%  $H_2O$ ,  $t_R = 5.013$  min; purity = 95.2%. **222b**:  $^1H$  NMR (500 MHz,  $CDCl_3$ )  $\delta$  7.43 (d,  $J = 0.7$ , 1H), 7.40 (t,  $J = 1.7$ , 1H), 6.39 (dd,  $J = 0.7, 1.7$ , 1H), 5.55 (dd,  $J = 5.1, 11.7$ , 1H), 5.19 (d,  $J = 4.6$ , 1H), 4.14 (dd,  $J = 7.3, 12.4$ , 1H), 3.97 (td,  $J = 6.0, 8.0$ , 1H), 3.82 (td,  $J = 6.1, 7.8$ , 1H), 3.71 (s, 3H), 2.66 (dd,  $J = 3.3, 13.5$ , 1H), 2.55 (dd,  $J = 5.1, 13.4$ , 1H), 2.40 (ddd,  $J = 3.3, 7.1, 13.3$ , 1H), 2.17 – 2.02 (m, 6H), 1.98 – 1.90 (m, 1H), 1.90 – 1.83 (m, 1H), 1.78 (dt,  $J = 3.1, 13.3$ , 1H), 1.67 – 1.57 (m, 2H), 1.53 (d,  $J = 4.3$ , 1H), 1.47 (s, 3H), 1.10 (s, 3H).  $^{13}C$  NMR (126 MHz,  $CDCl_3$ )  $\delta$  205.35, 171.98, 171.35, 143.71, 139.44, 125.37, 108.43, 102.04, 77.43, 72.03, 67.63, 64.35, 53.86, 51.85, 51.54, 43.47, 42.03, 38.23, 35.48, 32.33, 31.82, 23.30, 18.18, 16.39, 15.18. HRMS ( $m/z$ ):  $[M+K]$  calcd for  $C_{25}H_{32}O_8K$ , 499.1734; found 499.1731, 0.6 ppm. HPLC in 60% MeCN/40%  $H_2O$ ,  $t_R = 4.393$  min; purity = 95.2%.



(2S,4aR,6aR,7R,9S,10aS,10bR)-methyl 9-((R)-1-ethoxyethoxy)-2-(furan-3-yl)-6a,10b-dimethyl-4,10-dioxododecahydro-1H-benzo[f]isochromene-7-carboxylate and (2S,4aR,6aR,7R,9S,10aS,10bR)-methyl 9-((S)-1-ethoxyethoxy)-2-(furan-3-yl)-6a,10b-dimethyl-4,10-dioxododecahydro-1H-benzo[f]isochromene-7-carboxylate (**223a** and **223b**).

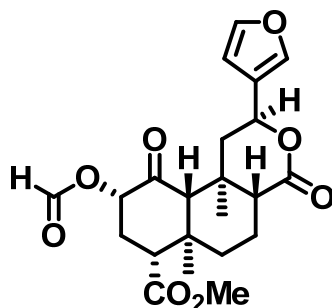
A suspension of **123** (0.200 g, 0.512 mmol) and pyridinium *p*-toluene sulfonate (20 mg, cat.) in ethyl vinyl ether (20 mL) was heated to reflux for 2 h. The solvent was removed *in vacuo* and the remaining residue was purified by flash column chromatography using EtOAc/*n*-hexanes (3:7) to give 0.0350 g (**223a**)  $R_f = 0.28$  (EtOAc/*n*-hexanes 3:7) and 0.0156 g (**223b**)  $R_f = 0.21$

(EtOAc/*n*-hexanes 3:7) as white powders (21% combined yield). HPLC in 50% MeCN/50% H<sub>2</sub>O, *t<sub>R</sub>* = 10.596 min; purity = 95.0% (**223a**) and HPLC in 50% MeCN/50% H<sub>2</sub>O, *t<sub>R</sub>* = 8.769 min; purity = 81.9% (**223b**). Spectroscopic information was in agreement with reported data.<sup>319</sup>



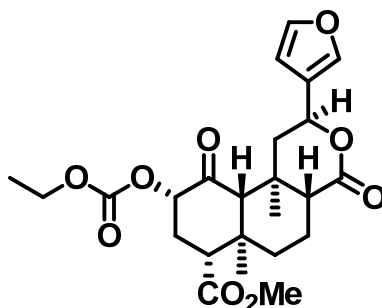
(2*S*,4*aR*,6*aR*,7*R*,9*S*,10*aS*,10*bR*)-methyl 9-((*R*)-1-bromo-2-ethoxypropan-2-yloxy)-2-(furan-3-yl)-6*a*,10*b*-dimethyl-4,10-dioxododecahydro-1*H*-benzo[*f*]isochromene-7-carboxylate and (2*S*,4*aR*,6*aR*,7*R*,9*S*,10*aS*,10*bR*)-methyl 9-((*S*)-1-bromo-2-ethoxypropan-2-yloxy)-2-(furan-3-yl)-6*a*,10*b*-dimethyl-4,10-dioxododecahydro-1*H*-benzo[*f*]isochromene-7-carboxylate (**224a** and **224b**). Ethyl vinyl ether (0.184 mL, 1.92 mmol, 2.5 equiv) was added in a dropwise fashion to a solution of bromine (0.080 mL, 1.54 mmol, 2 equiv) in anhydrous methylene chloride (15 mL) at 0° C under an argon atmosphere, turning the solution colorless. The reaction was allowed to stir for 15 minutes. *N,N*-diisopropylethylamine (0.535 mL, 3.07 mmol, 4 equiv) was then added to the reaction mixture, followed by the dropwise addition of a suspension of **123** (0.300 g, 0.768 mmol, 1 equiv) in anhydrous methylene chloride (15 mL). The reaction stirred for 24 h without recharging the ice bath. The reaction mixture was then diluted with methylene chloride (20 mL) and extracted with saturated aqueous NaHCO<sub>3</sub> (3 × 50 mL). The combined aqueous layers were washed with methylene chloride (50 mL). The combined organic layers were washed with brine (50 mL), dried over Na<sub>2</sub>SO<sub>4</sub>, filtered, and the solvent removed *in vacuo*. The remaining residue was purified by HPLC with an isocratic

solvent gradient of 50% MeCN/50% H<sub>2</sub>O and a flow rate of 3 mL/min to give 0.0230 g (**224a**)  $R_f$  = 0.63 (EtOAc/*n*-hexanes 2:5) and 0.0239 g (**224b**)  $R_f$  = 0.56 (EtOAc/*n*-hexanes 2:5) as white powders (11% combined yield). **224a**: <sup>1</sup>H NMR (500 MHz, C<sub>6</sub>D<sub>6</sub>) δ 7.11 – 7.09 (m, 1H), 7.04 (t,  $J$  = 1.7, 1H), 6.13 (dd,  $J$  = 0.7, 1.7, 1H), 5.16 (dd,  $J$  = 5.0, 11.8, 1H), 4.65 (dd,  $J$  = 4.2, 6.3, 1H), 3.76 – 3.70 (m, 1H), 3.65 – 3.54 (m, 2H), 3.30 (s, 3H), 3.27 (dd,  $J$  = 4.2, 10.7, 1H), 3.16 (dd,  $J$  = 6.3, 10.7, 1H), 2.29 (dd,  $J$  = 5.2, 13.1, 1H), 2.24 – 2.19 (m, 2H), 2.17 – 2.09 (m, 1H), 2.06 (dd,  $J$  = 7.3, 9.9, 1H), 1.46 (ddd,  $J$  = 3.3, 5.9, 10.2, 2H), 1.38 (d,  $J$  = 14.6, 3H), 1.25 (d,  $J$  = 2.5, 4H), 1.04 (t,  $J$  = 7.0, 3H), 0.86 (s, 3H). <sup>13</sup>C NMR (126 MHz, C<sub>6</sub>D<sub>6</sub>) δ 205.44, 171.96, 170.34, 144.15, 139.69, 126.91, 108.98, 100.90, 77.37, 71.82, 64.19, 62.26, 53.97, 51.66, 51.58, 43.93, 42.04, 38.52, 35.88, 33.40, 32.51, 19.01, 16.54, 15.63, 15.46. HRMS ( $m/z$ ): [M+Na] calcd for C<sub>25</sub>H<sub>33</sub>BrO<sub>8</sub>Na, 563.1257; found 563.1265, 1.4 ppm. HPLC in 60% MeCN/40% H<sub>2</sub>O,  $t_R$  = 9.104 min; purity = >99.9%. **224b**: <sup>1</sup>H NMR (500 MHz, C<sub>6</sub>D<sub>6</sub>) δ 7.10 – 7.07 (m, 1H), 7.05 (t,  $J$  = 1.7, 1H), 6.12 (dd,  $J$  = 0.8, 1.8, 1H), 5.17 (dd,  $J$  = 5.0, 11.7, 1H), 4.92 (dd,  $J$  = 3.8, 7.4, 1H), 3.85 – 3.79 (m, 1H), 3.55 (dd,  $J$  = 3.8, 10.9, 1H), 3.41 (dq,  $J$  = 7.0, 9.0, 1H), 3.33 – 3.23 (m, 5H), 2.29 – 2.18 (m, 3H), 2.10 (ddd,  $J$  = 6.5, 9.1, 9.5, 2H), 1.46 (dd,  $J$  = 7.8, 10.4, 3H), 1.24 (s, 3H), 1.23 (s, 1H), 1.12 (dd,  $J$  = 13.4, 26.2, 2H), 1.04 (t,  $J$  = 7.0, 3H), 0.85 (s, 3H). <sup>13</sup>C NMR (126 MHz, C<sub>6</sub>D<sub>6</sub>) δ 206.22, 171.92, 170.31, 144.13, 139.76, 126.86, 109.03, 101.22, 77.96, 71.79, 63.99, 60.75, 53.89, 51.61, 51.58, 43.96, 42.05, 38.45, 35.88, 33.32, 31.61, 18.99, 16.56, 15.73, 15.41. HRMS ( $m/z$ ): [M+Na] calcd for C<sub>25</sub>H<sub>33</sub>BrO<sub>8</sub>Na, 563.1257; found 563.1265, 1.4 ppm. HPLC in 60% MeCN/40% H<sub>2</sub>O,  $t_R$  = 9.799 min; purity = 98.5%.



(2S,4aR,6aR,7R,9S,10aS,10bR)-methyl 9-(formyloxy)-2-(furan-3-yl)-6a,10b-dimethyl-4,10-dioxododecahydro-1H-benzo[f]isochromene-7-carboxylate (225).

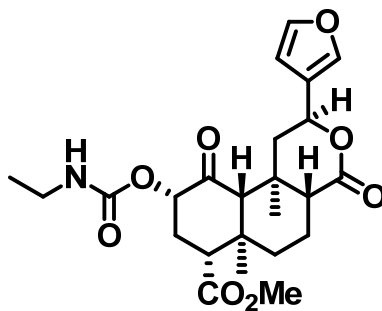
Synthesized according to the procedures of Munro et al.<sup>322</sup> HPLC in 60% MeCN/40% H<sub>2</sub>O,  $t_R$  = 5.905 min; purity = 95%. Spectroscopic information was in agreement with reported data.<sup>322</sup>



(2S,4aR,6aR,7R,9S,10aS,10bR)-methyl 9-(ethoxycarbonyloxy)-2-(furan-3-yl)-6a,10b-dimethyl-4,10-dioxododecahydro-1H-benzo[f]isochromene-7-carboxylate (226).<sup>311</sup>

<sup>319</sup> Ethyl chloroformate (0.055 mL, 0.576 mmol, 3 equiv) was added in a dropwise fashion to a solution of **123** (0.075 g, 0.192 mmol, 1 equiv), DMAP (0.070 g, 0.576 mmol, 3 equiv), and triethylamine (0.080 mL, 0.576 mmol, 3 equiv) in anhydrous methylene chloride (15 mL) under an atmosphere of argon. The reaction stirred at room temperature for 24 h. After TLC indicated completion of the reaction, the mixture was diluted with EtOAc (20 mL) and then extracted with saturated aqueous NaHCO<sub>3</sub> (3 × 50 mL). The combined organic layers were washed with H<sub>2</sub>O

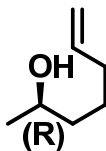
(50 mL) and brine (50 mL), and then dried over Na<sub>2</sub>SO<sub>4</sub>, filtered, and the solvent was removed *in vacuo*. The remaining residue was purified by flash column chromatography using EtOAc/*n*-hexanes (2:5) to give 0.0681 g (77% yield) *R<sub>f</sub>* = 0.40 (EtOAc/*n*-hexanes 2:5) and as white powder. <sup>1</sup>H NMR (500 MHz, CDCl<sub>3</sub>) δ 7.42 (s, 1H), 7.40 (t, *J* = 1.7, 1H), 6.38 (d, *J* = 1.0, 1H), 5.54 (dd, *J* = 5.1, 11.7, 1H), 4.98 (dd, *J* = 7.7, 12.4, 1H), 4.30 – 4.18 (m, 2H), 3.73 (s, 3H), 2.75 (dd, *J* = 3.7, 13.1, 1H), 2.54 (dd, *J* = 5.2, 13.4, 1H), 2.43 – 2.28 (m, 2H), 2.20 – 2.17 (m, 1H), 2.08 (dd, *J* = 2.9, 11.7, 1H), 1.83 – 1.76 (m, 1H), 1.68 – 1.62 (m, 1H), 1.58 (s, 3H), 1.46 (s, 3H), 1.34 (t, *J* = 7.1, 3H), 1.12 (s, 3H). <sup>13</sup>C NMR (126 MHz, CDCl<sub>3</sub>) δ 201.77, 171.40, 171.09, 154.19, 143.74, 139.48, 125.18, 108.41, 77.61, 72.01, 64.74, 64.02, 53.43, 52.04, 51.39, 43.34, 42.04, 38.11, 35.46, 30.65, 18.12, 16.40, 15.17, 14.17. HRMS (*m/z*): [M+Na] calcd for C<sub>24</sub>H<sub>30</sub>O<sub>9</sub>Na, 485.1788; found 485.1804, 3.3 ppm. HPLC in 60% MeCN/40% H<sub>2</sub>O, *t<sub>R</sub>* = 7.645 min; purity = 95.8%.



**(2S,4aR,6aR,7R,9S,10aS,10bR)-methyl 9-(ethylcarbamoyloxy)-2-(furan-3-yl)-6a,10b-dimethyl-4,10-dioxododecahydro-1H-benzo[f]isochromene-7-carboxylate (227).**

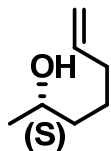
Synthesized according to the procedures of Beguin et al.<sup>311</sup> HPLC in 60% MeCN/40% H<sub>2</sub>O, *t<sub>R</sub>* = 5.074 min; purity = >99.9%. Spectroscopic information was in agreement with reported data.<sup>311</sup>



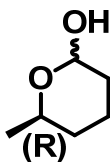


**(R)-hept-6-en-2-ol (R-228)**. Synthesized according to the procedures of Elzner et al.<sup>329</sup>

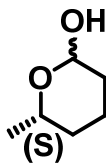
To Mg turnings (834 mg, 34.3 mmol, 2 equiv.) and I<sub>2</sub> (cat.) in an oven-dried 3-neck flask under an atmosphere of argon was added approximately 5 mL of a solution of 4-bromo-1-butene (2.6 mL, 25.7 mmol, 1.5 equiv.) in 25 mL anhydrous THF via dropping funnel. The suspension turned orange-brown and was heated with a heat gun until the color spontaneously lightened to a very light grey-brown (approximately 2 minutes of heating). The rest of the 4-bromo-1-butene solution was then added slowly via dropping funnel, as the reaction mixture was heated to reflux. When the addition was finished, the reaction mixture was allowed to continue refluxing for an additional 20 minutes. The mixture was allowed to cool to room temperature, then cooled to -78 °C, and CuI (490 mg, 2.57 mmol, 0.15 equiv.) was added followed by an additional 10 mL of anhydrous THF. The reaction stirred at -78 °C for 30 minutes. After this time (*R*)-(+)-propylene oxide (1.2 mL, 17.1 mmol) was added at -78 °C in a dropwise manner. The reaction mixture was then warmed to -10 °C and allowed to stir overnight without recharging the ice-brine bath. The now dark brown-black reaction mixture was quenched by carefully pouring it into 200 mL of 1:1 sat. aq. NH<sub>4</sub>Cl:H<sub>2</sub>O at 0 °C and stirring for 1 h. After this time, the mixture had turned bright blue and was then extracted with diethyl ether (3 × 50 mL). The organic layers were collected, dried over Na<sub>2</sub>SO<sub>4</sub>, filtered, and the solvent removed *in vacuo*. The residue was purified by flash column chromatography using EtOAc/*n*-hexanes (1:5) to give 1.3826 g (71% yield) *R<sub>f</sub>* = 0.34 as a light yellow oil. <sup>1</sup>H NMR (500 MHz, CDCl<sub>3</sub>) δ 5.81 (ddt, *J* = 6.7, 10.2, 16.9, 1H), 5.07 – 4.92 (m, 2H), 3.80 (s, 1H), 2.13 – 2.02 (m, 2H), 1.61 – 1.40 (m, 4H), 1.19 (d, *J* = 6.2, 3H). <sup>13</sup>C NMR (126 MHz, CDCl<sub>3</sub>) δ 138.71, 114.61, 68.02, 38.73, 33.69, 25.03, 23.53.



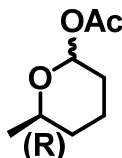
**(S)-hept-6-en-2-ol (S-228).** Synthesized from (S)-(-)-propylene oxide following the procedure described for **R-228** to give 1.3727 g (70% yield)  $R_f = 0.34$  (EtOAc/*n*-hexanes 1:4) as a light yellow oil.  $^1\text{H}$  NMR (500 MHz,  $\text{CDCl}_3$ )  $\delta$  5.81 (ddt,  $J = 6.7, 10.2, 16.9$ , 1H), 5.07 – 4.91 (m, 2H), 3.81 (dd,  $J = 5.7, 11.5$ , 1H), 2.14 – 2.01 (m, 2H), 1.57 – 1.40 (m, 4H), 1.19 (d,  $J = 6.2, 3\text{H}$ ).  $^{13}\text{C}$  NMR (126 MHz,  $\text{CDCl}_3$ )  $\delta$  138.71, 114.61, 68.03, 38.73, 33.69, 25.03, 23.53.



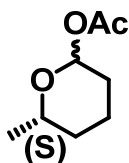
**(6R)-6-methyltetrahydro-2H-pyran-2-ol (R-229).** Synthesized according to the procedures of Yang et al.<sup>330</sup> To a solution of alcohol **R-228** (500 mg, 4.38 mmol) and  $\text{RuCl}_3 \cdot 3\text{H}_2\text{O}$  (40 mg, 0.153 mmol, 3.5 mol%) in  $\text{CH}_3\text{CN}:\text{H}_2\text{O}$  (6:1, 28 mL) was added  $\text{NaIO}_4$  (1.87 g, 8.76 mmol, 2 equiv.) in portions over 5 min. The reaction mixture stirred for 1 h and was complete by TLC observation,  $R_f = 0.29$  (EtOAc/*n*-hexanes 1:4). The mixture was quenched with sat. aq.  $\text{Na}_2\text{S}_2\text{O}_3$  (30 mL), stirring for 20 min. The layers were allowed to separate, and the aqueous layer was extracted with diethyl ether ( $3 \times 30$  mL). The combined organic layers were washed with  $\text{H}_2\text{O}$  (50 mL), brine (50 mL), dried over  $\text{Na}_2\text{SO}_4$ , filtered, and the solvent very carefully removed *in vacuo* to afford the crude pyranol **R-229** as a light yellow to orange oil which was immediately and entirely carried on to acetylation without further purification.



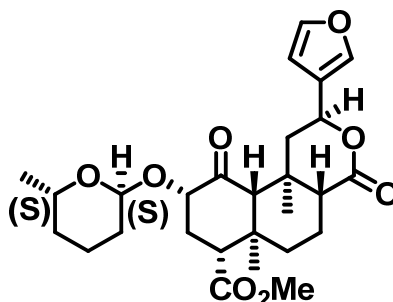
**(6S)-6-methyltetrahydro-2H-pyran-2-ol (S-229)**. Synthesized from **S-228** following the procedure described for **R-229**.



**(6R)-6-methyltetrahydro-2H-pyran-2-yl acetate (R-230)**. Synthesized from the crude product **R-229** according to the procedures of Coombs et al.<sup>331</sup> To a solution of crude alcohol **R-229** (4.38 mmol) in anhydrous methylene chloride (15 mL) at 0 °C under an atmosphere of argon was added DMAP (54 mg, 0.438 mmol, 0.1 equiv.) and acetic anhydride (621  $\mu$ L, 6.57 mmol, 1.5 equiv.), followed by triethylamine (1.22 mL, 8.76 mmol, 2 equiv.) in a dropwise manner. The reaction stirred at 0 °C for 20 min and was complete by TLC observation,  $R_f = 0.71$  (EtOAc/*n*-hexanes 1:2). The reaction was quenched by the addition of sat. aq.  $\text{NaHCO}_3$  (20 mL). The organic layer was washed with 1:1  $\text{H}_2\text{O}:\text{NaHCO}_3$  ( $2 \times 20$  mL). The combined aqueous layers were extracted with methylene chloride ( $2 \times 20$  mL). Finally, the combined organic layers were washed with  $\text{H}_2\text{O}$  (50 mL), brine (50 mL), dried over  $\text{Na}_2\text{SO}_4$ , filtered, and the solvent very carefully removed *in vacuo* to afford the crude acetylated pyran **R-230** as a light yellow to orange-brown oil which was entirely carried on to coupling reactions without further purification.

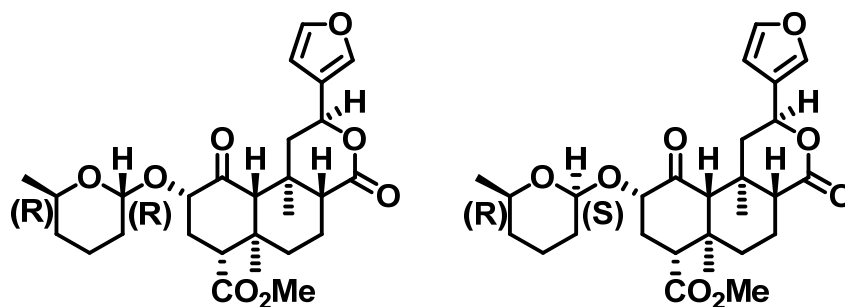


**(6S)-6-methyltetrahydro-2H-pyran-2-yl acetate (S-230).** Synthesized from **S-229** following the procedure described for **R-230**.



**(2S,4aR,6aR,7R,9S,10aS,10bR)-methyl 2-(furan-3-yl)-6a,10b-dimethyl-9-(((2S,6S)-6-methyltetrahydro-2H-pyran-2-yl)oxy)-4,10-dioxododecahydro-1H-benzo[f]isochromene-7-carboxylate (231).** Synthesized following the procedures of Magauer et al.<sup>332</sup> To a solution of **123** (250 mg, 0.640 mmol) in anhydrous 1,2-dichloroethane (20 mL) under an atmosphere of argon was added pyridinium *p*-toluene sulfonate (8 mg, 0.032 mmol, 0.05 equiv.) followed by crude pyran **S-230** (4.38 mmol, 6.8 equiv.) in anhydrous 1,2-dichloroethane (5 mL). The reaction was heated to 80 °C for 6 – 8 h, after which time additional pyridinium *p*-toluene sulfonate (8 mg, 0.032 mmol, 0.05 equiv.) was added, and the reaction was continued through 24 h. The reaction mixture was then allowed to cool to room temperature and diluted with EtOAc (70 mL). The organic layers were washed with sat. aq. NaHCO<sub>3</sub> (3 × 50 mL), H<sub>2</sub>O (50 mL), brine (50 mL), dried over Na<sub>2</sub>SO<sub>4</sub>, filtered, and the solvent removed *in vacuo*. The single product was purified by flash column chromatography using EtOAc/*n*-hexanes (1:2) and triturated from EtOAc/Et<sub>2</sub>O/*n*-hexanes to give 0.0277 g (9% yield) R<sub>f</sub> = 0.49 (EtOAc/*n*-hexanes 2:3) as a white powder. <sup>1</sup>H NMR (500 MHz, CDCl<sub>3</sub>) δ 7.43 – 7.38 (m, 2H), 6.37 (s, 1H), 5.53

(dd,  $J = 5.0, 11.7, 1\text{H}$ ), 4.92 (d,  $J = 3.0, 1\text{H}$ ), 4.26 (dd,  $J = 7.9, 11.9, 1\text{H}$ ), 3.83 (dd,  $J = 5.4, 10.1, 1\text{H}$ ), 3.73 (s, 3H), 2.73 (dd,  $J = 4.0, 12.9, 1\text{H}$ ), 2.52 (dd,  $J = 5.1, 13.3, 1\text{H}$ ), 2.34 – 2.09 (m, 4H), 2.06 – 2.02 (m, 1H), 1.94 – 1.74 (m, 4H), 1.63 (dd,  $J = 8.2, 12.9, 2\text{H}$ ), 1.56 – 1.48 (m, 2H), 1.46 (s, 3H), 1.34 – 1.21 (m, 2H), 1.12 (d,  $J = 4.7, 6\text{H}$ ).  $^{13}\text{C}$  NMR (126 MHz,  $\text{CDCl}_3$ )  $\delta$  207.05, 171.99, 171.28, 143.74, 139.35, 125.29, 108.32, 97.12, 76.52, 72.01, 65.61, 64.23, 54.09, 51.88, 51.53, 43.55, 42.02, 38.26, 35.49, 32.89, 32.77, 29.03, 21.88, 18.16, 17.66, 16.49, 15.22. HRMS ( $m/z$ ):  $[\text{M}+\text{Na}]$  calcd for  $\text{C}_{27}\text{H}_{36}\text{O}_8\text{Na}$ , 511.2308; found 511.2297, 2.2 ppm. HPLC in 60% MeCN/40%  $\text{H}_2\text{O}$ ,  $t_{\text{R}} = 13.376$  min; purity = 98.2%.



(2S,4aR,6aR,7R,9S,10aS,10bR)-methyl 2-(furan-3-yl)-6a,10b-dimethyl-9-(((2R,6R)-6-methyltetrahydro-2H-pyran-2-yl)oxy)-4,10-dioxododecahydro-1H-benzo[f]isochromene-7-carboxylate (**232a**) and (2S,4aR,6aR,7R,9S,10aS,10bR)-methyl 2-(furan-3-yl)-6a,10b-dimethyl-9-(((2S,6R)-6-methyltetrahydro-2H-pyran-2-yl)oxy)-4,10-dioxododecahydro-1H-benzo[f]isochromene-7-carboxylate (**232b**). Synthesized following the procedures of Magauer et al.<sup>332</sup> To a solution of **123** (250 mg, 0.640 mmol) in anhydrous 1,2-dichloroethane (20 mL) under an atmosphere of argon was added pyridinium *p*-toluene sulfonate (8 mg, 0.032 mmol, 0.05 equiv.) followed by crude pyran **R-230** (4.38 mmol, 6.8 equiv.) in anhydrous 1,2-dichloroethane (5 mL). The reaction was heated to 80 °C for 6 – 8 h, after which time additional pyridinium *p*-toluene sulfonate (8 mg, 0.032 mmol, 0.05 equiv.) was added, and the reaction was continued through 24 h. The reaction mixture was then allowed to cool to room temperature and

diluted with EtOAc (70 mL). The organic layers were washed with sat. aq. NaHCO<sub>3</sub> (3 × 50 mL), H<sub>2</sub>O (50 mL), brine (50 mL), dried over Na<sub>2</sub>SO<sub>4</sub>, filtered, and the solvent removed *in vacuo*. The diastereomer products were purified from unreacted and excess starting material by flash column chromatography using EtOAc/*n*-hexanes (3:7) to give 0.5911 g as a light yellow powder. The diastereomer products were then separated from each other by HPLC with an isocratic solvent gradient of 50% MeCN/50% H<sub>2</sub>O and a flow rate of 5 mL/min to give 0.0226 g (**232a**) *R<sub>f</sub>* = 0.31 (EtOAc/*n*-hexanes 2:3) and 0.0246 g (**232b**) *R<sub>f</sub>* = 0.27 (EtOAc/*n*-hexanes 2:3) as off-white powders (15% combined yield). **232a**: <sup>1</sup>H NMR (500 MHz, CDCl<sub>3</sub>) δ 7.46 – 7.38 (m, 2H), 6.41 (s, 1H), 5.55 (dd, *J* = 5.0, 11.8, 1H), 4.44 (dd, *J* = 2.0, 9.3, 1H), 4.32 (dd, *J* = 7.5, 12.2, 1H), 3.70 (s, 3H), 3.48 – 3.40 (m, 1H), 2.71 (dd, *J* = 3.2, 13.5, 1H), 2.56 (dd, *J* = 5.1, 13.3, 1H), 2.46 – 2.38 (m, *J* = 7.4, 1H), 2.31 – 2.09 (m, 3H), 2.06 – 1.93 (m, 2H), 1.90 – 1.73 (m, *J* = 13.3, 3H), 1.70 – 1.60 (m, 2H), 1.52 (d, *J* = 16.8, 2H), 1.47 (s, 3H), 1.25 (s, 2H), 1.19 (d, *J* = 6.2, 3H), 1.12 (s, 3H). <sup>13</sup>C NMR (126 MHz, CDCl<sub>3</sub>) δ 206.90, 171.82, 171.25, 143.73, 139.43, 125.42, 108.35, 101.68, 78.26, 72.31, 71.97, 64.24, 53.98, 51.83, 51.65, 43.78, 41.97, 38.19, 35.54, 32.94, 32.25, 30.61, 21.98, 21.62, 18.16, 16.49, 15.18. HRMS (*m/z*): [M+Na] calcd for C<sub>27</sub>H<sub>36</sub>O<sub>8</sub>Na, 511.2308; found 511.2323, 2.9 ppm. HPLC in 60% MeCN/40% H<sub>2</sub>O, *t<sub>R</sub>* = 10.260 min; purity = 95.3%. **232b**: <sup>1</sup>H NMR (500 MHz, CDCl<sub>3</sub>) δ 7.42 – 7.38 (m, *J* = 1.7, 2H), 6.37 (s, 1H), 5.56 (dd, *J* = 5.1, 11.7, 1H), 4.89 (d, *J* = 2.6, 1H), 4.18 (dd, *J* = 7.3, 12.3, 1H), 4.05 – 3.96 (m, *J* = 4.4, 11.2, 1H), 3.71 (s, 3H), 2.67 (dd, *J* = 3.3, 13.4, 1H), 2.57 (dd, *J* = 5.1, 13.3, 1H), 2.39 (ddd, *J* = 3.3, 7.2, 13.3, 1H), 2.20 – 2.12 (m, 2H), 2.06 (dd, *J* = 3.0, 12.0, 1H), 1.99 – 1.90 (m, *J* = 13.0, 1H), 1.82 – 1.73 (m, 2H), 1.68 – 1.59 (m, 4H), 1.56 – 1.50 (m, 2H), 1.49 (s, 3H), 1.25 (t, *J* = 19.0, 2H), 1.13 (s, 3H), 1.03 (d, *J* = 6.3, 3H). <sup>13</sup>C NMR (126 MHz, CDCl<sub>3</sub>) δ 205.52, 171.98, 171.30, 143.74, 139.24, 125.44, 108.28, 95.63, 77.32, 72.04, 65.64, 64.49, 53.82, 51.87, 51.55,

43.40, 42.08, 38.24, 35.50, 32.66, 31.80, 29.27, 21.73, 18.18, 18.05, 16.45, 15.21. HRMS ( $m/z$ ): [M+Na] calcd for C<sub>27</sub>H<sub>36</sub>O<sub>8</sub>Na, 511.2308; found 511.2310, 0.4 ppm. HPLC in 60% MeCN/40% H<sub>2</sub>O,  $t_R$  = 11.917 min; purity = 99.5%

### *Binding and Efficacy Studies*

**Radioligand Binding Studies.**<sup>213</sup> MOP receptor binding sites were labeled using [<sup>3</sup>H]D-Ala<sup>2</sup>-MePhe<sup>4</sup>,Gly-ol<sup>5</sup>]-enkephalin ([<sup>3</sup>H]DAMGO, SA = 44 – 48 Ci/mmol) while DOP receptor binding sites were labeled using [<sup>3</sup>H][D-Ala<sup>2</sup>, D-Leu<sup>5</sup>]-enkephalin ([<sup>3</sup>H]DADLE, SA = 40 – 50 Ci/mmol) in rat brain homogenates. KOP receptor binding sites were labeled using [<sup>3</sup>H]*N*-methyl-2-phenyl-*N*-[(5*R*,7*S*,8*S*)-7-(pyrrolidin-1-yl)-1-oxaspiro[4.5]dec-8-yl]acetamide ([<sup>3</sup>H]U69,593, SA = 50 Ci/mmol). On the day of the assay, Cell pellets were thawed on ice for 15 minutes followed by homogenization with a polytron in 10 mL/pellet of ice-cold 10mM Tris-HCl, pH 7.4. The membranes were centrifuged at 30,000 × *g* for 10 minutes, then resuspended in 10 mL/pellet ice-cold 10mM Tris-HCl, pH 7.4 followed again by centrifugation at 30,000 × *g* for 10 minutes. Membranes were then resuspended in 25°C 50 mM Tris-HCl, pH 7.4 (~100 mL/pellet hMOP-CHO, 50 mL/pellet hDOP-CHO, and 120 mL/pellet hKOP-CHO). All assays were performed in 50 mM Tris-HCl, pH 7.4 in a final assay volume of 1.0 mL, with a protease inhibitor cocktail: bacitracin (100 µg/mL), bestatin (10 µg/mL), leupeptin (4 µg/mL) and chymostatin (2 µg/mL). Drug dilution curves were determined with buffer containing 1 mg/mL BSA. 20 µM levallorphan ([<sup>3</sup>H]DAMGO and [<sup>3</sup>H]DADLE) or 10 µM (-)-U69,593 (for [<sup>3</sup>H]U69,593 binding) was used to account for nonspecific binding. [<sup>3</sup>H]Radioligands were used at concentrations of approximately 2 nM. After 2 hours of incubation at 25°C, triplicate samples were filtered with Brandell Cell Harvesters (Biomedical Research & Development Inc., Gaithersburg, MD), over Whatman GF/B filters. The filters were the punched into 24-well

plates in which 0.6 mL of LSC-cocktail (Cytoscint) was added. After an overnight extraction, the samples were counted in a Trilux liquid scintillation counter at 44% efficiency. Approximately 30 µg protein was in each assay tube for the opioid binding assays. The inhibition curves were determined by displacing a single concentration of radioligand by 10 concentrations of drug.

**[<sup>35</sup>S]GTP-γ-S Functional Assay.**<sup>68</sup> The [<sup>35</sup>S]GTP-γ-S assays were conducted as previously described. Buffer A is 50 mM Tris-HCl, pH 7.4, containing 100 mM NaCl, 10 mM MgCl<sub>2</sub>, 1 mM EDTA and buffer B is buffer A with the addition of 1.67 mM dithiothreitol (DTT) and 0.15% bovine serum albumin (BSA). On the day of the assay, cells were thawed on ice for 15 min and homogenized using a polytron in 50 mM Tris-HCl, pH 7.4, containing a protease inhibitor cocktail: bacitracin (100 µg/mL), bestatin (10 µg/mL), leupeptin (4 µg/mL) and chymostatin (2 µg/mL). The homogenate was centrifuged at 30,000 × g for 10 minutes at 4°C, and the supernatant discarded. The membrane pellets were then resuspended in buffer B and used for [<sup>35</sup>S]GTP-γ-S binding assays. 50 µL of buffer A plus 0.1% BSA, 50 µL of GDP in buffer A/0.1% BSA (final concentration = 40 µM), 50 µL of drug in buffer A/0.1% bovine serum albumin, 50 µL of [<sup>35</sup>S]GTP-γ-S in buffer A/0.1% BSA (final concentration = 50 pM), and 300 µL of cell membranes (50 µg of protein) in buffer B were added in test tubes. Final concentration of reagents in assay were: 50 mM Tris-HCl, pH 7.4, containing 100 mM NaCl, 10 mM MgCl<sub>2</sub>, 1 mM EDTA, 1 mM DTT, 40 µM GDP, and 0.1% BSA. Media was incubated at 55°C for 3 hours. Non-specific binding was accounted for and determined using GTP-γ-S (40 µM). Vacuum filtration through Whatman GF/B filters separated bound and free [<sup>35</sup>S]GTP-γ-S. The filters were punched into 24-well plates followed by the addition of 0.6 mL of liquid



scintillation media (Cytoscint). An overnight extraction was performed and samples were counted in a Trilux liquid scintillation counter at an efficiency of 27%.

**Calcium Mobilization Assay.**<sup>214</sup> All cells were maintained in F-12 nutrient medium (Ham), supplemented with 10% fetal bovine serum (FBS), 1% penicillin and streptomycin (p/s), and 0.2% normocin. Cell culture supplies were from Invitrogen (Carlsbad, CA) unless otherwise specified. Chinese hamster ovary (CHO) cells stably expressing MOR-, KOR-, DOR-, or CB1-Gαq16 were removed from their flasks using Versene and quenched with the Ham media, centrifuged and re-suspended in media. Cells were counted with a Cellometer Auto T4 (Nexcelom Bioscience, Lawrence, MA) and 30,000 cells were transferred to each well of a black Costar 96-well optical bottom plate (Corning Corporation, Corning, NY). Each plate was incubated at 37°C/5% CO<sub>2</sub> overnight to confluence. The culture media was removed from the plates and cells were subsequently loaded with a fluorescent calcium probe (Calcium 5 dye, Molecular Devices, Sunnyvale, CA) in an HBSS-based buffer containing 20 mM HEPES, 0.25% BSA, 1% DMSO (or 0.5% DMSO + 0.5% EtOH for CB1-expressing cells), and 10 μM probenecid (Sigma) in a total volume of 225 μL. Cells were incubated at 37°C/5% CO<sub>2</sub> for 1 h and then stimulated with DMSO solutions of DAMGO, U69,593, DPDPE, ethanol solutions of CP55,940 or DMSO solutions of test compounds at various concentrations using a Flexstation 3 plate-reader, which automatically added 25 μL of the compounds at 10X concentration to each well after reading baseline values for ~17 sec. Agonist-mediated change in fluorescence (485 nm excitation, 525 nm emission) was monitored in each well at 1.52 sec intervals for 60 sec and reported for each well. Data were collected using Softmax version 4.8 (MDS Analytical Technologies) and analyzed using Prism software (GraphPad, La Jolla, CA). Nonlinear regression analysis was performed to fit data and obtain maximum response ( $E_{max}$ ),  $EC_{50}$ ,

correlation coefficient ( $r_2$ ) and other parameters. All experiments were performed at least 2 times to ensure reproducibility and data reported as mean  $\pm$  standard error, unless noted otherwise.

**X-ray Crystallography for 220.** The asymmetric unit contains one  $C_{26}H_{34}O_8$  molecule that has two slightly different conformations. All displacement ellipsoids are drawn at the 50% probability level.

Needle-shaped single crystals of  $C_{26}H_{34}O_8$  are, at 100(2) K, orthorhombic, space group  $P2_12_12_1 - D_2^4$  (No. 19)<sup>[336]</sup> with  $\mathbf{a} = 6.1944(1) \text{ \AA}$ ,  $\mathbf{b} = 11.2496(3) \text{ \AA}$ ,  $\mathbf{c} = 35.8673(8) \text{ \AA}$ ,  $V = 2499.4(1) \text{ \AA}^3$  and  $Z = 4$  molecules  $\{d_{\text{calcd}} = 1.261 \text{ g/cm}^3; \mu_a(\text{CuK}\alpha) = 0.767 \text{ mm}^{-1}\}$ . A full set of unique diffracted intensities was measured<sup>[337]</sup> (5711  $0.50^\circ$ -wide  $\omega$ - or  $\phi$ -scan frames with counting times of 1–6 seconds) for a single-domain specimen using monochromated  $\text{CuK}\alpha$  radiation ( $\lambda = 1.54178 \text{ \AA}$ ) on a Bruker Single Crystal Diffraction System equipped with Helios multilayer optics, an APEX II CCD detector and a Bruker MicroSTAR microfocus rotating anode x-ray source operating at 45kV and 60mA. Lattice constants were determined with the Bruker SAINT software package using peak centers for 9928 reflections. A total of 26136 integrated reflection intensities having  $2\theta(\text{CuK}\alpha) < 127.30^\circ$  were produced using the Bruker program SAINT<sup>[338]</sup>; 4076 of these were unique and gave  $R_{\text{int}} = 0.041$  with a coverage which was 99.5% complete. The data were corrected empirically for variable absorption effects using equivalent reflections; the relative transmission factors ranged from 0.905 to 1.000. The Bruker software package SHELXTL was used to solve the structure using “direct methods” techniques. All stages of weighted full-matrix least-squares refinement were conducted using  $F_o^2$  data with the SHELXTL Version 6.10 software package.<sup>[339]</sup>

The initial structure solution revealed that the 6-membered tetrahydropyran ring was disordered with two preferred orientations in the crystal. A second molecule having this conformation was therefore introduced into the model and the structure was refined with “whole molecule disorder” by restraining the bond lengths and angles for nonhydrogen atoms of the two molecules to have similar values. The major conformation is present 64% of the time and the minor conformation is present 36% of the time.

The final structural model incorporated anisotropic thermal parameters for all nonhydrogen atoms except minor-occupancy carbon atoms C1' and C26'. Hydrogen atoms were included with fixed isotropic thermal parameters and carbon atoms C1' and C26' were included with variable isotropic thermal parameters. Mild restraints were applied to the anisotropic thermal parameters for 2 nonhydrogen atoms of the major-occupancy conformer and 22 nonhydrogen atoms of the minor-occupancy conformer. Identical anisotropic thermal parameters were used for oxygen atoms O4 and O4' which refined to essentially the same position in the unit cell. All methyl groups were incorporated into the structural model as rigid groups (using idealized  $sp^3$ -hybridized geometry and a C–H bond length of 0.98 Å) with a “staggered” orientation. The remaining hydrogen atoms were included in the structural model at idealized positions ( $sp^2$ - or  $sp^3$ -hybridized geometry with C–H bond lengths of 0.95 – 1.00 Å). All hydrogen atoms utilized isotropic thermal parameters that were fixed at values 1.20 (nonmethyl) or 1.50 (methyl) times the equivalent isotropic thermal parameter of the carbon atom to which they were covalently bonded. A total of 598 parameters were refined using 240 restraints, 4076 data and weights of  $w = 1 / [\sigma^2(F^2) + (0.0785 P)^2 + (0.9339 P)]$ , where  $P = [F_o^2 + 2F_c^2] / 3$ . Final agreement factors at convergence are:  $R_1$ (unweighted, based on F) = 0.046 for 3704 independent absorption-corrected “observed” reflections having  $2\theta(\text{CuK}\alpha) < 127.30^\circ$  and

$I > 2\sigma(I)$ ;  $R_1$ (unweighted, based on  $F$ ) = 0.052 and  $wR_2$ (weighted, based on  $F^2$ ) = 0.126 for all 4076 independent absorption-corrected reflections having  $2\theta(\text{CuK}\alpha) < 127.30^\circ$ . The largest shift/s.u. was 0.001 in the final refinement cycle. The final difference map had maxima and minima of 0.38 and  $-0.34 \text{ e}^-/\text{\AA}^3$ , respectively. Since oxygen was the “heaviest” element present, the absolute configuration could not be reliably established using anomalous dispersion of the x-rays; the “Flack” absolute structure parameter refined to a final value of 0.0(2).

## CHAPTER 6: DISSERTATION CONCLUSIONS

Opioid analgesics are a mainstay in the clinic for the management and treatment of pain. The opioid receptor system itself has been implicated in the etiology of depression, mood regulation, and drug abuse. However, there are several important drawbacks associated with currently known opioid receptor ligands. Compounds that are selective agonists for the MOP receptor tend to produce constipation, respiratory depression, tolerance, and dependence. While there is an abundance of seemingly structurally diverse MOP ligands, these molecules can actually be related to each other through the systematic dismantling of the morphine scaffold. Unfortunately, the adverse effects associated with morphine tend to carry through to synthetic analogs, despite extensive scaffold manipulation. Compounds that are selective agonists for the KOP receptor can have a dysphoric effect, and selective antagonists of the KOP receptor tend to have an unusually long duration of action *in vivo* making for generally poor candidates for pharmacotherapies. Thus there is a critical need for the identification and development of novel, non-morphine-based opioid ligands. Novel chemical scaffolds that are active at opioid receptors have the potential to be biological probes as well as pharmacotherapies that improve upon or lack utterly the shortcomings associated with currently known ligands.

This study was conducted in search of novel, non-morphine-based opioid ligands. The flavonoid structural class was investigated based on literature precedent that molecules belonging to this class had been found to have affinity and potency at opioid receptors, as well as some receptor subtype selectivity.<sup>179</sup> Two flavonoid compounds isolated from the Brazilian vine *Dioclea grandiflora*, dioclein (**86**) and dioflorin (**87**), were reported to have antinociceptive effects in rodents that were reversed by the opioid antagonist naloxone.<sup>200-201</sup> However no *in*

*vitro* pharmacological evaluation of these compounds had been published. In order to determine if dioclein and dioflorin were indeed opioid ligands and generate some SAR, dioclein and several simplified analogs of dioflorin were synthesized and evaluated for affinity and potency using radioligand binding assays (opioid receptors), the fluorescent calcium mobilization assay (opioid and cannabinoid receptors), and the luminescent  $\beta$ -arrestin assay (opioid and GPR-55 receptors). Unfortunately, despite extensive investigation of possible biological targets, none of the flavonoids in this study appeared to have any activity that could explain the antinociceptive effects reported in rodents. One possible explanation is that the simplifications made to the dioflorin scaffold abolished any receptor activity. Another possibility is that the compounds identified in the literature as the ones responsible for antinociceptive effects were contaminated with an undetected impurity that was actually the active constituent. A third possibility is that these compounds exert their antinociceptive effects through a receptor system not examined in this report. In any case, the antinociceptive effects of flavonoids isolated from *Dioclea grandiflora* require confirmation before further analog synthesis and pharmacological evaluation can take place.

The neoclerodane diterpene structural class was also investigated as a source of novel opioid ligands. Salvinorin A (**108**), a member of this class, is the first non-nitrogenous opioid ligand ever reported and is a selective and potent agonist at the KOP receptor.<sup>180</sup> Modifications to the C-2 acetate of salvinorin A have been reported to change receptor selectivity; herkinorin (**141**), a C-2 benzoyl derivative of salvinorin A, is a selective and potent MOP receptor agonist.<sup>281</sup> Alkoxy ethers at the C-2 position (e.g. **190** and **191**) have been reported to improve KOP receptor affinity and potency.<sup>322</sup> However, as these ethers have a significant amount of rotational flexibility, the structural basis for their improved profile is unknown; for example, it is

possible for ethoxymethyl ether **191** to adopt either an extended or an eclipsed conformation (Figure 35). It is also possible that C-2 alkoxy ethers can participate in hydrogen bonding interactions not exploited by salvinorin A. In order to determine the KOP receptor binding mode of alkoxy ethers at the C-2 position, a series of analogs was synthesized and evaluated at opioid receptors via radioligand binding, the [<sup>35</sup>S]GTP- $\gamma$ -S functional assay, and the fluorescent calcium mobilization functional assay.

Analysis of this series of C-2 derivatives revealed several details about the salvinorin A–KOP receptor binding pocket. First, there is a stereochemical preference; tetrahydropyranyl ligands with the anomeric hydrogen in the  $\beta$  position (e.g. **220** and **231**) had better affinity and potency than their epimers. This trend likely carries through to acyclic ligands that are able to adopt a conformation similar to **220**; ether compound **223a** had higher affinity than its epimer **223b**, although the absolute configurations were not determined. Second, there are steric limitations within the binding pocket. Tetrahydrofuran derivatives **222a,b** had only modest affinity for the KOP receptor and poor potency and, though epimers, were not different from each other. This suggests that their smaller size may fail to achieve key interactions within the receptor binding pocket that would differentiate them from each other and lead to potent KOP receptor activation. Conversely, brominated ethers **224a,b** had no affinity for the KOP receptor, suggesting that their increased size precluded binding. Thirdly, in examining an overlay of the crystal structures of salvinorin A and **220** (Figure 42B), it is possible that **220** is able to take advantage of binding interactions within the receptor that salvinorin A cannot exploit; the tetrahydropyranyl oxygen of **220** occupies a region in space that is not occupied by heteroatoms in salvinorin A. This may explain the affinity and potency of compounds like **220** and **191** as well; the KOP receptor binding pocket prefers an eclipsed conformation for these types of

ligands. This hypothesis is supported by examining overlays of the crystal structures of salvinorin A, **220**, and **231** (Figures 42C and 42D); the extended, methyltetrahydropyranyl ring of **231** is flipped and the oxygen is in roughly the same space as the carbonyl oxygen on the C-2 acetate of salvinorin A, pushing the additional methyl group out into an empty region of space. The methyl group of **231** may have unfavorable interactions with the KOP receptor, resulting in lower potency relative to **220** and salvinorin A.

Finally, tetrahydropyranyl compound **220** was evaluated for its ability to effect cocaine-primed reinstatement of extinguished cocaine-seeking behavior in a rodent model of relapse. Compound **220** was able to attenuate drug-seeking behavior at a dose of 1.0 mg/kg,<sup>320</sup> comparable to the effects of 0.3 mg/kg salvinorin A, which was previously reported to attenuate reinstatement.<sup>289</sup> This represents the first example of a salvinorin A derivative with demonstrated anti-addictive capabilities.

Collectively, these results underscore the importance of continuing to search for novel scaffolds that have opioid receptor activity. Although investigation of compounds in the flavonoid structural class from *Dioclea grandiflora* did not yield any promising molecules for biological probes or pharmacotherapies, investigation of the neoclerodane diterpene structural class was more fruitful. Stereochemical and steric preferences of the salvinorin A–KOP receptor binding pocket were further elucidated, which will aid further ligand design and SAR development. Further, one analog, tetrahydropyran **220**, was found to have potential as a pharmacotherapy for drug abuse. This confirms the utility of the salvinorin A scaffold as a source of novel, non-morphine-based opioid ligands.



## References

- (1) Borchardt, J. K. The Beginnings of Drug Therapy: Ancient Mesopotamian Medicine. *Drug News Perspect.* **2002**, *15*, 187-192.
- (2) Wasson, R. G. The Soma of the Rig Veda: What Was It? *J. Am. Orient. Soc.* **1971**, *91*, 169-187.
- (3) Ingalls, D. H. H. Remarks on Mr. Wasson's Soma. *J. Am. Orient. Soc.* **1971**, *91*, 188-191.
- (4) Borchardt, J. K. Traditional Chinese Drug Therapy. *Drug News Perspect.* **2003**, *16*, 698-702.
- (5) Diaz, J. L. Ethnopharmacology of Sacred Psychoactive Plants Used by the Indians of Mexico. *Annu. Rev. Pharmacol. Toxicol.* **1977**, *17*, 647-675.
- (6) Rhizopoulou, S.; Katsarou, A. The plant material of medicine. *Adv. Nat. Appl. Sci.* **2008**, *2*, 94-98.
- (7) World Health Organization. Traditional Medicine. **2008**. <http://www.who.int/mediacentre/factsheets/fs134/en/> (accessed March 5, 2012).
- (8) Barnes, P. M.; Bloom, B. Complementary and Alternative Medicine Use Among Adults and Children: United States, 2007. *National Health Statistics Reports* [Online]. **2008**. Number 12. <http://nccam.nih.gov/sites/nccam.nih.gov/files/news/nhsr12.pdf> (accessed March 14, 2012).
- (9) Strohl, W. R. The role of natural products in a modern drug discovery program. *Drug Discov. Today.* **2000**, *5*, 39-41.
- (10) Mishra, B. B.; Tiwari, V. K. Natural products: An evolving role in future drug discovery. *Eur. J. Med. Chem.* **2011**, *46*, 4769-4807.
- (11) Vainio, H.; Morgan, G. Aspirin for the Second Hundred Years: New Uses for an Old Drug. *Pharmacol. Toxicol.* **1997**, *81*, 151-152.
- (12) Sneader, W. The discovery of aspirin: a reappraisal. *Br. Med. J.* **2000**, *321*, 1591-1594.
- (13) Rishton, G. M. Natural products as a robust source of new drugs and drug leads: past successes and present day issues. *Am. J. Cardiol.* **2008**, *101*, 43D-49D.
- (14) Fries, D. S. Opioid Analgesics. In *Foye's Principles of Medicinal Chemistry*. 6 ed.; Lemke, T. L.; Williams, D. A., Eds. Lippincott Williams & Wilkins. Baltimore, MD. **2008**. pp 652-678.
- (15) Aldrich, J. V.; Vigil-Cruz, S. C. Narcotic Analgesics. In *Burger's Medicinal Chemistry and Drug Discovery*. Abraham, D. A., Ed. John Wiley. New York. **2003**. Vol. 6, pp 329-441.
- (16) McCurdy, C. R.; Prisinzano, T. E. Opioid Receptor Ligands. In *Burger's Medicinal Chemistry, Drug Discovery, and Development*. John Wiley & Sons, Inc. **2010**. pp 1-168.
- (17) Gulland, J. M.; Robinson, R. The morphine group. Part I. A discussion of the constitutional problem. *J. Chem. Soc.* **1923**, *123*, 980-998.
- (18) Gulland, J. M.; Robinson, R. The morphine group. Part II. Thebainone, thebainol, and dihydrothebainone. *J. Chem. Soc.* **1923**, *123*, 998-1011.
- (19) Gulland, J. M.; Robinson, R. *Mem. Proc. Manchester Lit. Phil. Soc.* **1925**, *69*, 79.
- (20) Gates, M.; Tschudi, G. The Synthesis of Morphine. *J. Am. Chem. Soc.* **1952**, *74*, 1109-1110.
- (21) Gates, M.; Tschudi, G. The Synthesis of Morphine. *J. Am. Chem. Soc.* **1956**, *78*, 1380-1393.

- (22) Newman, D. J.; Cragg, G. M. Natural Products As Sources of New Drugs over the 30 Years from 1981 to 2010. *J. Nat. Prod.* **2012**, *75*, 311-335.
- (23) Mitscher, L. A. Coevolution: Mankind and Microbes. *J. Nat. Prod.* **2008**, *71*, 497-509.
- (24) Fleming, A. The antibacterial action of cultures of a *Penicillium*, with special reference to their use in the isolation of *B. influenzae*. *Br. J. Exp. Pathol.* **1929**, *10*, 226-236.
- (25) Waksman, S. A.; Reilly, H. C.; Johnstone, D. B. Isolation of Streptomycin-producing Strains of *Streptomyces griseus*. *J. Bacteriol.* **1946**, *52*, 393-397.
- (26) Finland, M. Twenty-fifth anniversary of the discovery of Aureomycin: the place of the tetracyclines in antimicrobial therapy. *Clin. Pharmacol. Ther.* **1974**, *15*, 3-8.
- (27) McGuire, J. M.; Bunch, R. L.; Anderson, R. C.; Boaz, H. E.; Flynn, E. H.; Powell, H. M.; Smith, J. W. Ilotycin, a new antibiotic. *Antibiot. Chemother.* **1952**, *2*, 281-283.
- (28) Centers for Disease Control and Prevention. Achievements in Public Health, 1900-1999: Control of Infectious Diseases. **1999**. <http://www.cdc.gov/mmwr/preview/mmwrhtml/mm4829a1.htm> (accessed March 16, 2012).
- (29) Noble, R. L.; Beer, C. T.; Cutts, J. H. Role of chance observations in chemotherapy: *Vinca rosea*. *Ann. N. Y. Acad. Sci.* **1958**, *76*, 882-894.
- (30) Svoboda, G. H.; Johnson, I. S.; Gorman, M.; Neuss, N. Current status of research on the alkaloids of *Vinca rosea* Linn. (*Catharanthus roseus* G. Don). *J. Pharm. Sci.* **1962**, *51*, 707-720.
- (31) Brana, M. F.; Sanchez-Migallon, A. Anticancer drug discovery and pharmaceutical chemistry: a history. *Clin. Transl. Oncol.* **2006**, *8*, 717-728.
- (32) Grothaus, P. G.; Cragg, G. M.; Newman, D. J. Plant natural products in anticancer drug discovery. *Curr. Org. Chem.* **2010**, *14*, 1781-1791.
- (33) Hartwell, J. L.; Schrecker, A. W. Components of podophyllin. V. The constitution of podophyllotoxin. *J. Am. Chem. Soc.* **1951**, *73*, 2909-2916.
- (34) Wall, M. E.; Wani, M. C.; Cook, C. E.; Palmer, K. H.; McPhail, A. T.; Sim, G. A. Plant antitumor agents. I. Isolation and structure of camptothecin, a novel alkaloidal leukemia and tumor inhibitor from *Camptotheca acuminata*. *J. Am. Chem. Soc.* **1966**, *88*, 3888-3890.
- (35) Kingsbury, W. D.; Boehm, J. C.; Jakas, D. R.; Holden, K. G.; Hecht, S. M.; Gallagher, G.; Caranfa, M. J.; McCabe, F. L.; Faucette, L. F.; et, a. Synthesis of water-soluble (aminoalkyl)camptothecin analogs: inhibition of topoisomerase I and antitumor activity. *J. Med. Chem.* **1991**, *34*, 98-107.
- (36) Sawada, S.; Okajima, S.; Aiyama, R.; Nokata, K.; Furuta, T.; Yokokura, T.; Sugino, E.; Yamaguchi, K.; Miyasaka, T. Synthesis and antitumor activity of 20(S)-camptothecin derivatives: carbamate-linked, water-soluble derivatives of 7-ethyl-10-hydroxycamptothecin. *Chem. Pharm. Bull.* **1991**, *39*, 1446-1454.
- (37) Wani, M. C.; Taylor, H. L.; Wall, M. E.; Coggon, P.; McPhail, A. T. Plant antitumor agents. VI. The isolation and structure of taxol, a novel antileukemic and antitumor agent from *Taxus brevifolia*. *J. Am. Chem. Soc.* **1971**, *93*, 2325-2327.
- (38) Wells, T. N. Natural products as starting points for future anti-malarial therapies: going back to our roots? *Malar. J.* **2011**, *10*(Suppl 1), S3.
- (39) Centers for Disease Control and Prevention. The History of Malaria, an Ancient Disease. **2010**. <http://www.cdc.gov/malaria/about/history/#chloroquine> (accessed March 16, 2012).

- (40) Kaur, K.; Jain, M.; Kaur, T.; Jain, R. Antimalarials from nature. *Bioorg. Med. Chem.* **2009**, *17*, 3229-3256.
- (41) Tu, Y. The discovery of artemisinin (qinghaosu) and gifts from Chinese medicine. *Nat. Med.* **2011**, *17*, 1217-1220.
- (42) Vennerstrom, J. L.; Arbe-Barnes, S.; Brun, R.; Charman, S. A.; Chiu, F. C. K.; Chollet, J.; Dong, Y.; Dorn, A.; Hunziker, D.; Matile, H.; McIntosh, K.; Padmanilayam, M.; Santo Tomas, J.; Scheurer, C.; Scorneaux, B.; Tang, Y.; Urwyler, H.; Wittlin, S.; Charman, W. N. Identification of an antimalarial synthetic trioxolane drug development candidate. *Nature*. **2004**, *430*, 900-904.
- (43) Prisinzano, T.; Gebhart, G. F. 6.13 - Pain Overview. In *Comprehensive Medicinal Chemistry II*. Editors-in-Chief: John, B. T.; David, J. T., Eds. Elsevier. Oxford. **2007**. pp 321-326.
- (44) McCurdy, C. R.; Scully, S. S. Analgesic substances derived from natural products (natureceuticals). *Life Sci.* **2005**, *78*, 476-484.
- (45) Smith, H. S. Opioids: maximizing efficacy, minimizing adverse effects. *Therapy*. **2009**, *6*, 629-631.
- (46) Pharmacological management of persistent pain in older persons. *J. Am. Geriatr. Soc.* **2009**, *57*, 1331-1346.
- (47) Chou, R.; Fanciullo, G. J.; Fine, P. G.; Adler, J. A.; Ballantyne, J. C.; Davies, P.; Donovan, M. I.; Fishbain, D. A.; Foley, K. M.; Fudin, J.; Gilson, A. M.; Kelter, A.; Mauskop, A.; O'Connor, P. G.; Passik, S. D.; Pasternak, G. W.; Portenoy, R. K.; Rich, B. A.; Roberts, R. G.; Todd, K. H.; Miaskowski, C. Clinical Guidelines for the Use of Chronic Opioid Therapy in Chronic Noncancer Pain. *J. Pain*. **2009**, *10*, 113-130.
- (48) U.S. National Library of Medicine. MedlinePlus: Acetaminophen and Propoxyphene. **2011**. <http://www.nlm.nih.gov/medlineplus/druginfo/meds/a601008.html> (accessed June 18, 2012).
- (49) Dhawan, B. N.; Cesselin, F.; Raghubir, R.; Reisine, T.; Bradley, P. B.; Portoghese, P. S.; Hamon, M. International Union of Pharmacology. XII. Classification of opioid receptors. *Pharmacol. Rev.* **1996**, *48*, 567-592.
- (50) Beckett, A. H.; Casy, A. F. Synthetic analgesics: stereochemical considerations. *J. Pharm. Pharmacol.* **1954**, *6*, 986-1001.
- (51) Goldstein, A.; Lowney, L. I.; Pal, B. K. Stereospecific and nonspecific interactions of the morphine congener levorphanol in subcellular fractions of mouse brain. *Proc. Natl. Acad. Sci. U. S. A.* **1971**, *68*, 1742-1747.
- (52) Pert, C. B.; Snyder, S. H. Opiate receptor. Demonstration in nervous tissue. *Science*. **1973**, *179*, 1011-1014.
- (53) Simon, E. J.; Hiller, J. M.; Edelman, I. Stereospecific binding of the potent narcotic analgesic tritium-labeled etorphine to rat-brain homogenate. *Proc. Natl. Acad. Sci. U. S. A.* **1973**, *70*, 1947-1949.
- (54) Terenius, L. Stereospecific interaction between narcotic analgesics and a synaptic plasma membrane fraction of rat cerebral cortex. *Acta Pharmacol. Toxicol.* **1973**, *32*, 317-320.
- (55) Martin, W. R.; Eades, C. G.; Thompson, J. A.; Huppler, R. E.; Gilbert, P. E. The effects of morphine- and nalorphine-like drugs in the nondependent and morphine-dependent chronic spinal dog. *J. Pharmacol. Exp. Ther.* **1976**, *197*, 517-532.
- (56) Lord, J. A. H.; Waterfield, A. A.; Hughes, J.; Kosterlitz, H. W. Endogenous opioid peptides: multiple agonists and receptors. *Nature*. **1977**, *267*, 495-499.

- (57) Hughes, J.; Smith, T. W.; Kosterlitz, H. W.; Fothergill, L. A.; Morgan, B. A.; Morris, H. R. Identification of two related pentapeptides from the brain with potent opiate agonist activity. *Nature*. **1975**, *258*, 577-579.
- (58) Teschemacher, H.; Opheim, K. E.; Cox, B. M.; Goldstein, A. Peptidlike substance from pituitary that acts like morphine. 1. Isolation. *Life Sci*. **1975**, *16*, 1771-1775.
- (59) Cox, B. M.; Opheim, K. E.; Teschemacher, H.; Goldstein, A. Peptidlike substance from pituitary that acts like morphine. 2. Purification and properties. *Life Sci*. **1975**, *16*, 1777-1782.
- (60) Li, C. H.; Chung, D. Isolation and structure of an untriakontapeptide with opiate activity from camel pituitary glands. *Proc. Natl. Acad. Sci. U. S. A.* **1976**, *73*, 1145-1148.
- (61) Kieffer, B. L.; Befort, K.; Gaveriaux-Ruff, C.; Hirth, C. G. The delta-opioid receptor : Isolation of a cDNA by expression cloning and pharmacological characterization. *Proc. Natl. Acad. Sci. U. S. A.* **1992**, *89*, 12048-12052.
- (62) Evans, C. J.; Keith, D. E., Jr.; Morrison, H.; Magendzo, K.; Edwards, R. H. Cloning of a delta opioid receptor by functional expression. *Science*. **1992**, *258*, 1952-1955.
- (63) Meng, F.; Xie, G. X.; Thompson, R. C.; Mansour, A.; Goldstein, A.; Watson, S. J.; Akil, H. Cloning and pharmacological characterization of a rat kappa opioid receptor. *Proc. Natl. Acad. Sci. U. S. A.* **1993**, *90*, 9954-9958.
- (64) Wang, J.-B.; Johnson, P. S.; Persico, A. M.; Hawkins, A. L.; Griffin, C. A.; Uhl, G. R. Human mu opiate receptor. cDNA and genomic clones, pharmacologic characterization and chromosomal assignment. *FEBS Lett.* **1994**, *338*, 217-222.
- (65) Corbett, A. D.; Henderson, G.; McKnight, A. T.; Paterson, S. J. 75 years of opioid research: the exciting but vain quest for the Holy Grail. *Br. J. Pharmacol.* **2006**, *147*, S153-S162.
- (66) Kosterlitz, H. W.; Lord, J. A. H.; Paterson, S. J.; Waterfield, A. A. Effects of changes in the structure of enkephalins and of narcotic analgesic drugs on their interactions with mu- and delta-receptors. *Br. J. Pharmacol.* **1980**, *68*, 333-342.
- (67) Handa, B. K.; Lane, A. C.; Lord, J. A. H.; Morgan, B. A.; Rance, M. J.; Smith, C. F. C. Analogs of beta-LPH61-64 possessing selective agonist activity at mu-opiate receptors. *Eur. J. Pharmacol.* **1981**, *70*, 531-540.
- (68) Xu, H.; Hashimoto, A.; Rice, K. C.; Jacobson, A. E.; Thomas, J. B.; Carroll, F. I.; Lai, J.; Rothman, R. B. Opioid peptide receptor studies. 14. Stereochemistry determines agonist efficacy and intrinsic efficacy in the [35S]GTP-gamma-S functional binding assay. *Synapse*. **2001**, *39*, 64-69.
- (69) Chipkin, R. E.; Stewart, J. M.; Stammer, C. H. Opiate activity of [DAla<sup>2</sup>,deltazPhe<sup>4</sup>]-methionine-enkephalinamide. *Biochem. Biophys. Res. Commun.* **1979**, *87*, 890-895.
- (70) Morley, J. S. Structure-activity relationships of enkephalin-like peptides. *Annu. Rev. Pharmacol. Toxicol.* **1980**, *20*, 81-110.
- (71) Shimohigashi, Y.; English, M. L.; Stammer, C. H.; Costa, T. Dehydroenkephalins. IV. Discriminative recognition of delta and mu opiate receptors by enkephalin analogs. *Biochem. Biophys. Res. Commun.* **1982**, *104*, 583-590.
- (72) Casy, A. F.; Parfitt, R. T. Enkephalins, Endorphins, and Other Opioid Peptides. In *Opioid Analgesics: Chemistry and Receptors*. Plenum Press. New York. **1986**. pp 333-384.
- (73) Chavkin, C.; Goldstein, A. Specific receptor for the opioid peptide dynorphin: Structure-activity relationships. *Proc. Natl. Acad. Sci. U. S. A.* **1981**, *78*, 6543-6547.

- (74) Schiller, P. W.; Weltrowska, G.; Nguyen, T. M. D.; Lemieux, C.; Chung, N. N.; Lu, Y. Conversion of delta-, kappa- and mu-receptor selective opioid peptide agonists into delta-, kappa- and mu-selective antagonists. *Life Sci.* **2003**, *73*, 691-698.
- (75) Bennett, M. A.; Murray, T. F.; Aldrich, J. V. Identification of Arodyn, a Novel Acetylated Dynorphin A-(1-11) Analogue, as a Kappa Opioid Receptor Antagonist. *J. Med. Chem.* **2002**, *45*, 5617-5619.
- (76) Wright, C. R. A. XLIX. On the action of organic acids and their anhydrides on the natural alkaloids. Part I. *J. Chem. Soc. Trans.* **1874**, *27*, 1031-1043.
- (77) Wright, C. I. Enzymatic deacetylation of heroin and closely related morphine derivatives by blood serum. *Science.* **1940**, *92*, 244-245.
- (78) Eddy, N. B.; Friebel, H.; Hahn, K. J.; Halbach, H. Codeine and its alternates for pain and cough relief. 4. Potential alternates for cough relief. *Bull. World Health Organ.* **1969**, *40*, 639-719.
- (79) Townsend, E. H., Jr. Prolonged cough suppression. *N. Engl. J. Med.* **1958**, *258*, 63-67.
- (80) Chou, D. T.; Wang, S. C. Studies on the localization of central cough mechanism; site of action of antitussive drugs. *J. Pharmacol. Exp. Ther.* **1975**, *194*, 499-505.
- (81) Blane, G. F.; Boura, A. L. A.; Fitzgerald, A. E.; Lister, R. E. Actions of etorphine hydrochloride, (M99): a potent morphine-like agent. *Br. J. Pharmacol. Chemother.* **1967**, *30*, 11-22.
- (82) Richards, M. L.; Sadee, W. Buprenorphine is an antagonist at the kappa opioid receptor. *Pharm. Res.* **1985**, 178-181.
- (83) Boothby, L. A.; Doering, P. L. Buprenorphine for the treatment of opioid dependence. *Am. J. Health-Syst. Pharm.* **2007**, *64*, 266-272.
- (84) Benson, W. M.; Stefko, P. L.; Randall, L. O. Comparative pharmacology of levorphan, racemorphan, and dextrorphan and related methyl ethers. *J. Pharmacol. Exp. Ther.* **1953**, *109*, 189-200.
- (85) Tortella, F. C.; Pellicano, M.; Bowery, N. G. Dextromethorphan and neuromodulation: old drug coughs up new activities. *Trends Pharmacol. Sci.* **1989**, *10*, 501-7.
- (86) Fullerton, S. E.; May, E. L.; Becker, E. D. Structures related to morphine. XXIII. Stereochemistry of 5,9-dialkyl-6,7-benzomorphans. *J. Org. Chem.* **1962**, *27*, 2144-2147.
- (87) Wood, P. L.; Pilapil, C.; Thakur, M.; Richard, J. W. WIN 44,441: a stereospecific and long-acting narcotic antagonist. *Pharm. Res.* **1984**, *1*, 46-48.
- (88) Roemer, D.; Buescher, H.; Hill, R. C.; Maurer, R.; Petcher, T. J.; Welle, H. B. A.; Bakel, H. C. C. K.; Akkerman, A. M. Bremazocine: a potent, long-acting opiate kappa-agonist. *Life Sci.* **1980**, *27*, 971-978.
- (89) Gutstein, H.; Akil, H. Opioid analgesics. In *Goodman and Gilman's The Pharmacological Basis of Therapeutics*. 10th ed.; Hardman, J.; Limbird, L.; Gilman, A., Eds. McGraw-Hill Medical Publishing Division. New York. **2001**. pp 569-619.
- (90) Elpern, B.; Carabateas, P.; Soria, A. E.; Gardner, L. N.; Grumbach, L. Strong analgesics. The preparation of some ethyl 1-anilinoalkyl-4-phenylpiperidine-4-carboxylates. *J. Am. Chem. Soc.* **1959**, *81*, 3784-3786.
- (91) Eddy, N. B.; Leimbach, D. Synthetic analgesics. II. Dithienylbutenylamines and dithienylbutylamines. *J. Pharmacol. Exp. Ther.* **1953**, *107*, 385-393.
- (92) Gardocki, J. F.; Yelnosky, J.; Kuehn, W. F.; Gunster, J. C. Interaction of nalorphine with fentanyl and Innovar. *Toxicol. Appl. Pharmacol.* **1964**, *6*, 593-601.

- (93) Gardocki, J. F.; Yelnosky, J. Some of the pharmacologic actions of fentanyl citrate. *Toxicol. Appl. Pharmacol.* **1964**, *6*, 48-62.
- (94) Yelnosky, J.; Gardocki, J. F. Some of the pharmacologic actions of fentanyl citrate and droperidol. *Toxicol. Appl. Pharmacol.* **1964**, *6*, 63-70.
- (95) Casy, A. F.; Ogungbamila, F. O. 3-Allyl analogs of fentanyl. *J. Pharm. Pharmacol.* **1982**, *34*, 210.
- (96) Kreek, M. J.; Schlussman, S. D.; Bart, G.; LaForge, K. S.; Butelman, E. R. Evolving perspectives on neurobiological research on the addictions: celebration of the 30th anniversary of NIDA. *Neuropharmacology.* **2004**, *47*, 324-344.
- (97) Braenden, O. J.; Eddy, N. B.; Halbach, H. Synthetic substances with morphine-like effect; relationship between chemical structure and analgesic action. *Bull. World Health Organ.* **1955**, *13*, 937-998.
- (98) Szmuszkovicz, J.; Von, V. P. F. Benzeneacetamide amines: structurally novel non-mu opioids. *J. Med. Chem.* **1982**, *25*, 1125-1126.
- (99) Vonvoigtlander, P. F.; Lahti, R. A.; Ludens, J. H. U-50,488: a selective and structurally novel non-mu (kappa) opioid agonist. *J. Pharmacol. Exp. Ther.* **1983**, *224*, 7-12.
- (100) Lahti, R. A.; Mickelson, M. M.; McCall, J. M.; Von, V. P. F. [3H]U-69593 a highly selective ligand for the opioid kappa receptor. *Eur. J. Pharmacol.* **1985**, *109*, 281-284.
- (101) Calderon, S. N.; Rothman, R. B.; Porreca, F.; Flippen-Anderson, J. L.; McNutt, R. W.; Xu, H.; Smith, L. E.; Bilsky, E. J.; Davis, P.; Rice, K. C. Probes for Narcotic Receptor Mediated Phenomena. 19. Synthesis of (+)-4-[(alphaR)-alpha-((2S,5R)-4-Allyl-2,5-dimethyl-1-piperazinyl)-3-methoxybenzyl]-N,N-diethylbenzamide (SNC 80): A Highly Selective, Nonpeptide Delta Opioid Receptor Agonist. *J. Med. Chem.* **1994**, *37*, 2125-2128.
- (102) Thomas, J. B.; Atkinson, R. N.; Rothman, R. B.; Fix, S. E.; Mascarella, S. W.; Vinson, N. A.; Xu, H.; Dersch, C. M.; Lu, Y. F.; Cantrell, B. E.; Zimmerman, D. M.; Carroll, F. I. Identification of the first trans-(3R,4R)- dimethyl-4-(3-hydroxyphenyl)piperidine derivative to possess highly potent and selective opioid kappa receptor antagonist activity. *J. Med. Chem.* **2001**, *44*, 2687-2690.
- (103) Brugel, T. A.; Smith, R. W.; Balestra, M.; Becker, C.; Daniels, T.; Hoerter, T. N.; Koether, G. M.; Throner, S. R.; Panko, L. M.; Folmer, J. J.; Cacciola, J.; Hunter, A. M.; Liu, R.; Edwards, P. D.; Brown, D. G.; Gordon, J.; Ledonne, N. C.; Pietras, M.; Schroeder, P.; Sygowski, L. A.; Hirata, L. T.; Zacco, A.; Peters, M. F. Discovery of 8-azabicyclo[3.2.1]octan-3-yloxy-benzamides as selective antagonists of the kappa opioid receptor. Part 1. *Bioorg. Med. Chem. Lett.* **2010**, *20*, 5847-5852.
- (104) Brugel, T. A.; Smith, R. W.; Balestra, M.; Becker, C.; Daniels, T.; Koether, G. M.; Throner, S. R.; Panko, L. M.; Brown, D. G.; Liu, R.; Gordon, J.; Peters, M. F. SAR development of a series of 8-azabicyclo[3.2.1]octan-3-yloxy-benzamides as kappa opioid receptor antagonists. Part 2. *Bioorg. Med. Chem. Lett.* **2010**, *20*, 5405-5410.
- (105) Peters, M. F.; Zacco, A.; Gordon, J.; Maciag, C. M.; Litwin, L. C.; Thompson, C.; Schroeder, P.; Sygowski, L. A.; Piser, T. M.; Brugel, T. A. Identification of short-acting kappa-opioid receptor antagonists with anxiolytic-like activity. *Eur. J. Pharmacol.* **2011**, *661*, 27-34.
- (106) Mitch, C. H.; Quimby, S. J.; Diaz, N.; Pedregal, C.; de, I. T. M. G.; Jimenez, A.; Shi, Q.; Canada, E. J.; Kahl, S. D.; Statnick, M. A.; McKinzie, D. L.; Benesh, D. R.; Rash, K. S.; Barth, V. N. Discovery of Aminobenzyloxyarylamides as Kappa Opioid Receptor

- Selective Antagonists: Application to Preclinical Development of a Kappa Opioid Receptor Antagonist Receptor Occupancy Tracer. *J. Med. Chem.* **2011**, *54*, 8000-8012.
- (107) Frankowski, K. J.; Ghosh, P.; Setola, V.; Tran, T. B.; Roth, B. L.; Aube, J. N-Alkyl-octahydroisoquinolin-1-one-8-carboxamides: Selective and Nonbasic Kappa-Opioid Receptor Ligands. *ACS Med. Chem. Lett.* **2010**, *1*, 189-193.
- (108) Frankowski, K. J.; Hedrick, M. P.; Gosalia, P.; Li, K.; Shi, S.; Whipple, D.; Ghosh, P.; Prisinzano, T. E.; Schoenen, F. J.; Su, Y.; Vasile, S.; Sergienko, E.; Gray, W.; Hariharan, S.; Milan, L.; Heynen-Genel, S.; Mangravita-Novo, A.; Vicchiarelli, M.; Smith, L. H.; Streicher, J. M.; Caron, M. G.; Barak, L. S.; Bohn, L. M.; Chung, T. D. Y.; Aube, J. Discovery of small molecule kappa opioid receptor agonist and antagonist chemotypes through a HTS and Hit refinement strategy. *ACS Chem. Neurosci.* **2012**, *3*, 221-236.
- (109) Verhoest, P. R.; Sawant, B. A.; Parikh, V.; Hayward, M.; Kauffman, G. W.; Paradis, V.; McHardy, S. F.; McLean, S.; Grimwood, S.; Schmidt, A. W.; Vanase-Frawley, M.; Freeman, J.; Van, D. J.; Cox, L.; Wong, D.; Liras, S. Design and Discovery of a Selective Small Molecule Kappa Opioid Antagonist (2-Methyl-N-((2'-(pyrrolidin-1-ylsulfonyl)biphenyl-4-yl)methyl)propan-1-amine, PF-4455242). *J. Med. Chem.* **2011**, *54*, 5868-5877.
- (110) Pan, H.-L.; Wu, Z.-Z.; Zhou, H.-Y.; Chen, S.-R.; Zhang, H.-M.; Li, D.-P. Modulation of pain transmission by G-protein-coupled receptors. *Pharmacol. Ther.* **2008**, *117*, 141-161.
- (111) Wheatley, M.; Wootten, D.; Conner, M. T.; Simms, J.; Kendrick, R.; Logan, R. T.; Poyner, D. R.; Barwell, J. Lifting the lid on GPCRs: the role of extracellular loops. *Br. J. Pharmacol.* **2012**, *165*, 1688-1703.
- (112) Lu, Z.-L.; Saldanha, J. W.; Hulme, E. C. Seven-transmembrane receptors: crystals clarify. *Trends Pharmacol. Sci.* **2002**, *23*, 140-146.
- (113) Kristiansen, K. Molecular mechanisms of ligand binding, signaling, and regulation within the superfamily of G-protein-coupled receptors: molecular modeling and mutagenesis approaches to receptor structure and function. *Pharmacol. Ther.* **2004**, *103*, 21-80.
- (114) Neves, S. R.; Ram, P. T.; Iyengar, R. G Protein Pathways. *Science.* **2002**, *296*, 1636-1639.
- (115) Sadjia, R.; Alagem, N.; Reuveny, E. Gating of GIRK Channels: Details of an Intricate, Membrane-Delimited Signaling Complex. *Neuron.* **2003**, *39*, 9-12.
- (116) Magalhaes, A. C.; Dunn, H.; Ferguson, S. S. G. Regulation of GPCR activity, trafficking and localization by GPCR-interacting proteins. *Br. J. Pharmacol.* **2012**, *165*, 1717-1736.
- (117) Shukla, A. K.; Xiao, K.; Lefkowitz, R. J. Emerging paradigms of beta-arrestin-dependent seven transmembrane receptor signaling. *Trends Biochem. Sci.* **2011**, *36*, 457-469.
- (118) Pitcher, J. A.; Tesmer, J. J. G.; Freeman, J. L. R.; Capel, W. D.; Stone, W. C.; Lefkowitz, R. J. Feedback inhibition of G protein-coupled receptor kinase 2 (GRK2) activity by extracellular signal-regulated kinases. *J. Biol. Chem.* **1999**, *274*, 34531-34534.
- (119) Violin, J. D.; Lefkowitz, R. J. Beta-arrestin-biased ligands at seven-transmembrane receptors. *Trends Pharmacol. Sci.* **2007**, *28*, 416-422.
- (120) Kivell, B.; Prisinzano, T. E. Kappa opioids and the modulation of pain. *Psychopharmacol.* **2010**, *210*, 109-119.
- (121) Friedman, J. D.; Buono, F. A. D. Opioid antagonists in the treatment of opioid-induced constipation and pruritus. *Ann. Pharmacother.* **2001**, *35*, 85-91.
- (122) Pappagallo, M. Incidence, prevalence, and management of opioid bowel dysfunction. *Am. J. Surg.* **2001**, *182*, 11S-18S.

- (123) Foss, J. F. A Review of the Potential Role of Methylnaltrexone in Opioid Bowel Dysfunction. *Am. J. Surg.* **2001**, *182*, 19S-26S.
- (124) Cherny, N. I. Opioid analgesics: comparative features and prescribing guidelines. *Drugs.* **1996**, *51*, 713-737.
- (125) Principles of Analgesic Use in the Treatment of Acute Pain and Cancer Pain. 4th ed.; American Pain Society: Glenview, IL, **1999**; p. 64.
- (126) Savage, S.; Covington, E. C.; Heit, H. A.; Hunt, J.; Joranson, D.; Schnoll, S. H. Definitions Related to the Use of Opioids for the Treatment of Pain. American Academy of Pain Medicine, American Pain Society, American Society of Addiction Medicine: Glenview, IL, **2001**.
- (127) Pfeiffer, A.; Brantl, V.; Herz, A.; Emrich, H. M. Psychotomimesis Mediated by Kappa-Opiate Receptors. *Science.* **1986**, *233*, 774-776.
- (128) Carlezon, W. A.; Beguin, C.; Knoll, A. T.; Cohen, B. M. Kappa-opioid ligands in the study and treatment of mood disorders. *Pharmacol. Ther.* **2009**, *123*, 334-343.
- (129) Turgeon, S. M.; Pollack, A. E.; Fink, J. S. Enhanced CREB phosphorylation and changes in c-Fos and FRA expression in striatum accompany amphetamine sensitization. *Brain Res.* **1997**, *749*, 120-126.
- (130) Pliakas, A. M.; Carlson, R. R.; Neve, R. L.; Konradi, C.; Nestler, E. J.; Carlezon, W. A., Jr. Altered responsiveness to cocaine and increased immobility in the forced swim test associated with elevated cAMP response element-binding protein expression in nucleus accumbens. *J. Neurosci.* **2001**, *21*, 7397-7403.
- (131) Chartoff, E. H.; Papadopoulou, M.; MacDonald, M. L.; Parsegian, A.; Potter, D.; Konradi, C.; Carlezon, W. A., Jr. Desipramine reduces stress-activated dynorphin expression and CREB phosphorylation in NAc tissue. *Mol. Pharmacol.* **2009**, *75*, 704-712.
- (132) Carlezon, W. A., Jr.; Thome, J.; Olson, V. G.; Lane-Ladd, S. B.; Brodtkin, E. S.; Hiroi, N.; Duman, R. S.; Neve, R. L.; Nestler, E. J. Regulation of cocaine reward by CREB. *Science.* **1998**, *282*, 2272-2275.
- (133) Mague, S. D.; Pliakas, A. M.; Todtenkopf, M. S.; Tomasiewicz, H. C.; Zhang, Y.; Stevens, W. C., Jr.; Jones, R. M.; Portoghese, P. S.; Carlezon, W. A., Jr. Antidepressant-like effects of kappa-opioid receptor antagonists in the forced swim test in rats. *J. Pharmacol. Exp. Ther.* **2003**, *305*, 323-330.
- (134) Beardsley, P. M.; Howard, J. L.; Shelton, K. L.; Carroll, F. I. Differential effects of the novel kappa opioid receptor antagonist, JD1c, on reinstatement of cocaine-seeking induced by footshock stressors vs cocaine primes and its antidepressant-like effects in rats. *Psychopharmacol.* **2005**, *183*, 118-126.
- (135) Spanagel, R.; Shippenberg, T. S. Modulation of morphine-induced sensitization by endogenous kappa opioid systems in the rat. *Neurosci. Lett.* **1993**, *153*, 232-236.
- (136) Bruchas, M. R.; Yang, T.; Schreiber, S.; DeFino, M.; Kwan, S. C.; Li, S.; Chavkin, C. Long-Acting Kappa Opioid Antagonists Disrupt Receptor Signaling And Produce Noncompetitive Effects By Activating C-Jun N-Terminal Kinase. *J. Biol. Chem.* **2007**, *282*, 29803-29811.
- (137) Melief, E. J.; Miyatake, M.; Carroll, F. I.; Béguin, C.; Carlezon, W. A.; Cohen, B. M.; Grimwood, S.; Mitch, C. H.; Rorick-Kehn, L.; Chavkin, C. Duration of Action of a Broad Range of Selective Kappa-Opioid Receptor Antagonists Is Positively Correlated with c-Jun N-Terminal Kinase-1 Activation. *Mol. Pharmacol.* **2011**, *80*, 920-929.



- (138) Ma, J.; Ye, N.; Lange, N.; Cohen, B. M. Dynorphinergic GABA neurons are a target of both typical and atypical antipsychotic drugs in the nucleus accumbens shell, central amygdaloid nucleus and thalamic central medial nucleus. *Neurosci.* **2003**, *121*, 991-998.
- (139) Prisinzano, T. E.; Tidgewell, K.; Harding, W. W. Kappa opioids as potential treatments for stimulant dependence. *AAPS J.* **2005**, *7*, E592-E599.
- (140) Shippenberg, T. S.; Zapata, A.; Chefer, V. I. Dynorphin and the pathophysiology of drug addiction. *Pharmacol. Ther.* **2007**, *116*, 306-321.
- (141) Wee, S.; Koob, G. F. The role of the dynorphin-kappa opioid system in the reinforcing effects of drugs of abuse. *Psychopharmacol.* **2010**, *210*, 121-135.
- (142) Wang, Y.-h.; Sun, J.-f.; Tao, Y.-m.; Chi, Z.-q.; Liu, J.-g. The role of kappa-opioid receptor activation in mediating antinociception and addiction. *Acta Pharmacol. Sin.* **2010**, *31*, 1065-1070.
- (143) Association, A. P. *Diagnostic and statistical manual of mental disorders*. 4th ed. American Psychiatric Press: Washington D.C. **1994**.
- (144) Gawin, F. H. Cocaine addiction: psychology and neurophysiology. *Science.* **1991**, *251*, 1580-1586.
- (145) Koob, G. F.; Le, M. M. Drug abuse: hedonic homeostatic dysregulation. *Science.* **1997**, *278*, 52-58.
- (146) Koob, G. F. Allostatic view of motivation: implications for psychopathology. *Nebr. Symp. Motiv.* **2004**, *50*, 1-18.
- (147) Bruijnzeel, A. W. Kappa-opioid receptor signaling and brain reward function. *Brain Res. Rev.* **2009**, *62*, 127-146.
- (148) Mysels, D.; Sullivan, M. A. The kappa-opiate receptor impacts the pathophysiology and behavior of substance use. *Am. J. Addict.* **2009**, *18*, 272-276.
- (149) Chartoff, E. H.; Potter, D.; Damez-Werno, D.; Cohen, B. M.; Carlezon, W. A., Jr. Exposure to the Selective Kappa-Opioid Receptor Agonist Salvinorin A Modulates the Behavioral and Molecular Effects of Cocaine in Rats. *Neuropsychopharmacol.* **2008**, *33*, 2676-2687.
- (150) Di Chiara, G.; Imperato, A. Drugs abused by humans preferentially increase synaptic dopamine concentrations in the mesolimbic system of freely moving rats. *Proc. Natl. Acad. Sci. U. S. A.* **1988**, *85*, 5274-5278.
- (151) Margolis, E. B.; Hjelmstad, G. O.; Bonci, A.; Fields, H. L. Kappa-opioid agonists directly inhibit midbrain dopaminergic neurons. *J. Neurosci.* **2003**, *23*, 9981-9986.
- (152) Crawford, C. A.; McDougall, S. A.; Bolanos, C. A.; Hall, S.; Berger, S. P. The effects of the kappa agonist U-50,488 on cocaine-induced conditioned and unconditioned behaviors and Fos immunoreactivity. *Psychopharmacol.* **1995**, *120*, 392-399.
- (153) Suzuki, T.; Shiozaki, Y.; Masukawa, Y.; Misawa, M.; Nagase, H. The role of mu- and kappa-opioid receptors in cocaine-induced conditioned place preference. *Jpn. J. Pharmacol.* **1992**, *58*, 435-442.
- (154) Shippenberg, T. S.; LeFevour, A.; Heidbreder, C. Kappa-opioid receptor agonists prevent sensitization to the conditioned rewarding effects of cocaine. *J. Pharmacol. Exp. Ther.* **1996**, *276*, 545-554.
- (155) Glick, S. D.; Maisonneuve, I. M.; Raucci, J.; Archer, S. Kappa opioid inhibition of morphine and cocaine self-administration in rats. *Brain Res.* **1995**, *681*, 147-152.

- (156) Negus, S. S.; Mello, N. K.; Portoghese, P. S.; Lin, C.-E. Effects of kappa opioids on cocaine self-administration by rhesus monkeys. *J. Pharmacol. Exp. Ther.* **1997**, *282*, 44-55.
- (157) Mello, N. K.; Negus, S. S. Effects of kappa opioid agonists on cocaine- and food-maintained responding by rhesus monkeys. *J. Pharmacol. Exp. Ther.* **1998**, *286*, 812-824.
- (158) Schenk, S.; Partridge, B.; Shippenberg, T. S. U69,593, a kappa-opioid agonist, decreases cocaine self-administration and decreases cocaine-produced drug-seeking. *Psychopharmacol.* **1999**, *144*, 339-346.
- (159) Bals-Kubik, R.; Herz, A.; Shippenberg, T. S. Evidence that the aversive effects of opioid antagonists and  $\kappa$ -agonists are centrally mediated. *Psychopharmacol.* **1989**, *98*, 203-206.
- (160) Schenk, S.; Partridge, B.; Shippenberg, T. S. Reinstatement of extinguished drug-taking behavior in rats: effect of the kappa-opioid receptor agonist, U69,593. *Psychopharmacol.* **2000**, *151*, 85-90.
- (161) Maisonneuve, I. M.; Archer, S.; Glick, S. D. U50,488, a kappa opioid receptor agonist, attenuates cocaine-induced increases in extracellular dopamine in the nucleus accumbens of rats. *Neurosci. Lett.* **1994**, *181*, 57-60.
- (162) Thompson, A. C.; Zapata, A.; Justice, J. B., Jr.; Vaughan, R. A.; Sharpe, L. G.; Shippenberg, T. S. Kappa-opioid receptor activation modifies dopamine uptake in the nucleus accumbens and opposes the effects of cocaine. *J. Neurosci.* **2000**, *20*, 9333-9340.
- (163) Collins, S. L.; Gerdes, R. M.; D'Addario, C.; Izenwasser, S. Kappa opioid agonists alter dopamine markers and cocaine-stimulated locomotor activity. *Behav. Pharmacol.* **2001**, *12*, 237-245.
- (164) Collins, S. L.; D'Addario, C.; Izenwasser, S. Effects of kappa-opioid receptor agonists on long-term cocaine use and dopamine neurotransmission. *Eur. J. Pharmacol.* **2001**, *426*, 25-34.
- (165) McLaughlin, J. P.; Land, B. B.; Li, S.; Pintar, J. E.; Chavkin, C. Prior Activation of Kappa Opioid Receptors by U50,488 Mimics Repeated Forced Swim Stress to Potentiate Cocaine Place Preference Conditioning. *Neuropsychopharmacol.* **2006**, *31*, 787-794.
- (166) McLaughlin, J. P.; Marton-Popovici, M.; Chavkin, C. Kappa-opioid receptor antagonism and prodynorphin gene disruption block stress-induced behavioral responses. *J. Neurosci.* **2003**, *23*, 5674-5683.
- (167) Wee, S.; Orio, L.; Ghirmai, S.; Cashman, J. R.; Koob, G. F. Inhibition of kappa opioid receptors attenuated increased cocaine intake in rats with extended access to cocaine. *Psychopharmacol.* **2009**, *205*, 565-575.
- (168) Devane, W. A.; Dysarz, F. A.; Johnson, M. R.; Melvin, L. S.; Howlett, A. C. Determination and Characterization of a Cannabinoid Receptor in Rat Brain. *Mol. Pharmacol.* **1988**, *34*, 605-613.
- (169) Matsuda, L. A.; Lolait, S. J.; Brownstein, M. J.; Young, A. C.; Bonner, T. I. Structure of a Cannabinoid Receptor and Functional Expression of the Cloned cDNA. *Nature.* **1990**, *346*, 561-564.
- (170) Munro, S.; Thomas, K. L.; Abushaar, M. Molecular Characterization of a Peripheral Receptor for Cannabinoids. *Nature.* **1993**, *365*, 61-65.
- (171) Parolaro, D.; Rubino, T.; Vigano, D.; Massi, P.; Guidali, C.; Realini, N. Cellular mechanisms underlying the interaction between cannabinoid and opioid system. *Curr. Drug Targets.* **2010**, *11*, 393-405.

- (172) Vigano, D.; Rubino, T.; Parolaro, D. Molecular and cellular basis of cannabinoid and opioid interactions. *Pharmacol. Biochem. Behav.* **2005**, *81*, 360-368.
- (173) Rubino, T.; Tizzoni, L.; Vigano, D.; Massi, P.; Parolaro, D. Modulation of rat brain cannabinoid receptors after chronic morphine treatment. *NeuroReport*. **1997**, *8*, 3219-3223.
- (174) Cichewicz, D. L. Synergistic interactions between cannabinoid and opioid analgesics. *Life Sci.* **2004**, *74*, 1317-1324.
- (175) Robledo, P.; Berrendero, F.; Ozaita, A.; Maldonado, R. Advances in the field of cannabinoid-opioid cross-talk. *Addict. Biol.* **2008**, *13*, 213-224.
- (176) Welch, S. P. Blockade of cannabinoid-induced antinociception by norbinaltorphimine, but not N,N-diallyl-tyrosine-Aib-phenylalanine-leucine, ICI 174,864 or naloxone in mice. *J. Pharmacol. Exp. Ther.* **1993**, *265*, 633-640.
- (177) Welch, S. P.; Eads, M. Synergistic interactions of endogenous opioids and cannabinoid systems. *Brain Res.* **1999**, *848*, 183-190.
- (178) Mason, D. J., Jr.; Lowe, J.; Welch, S. P. Cannabinoid modulation of dynorphin A: correlation to cannabinoid-induced antinociception. *Eur. J. Pharmacol.* **1999**, *378*, 237-248.
- (179) Katavic, P. L.; Lamb, K.; Navarro, H.; Prisinzano, T. E. Flavonoids as Opioid Receptor Ligands: Identification and Preliminary Structure-Activity Relationships. *J. Nat. Prod.* **2007**, *70*, 1278-1282.
- (180) Roth, B. L.; Baner, K.; Westkaemper, R.; Siebert, D.; Rice, K. C.; Steinberg, S.; Ernsberger, P.; Rothman, R. B. Salvinorin A: a potent naturally occurring nonnitrogenous kappa opioid selective agonist. *Proc. Natl. Acad. Sci. U. S. A.* **2002**, *99*, 11934-11939.
- (181) Benavente-García, O.; Castillo, J. Update on Uses and Properties of Citrus Flavonoids: New Findings in Anticancer, Cardiovascular, and Anti-inflammatory Activity. *J. Agric. Food Chem.* **2008**, *56*, 6185-6205.
- (182) Hodek, P.; Trefil, P.; Stiborova, M. Flavonoids - potent and versatile biologically active compounds interacting with cytochromes P 450. *Chem.-Biol. Interact.* **2002**, *139*, 1-21.
- (183) Jaganath, I. B.; Crozier, A. Flavonoid biosynthesis. In *Plant Metabolism and Biotechnology*. 1st ed.; Ashihara, H.; Crozier, A.; Komamine, A., Eds. John Wiley & Sons Ltd. **2011**. pp 293-320.
- (184) Lovell, K. M.; Simpson, D. S.; Cunningham, C. W.; Prisinzano, T. E. Utilizing nature as a source of new probes for opioid pharmacology. *Future Med. Chem.* **2009**, *1*, 285-301.
- (185) Pietta, P.-G. Flavonoids as Antioxidants. *J. Nat. Prod.* **2000**, *63*, 1035-1042.
- (186) Heller, W.; Forkmann, G. Biosynthesis of flavonoids. In *The Flavonoids: Advances in research since 1986*. Harborne, J. B., Ed. Chapman & Hall. London. **1993**. pp 499-535.
- (187) Kummer, V.; Maskova, J.; Canderle, J.; Zraly, Z.; Neca, J.; Machala, M. Estrogenic effects of silymarin in ovariectomized rats. *Vet. Med.* **2001**, *46*, 17-23.
- (188) Rezvani, A. H.; Overstreet, D. H.; Perfumi, M.; Massi, M. Plant derivatives in the treatment of alcohol dependency. *Pharmacol. Biochem. Behav.* **2003**, *75*, 593-606.
- (189) Overstreet, D. H.; Keung, W.-M.; Rezvani, A. H.; Massi, M.; Lee, D. Y. W. Herbal remedies for alcoholism: promises and possible pitfalls. *Alcohol Clin. Exp. Res.* **2003**, *27*, 177-185.
- (190) Perfumi, M.; Santoni, M.; Cippitelli, A.; Ciccocioppo, R.; Frolidi, R.; Massi, M. *Hypericum perforatum* CO<sub>2</sub> Extract and Opioid Receptor Antagonists Act

- Synergistically to Reduce Ethanol Intake in Alcohol-Preferring Rats. *Alcohol Clin. Exp. Res.* **2003**, *27*, 1554-1562.
- (191) Kumar, V.; Singh, P. N.; Bhattacharya, S. K. Anti-inflammatory and analgesic activity of Indian *Hypericum perforatum* L. *Indian J. Exp. Biol.* **2001**, *39*, 339-343.
- (192) Raso, G. M.; Pacilio, M.; Di, C. G.; Esposito, E.; Pinto, L.; Meli, R. *In vivo* and *in vitro* anti-inflammatory effect of *Echinacea purpurea* and *Hypericum perforatum*. *J. Pharm. Pharmacol.* **2002**, *54*, 1379-1383.
- (193) Mahmoudi, M.; Morteza-Semnani, K.; Saeedi, M.; Javanmardi, A. Anti-inflammatory activity and acute toxicity of Iranian *Hypericum perforatum*. *Toxicol. Lett.* **2003**, *144* (S1), s89.
- (194) Morteza-Semnani, K.; Mahmoudi, M.; Saeedi, M.; Javanmardi, A. Analgesic activity of Iranian *Hypericum perforatum*. *Toxicol. Lett.* **2003**, *144* (S1), s88.
- (195) Joris, J.; Costello, A.; Dubner, R.; Hargreaves, K. M. Opiates suppress carrageenan-induced edema and hyperthermia at doses that inhibit hyperalgesia. *Pain.* **1990**, *43*, 95-103.
- (196) Abbott, F. V.; Franklin, K. B. J.; Libman, R. B. A dose-ratio comparison of mu and kappa agonists in formalin and thermal pain. *Life Sci.* **1986**, *39*, 2017-2024.
- (197) Simmen, U.; Schweitzer, C.; Burkard, W.; Schaffner, W.; Lundstrom, K. *Hypericum perforatum* inhibits the binding of mu- and kappa-opioid receptor expressed with the Semliki Forest virus system. *Pharm. Acta Helv.* **1998**, *73*, 53-56.
- (198) Simmen, U.; Burkard, W.; Berger, K.; Schaffner, W.; Lundstrom, K. Extracts and constituents of *Hypericum perforatum* inhibit the binding of various ligands to recombinant receptors expressed with the Semliki Forest virus system. *J. Recept. Signal Transduct. Res.* **1999**, *19*, 59-74.
- (199) Butterweck, V.; Nahrstedt, A.; Evans, J.; Hufeisen, S.; Rauser, L.; Savage, J.; Popadak, B.; Ernsberger, P.; Roth, B. L. *In vitro* receptor screening of pure constituents of St. John's wort reveals novel interactions with a number of GPCRs. *Psychopharmacol.* **2002**, *162*, 193-202.
- (200) Batista, J. S.; Almeida, R. N.; Bhattacharyya, J. Analgesic effect of *Dioclea grandiflora* constituents in rodents. *J. Ethnopharmacol.* **1995**, *45*, 207-210.
- (201) Almeida, R. N.; Navarro, D. S.; De, F. A. M.; Almeida, E. R.; Majetich, G.; Bhattacharyya, J. Analgesic effect of Dioclenol and Dioflorin isolated from *Dioclea grandiflora*. *Pharm. Biol.* **2000**, *38*, 394-395.
- (202) Bhattacharyya, J.; Batista, J. S.; Almeida, R. N. Dioclein, a flavanone from the roots of *Dioclea grandiflora*. *Phytochemistry.* **1995**, *38*, 277-278.
- (203) Bhattacharyya, J.; Majetich, G.; Jenkins, T. M.; Almeida, R. N. Dioflorin, a minor flavonoid from *Dioclea grandiflora*. *J. Nat. Prod.* **1998**, *61*, 413-414.
- (204) Almeida, E. R.; Almeida, R. N.; Navarro, D. S.; Bhattacharyya, J.; Silva, B. A.; Birnbaum, J. S. P. Central antinociceptive effect of hydroalcoholic extract of *Dioclea grandiflora* seeds in rodents. *J. Ethnopharmacol.* **2003**, *88*, 1-4.
- (205) da Silveira e Sa, R. d. C.; de Oliveira, L. E. G.; de Farias Nobrega, F. F.; Bhattacharyya, J.; de Almeida, R. N. Antinociceptive and toxicological effects of *Dioclea grandiflora* seed pod in mice. *J. Biomed. Biotechnol.* **2010**, *2010*, 606748.
- (206) United Nations. Convention on Biological Diversity. **1992**. <http://www.cbd.int/doc/legal/cbd-en.pdf> (accessed May 17, 2012).

- (207) Spearing, P.; Majetich, G.; Bhattacharyya, J. Synthesis of (R,S)-Dioclein, a Bioactive Flavanone from the Root Bark of *Diocleia grandiflora*. *J. Nat. Prod.* **1997**, *60*, 399-400.
- (208) Khupse, R. S.; Erhardt, P. W. Total synthesis of xanthohumol. *J. Nat. Prod.* **2007**, *70*, 1507-1509.
- (209) Kagawa, H.; Shigematsu, A.; Ohta, S.; Harigaya, Y. Preparative Monohydroxyflavanone Syntheses and a Protocol for Gas Chromatography-Mass Spectrometry Analysis of Monohydroxyflavanones. *Chem. Pharm. Bull.* **2005**, *53*, 547-554.
- (210) Vogel, S.; Ohmayer, S.; Brunner, G.; Heilmann, J. Natural and non-natural prenylated chalcones: Synthesis, cytotoxicity and anti-oxidative activity. *Bioorg. Med. Chem.* **2008**, *16*, 4286-4293.
- (211) Isleyen, A.; Dogan, O. Application of ferrocenyl substituted aziridinylmethanols (FAM) as chiral ligands in enantioselective conjugate addition of diethylzinc to enones. *Tetrahedron: Asymmetry.* **2007**, *18*, 679-684.
- (212) Dong, X.; Fan, Y.; Yu, L.; Hu, Y. Synthesis of four natural prenylflavonoids and their estrogen-like activities. *Arch. Pharm.* **2007**, *340*, 372-376.
- (213) Fontana, G.; Savona, G.; Rodríguez, B.; Dersch, C. M.; Rothman, R. B.; Prisinzano, T. E. Synthetic studies of neoclerodane diterpenoids from *Salvia splendens* and evaluation of opioid receptor affinity. *Tetrahedron.* **2008**, *64*, 10041-10048.
- (214) Holden, K. G.; Tidgewell, K.; Marquam, A.; Rothman, R. B.; Navarro, H.; Prisinzano, T. E. Synthetic studies of neoclerodane diterpenes from *Salvia divinorum*: Exploration of the 1-position. *Bioorg. Med. Chem. Lett.* **2007**, *17*, 6111-6115.
- (215) Coward, P.; Chan, S. D. H.; Wada, H. G.; Humphries, G. M.; Conklin, B. R. Chimeric G Proteins Allow a High-Throughput Signaling Assay of Gi-Coupled Receptors. *Anal. Biochem.* **1999**, *270*, 242-248.
- (216) Balenga, N. A. B.; Henstridge, C. M.; Kargl, J.; Waldhoer, M. Pharmacology, signaling and physiological relevance of the G protein-coupled receptor 55. *Adv. Pharmacol.* **2011**, *62*, 251-277.
- (217) Henstridge, C. M.; Balenga, N. A. B.; Kargl, J.; Andradas, C.; Brown, A. J.; Irving, A.; Sanchez, C.; Waldhoer, M. Minireview: recent developments in the physiology and pathology of the lysophosphatidylinositol-sensitive receptor GPR55. *Mol. Endocrinol.* **2011**, *25*, 1835-1848.
- (218) PathHunter™ Detection Kit, Product Booklet: 93-0001. **2009**. DiscoverRx Corporation. 42501 Albrae Street, Fremont, CA, 94538.
- (219) Zhang, J.; Liu, X.; Lei, X.; Wang, L.; Guo, L.; Zhao, G.; Lin, G. Discovery and synthesis of novel luteolin derivatives as DAT agonists. *Bioorg. Med. Chem.* **2010**, *18*, 7842-7848.
- (220) Bu, X. Y.; Zhao, L. Y.; Li, Y. L. A facile synthesis of 6-C-prenylflavanones. *Synthesis.* **1997**, 1246-1248.
- (221) Dong, X.; Fan, Y.; Yu, L.; Hu, Y. Synthesis of four natural prenylflavonoids and their estrogen-like activities. *Arch. Pharm. (Weinheim, Ger.)*. **2007**, *340*, 372-376.
- (222) Valdes, L. J.; Butler, W. M.; Hatfield, G. M.; Paul, A. G.; Koreeda, M. Divinorin A, a psychotropic terpenoid, and divinorin B from the hallucinogenic Mexican mint, *Salvia divinorum*. *J. Org. Chem.* **1984**, *49*, 4716-4720.
- (223) Ortega, A.; Blount, J. F.; Manchand, P. S. Salvinorin, a new trans-neoclerodane diterpene from *Salvia divinorum* (Labiatae). *J. Chem. Soc. Perkin Trans. 1.* **1982**, *1*, 2505-2508.
- (224) Koreeda, M.; Brown, L.; Valdes, L. J. The Absolute Stereochemistry of Salvinorins. *Chem. Lett.* **1990**, *19*, 2015-2018.

- (225) Valdes, L. J., 3rd; Diaz, J. L.; Paul, A. G. Ethnopharmacology of ska Maria Pastora (*Salvia divinorum*, Epling and Jativa-M.). *J. Ethnopharmacol.* **1983**, *7*, 287-312.
- (226) Siebert, D. J. *Salvia divinorum* and salvinorin A: New pharmacologic findings. *J. Ethnopharmacol.* **1994**, *43*, 53-56.
- (227) Valdes, L. J., 3rd. *Salvia divinorum* and the unique diterpene hallucinogen, Salvinorin (divinorin) A. *J Psychoactive Drugs.* **1994**, *26*, 277-283.
- (228) Gonzalez, D.; Riba, J.; Bouso, J. C.; Gomez-Jarabo, G.; Barbanoj, M. J. Pattern of use and subjective effects of *Salvia divinorum* among recreational users. *Drug Alcohol Depend.* **2006**, *85*, 157-162.
- (229) Lange, J. E.; Reed, M. B.; Croff, J. M. K.; Clapp, J. D. College student use of *Salvia divinorum*. *Drug Alcohol Depend.* **2008**, *94*, 263-266.
- (230) Drug Enforcement Administration. Drugs and Chemicals of Concern. [http://www.deadiversion.usdoj.gov/drugs\\_concern/index.html](http://www.deadiversion.usdoj.gov/drugs_concern/index.html) (accessed May 14, 2012).
- (231) Drug Enforcement Administration. *Salvia Divinorum* and Salvinorin A. **2010**. [http://www.deadiversion.usdoj.gov/drugs\\_concern/salvia\\_d.pdf](http://www.deadiversion.usdoj.gov/drugs_concern/salvia_d.pdf) (accessed May 14, 2012).
- (232) Eguchi, M. Recent advances in selective opioid receptor agonists and antagonists. *Med. Res. Rev.* **2004**, *24*, 182-212.
- (233) Lu, Y.; Weltrowska, G.; Lemieux, C.; Chung, N. N.; Schiller, P. W. Stereospecific synthesis of (2S)-2-methyl-3-(2',6'-dimethyl-4'-hydroxyphenyl)propionic acid (Mdp) and its incorporation into an opioid peptide. *Bioorg. Med. Chem. Lett.* **2001**, *11*, 323-325.
- (234) Surratt, C. K.; Johnson, P. S.; Moriwaki, A.; Seidleck, B. K.; Blaschak, C. J.; Wang, J. B.; Uhl, G. R. Mu opiate receptor. Charged transmembrane domain amino acids are critical for agonist recognition and intrinsic activity. *J. Biol. Chem.* **1994**, *269*, 20548-20553.
- (235) Weltrowska, G.; Chung, N. N.; Lemieux, C.; Guo, J.; Lu, Y.; Wilkes, B. C.; Schiller, P. W. "Carba"-Analogues of Fentanyl are Opioid Receptor Agonists. *J. Med. Chem.* **2010**, *53*, 2875-2881.
- (236) Lovell, K. M.; Prevatt-Smith, K. M.; Lozama, A.; Prisinzano, T. E. Synthesis of neoclerodane diterpenes and their pharmacological effects. *Top. Curr. Chem.* **2011**, *299*, 141-185.
- (237) Ruzicka, L. Isoprene rule and the biogenesis of terpenic compounds. *Experientia.* **1953**, *9*, 357-367.
- (238) Katsuki, H.; Bloch, K. Biosynthesis of ergosterol in yeast; formation of methylated intermediates. *J. Biol. Chem.* **1967**, *242*, 222-227.
- (239) Lynen, F. Biosynthetic pathways from acetate to natural products. *Pure Appl. Chem.* **1967**, *14*, 137-167.
- (240) Rohmer, M. The discovery of a mevalonate-independent pathway for isoprenoid biosynthesis in bacteria, algae and higher plants. *Nat. Prod. Rep.* **1999**, *16*, 565-574.
- (241) Rohmer, M.; Knani, M. h.; Simonin, P.; Sutter, B.; Sahn, H. Isoprenoid biosynthesis in bacteria: A novel pathway for the early steps leading to isopentenyl diphosphate. *Biochem. J.* **1993**, *295*, 517-524.
- (242) Sprenger, G. A.; Schorken, U.; Wiegert, T.; Grolle, S.; De, G. A. A.; Taylor, S. V.; Begley, T. P.; Bringer-Meyer, S.; Sahn, H. Identification of a thiamin-dependent synthase in *Escherichia coli* required for the formation of the 1-deoxy-D-xylulose 5-phosphate precursor to isoprenoids, thiamin, and pyridoxol. *Proc. Natl. Acad. Sci. U. S. A.* **1997**, *94*, 12857-12862.

- (243) Kuzuyama, T.; Seto, H. Two distinct pathways for essential metabolic precursors for isoprenoid biosynthesis. *Proc. Jpn. Acad., Ser. B.* **2012**, *88*, 41-52.
- (244) Poulter, C. D.; Satterwhite, D. M. Mechanism of the prenyl transfer reaction. Studies with (E)- and (Z)-3-trifluoromethyl-2-buten-1-yl pyrophosphate. *Biochemistry.* **1977**, *16*, 5470-5478.
- (245) Kellogg, B. A.; Poulter, C. D. Chain elongation in the isoprenoid biosynthetic pathway. *Curr. Opin. Chem. Biol.* **1997**, *1*, 570-578.
- (246) Breitmaier, E. *Terpenes: Flavors, Fragrances, Pharmaca, Pheromones*. 1st ed. Wiley-VCH: **2006**.
- (247) Tokoroyama, T. Synthesis of clerodane diterpenoids and related compounds - stereoselective construction of the decalin skeleton with multiple contiguous stereogenic centers. *Synthesis.* **2000**, *5*, 611-633.
- (248) Kohno, H.; Maeda, M.; Tanino, M.; Tsukio, Y.; Ueda, N.; Wada, K.; Sugie, S.; Mori, H.; Tanaka, T. A bitter diterpenoid furanolactone columbin from *Calumbae Radix* inhibits azoxymethane-induced rat colon carcinogenesis. *Cancer Lett.* **2002**, *183*, 131-139.
- (249) Moody, J. O.; Robert, V. A.; Connolly, J. D.; Houghton, P. J. Anti-inflammatory activities of the methanol extracts and an isolated furanoditerpene constituent of *Sphenocentrum jollyanum* Pierre (Menispermaceae). *J. Ethnopharmacol.* **2006**, *104*, 87-91.
- (250) Shi, Q.; Liang, M.; Zhang, W.; Zhang, C.; Liu, R.; Shen, Y.; Li, H.; Wang, X.; Wang, X.; Pan, Q.; Chen, C. Quantitative LC/MS/MS method and pharmacokinetic studies of columbin, an anti-inflammation furanoditerpen isolated from *Radix Tinosporae*. *Biomed. Chromatogr.* **2007**, *21*, 642-648.
- (251) Bruno, M.; Fazio, C.; Arnold, N. A. Neo-clerodane diterpenoids from *Scutellaria cypria*. *Phytochemistry.* **1996**, *42*, 555-557.
- (252) Lallemand, J.-Y.; Six, Y.; Ricard, L. A concise synthesis of an advanced clerodin intermediate through a Valtier tandem reaction. *Eur. J. Org. Chem.* **2002**, 503-513.
- (253) Ley, S. V.; Denholm, A. A.; Wood, A. The chemistry of azadirachtin. *Nat. Prod. Rep.* **1993**, *10*, 109-157.
- (254) Merritt, A. T.; Ley, S. V. Clerodane diterpenoids. *Nat. Prod. Rep.* **1992**, *9*, 243-287.
- (255) Rogers, D.; Unal, G. G.; Williams, D. J.; Ley, S. V.; Sim, G. A.; Joshi, B. S.; Ravindranath, K. R. The crystal structure of 3-epicaryoptin and the reversal of the currently accepted absolute configuration of clerodin. *J. Chem. Soc. Chem. Commun.* **1979**, *3*, 97-99.
- (256) Chavkin, C.; Sud, S.; Jin, W.; Stewart, J.; Zjawiony, J. K.; Siebert, D. J.; Toth, B. A.; Hufeisen, S. J.; Roth, B. L. Salvinorin A, an active component of the hallucinogenic sage *Salvia divinorum* is a highly efficacious kappa-opioid receptor agonist: Structural and functional considerations. *J. Pharmacol. Exp. Ther.* **2004**, *308*, 1197-1203.
- (257) Wang, Y.; Tang, K.; Inan, S.; Siebert, D.; Holzgrabe, U.; Lee, D. Y. W.; Huang, P.; Li, J.-G.; Cowan, A.; Liu-Chen, L.-Y. Comparison of pharmacological activities of three distinct kappa ligands (salvinorin A, TRK-820 and 3FLB) on kappa opioid receptors *in vitro* and their antipruritic and antinociceptive activities *in vivo*. *J. Pharmacol. Exp. Ther.* **2005**, *312*, 220-230.
- (258) Sheffler, D. J.; Roth, B. L. Salvinorin A: the 'magic mint' hallucinogen finds a molecular target in the kappa opioid receptor. *Trends Pharmacol. Sci.* **2003**, *24*, 107-109.

- (259) Johnson, M. W.; MacLean, K. A.; Reissig, C. J.; Prisinzano, T. E.; Griffiths, R. R. Human psychopharmacology and dose-effects of salvinorin A, a kappa opioid agonist hallucinogen present in the plant *Salvia divinorum*. *Drug Alcohol Depend.* **2011**, *115*, 150-155.
- (260) Addy, P. H. Acute and post-acute behavioral and psychological effects of salvinorin A in humans. *Psychopharmacol.* **2012**, *220*, 195-204.
- (261) Butelman, E. R.; Mandau, M.; Tidgewell, K.; Prisinzano, T. E.; Yuferov, V.; Kreek, M. J. Effects of salvinorin A, a kappa-opioid hallucinogen, on a neuroendocrine biomarker assay in nonhuman primates with high kappa-receptor homology to humans. *J. Pharmacol. Exp. Ther.* **2007**, *320*, 300-306.
- (262) Bowen, C. A.; Stevens, N. S.; Kelly, M.; Mello, N. K. The effects of heroin on prolactin levels in male rhesus monkeys: use of cumulative-dosing procedures. *Psychoneuroendocrinology.* **2002**, *27*, 319-336.
- (263) Butelman, E. R.; Ball, J. W.; Kreek, M.-J. Comparison of the discriminative and neuroendocrine effects of centrally penetrating kappa-opioid agonists in rhesus monkeys. *Psychopharmacol.* **2002**, *164*, 115-120.
- (264) Butelman, E. R.; Prisinzano, T. E.; Deng, H.; Rus, S.; Kreek, M. J. Unconditioned behavioral effects of the powerful kappa-opioid hallucinogen salvinorin A in nonhuman primates: fast onset and entry into cerebrospinal fluid. *J. Pharmacol. Exp. Ther.* **2009**, *328*, 588-597.
- (265) Dykstra, L. A.; Gmerek, D. E.; Winger, G.; Woods, J. H. Kappa opioids in rhesus monkeys. I. Diuresis, sedation, analgesia and discriminative stimulus effects. *J. Pharmacol. Exp. Ther.* **1987**, *242*, 413-420.
- (266) Butelman, E. R.; Woods, J. H. Effects of clonidine, dexmedetomidine and xylazine on thermal antinociception in rhesus monkeys. *J. Pharmacol. Exp. Ther.* **1993**, *264*, 762-769.
- (267) Hooker, J. M.; Xu, Y.; Schiffer, W.; Shea, C.; Carter, P.; Fowler, J. S. Pharmacokinetics of the potent hallucinogen, salvinorin A in primates parallels the rapid onset and short duration of effects in humans. *Neuroimage.* **2008**, *41*, 1044-50.
- (268) Schmidt, M. S.; Prisinzano, T. E.; Tidgewell, K.; Harding, W.; Butelman, E. R.; Kreek, M. J.; Murry, D. J. Determination of Salvinorin A in body fluids by high performance liquid chromatography-atmospheric pressure chemical ionization. *J. Chromatogr. B: Anal. Technol. Biomed. Life Sci.* **2005**, *818*, 221-225.
- (269) Kutrzeba, L. M.; Karamyan, V. T.; Speth, R. C.; Williamson, J. S.; Zjawiony, J. K. In vitro studies on metabolism of salvinorin A. *Pharm. Biol.* **2010**, *47*, 1078-1084.
- (270) Schmidt, M. D.; Schmidt, M. S.; Butelman, E. R.; Harding, W. W.; Tidgewell, K.; Murry, D. J.; Kreek, M. J.; Prisinzano, T. E. Pharmacokinetics of the plant-derived kappa-opioid hallucinogen salvinorin A in nonhuman primates. *Synapse.* **2005**, *58*, 208-210.
- (271) Tsujikawa, K.; Kuwayama, K.; Miyaguchi, H.; Kanamori, T.; Iwata, Y. T.; Inoue, H. *In vitro* stability and metabolism of salvinorin A in rat plasma. *Xenobiotica.* **2009**, *39*, 391-398.
- (272) Roth, R. H.; Levy, R.; Giarman, N. J. Dependence of rat serum lactonase upon calcium. *Biochem. Pharmacol.* **1967**, *16*, 596-598.
- (273) Teksin, Z. S.; Lee, I. J.; Nemieboka, N. N.; Othman, A. A.; Upreti, V. V.; Hassan, H. E.; Syed, S. S.; Prisinzano, T. E.; Eddington, N. D. Evaluation of the transport, in vitro



- metabolism and pharmacokinetics of Salvinorin A, a potent hallucinogen. *Eur. J. Pharm. Biopharm.* **2009**, *72*, 471-477.
- (274) Mowry, M.; Mosher, M.; Briner, W. Acute physiologic and chronic histologic changes in rats and mice exposed to the unique hallucinogen salvinorin A. *J Psychoactive Drugs.* **2003**, *35*, 379-82.
- (275) Butelman, E. R.; Harris, T. J.; Kreek, M. J. The plant-derived hallucinogen, salvinorin A, produces kappa-opioid agonist-like discriminative effects in rhesus monkeys. *Psychopharmacol.* **2004**, *172*, 220-224.
- (276) Willmore-Fordham, C. B.; Krall, D. M.; McCurdy, C. R.; Kinder, D. H. The hallucinogen derived from *Salvia divinorum*, salvinorin A, has kappa-opioid agonist discriminative stimulus effects in rats. *Neuropharmacology.* **2007**, *53*, 481-486.
- (277) Baker, L. E.; Panos, J. J.; Killinger, B. A.; Peet, M. M.; Bell, L. M.; Haliw, L. A.; Walker, S. L. Comparison of the discriminative stimulus effects of salvinorin A and its derivatives to U69,593 and U50,488 in rats. *Psychopharmacol.* **2009**, *203*, 203-211.
- (278) Killinger, B. A.; Peet, M. M.; Baker, L. E. Salvinorin A fails to substitute for the discriminative stimulus effects of LSD or ketamine in Sprague-Dawley rats. *Pharmacol. Biochem. Behav.* **2010**, *96*, 260-265.
- (279) Butelman, E. R.; Rus, S.; Priszano, T. E.; Kreek, M. J. The discriminative effects of the kappa-opioid hallucinogen Salvinorin A in nonhuman primates: dissociation from classic hallucinogen effects. *Psychopharmacol.* **2010**, *210*, 253-262.
- (280) Li, J.-X.; Rice, K. C.; France, C. P. Discriminative stimulus effects of 1-(2,5-dimethoxy-4-methylphenyl)-2-aminopropane in Rhesus monkeys. *J. Pharmacol. Exp. Ther.* **2008**, *324*, 827-833.
- (281) Harding, W. W.; Tidgewell, K.; Byrd, N.; Cobb, H.; Dersch, C. M.; Butelman, E. R.; Rothman, R. B.; Priszano, T. E. Neoclerodane Diterpenes as a Novel Scaffold for Mu Opioid Receptor Ligands. *J. Med. Chem.* **2005**, *48*, 4765-4771.
- (282) McCurdy, C. R.; Sufka, K. J.; Smith, G. H.; Warnick, J. E.; Nieto, M. J. Antinociceptive profile of salvinorin A, a structurally unique kappa opioid receptor agonist. *Pharmacol. Biochem. Behav.* **2006**, *83*, 109-113.
- (283) John, T. F.; French, L. G.; Erlichman, J. S. The antinociceptive effect of Salvinorin A in mice. *Eur. J. Pharmacol.* **2006**, *545*, 129-133.
- (284) Fichna, J.; Dickey, M.; Lewellyn, K.; Janecka, A.; Zjawiony, J. K.; Macnaughton, W. K.; Storr, M. A. Salvinorin A has antiinflammatory and antinociceptive effects in experimental models of colitis in mice mediated by KOR and CB1 receptors. *Inflamm. Bowel Dis.* **2012**, *18*, 1137-11345.
- (285) Ansonoff, M. A.; Zhang, J.; Czyzyk, T.; Rothman, R. B.; Stewart, J.; Xu, H.; Zjawiony, J.; Siebert, D. J.; Yang, F.; Roth, B. L.; Pintar, J. E. Antinociceptive and hypothermic effects of salvinorin A are abolished in a novel strain of kappa-opioid receptor-1 knockout mice. *J. Pharmacol. Exp. Ther.* **2006**, *318*, 641-648.
- (286) Carlezon, W. A., Jr.; Beguin, C.; DiNieri, J. A.; Baumann, M. H.; Richards, M. R.; Todtenkopf, M. S.; Rothman, R. B.; Ma, Z.; Lee, D. Y. W.; Cohen, B. M. Depressive-like effects of the kappa-opioid receptor agonist salvinorin A on behavior and neurochemistry in rats. *J. Pharmacol. Exp. Ther.* **2006**, *316*, 440-447.
- (287) Braidà, D.; Capurro, V.; Zani, A.; Rubino, T.; Vigano, D.; Parolaro, D.; Sala, M. Potential anxiolytic- and antidepressant-like effects of salvinorin A, the main active ingredient of *Salvia divinorum*, in rodents. *Br. J. Pharmacol.* **2009**, *157*, 844-853.

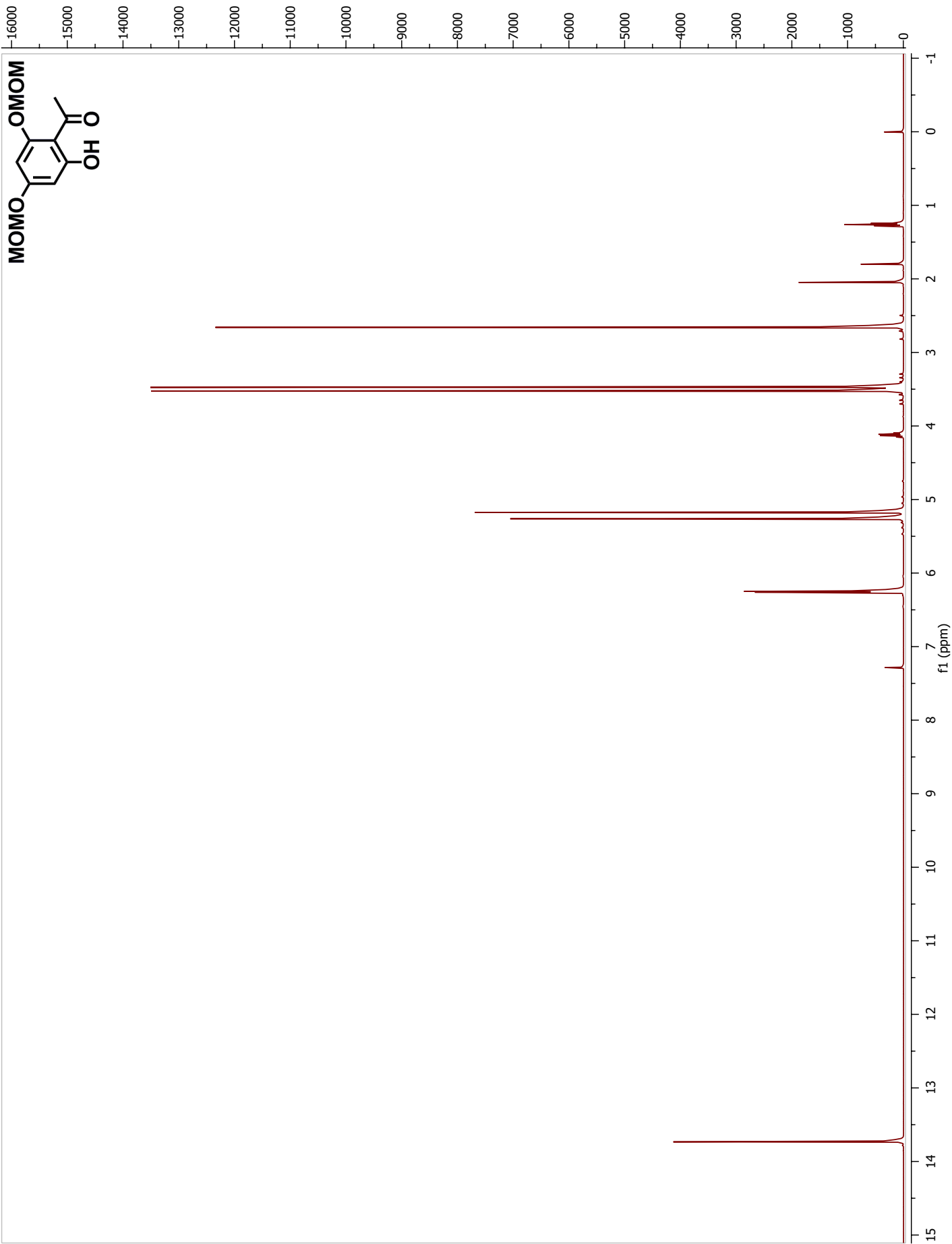
- (288) Ebner, S. R.; Roitman, M. F.; Potter, D. N.; Rachlin, A. B.; Chartoff, E. H. Depressive-like effects of the kappa opioid receptor agonist salvinorin A are associated with decreased phasic dopamine release in the nucleus accumbens. *Psychopharmacol.* **2010**, *210*, 241-252.
- (289) Morani, A. S.; Kivell, B.; Prisinzano, T. E.; Schenk, S. Effect of kappa-opioid receptor agonists U69593, U50488H, spiradoline and salvinorin A on cocaine-induced drug-seeking in rats. *Pharmacol. Biochem. Behav.* **2009**, *94*, 244-249.
- (290) Zhang, Y.; Butelman, E. R.; Schlussman, S. D.; Ho, A.; Kreek, M. J. Effects of the plant-derived hallucinogen salvinorin A on basal dopamine levels in the caudate putamen and in a conditioned place aversion assay in mice: agonist actions at kappa opioid receptors. *Psychopharmacol.* **2005**, *179*, 551-558.
- (291) Gehrke, B. J.; Chefer, V. I.; Shippenberg, T. S. Effects of acute and repeated administration of salvinorin A on dopamine function in the rat dorsal striatum. *Psychopharmacol.* **2008**, *197*, 509-517.
- (292) Potter, D. N.; Damez-Werno, D.; Carlezon, W. A., Jr.; Cohen, B. M.; Chartoff, E. H. Repeated Exposure to the Kappa-Opioid Receptor Agonist Salvinorin A Modulates Extracellular Signal-Regulated Kinase and Reward Sensitivity. *Biol. Psychiatry.* **2011**, *70*, 744-753.
- (293) Braidà, D.; Limonta, V.; Capurro, V.; Fadda, P.; Rubino, T.; Mascia, P.; Zani, A.; Gori, E.; Fratta, W.; Parolaro, D.; Sala, M. Involvement of Kappa-Opioid and Endocannabinoid System on Salvinorin A-Induced Reward. *Biol. Psychiatry.* **2008**, *63*, 286-292.
- (294) Beerepoot, P.; Lam, V.; Luu, A.; Tsoi, B.; Siebert, D.; Szechtman, H. Effects of salvinorin A on locomotor sensitization to D2/D3 dopamine agonist quinpirole. *Neurosci. Lett.* **2008**, *446*, 101-104.
- (295) Singh, N.; Nolan, T. L.; McCurdy, C. R. Chemical function-based pharmacophore development for novel, selective kappa opioid receptor agonists. *J. Mol. Graph. Model.* **2008**, *27*, 131-139.
- (296) Manglik, A.; Kruse, A. C.; Kobilka, T. S.; Thian, F. S.; Mathiesen, J. M.; Sunahara, R. K.; Pardo, L.; Weis, W. I.; Kobilka, B. K.; Granier, S. Crystal structure of the mu-opioid receptor bound to a morphinan antagonist. *Nature.* **2012**, *485*, 321-326.
- (297) Wu, H.; Wacker, D.; Mileni, M.; Katritch, V.; Han, G. W.; Vardy, E.; Liu, W.; Thompson, A. A.; Huang, X.-P.; Carroll, F. I.; Mascarella, S. W.; Westkaemper, R. B.; Mosier, P. D.; Roth, B. L.; Cherezov, V.; Stevens, R. C. Structure of the human kappa-opioid receptor in complex with JD(Tic). *Nature.* **2012**, *485*, 327-332.
- (298) Pogozheva, I. D.; Lomize, A. L.; Mosberg, H. I. Opioid receptor three-dimensional structures from distance geometry calculations with hydrogen bonding constraints. *Biophys. J.* **1998**, *75*, 612-634.
- (299) Yan, F.; Mosier, P. D.; Westkaemper, R. B.; Stewart, J.; Zjawiony, J. K.; Vortherms, T. A.; Sheffler, D. J.; Roth, B. L. Identification of the Molecular Mechanisms by Which the Diterpenoid Salvinorin A Binds to Kappa-Opioid Receptors. *Biochemistry.* **2005**, *44*, 8643-8651.
- (300) Kane, B. E.; Nieto, M. J.; McCurdy, C. R.; Ferguson, D. M. A unique binding epitope for salvinorin A, a non-nitrogenous kappa opioid receptor agonist. *FEBS J.* **2006**, *273*, 1966-1974.

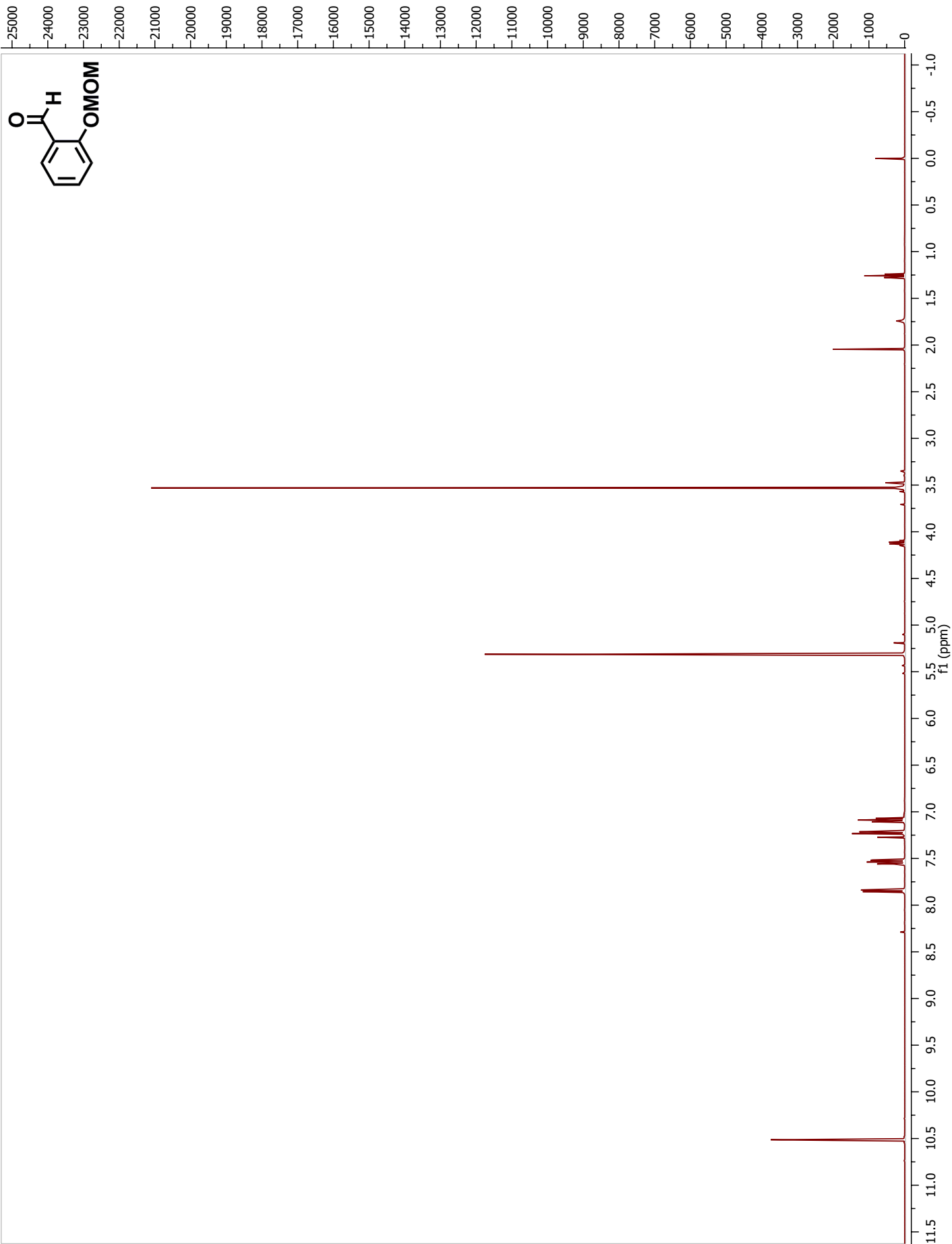
- (301) Vortherms, T. A.; Mosier, P. D.; Westkaemper, R. B.; Roth, B. L. Differential Helical Orientations among Related G Protein-coupled Receptors Provide Novel Mechanism for Selectivity. *J. Biol. Chem.* **2006**, *282*, 3146-3156.
- (302) Kane, B. E.; McCurdy, C. R.; Ferguson, D. M. Toward a Structure-Based Model of Salvinorin A Recognition of the Kappa-Opioid Receptor. *J. Med. Chem.* **2008**, *51*, 1824-1830.
- (303) Singh, N.; Cheve, G.; Ferguson, D. M.; McCurdy, C. R. A combined ligand-based and target-based drug design approach for G-protein coupled receptors: application to salvinorin A, a selective kappa opioid receptor agonist. *J. Comput. Aided Mol. Des.* **2006**, *20*, 471-493.
- (304) McGovern, D. L.; Mosier, P. D.; Roth, B. L.; Westkaemper, R. B. CoMFA analyses of C-2 position Salvinorin A analogs at the kappa-opioid receptor provides insights into epimer selectivity. *J. Mol. Graph. Model.* **2010**, *28*, 612-625.
- (305) Yan, F.; Bikbulatov, R. V.; Mocanu, V.; Dicheva, N.; Parker, C. E.; Wetsel, W. C.; Mosier, P. D.; Westkaemper, R. B.; Allen, J. A.; Zjawiony, J. K.; Roth, B. L. Structure-Based Design, Synthesis, and Biochemical and Pharmacological Characterization of Novel Salvinorin A Analogues as Active State Probes of the Kappa-Opioid Receptor. *Biochemistry.* **2009**, *48*, 6898-6908.
- (306) Prisinzano, T. E.; Rothman, R. B. Salvinorin A Analogs as Probes in Opioid Pharmacology. *Chem. Rev.* **2008**, *108*, 1732-1743.
- (307) Prisinzano, T. E. Natural Products as Tools for Neuroscience: Discovery and Development of Novel Agents to Treat Drug Abuse. *J. Nat. Prod.* **2009**, *72*, 581-587.
- (308) Cunningham, C. W.; Rothman, R. B.; Prisinzano, T. E. Neuropharmacology of the Naturally Occurring Kappa-Opioid Hallucinogen Salvinorin A. *Pharmacol. Rev.* **2011**, *63*, 316-347.
- (309) Tidgewell, K.; Harding, W. W.; Schmidt, M.; Holden, K. G.; Murry, D. J.; Prisinzano, T. E. A facile method for the preparation of deuterium labeled salvinorin A: synthesis of [2,2,2-2H<sub>3</sub>]-salvinorin A. *Bioorg. Med. Chem. Lett.* **2004**, *14*, 5099-5102.
- (310) Beguin, C.; Richards, M. R.; Li, J.-G.; Wang, Y.; Xu, W.; Liu-Chen, L.-Y.; Carlezon, W. A.; Cohen, B. M. Synthesis and *in vitro* evaluation of salvinorin A analogues: Effect of configuration at C(2) and substitution at C(18). *Bioorg. Med. Chem. Lett.* **2006**, *16*, 4679-4685.
- (311) Beguin, C.; Richards, M. R.; Wang, Y. L.; Chen, Y.; Liu-Chen, L. Y.; Ma, Z. Z.; Lee, D. Y. W.; Carlezon, W. A.; Cohen, B. M. Synthesis and *in vitro* pharmacological evaluation of salvinorin A analogues modified at C(2). *Bioorg. Med. Chem. Lett.* **2005**, *15*, 2761-2765.
- (312) Munro, T. A.; Rizzacasa, M. A.; Roth, B. L.; Toth, B. A.; Yan, F. Studies toward the Pharmacophore of Salvinorin A, a Potent Kappa Opioid Receptor Agonist. *J. Med. Chem.* **2005**, *48*, 345-348.
- (313) Tidgewell, K.; Harding, W. W.; Lozama, A.; Cobb, H.; Shah, K.; Kannan, P.; Dersch, C. M.; Parrish, D.; Deschamps, J. R.; Rothman, R. B.; Prisinzano, T. E. Synthesis of Salvinorin A Analogues as Opioid Receptor Probes. *J. Nat. Prod.* **2006**, *69*, 914-918.
- (314) Groer, C. E.; Tidgewell, K.; Moyer, R. A.; Harding, W. W.; Rothman, R. B.; Prisinzano, T. E.; Bohn, L. M. An opioid agonist that does not induce mu-opioid receptor-arrestin interactions or receptor internalization. *Mol. Pharmacol.* **2007**, *71*, 549-557.

- (315) Xu, H.; Partilla, J. S.; Wang, X.; Rutherford, J. M.; Tidgewell, K.; Prisinzano, T. E.; Bohn, L. M.; Rothman, R. B. A comparison of noninternalizing (herkinorin) and internalizing (DAMGO) mu-opioid agonists on cellular markers related to opioid tolerance and dependence. *Synapse*. **2007**, *61*, 166-175.
- (316) Butelman, E. R.; Rus, S.; Simpson, D. S.; Wolf, A.; Prisinzano, T. E.; Kreek, M. J. The effects of herkinorin, the first mu-selective ligand from a salvinorin A-derived scaffold, in a neuroendocrine biomarker assay in nonhuman primates. *J. Pharmacol. Exp. Ther.* **2008**, *327*, 154-160.
- (317) Lamb, K.; Tidgewell, K.; Simpson, D. S.; Bohn, L. M.; Prisinzano, T. E. Antinociceptive effects of herkinorin, a MOP receptor agonist derived from salvinorin A in the formalin test in rats: New concepts in mu opioid receptor pharmacology: From a symposium on new concepts in mu-opioid pharmacology. *Drug Alcohol Depend.* **2012**, *121*, 181-188.
- (318) Tidgewell, K.; Groer, C. E.; Harding, W. W.; Lozama, A.; Schmidt, M.; Marquam, A.; Hiemstra, J.; Partilla, J. S.; Dersch, C. M.; Rothman, R. B.; Bohn, L. M.; Prisinzano, T. E. Herkinorin Analogues with Differential Beta-Arrestin-2 Interactions. *J. Med. Chem.* **2008**, *51*, 2421-2431.
- (319) Lee, D. Y. W.; Karnati, V. V. R.; He, M.; Liu-Chen, L.-Y.; Kondaveti, L.; Ma, Z.; Wang, Y.; Chen, Y.; Beguin, C.; Carlezon, J. W. A.; Cohen, B. Synthesis and in vitro pharmacological studies of new C(2) modified salvinorin A analogues. *Bioorg. Med. Chem. Lett.* **2005**, *15*, 3744-3747.
- (320) Prevatt-Smith, K. M.; Lovell, K. M.; Simpson, D. S.; Day, V. W.; Douglas, J. T.; Bosch, P.; Dersch, C. M.; Rothman, R. B.; Kivell, B.; Prisinzano, T. E. Potential drug abuse therapeutics derived from the hallucinogenic natural product salvinorin A. *MedChemComm.* **2011**, *2*, 1217-1222.
- (321) Bikbulatov, R. V.; Yan, F.; Roth, B. L.; Zjawiony, J. K. Convenient synthesis and in vitro pharmacological activity of 2-thioanalogs of salvinorins A and B. *Bioorg. Med. Chem. Lett.* **2007**, *17*, 2229-2232.
- (322) Munro, T. A.; Duncan, K. K.; Xu, W.; Wang, Y.; Liu-Chen, L.-Y.; Carlezon Jr, W. A.; Cohen, B. M.; Béguin, C. Standard protecting groups create potent and selective kappa opioids: Salvinorin B alkoxymethyl ethers. *Bioorg. Med. Chem.* **2008**, *16*, 1279-1286.
- (323) Stewart, D. J.; Fahmy, H.; Roth, B. L.; Yan, F.; Zjawiony, J. K. Bioisosteric modification of salvinorin A, a potent and selective kappa-opioid receptor agonist. *Arzneimittelforschung.* **2006**, *56*, 269-75.
- (324) Lee, D. Y. W.; Yang, L.; Xu, W.; Deng, G.; Guo, L.; Liu-Chen, L.-Y. Synthesis and biological evaluation of C-2 halogenated analogs of salvinorin A. *Bioorg. Med. Chem. Lett.* **2010**, *20*, 5749-5752.
- (325) Harding, W. W.; Schmidt, M.; Tidgewell, K.; Kannan, P.; Holden, K. G.; Gilmour, B.; Navarro, H.; Rothman, R. B.; Prisinzano, T. E. Synthetic Studies of Neoclerodane Diterpenes from *Salvia divinorum*: Semisynthesis of Salvinicins A and B and Other Chemical Transformations of Salvinorin A. *J. Nat. Prod.* **2006**, *69*, 107-112.
- (326) Bock, K.; Lundt, I.; Pedersen, C. Assignment of anomeric structure to carbohydrates through geminal carbon-13-proton coupling constants. *Tetrahedron Lett.* **1973**, *14*, 1037-1040.
- (327) Haellgren, C. Use of the anomeric carbon-13 proton one bond scalar coupling constant as a tool for detecting 1,2-orthoester formation in oligosaccharide synthesis. *J. Carbohydr. Chem.* **1992**, *11*, 527-530.

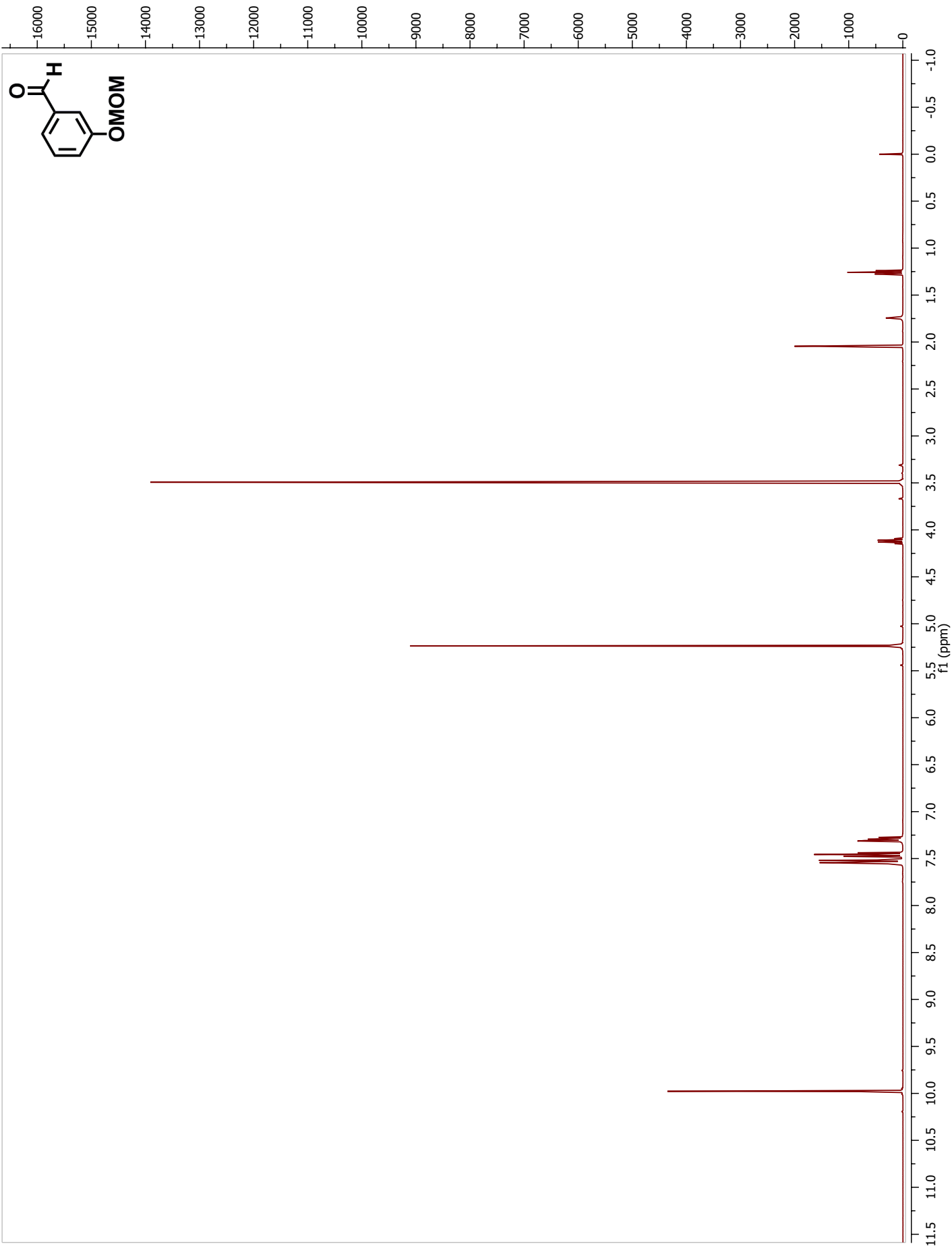
- (328) Tvaroska, I.; Taravel, F. R. Carbon-Proton Coupling Constants In The Conformational Analysis of Sugar Molecules. In *Advances in Carbohydrate Chemistry and Biochemistry*. Derek, H., Ed. Academic Press. **1995**. Vol. 51, pp 15-61.
- (329) Elzner, S.; Schmidt, D.; Schollmeyer, D.; Erkel, G.; Anke, T.; Kleinert, H.; Foerstermann, U.; Kunz, H. Inhibitors of inducible NO synthase expression: total synthesis of (S)-curvularin and its ring homologues. *ChemMedChem*. **2008**, *3*, 924-939.
- (330) Yang, D.; Zhang, C. Ruthenium-Catalyzed Oxidative Cleavage of Olefins to Aldehydes. *J. Org. Chem*. **2001**, *66*, 4814-4818.
- (331) Coombs, T. C.; Lee, M. D.; Wong, H.; Armstrong, M.; Cheng, B.; Chen, W.; Moretto, A. F.; Liebeskind, L. S. Practical, Scalable, High-Throughput Approaches to  $\eta^3$ -Pyranyl and  $\eta^3$ -Pyridinyl Organometallic Enantiomeric Scaffolds Using the Achmatowicz Reaction. *J. Org. Chem*. **2008**, *73*, 882-888.
- (332) Magauer, T.; Myers, A. G. Short and Efficient Synthetic Route to Methyl  $\alpha$ -Trioxacarcinocide B and Anomerically Activated Derivatives. *Org. Lett*. **2011**, *13*, 5584-5587.
- (333) Wang, Y.; Chen, Y.; Xu, W.; Lee, D. Y. W.; Ma, Z.; Rawls, S. M.; Cowan, A.; Liu-Chen, L.-Y. 2-Methoxymethylsalvinorin B is a potent kappa opioid receptor agonist with longer lasting action *in vivo* than salvinorin A. *J. Pharmacol. Exp. Ther*. **2008**, *324*, 1073-1083.
- (334) Carroll, M. E.; Meisch, R. A. Acquisition of drug self-administration. *Neuromethods*. **2011**, *53*, 237-265.
- (335) Panlilio, L. V. Stimulant self-administration. *Neuromethods*. **2011**, *53*, 57-81.
- (336) *International Tables for Crystallography*. 4 ed. Kluwer: Boston. **1996**. Vol. A.
- (337) Data Collection: SMART Software in APEX2 v2010.3-0 Suite. **2010**. Bruker-AXS. 5465 E. Cheryl Parkway, Madison, WI 53711-5373 USA.
- (338) Data Reduction: SAINT Software in APEX2 v2010.3-0 Suite. **2010**. Bruker-AXS. 5465 E. Cheryl Parkway, Madison, WI 53711-5373 USA.
- (339) Refinement: SHELXTL v2010.3-0. **2010**. Bruker-AXS. 5465 E. Cheryl Parkway, Madison, WI 53711-5373 USA.

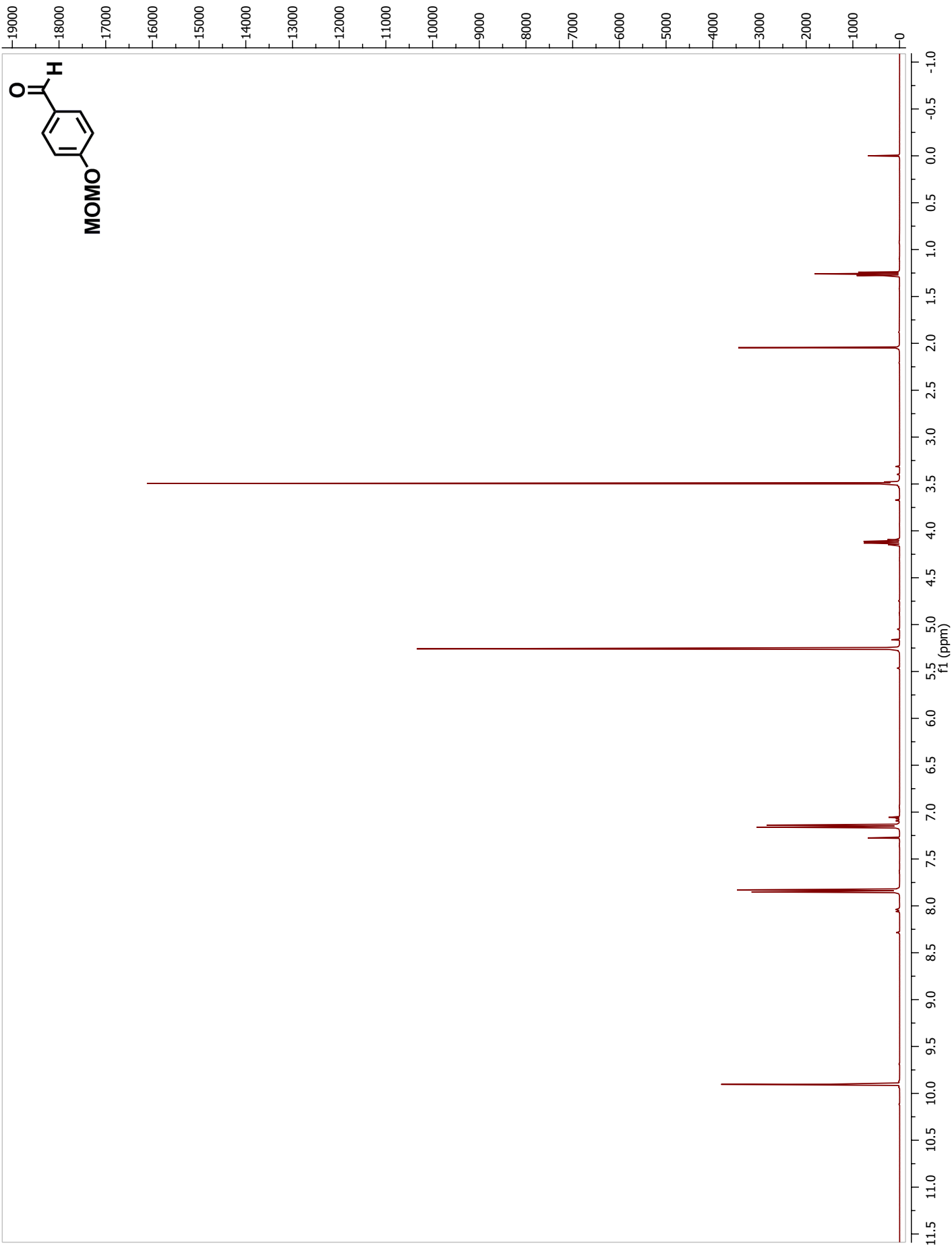
## APPENDIX A: $^1\text{H}$ NMR SPECTRA

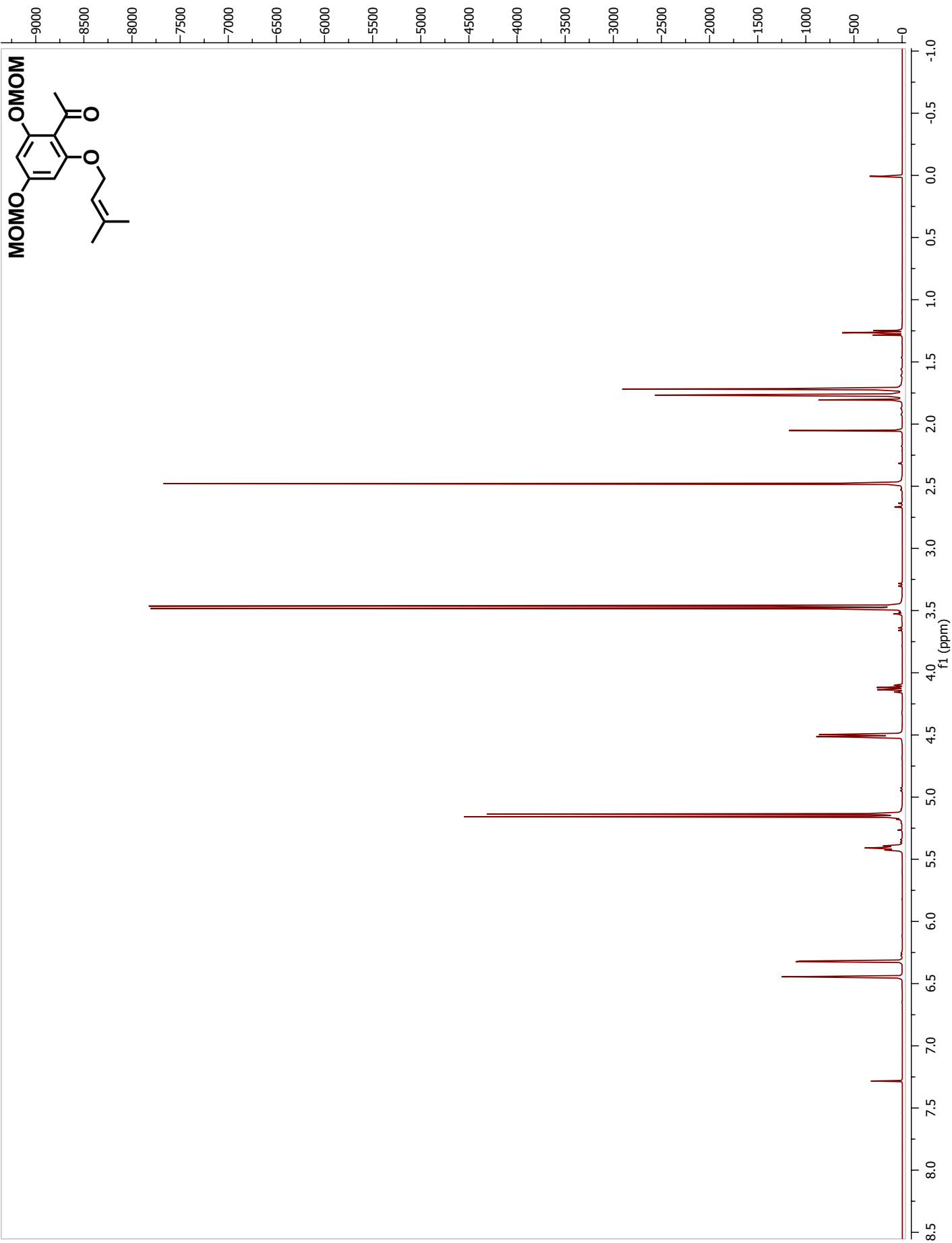


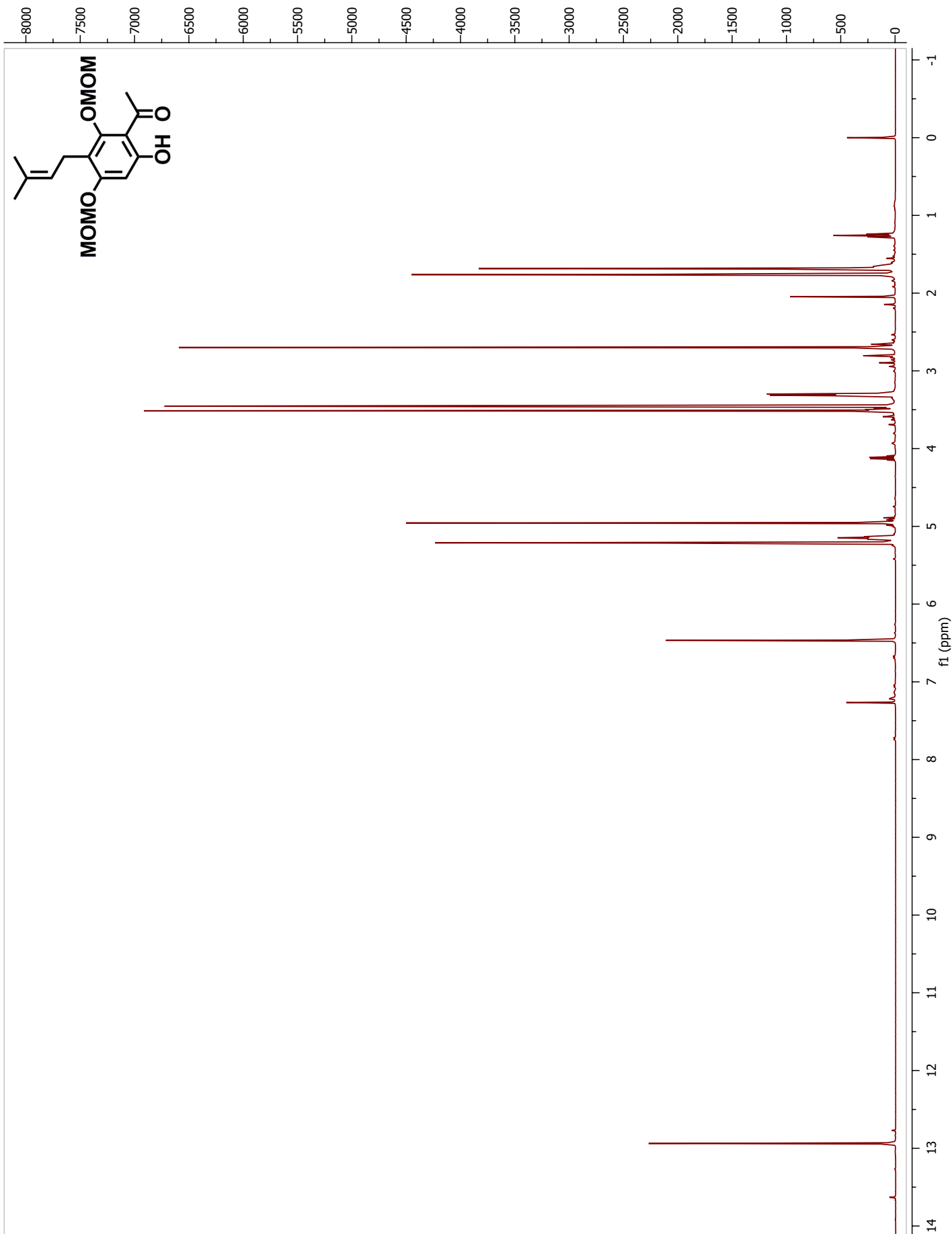


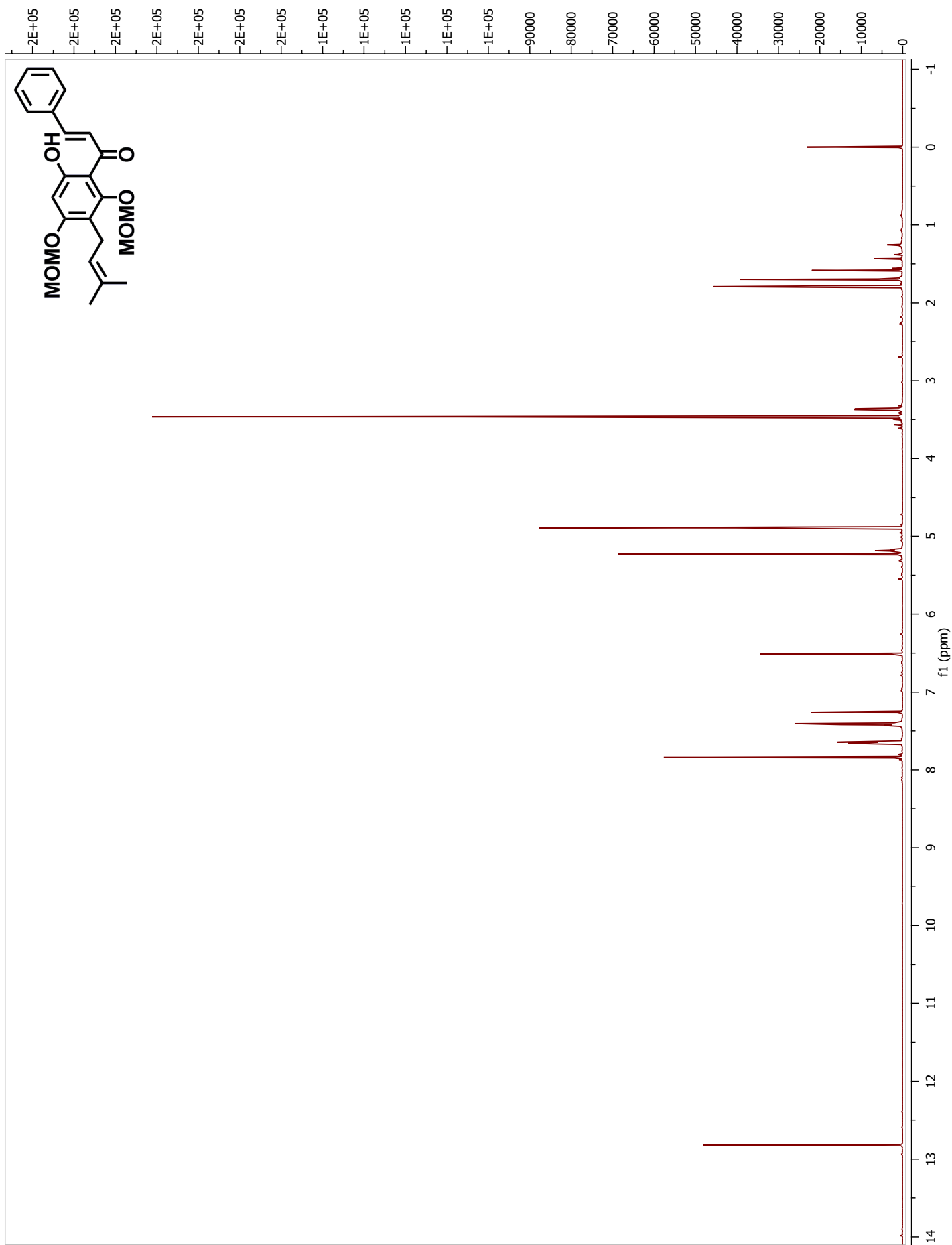


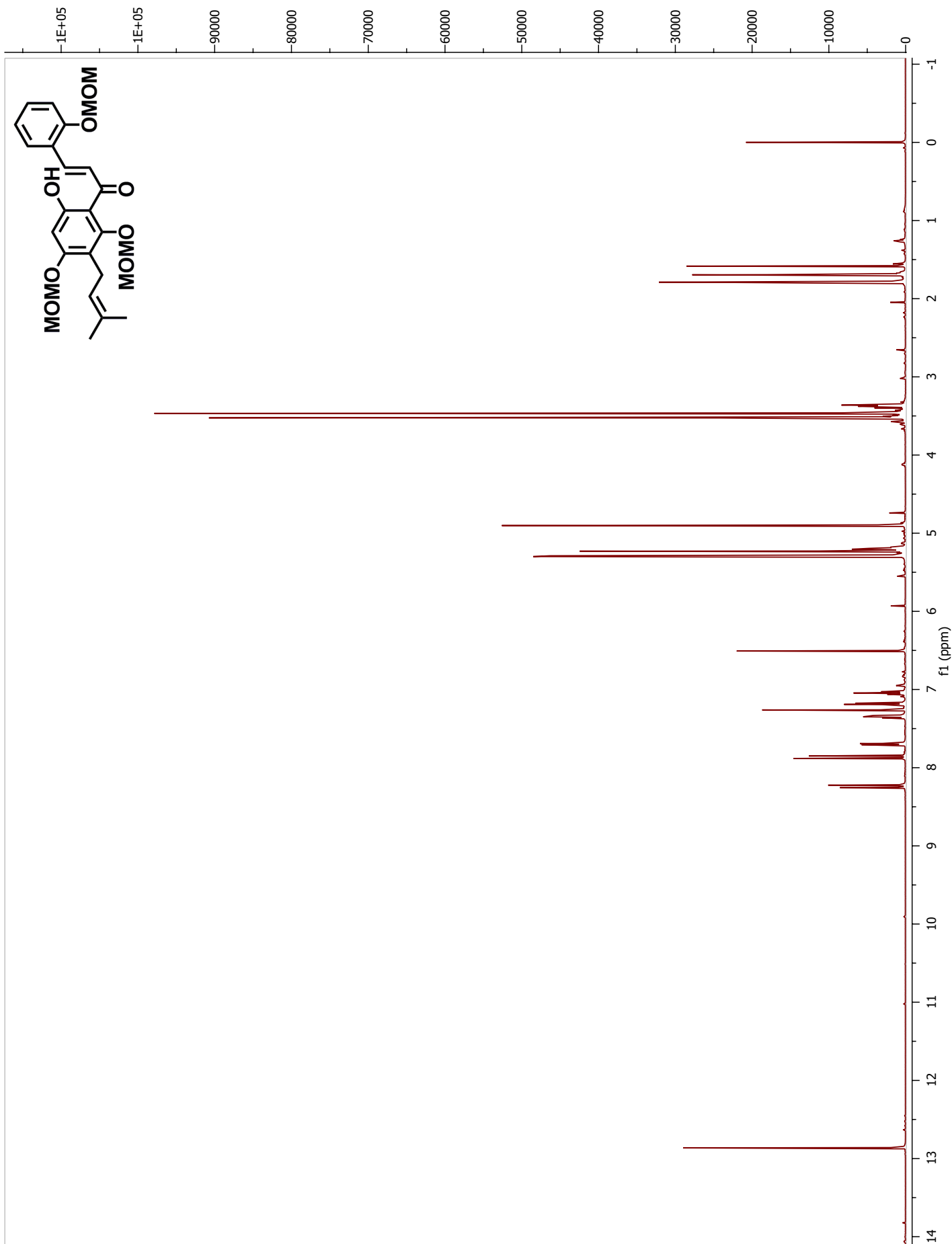


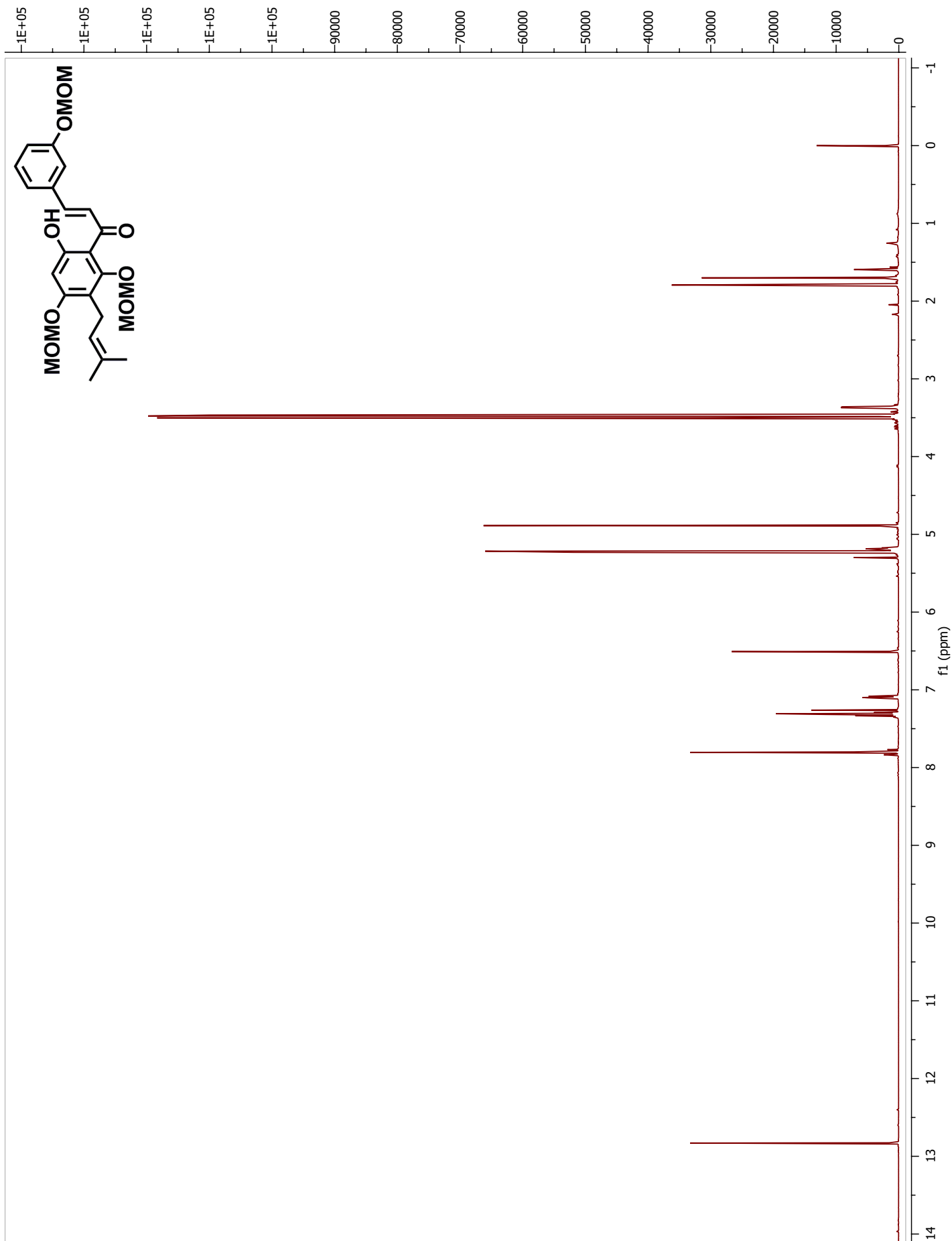


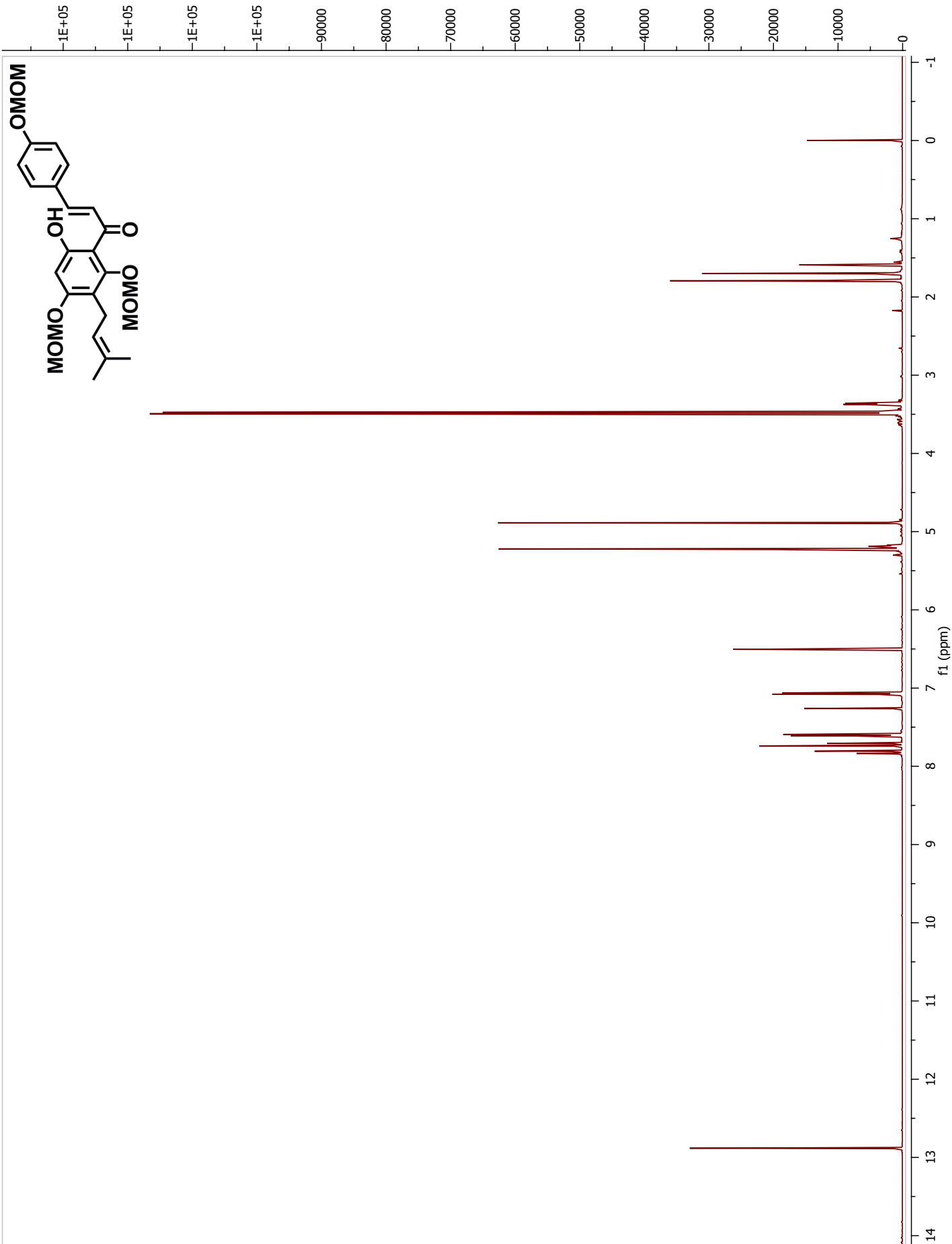




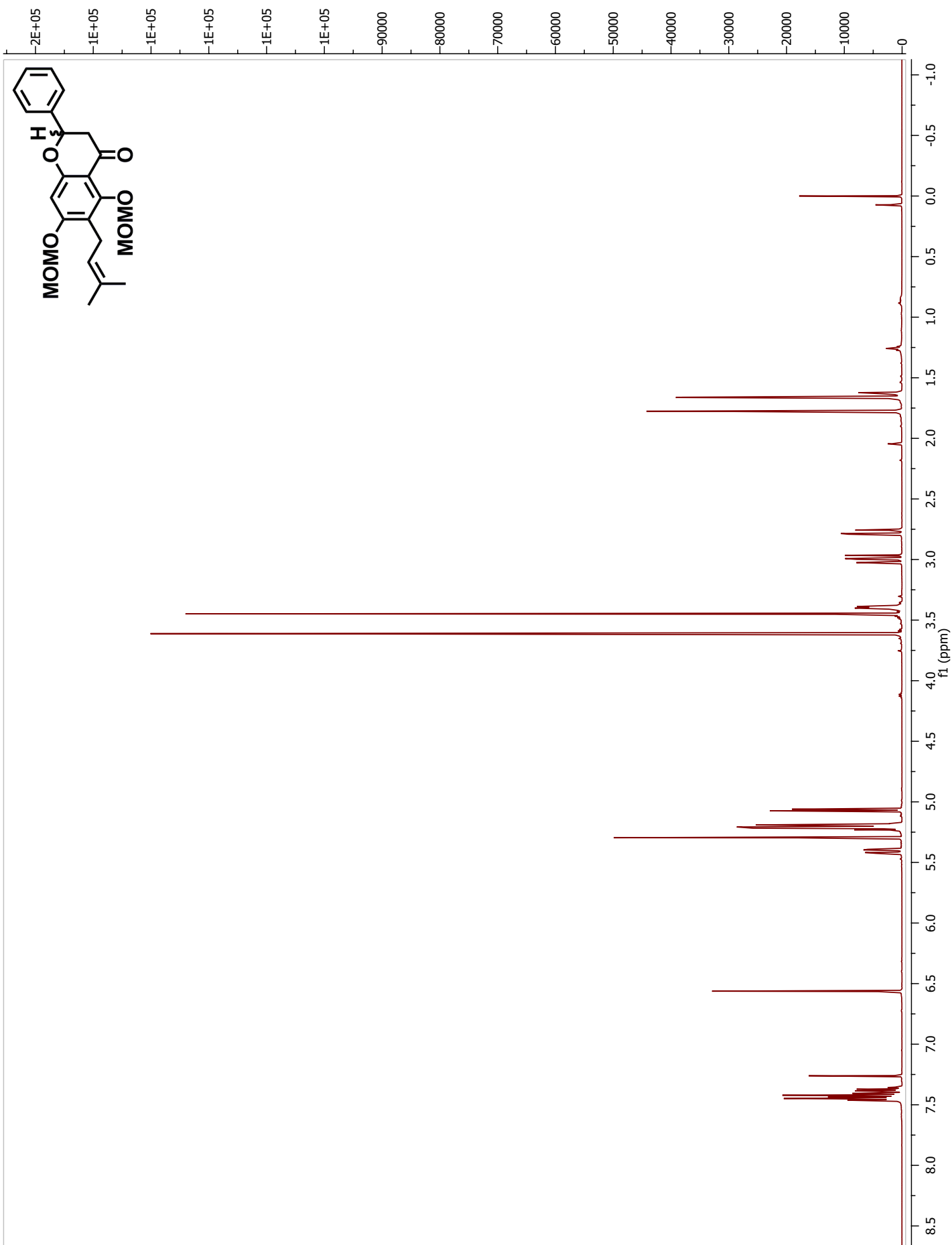


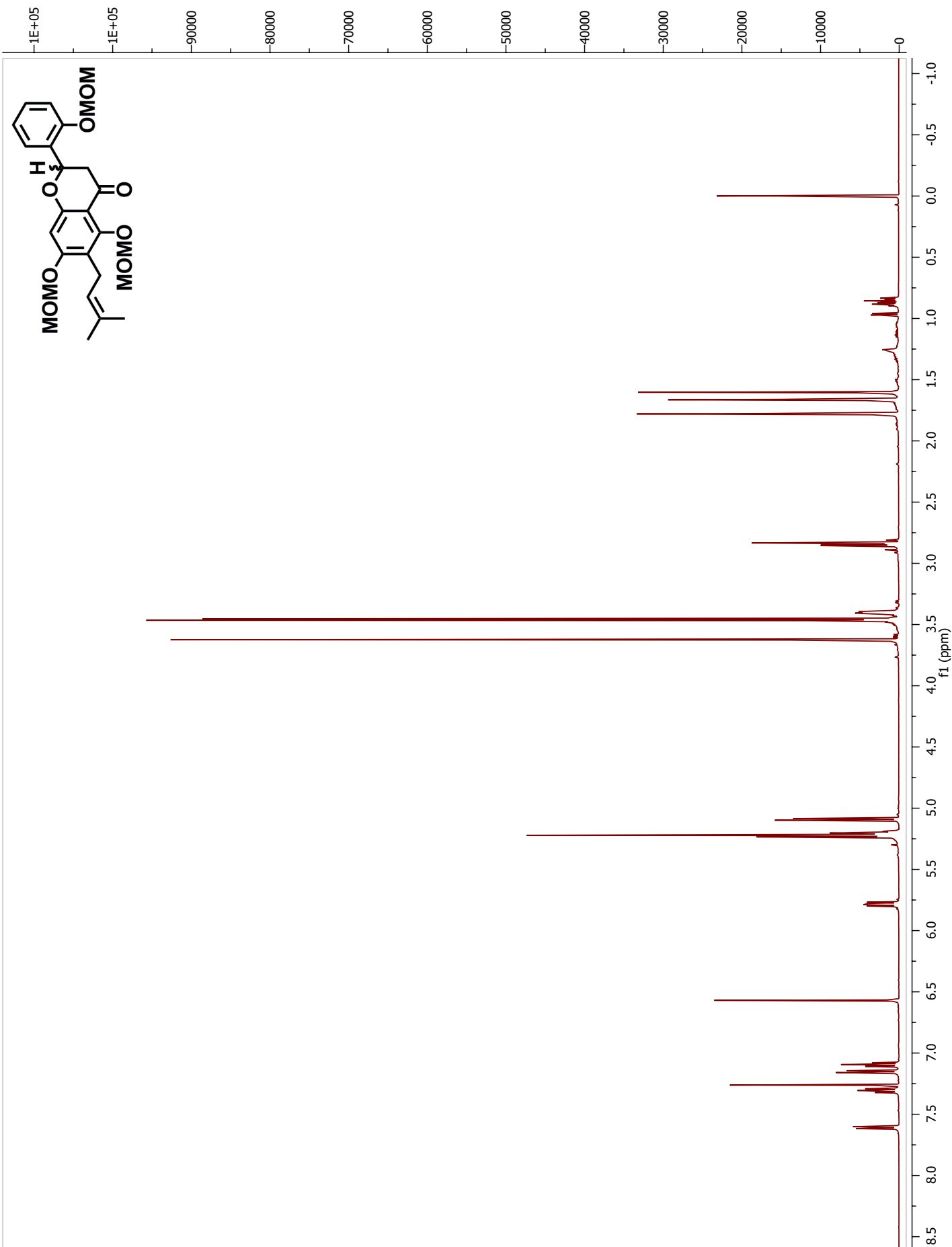


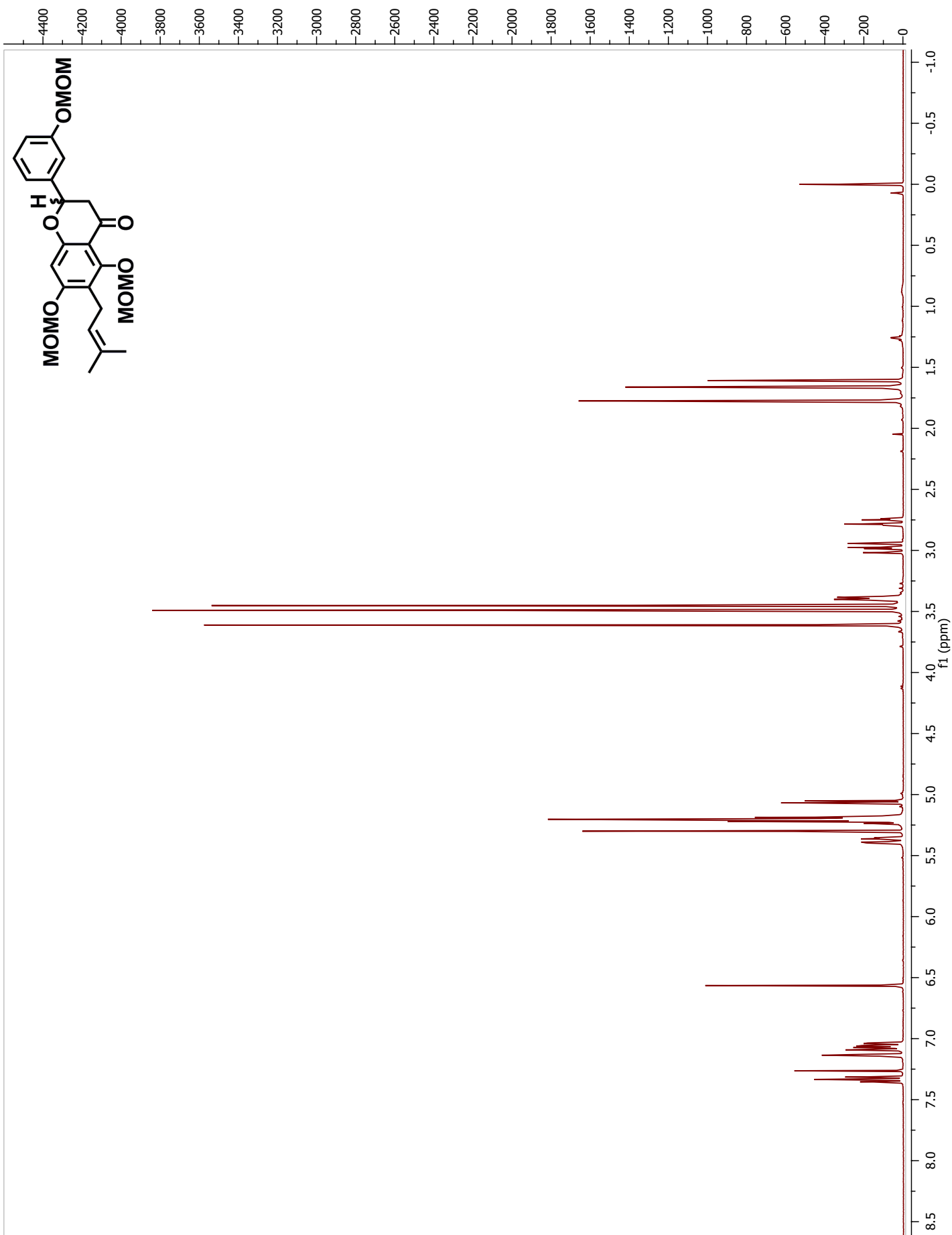


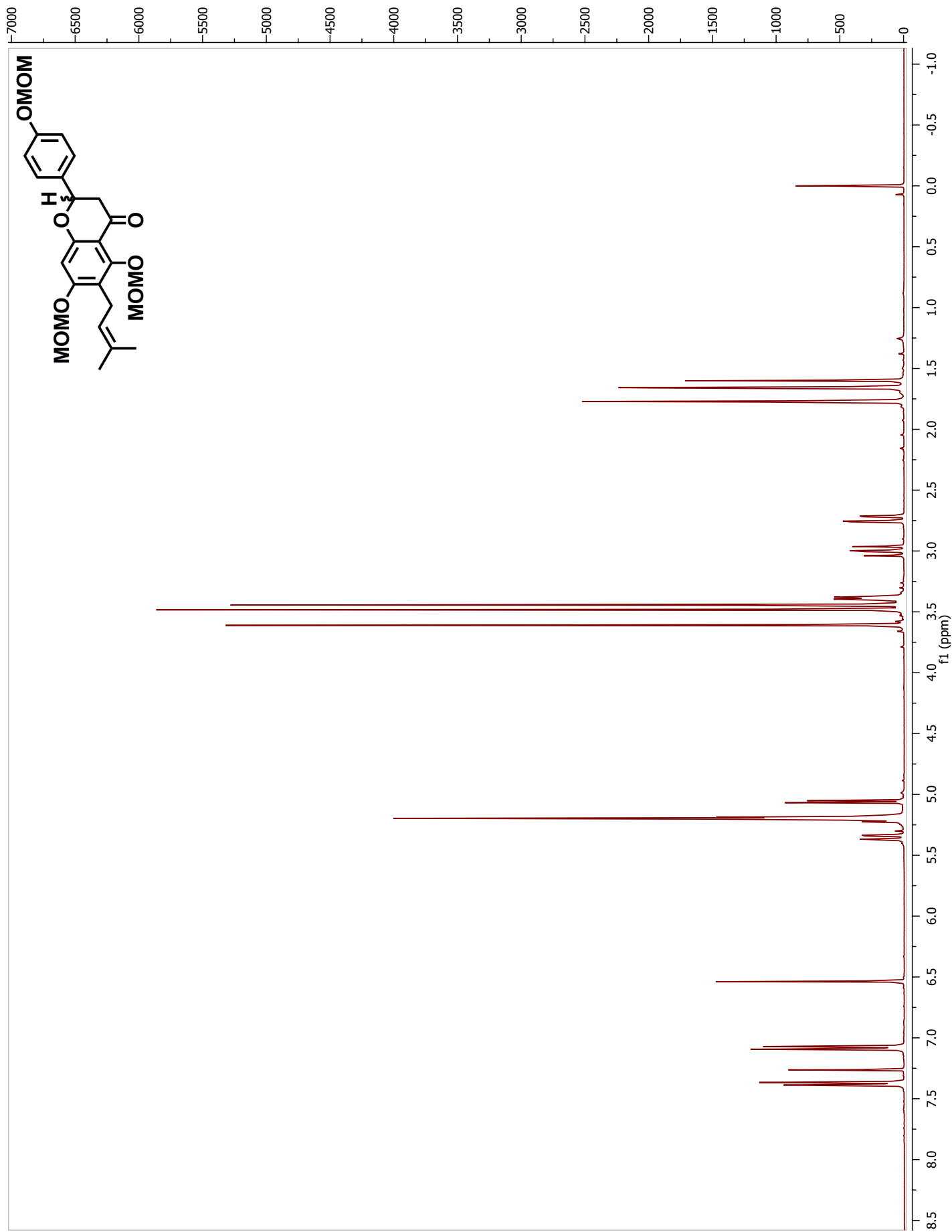


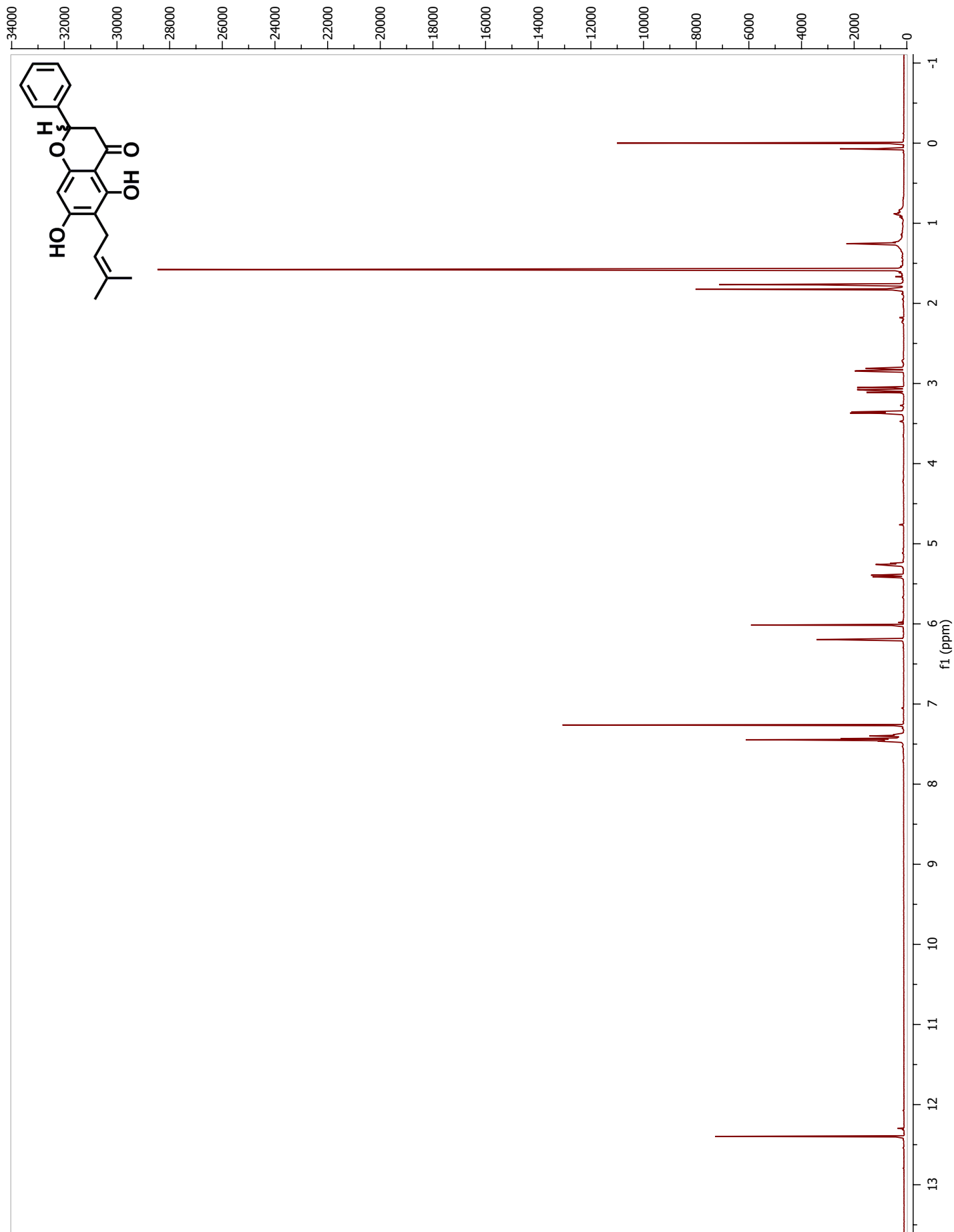


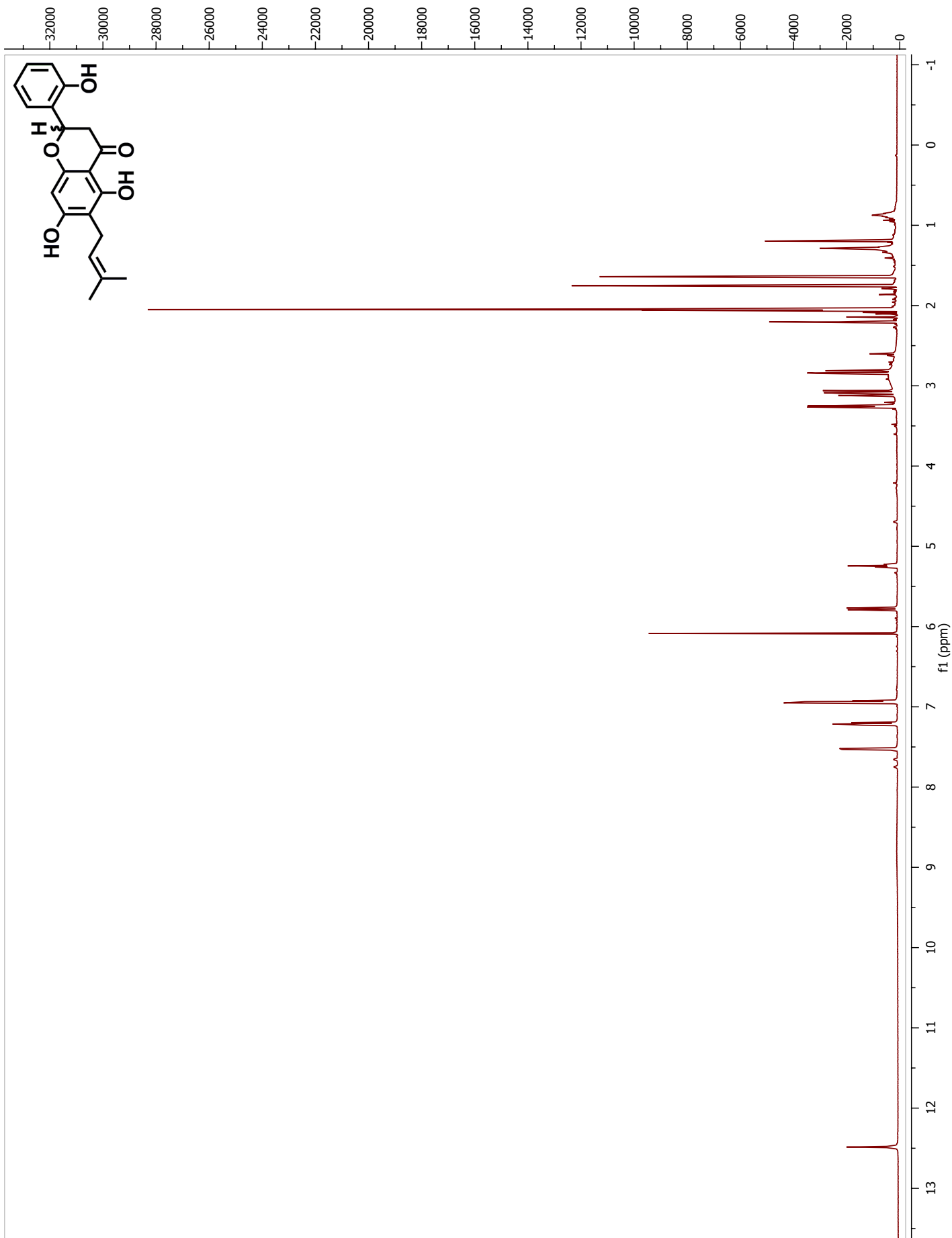


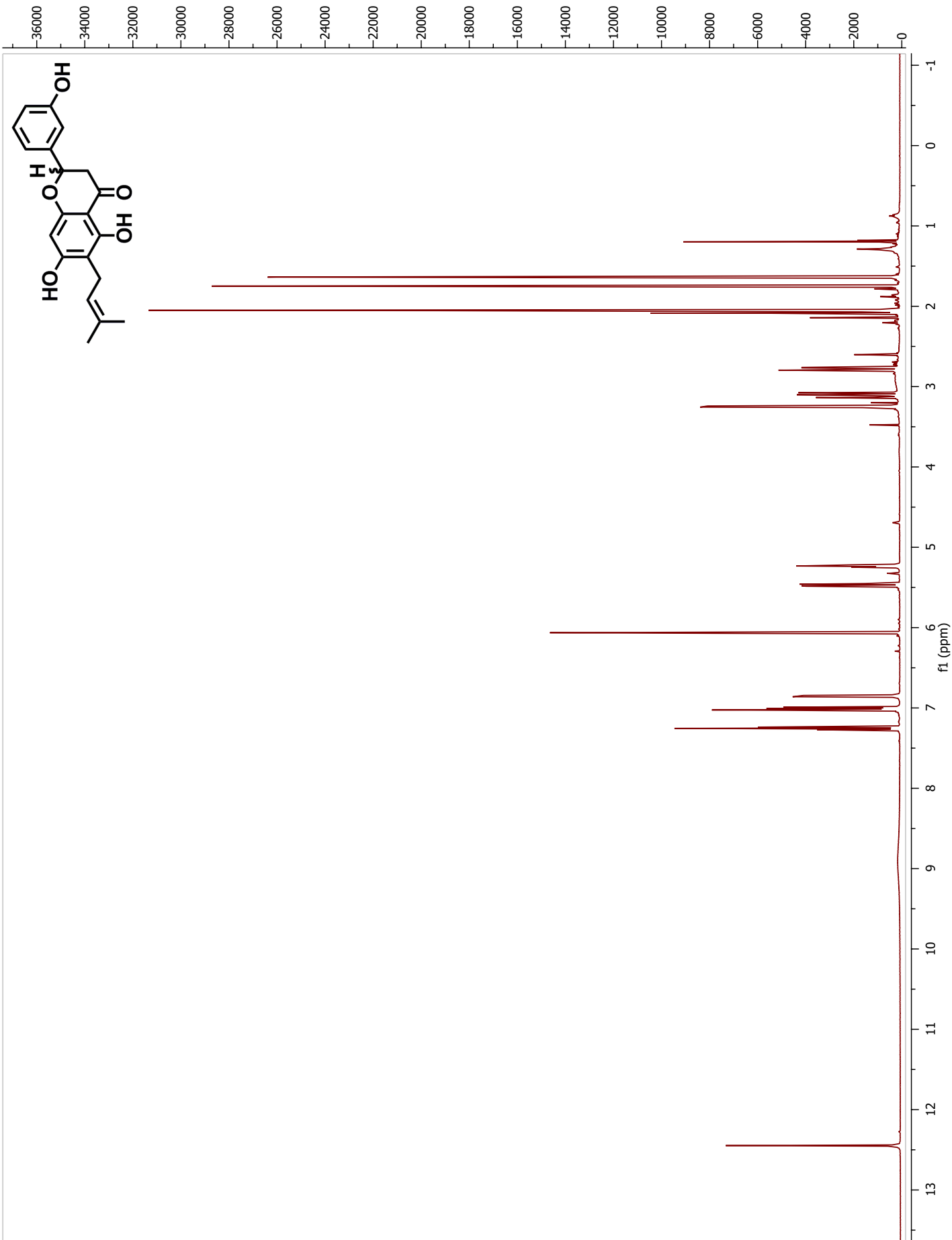


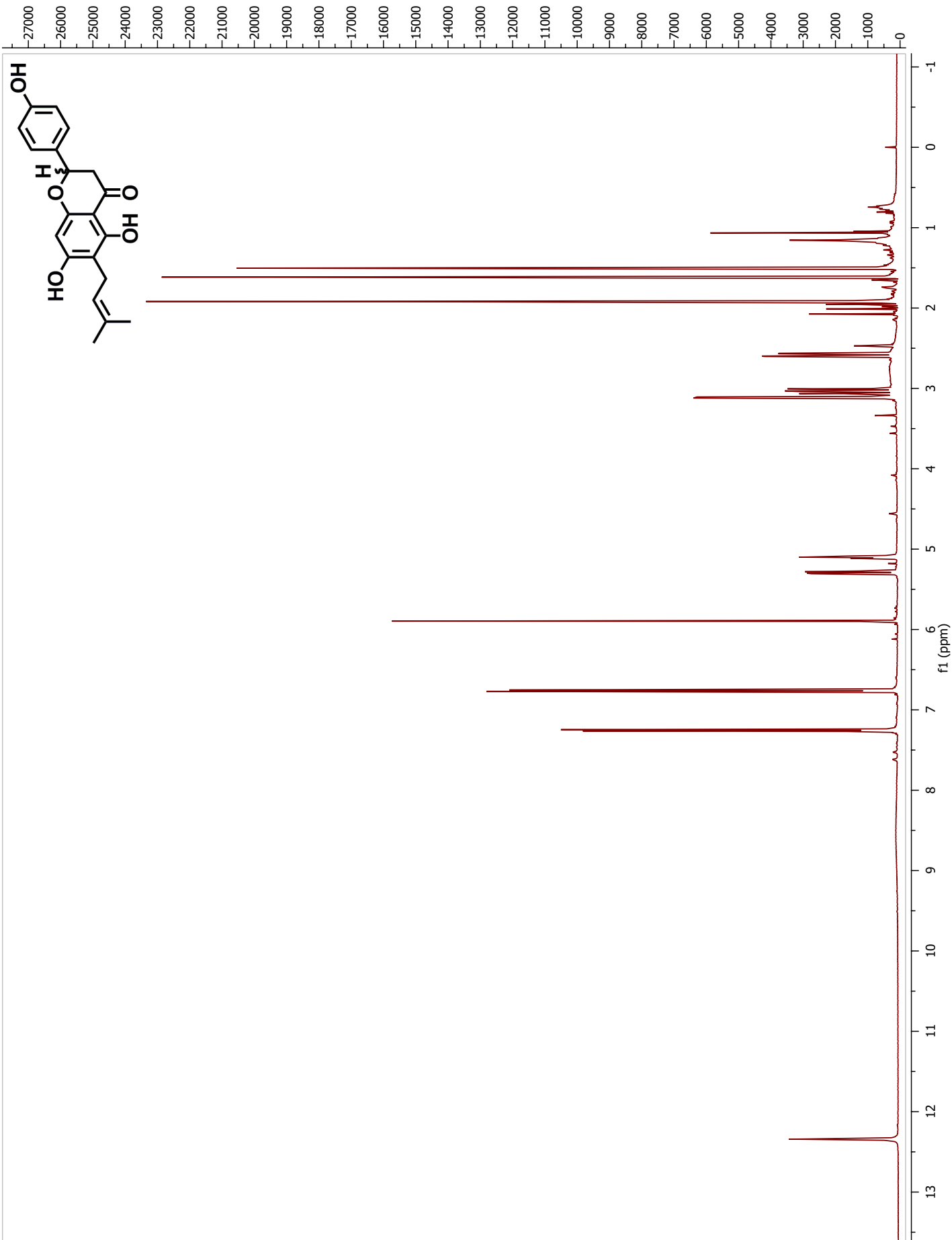




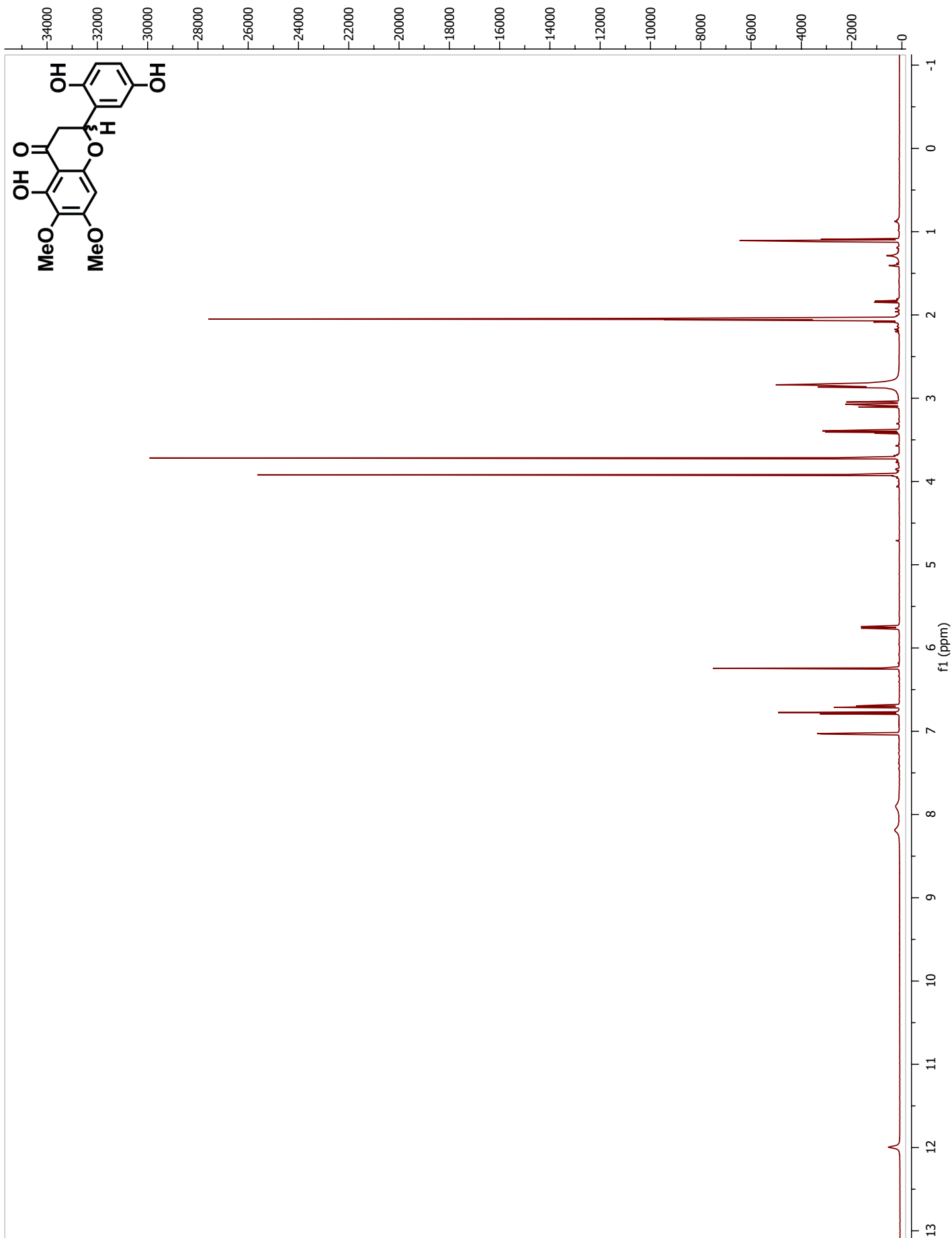


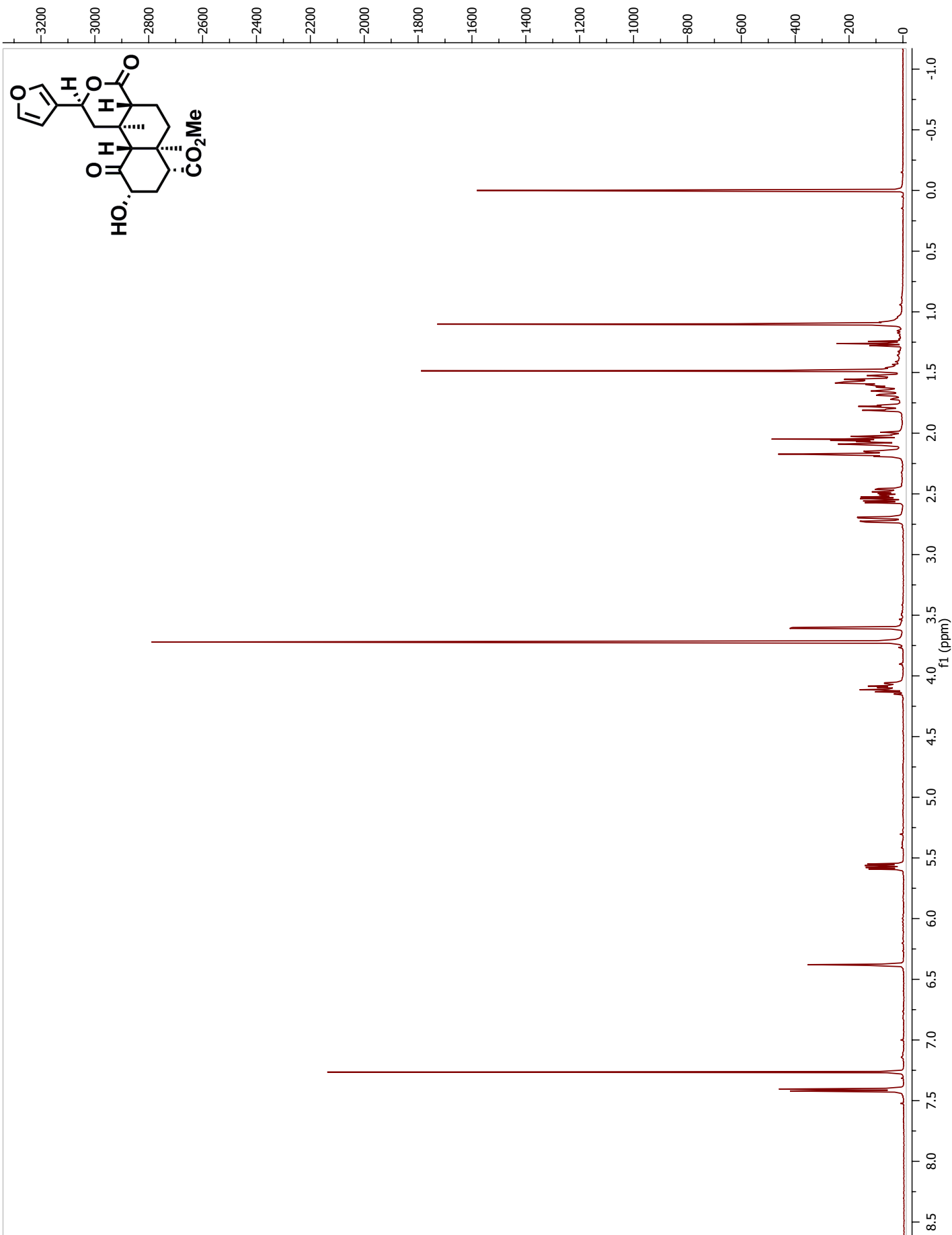


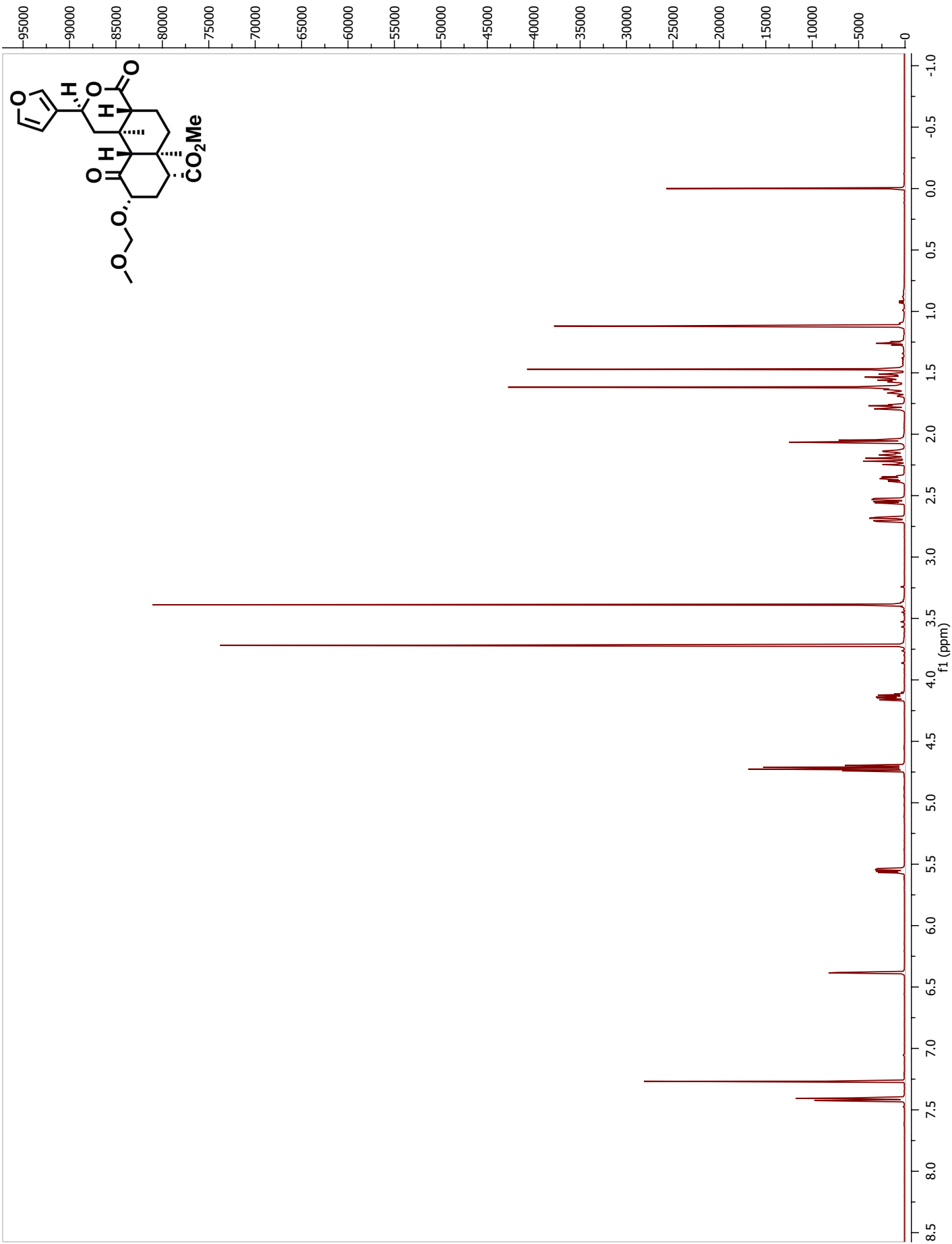


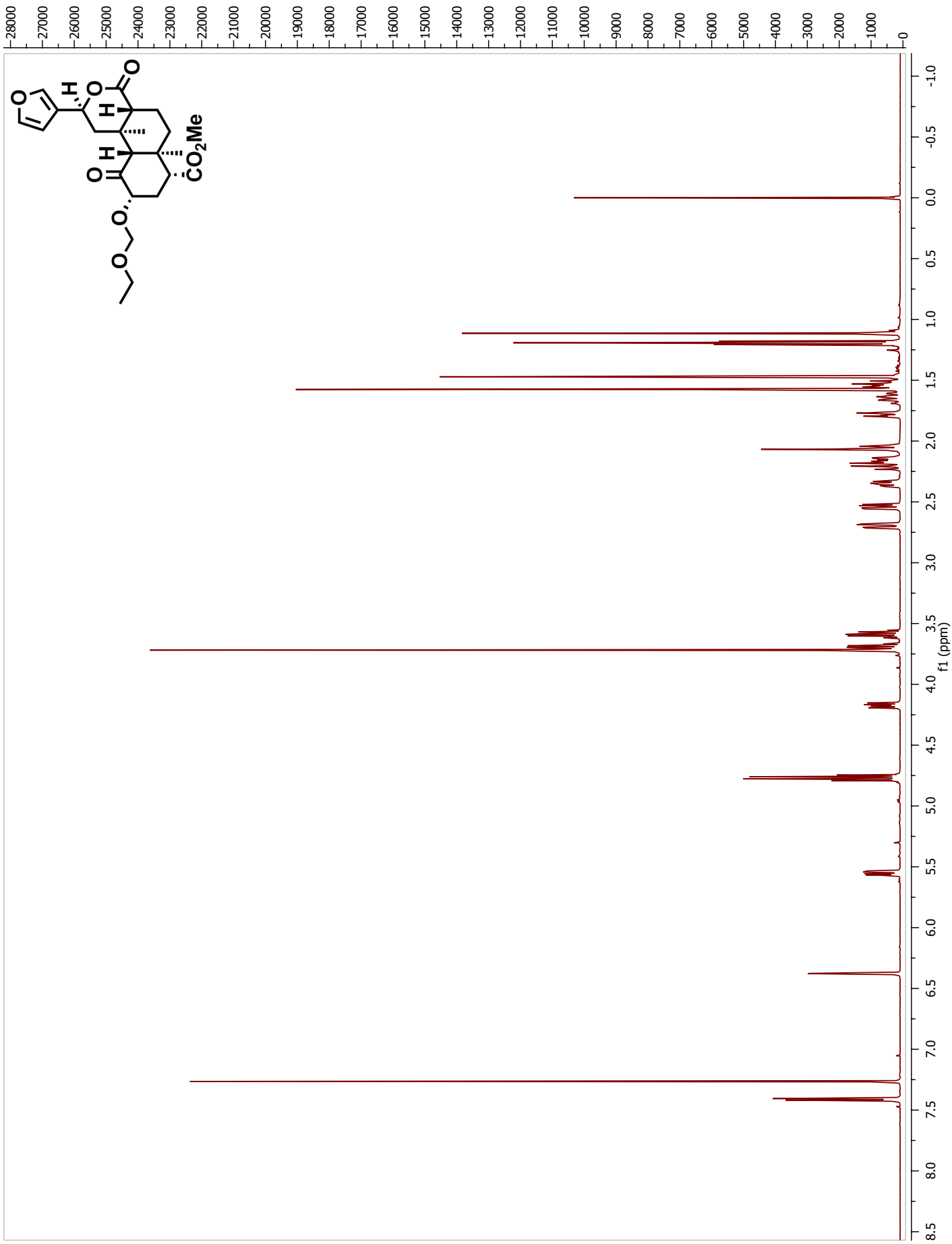


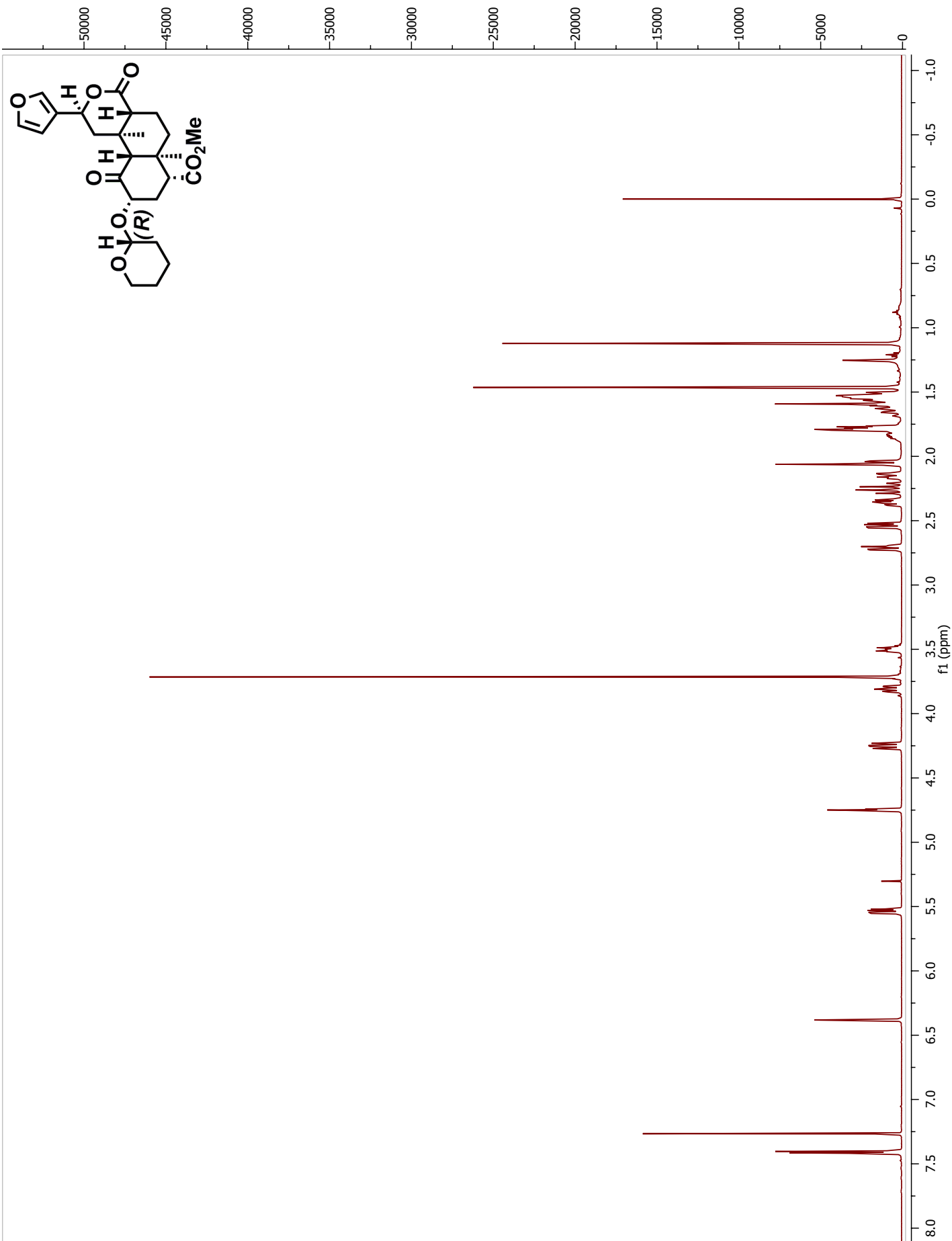


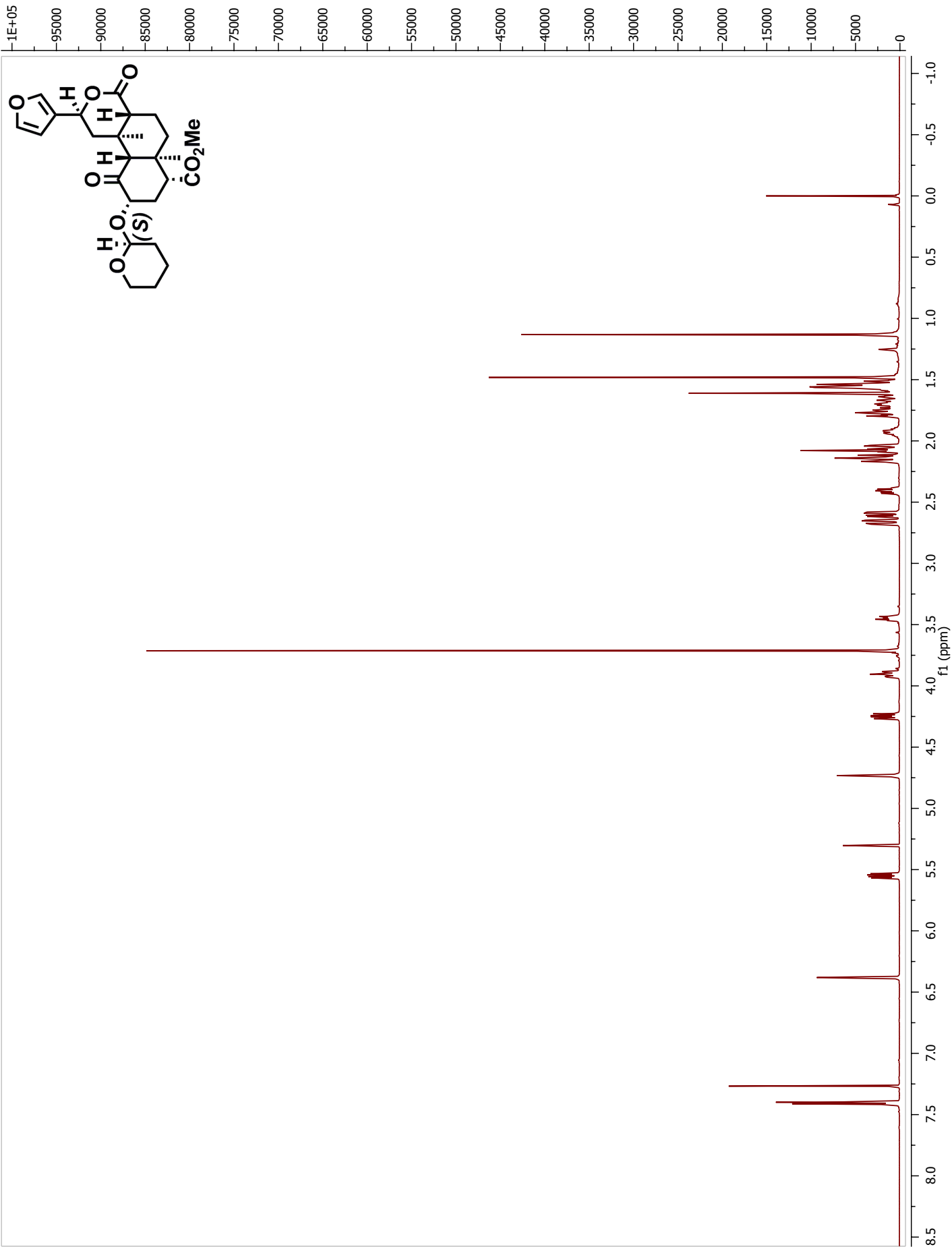


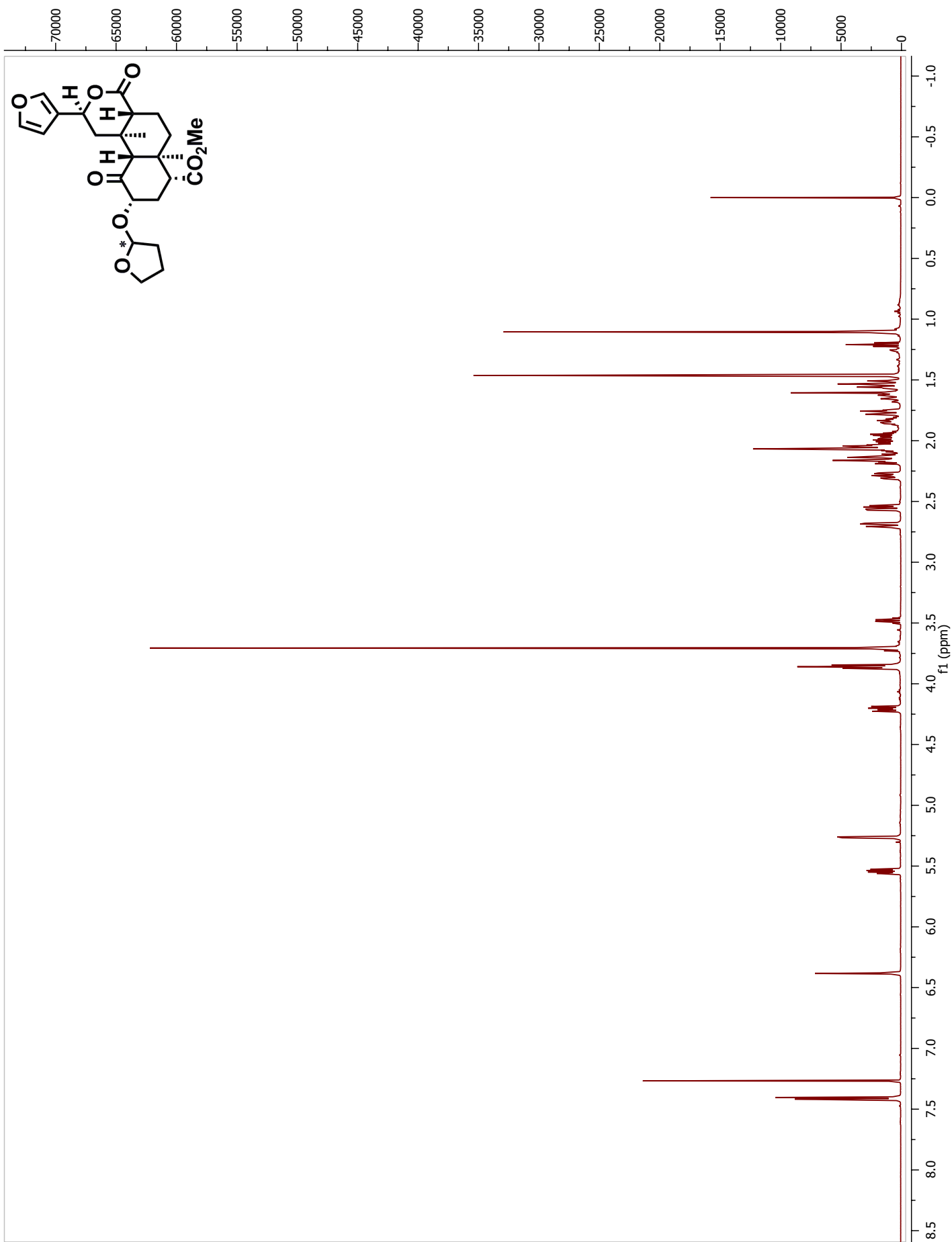


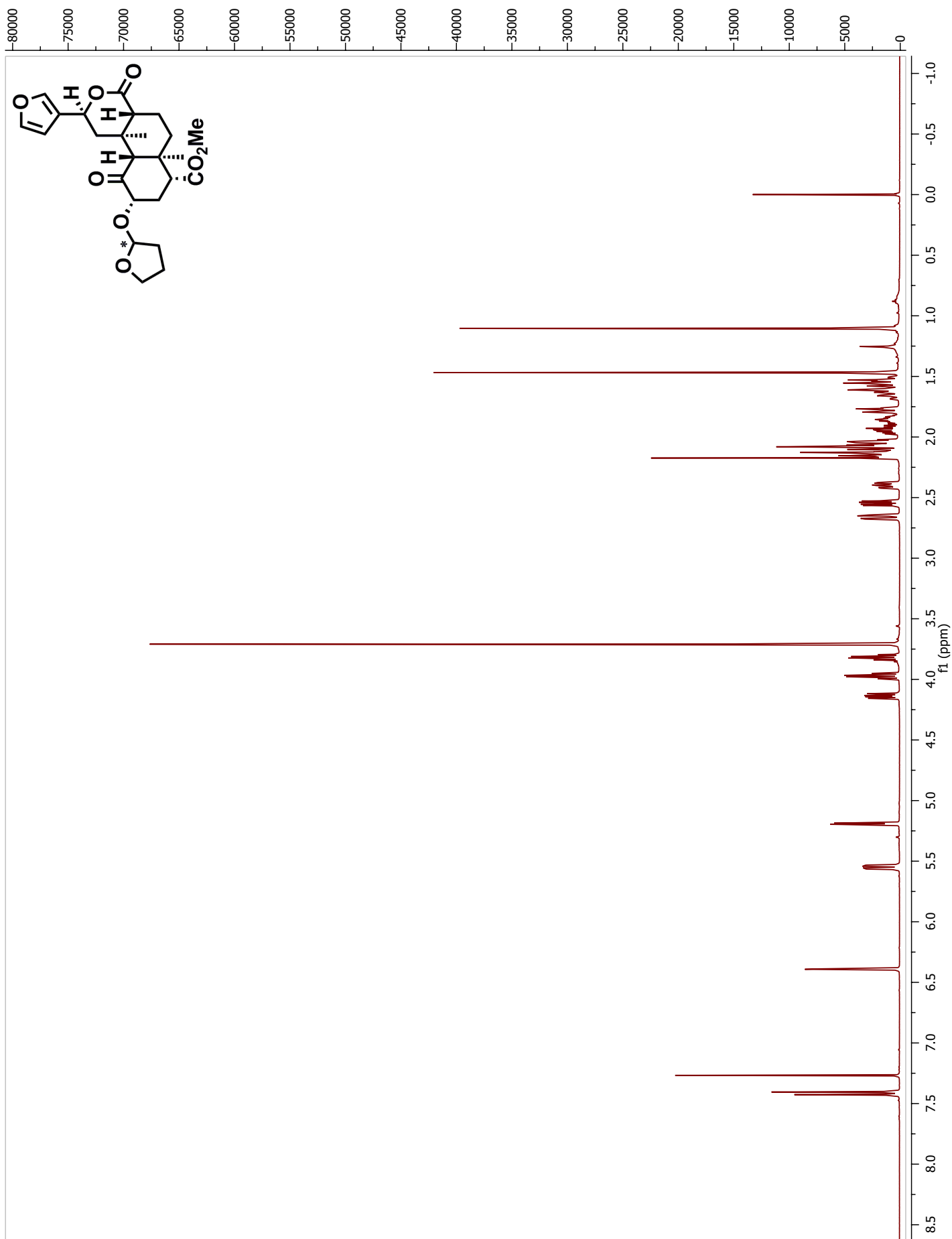




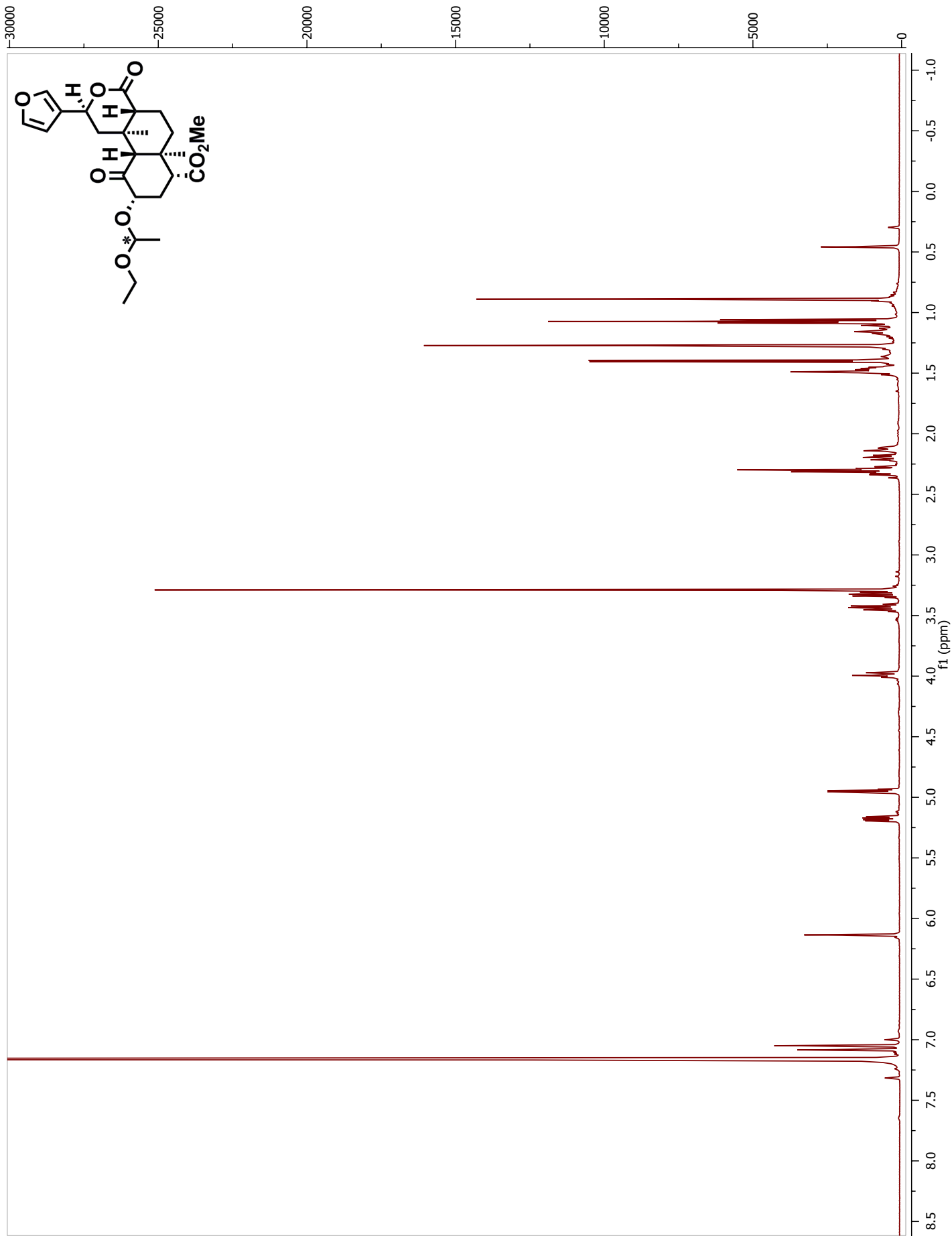


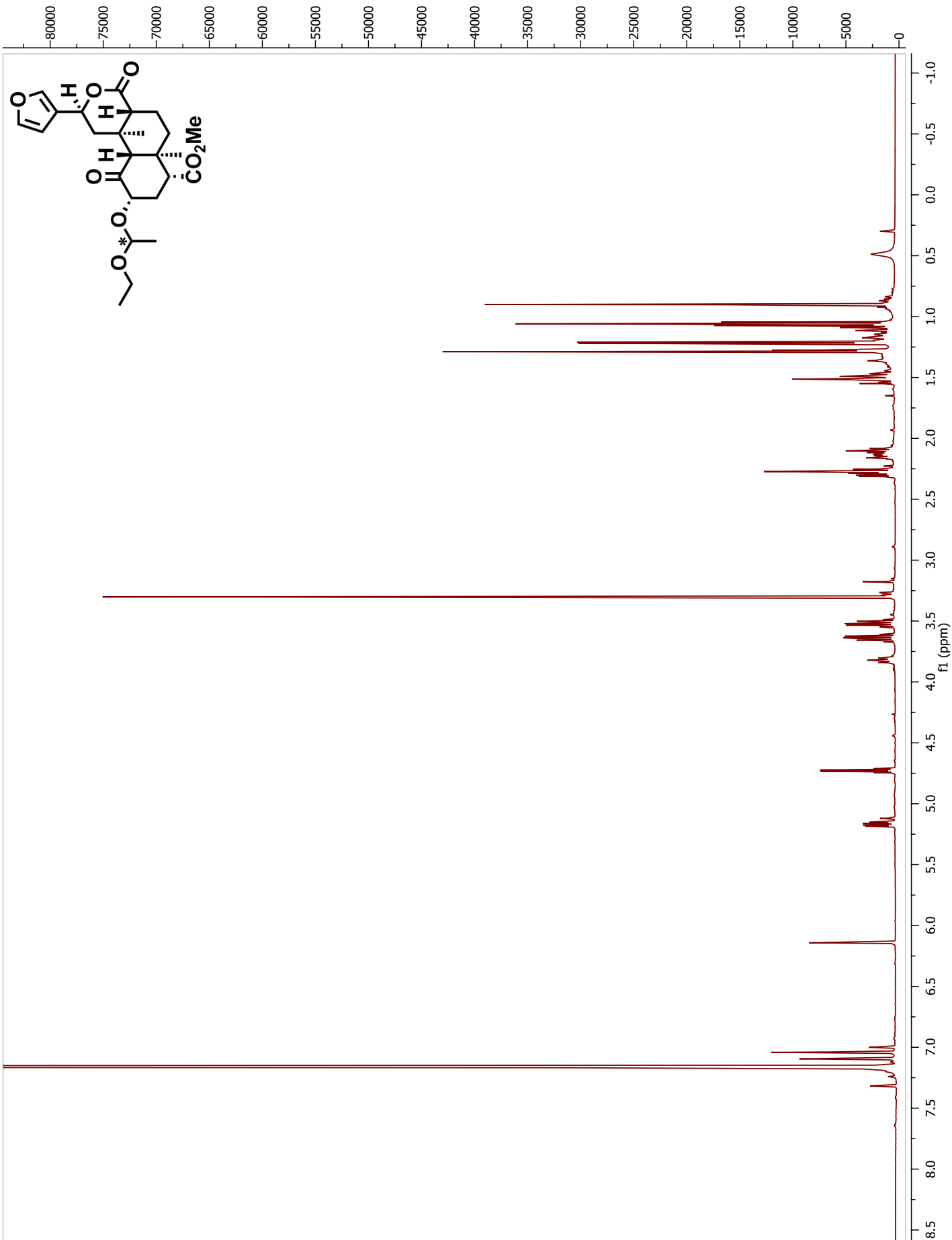


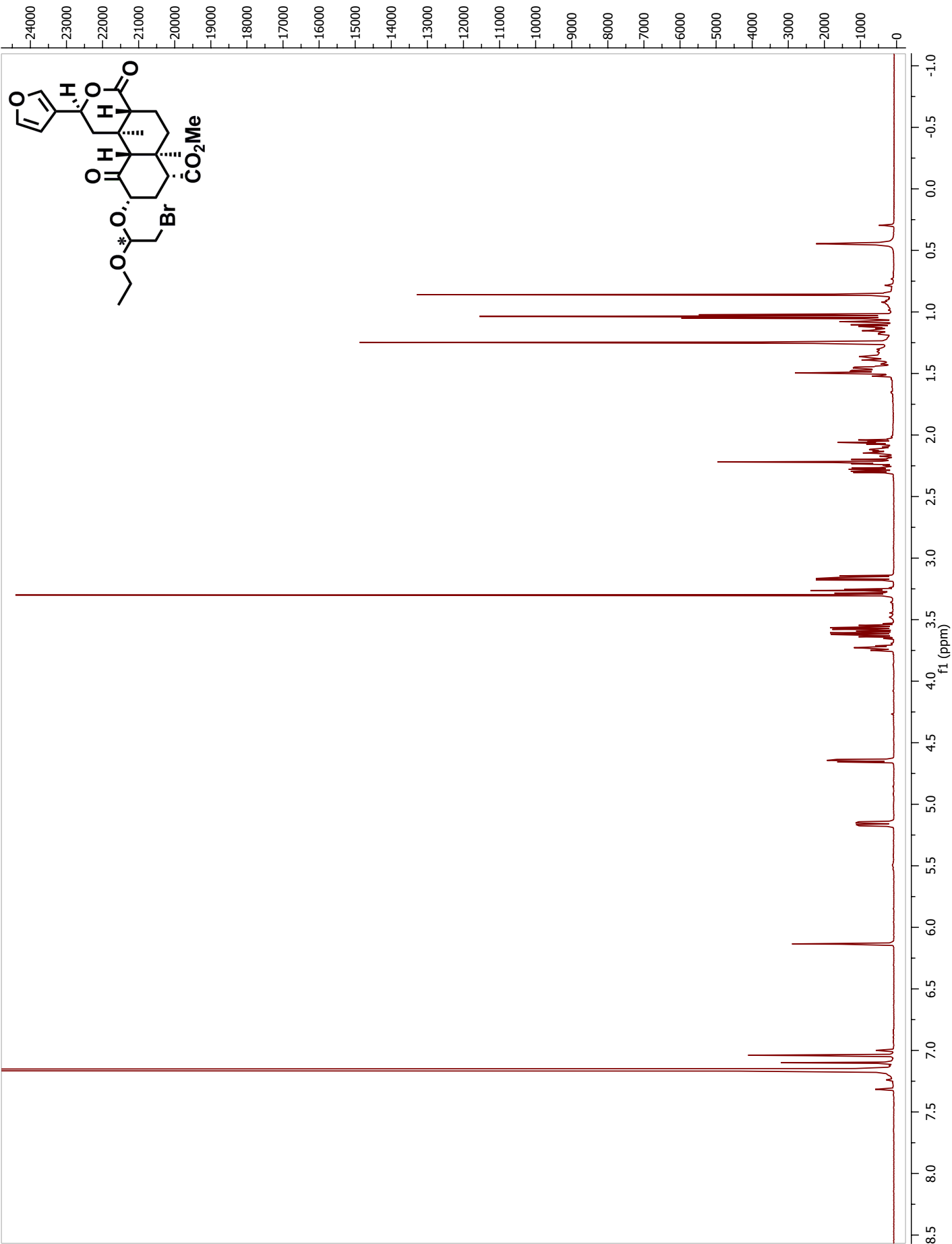


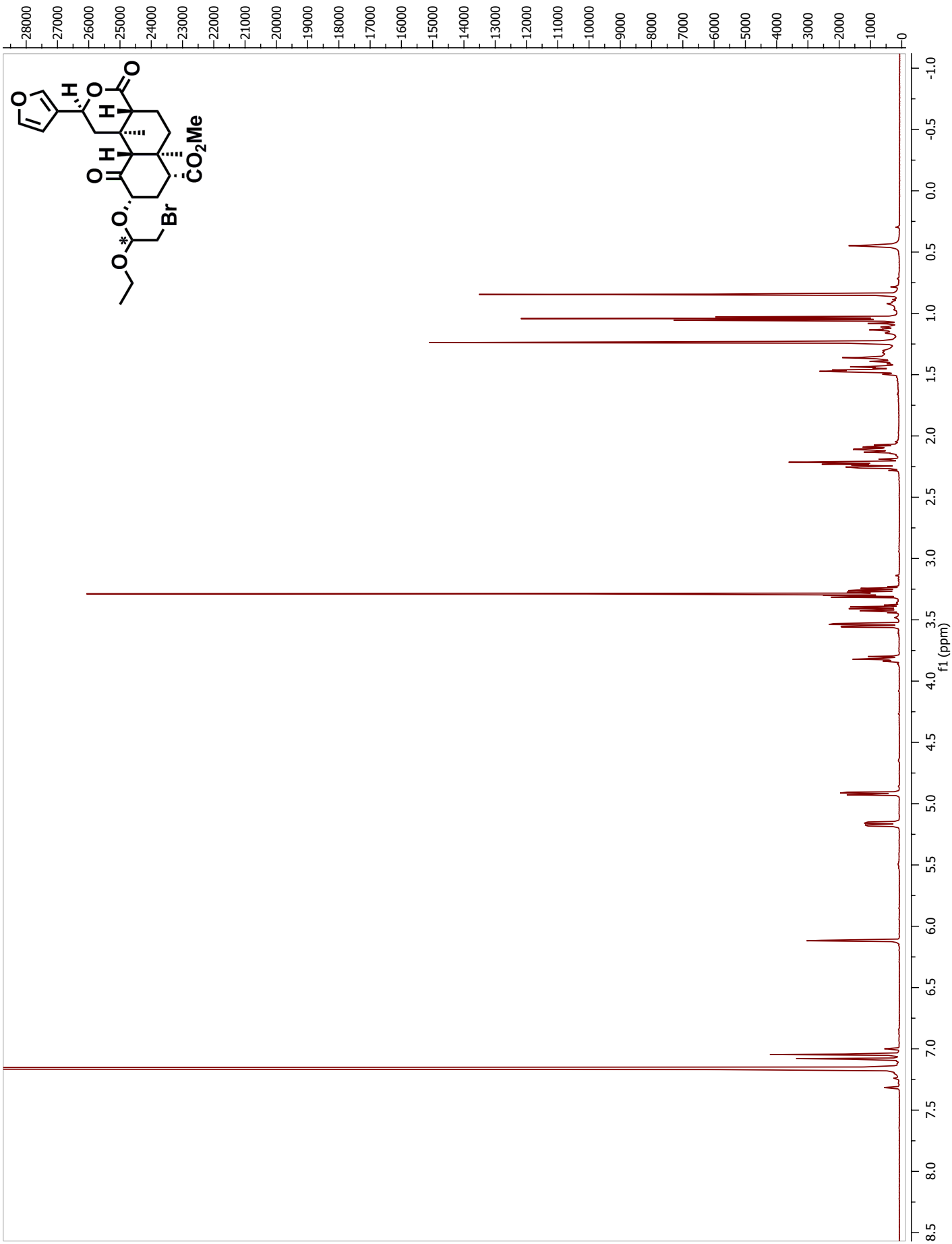


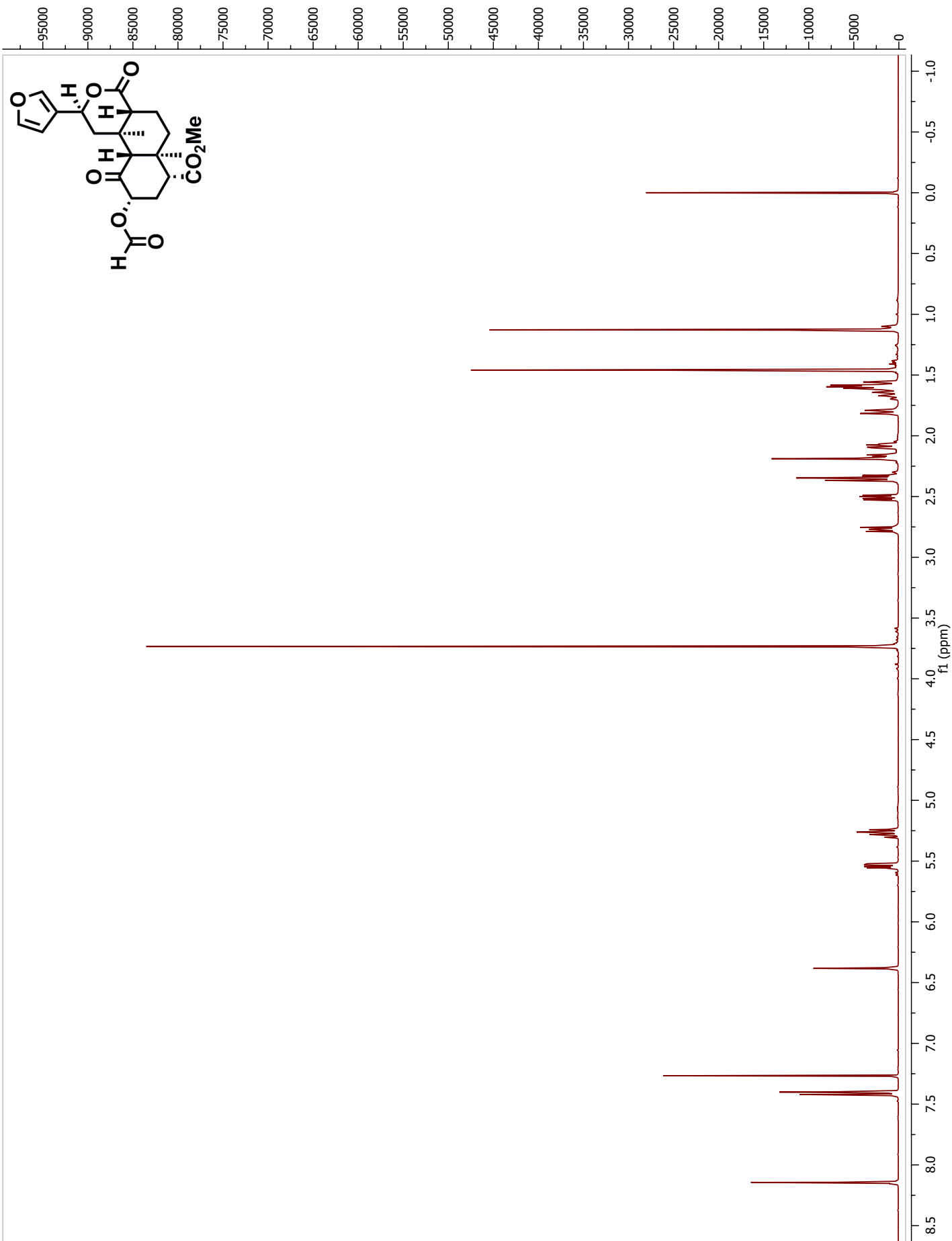


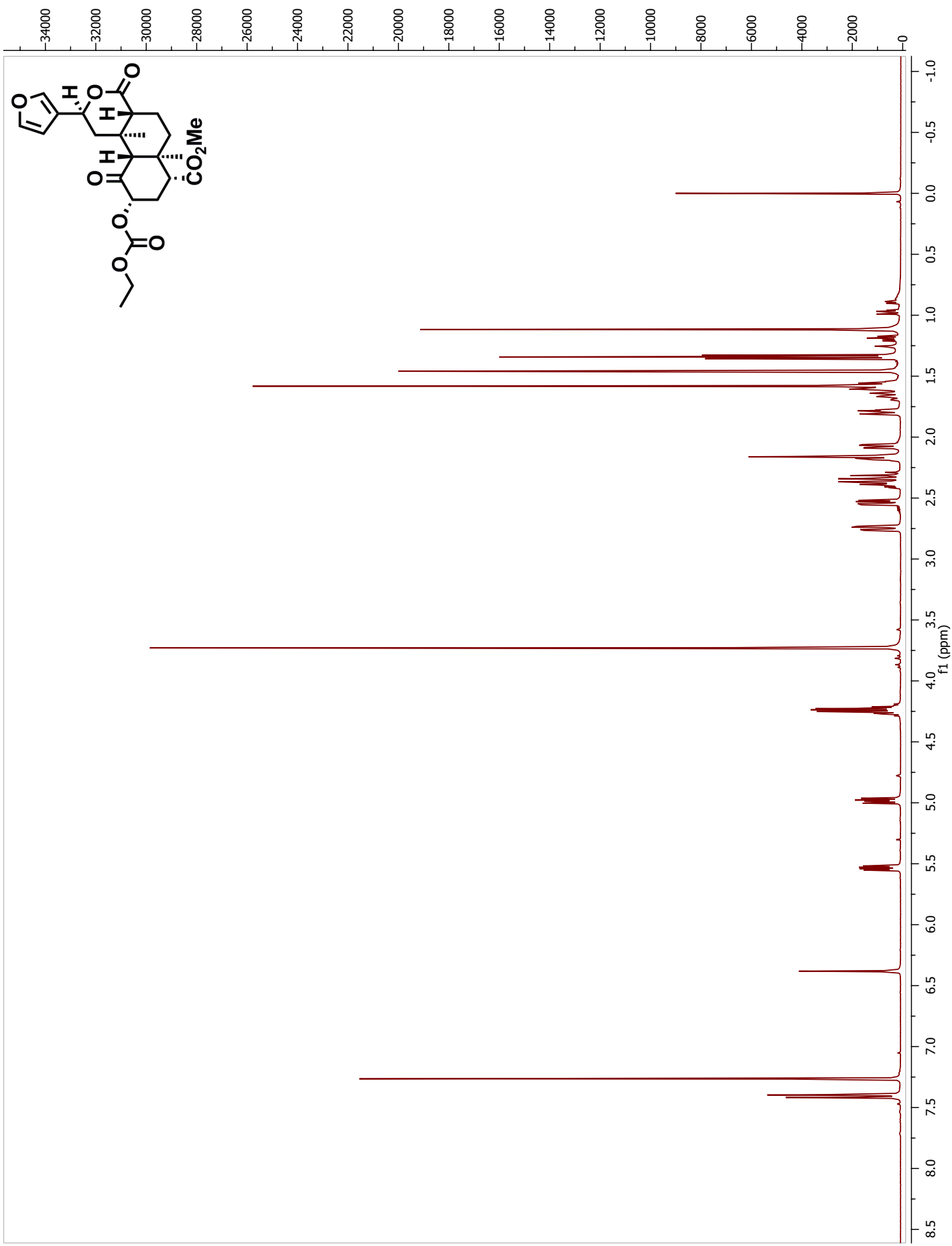


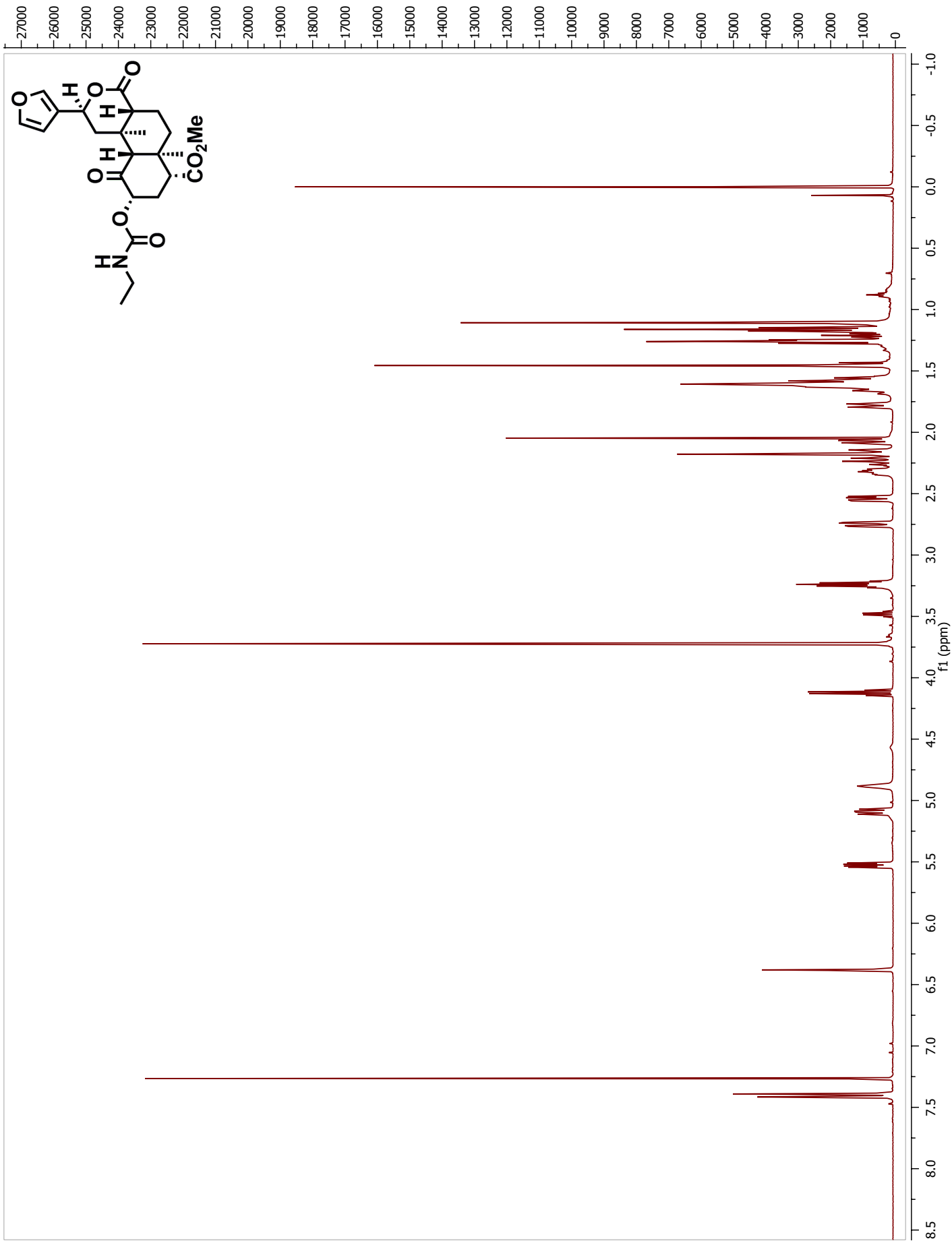


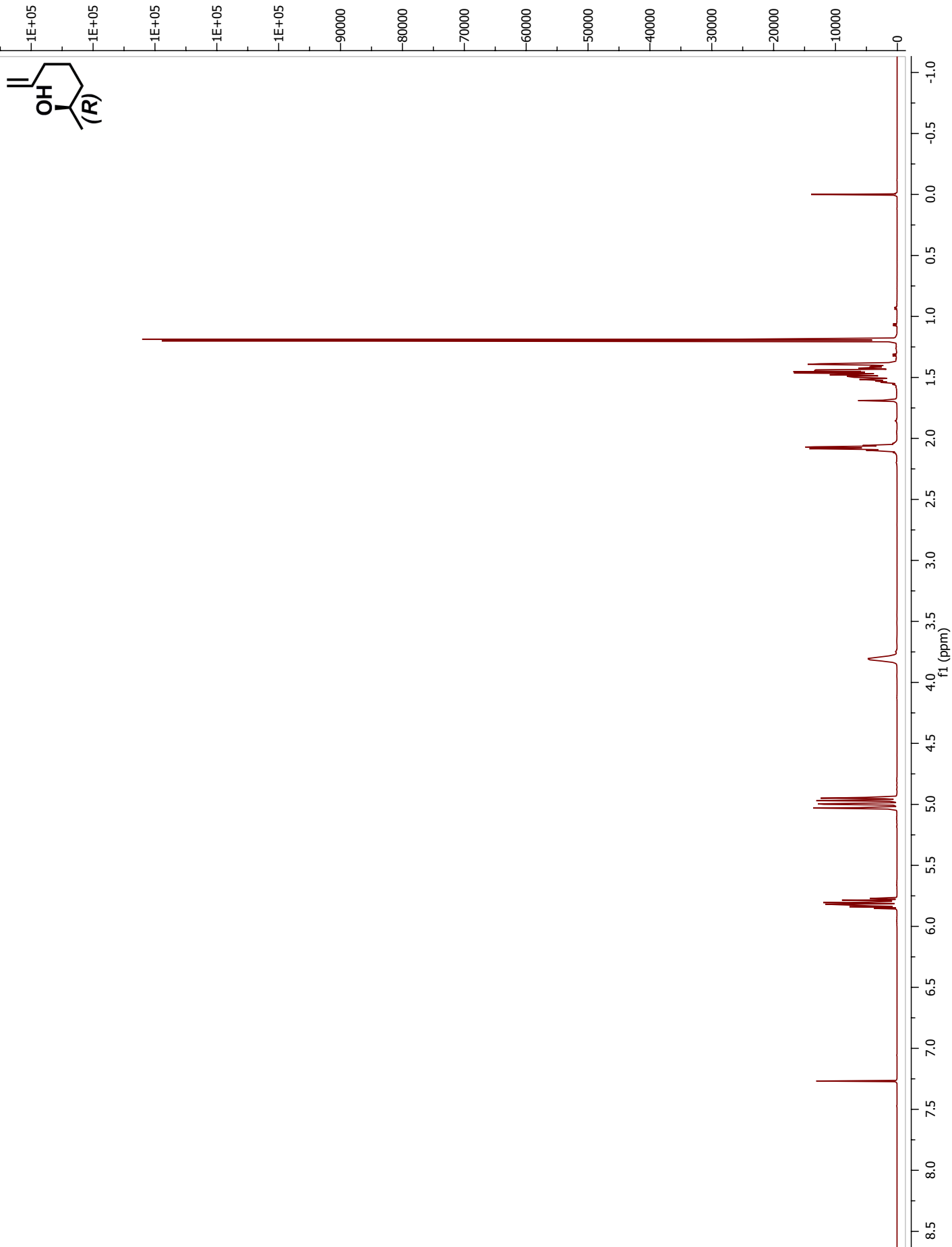




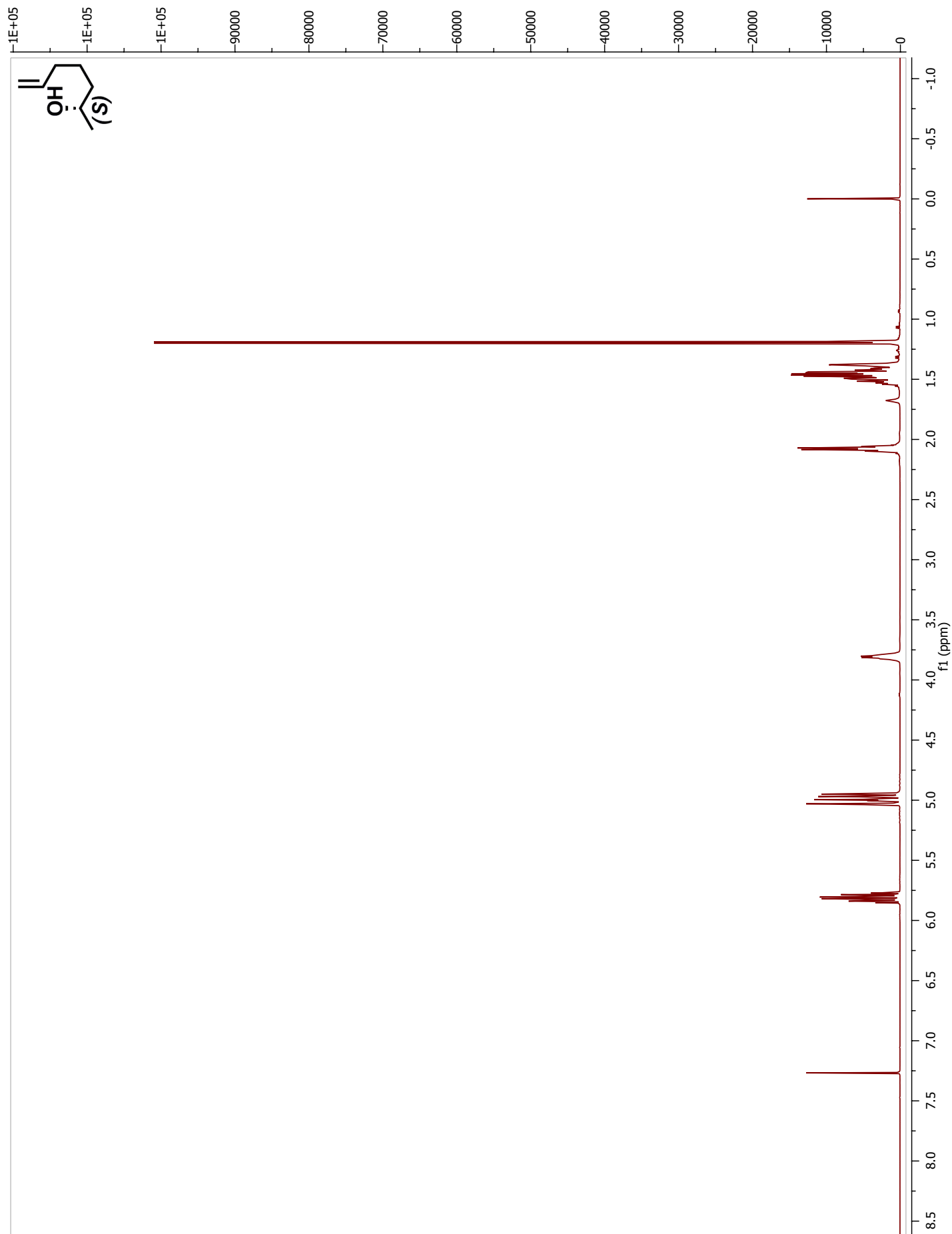


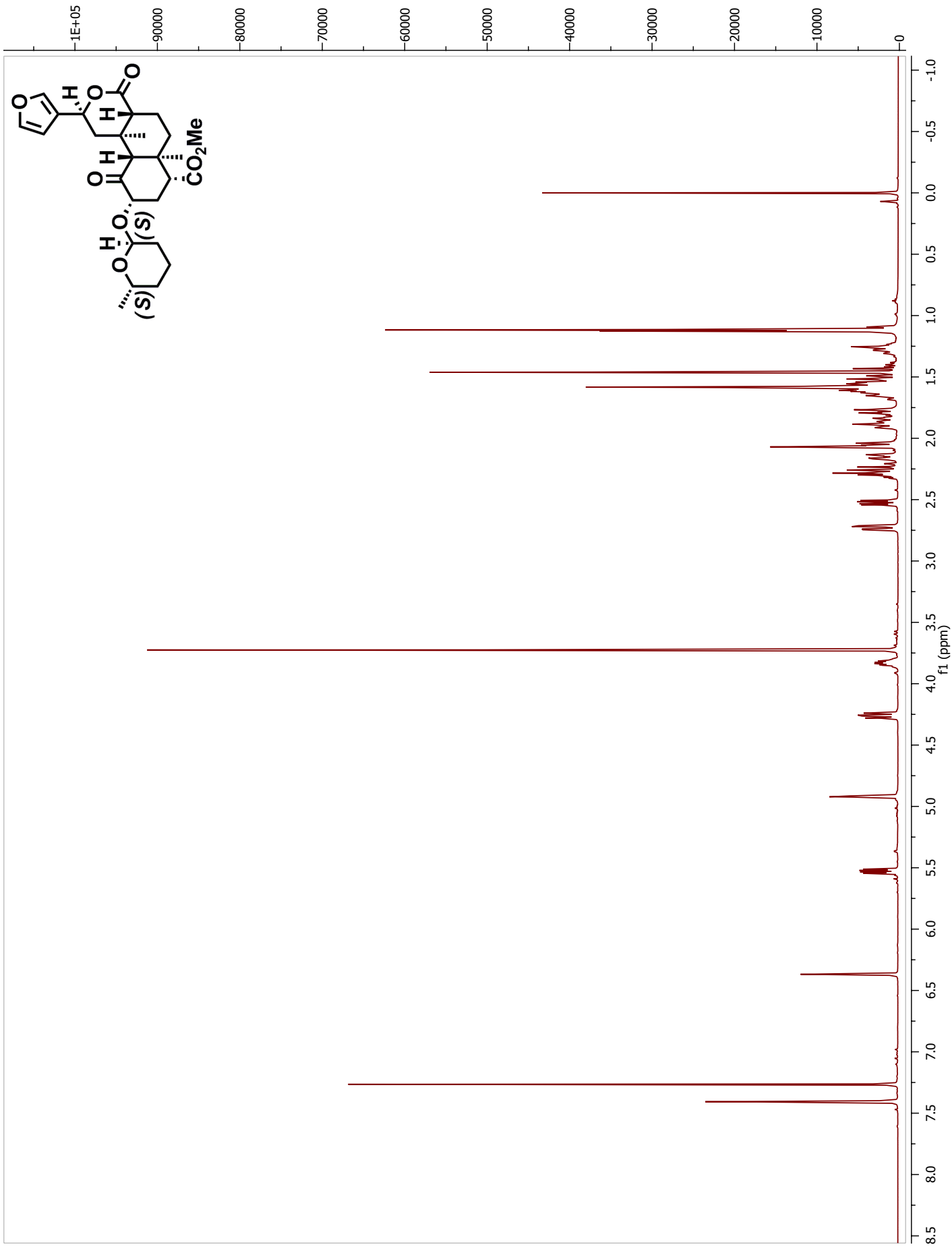


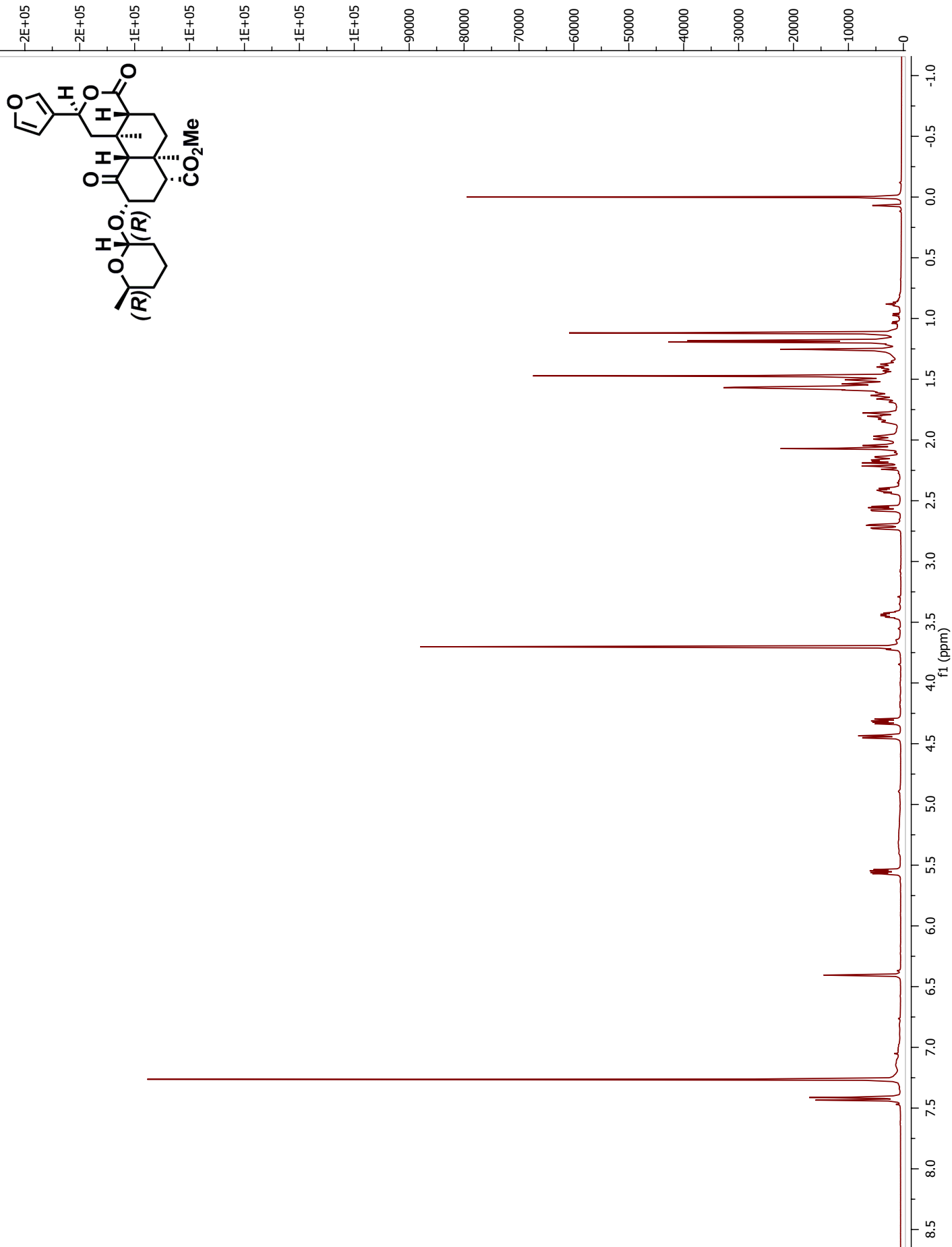


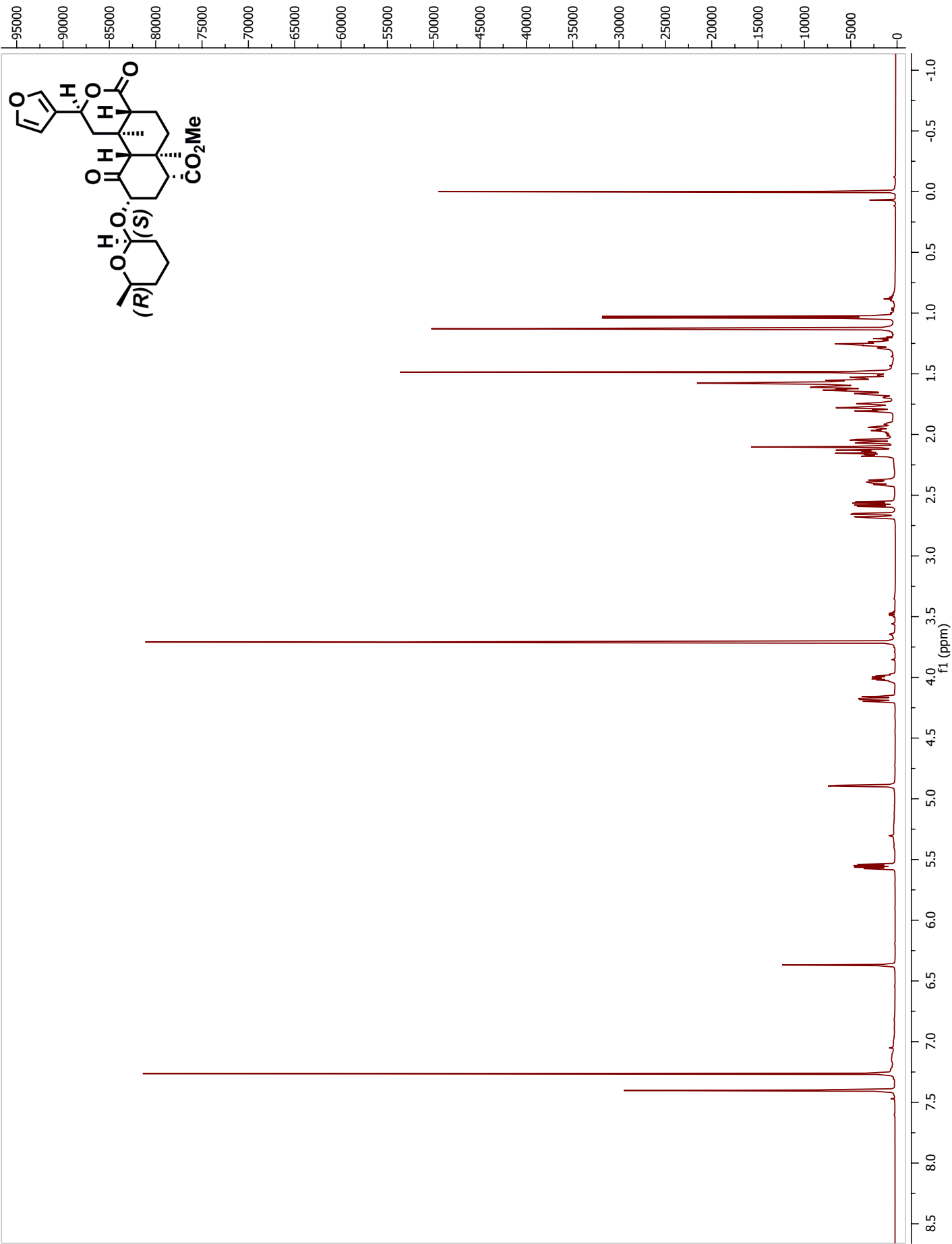




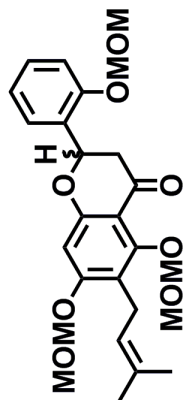
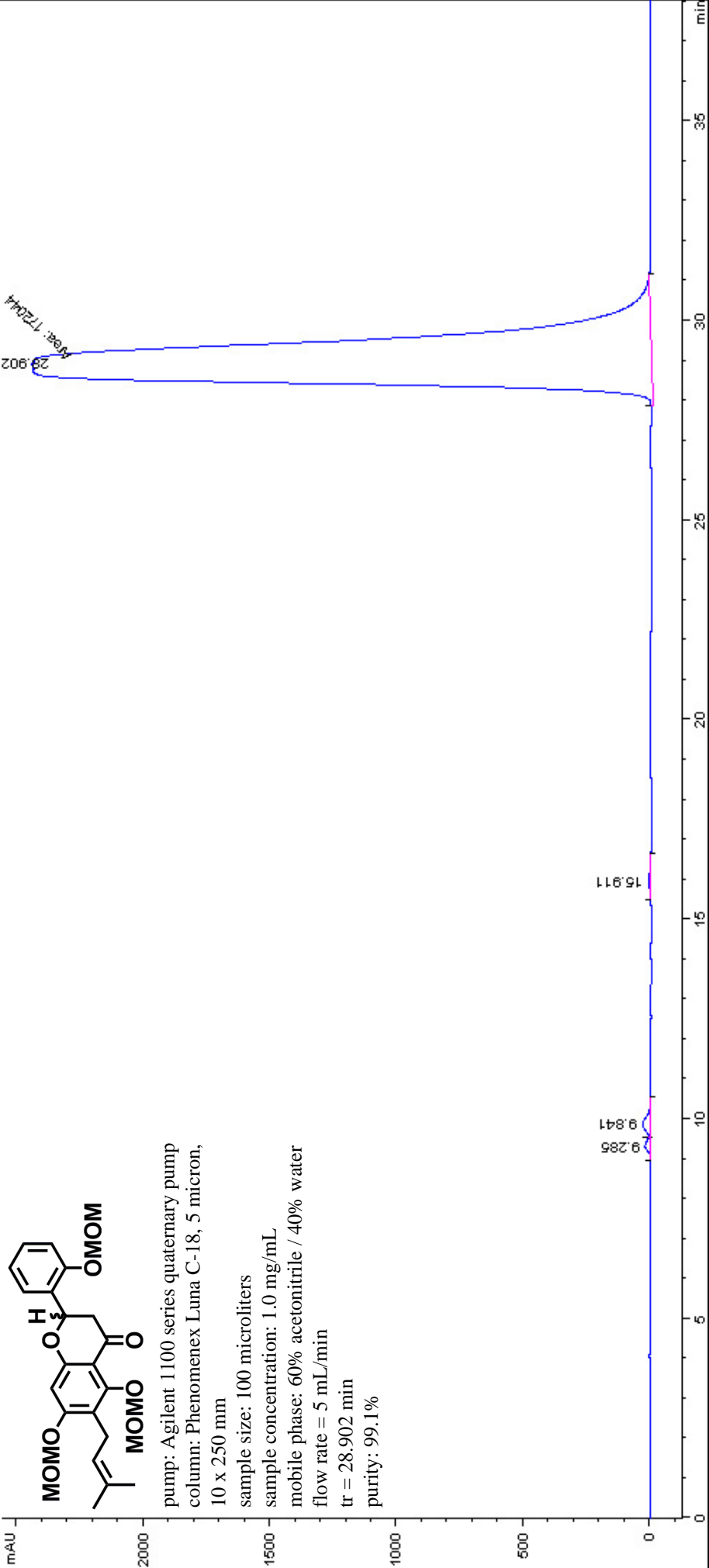






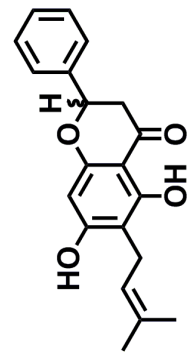


## APPENDIX B: HPLC CHROMATOGRAMS

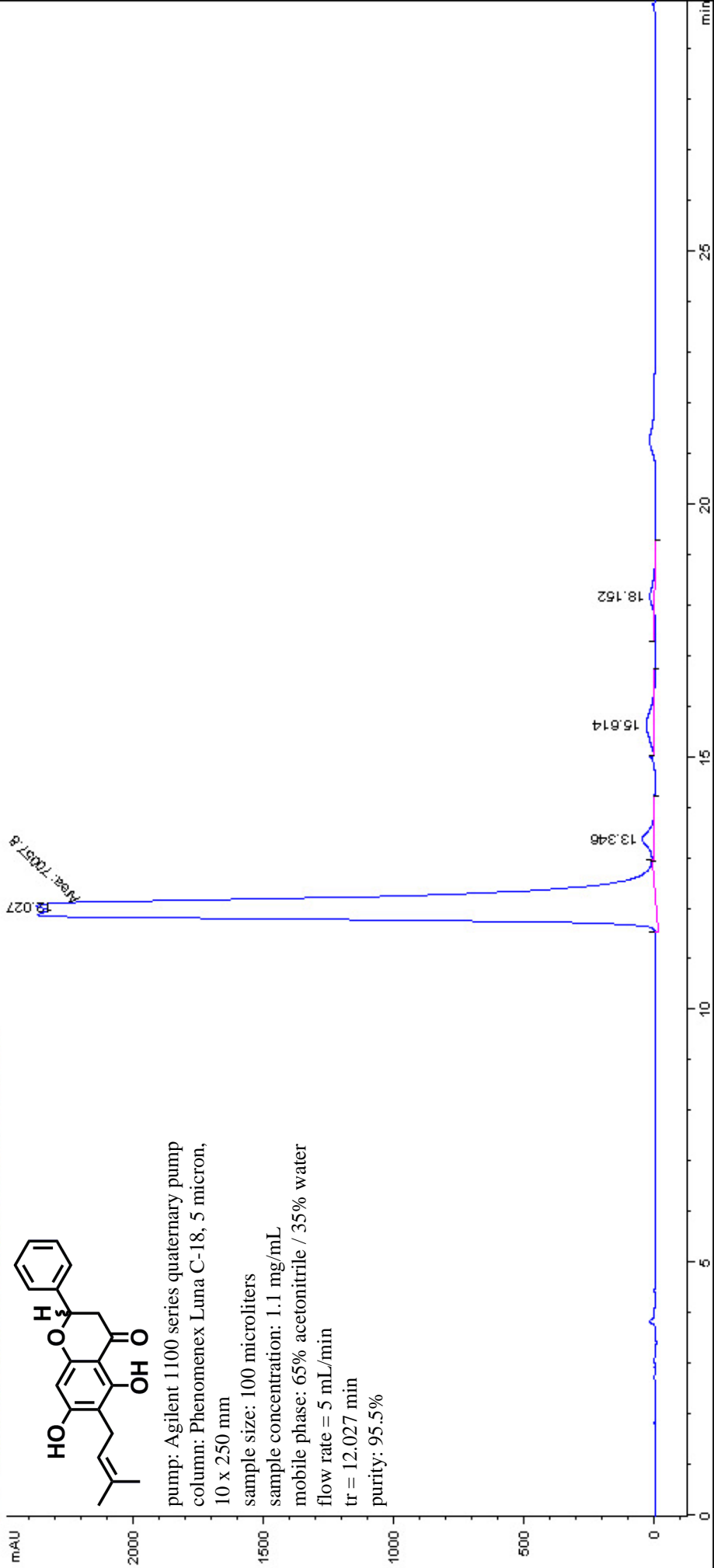


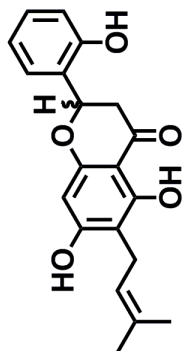
pump: Agilent 1100 series quaternary pump  
column: Phenomenex Luna C-18, 5 micron,  
10 x 250 mm  
sample size: 100 microliters  
sample concentration: 1.0 mg/mL  
mobile phase: 60% acetonitrile / 40% water  
flow rate = 5 mL/min  
tr = 28.902 min  
purity: 99.1%

DAD1 A, Sig=209,4 Ref=360,100 (KARRIEVIMS-1-2066000002.D)



pump: Agilent 1100 series quaternary pump  
column: Phenomenex Luna C-18, 5 micron,  
10 x 250 mm  
sample size: 100 microliters  
sample concentration: 1.1 mg/mL  
mobile phase: 65% acetonitrile / 35% water  
flow rate = 5 mL/min  
tr = 12.027 min  
purity: 95.5%





pump: Agilent 1100 series quaternary pump  
column: Phenomenex Luna C-18, 5 micron,  
10 x 250 mm

sample size: 100 microliters

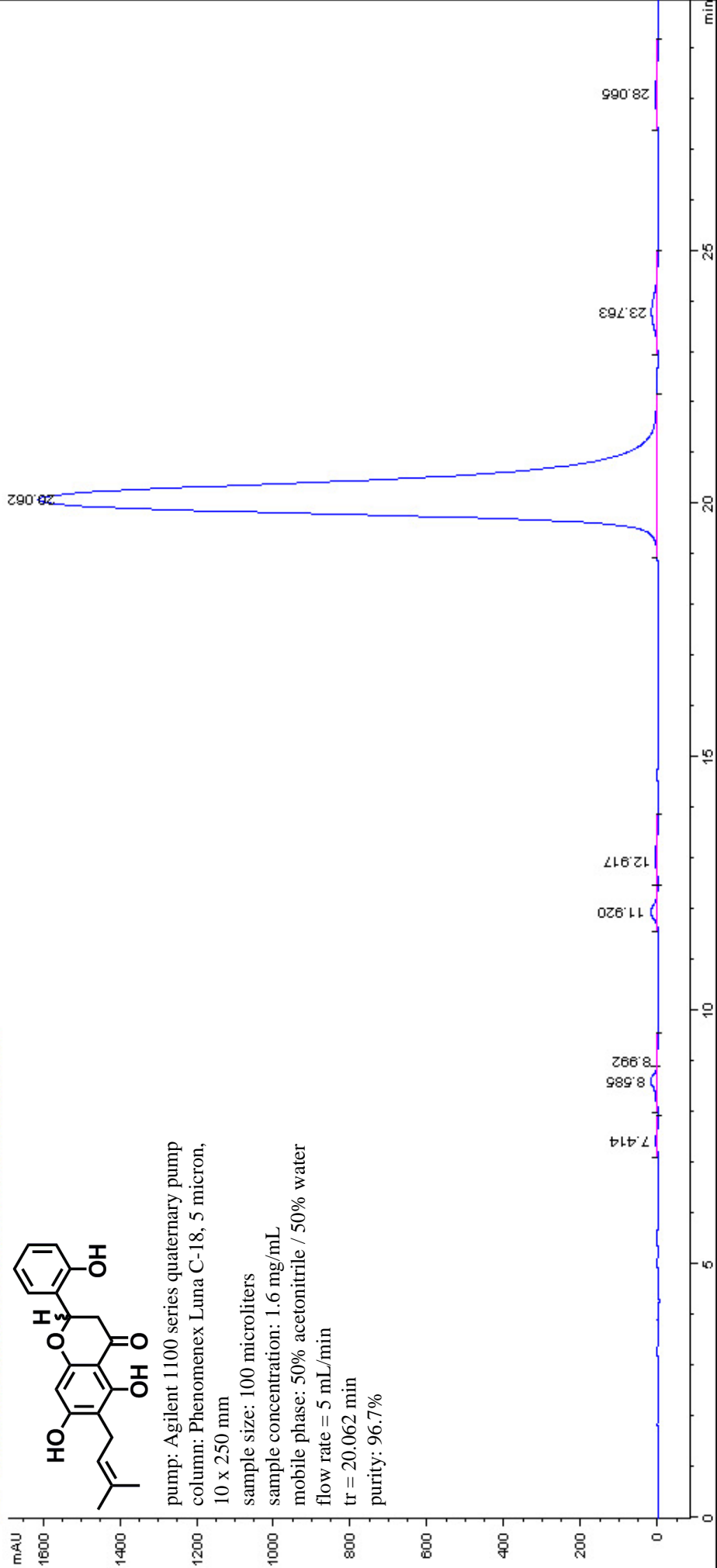
sample concentration: 1.6 mg/mL

mobile phase: 50% acetonitrile / 50% water

flow rate = 5 mL/min

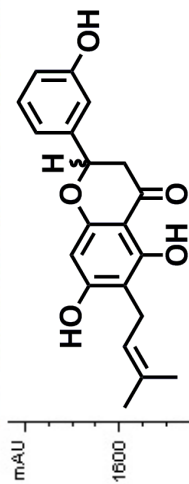
tr = 20.062 min

purity: 96.7%





DAD1 A, Sig=208.4 Ref=360,100 (KARRIEIKMS-1-187B000001.D)



pump: Agilent 1100 series quaternary pump

column: Phenomenex Luna C-18, 5 micron,  
10 x 250 mm

sample size: 100 microliters

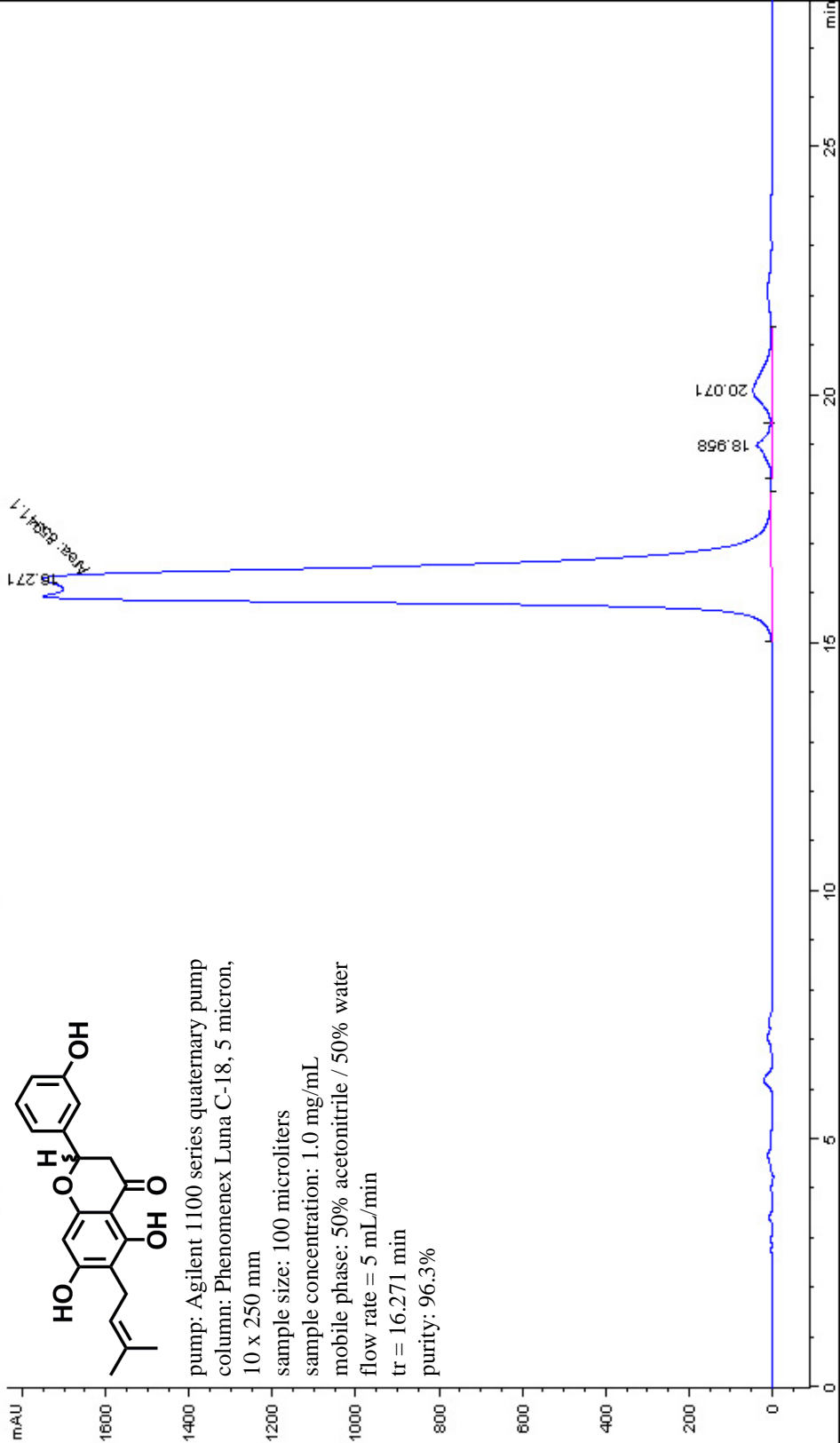
sample concentration: 1.0 mg/mL

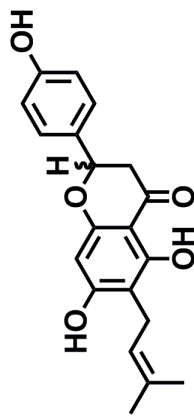
mobile phase: 50% acetonitrile / 50% water

flow rate = 5 mL/min

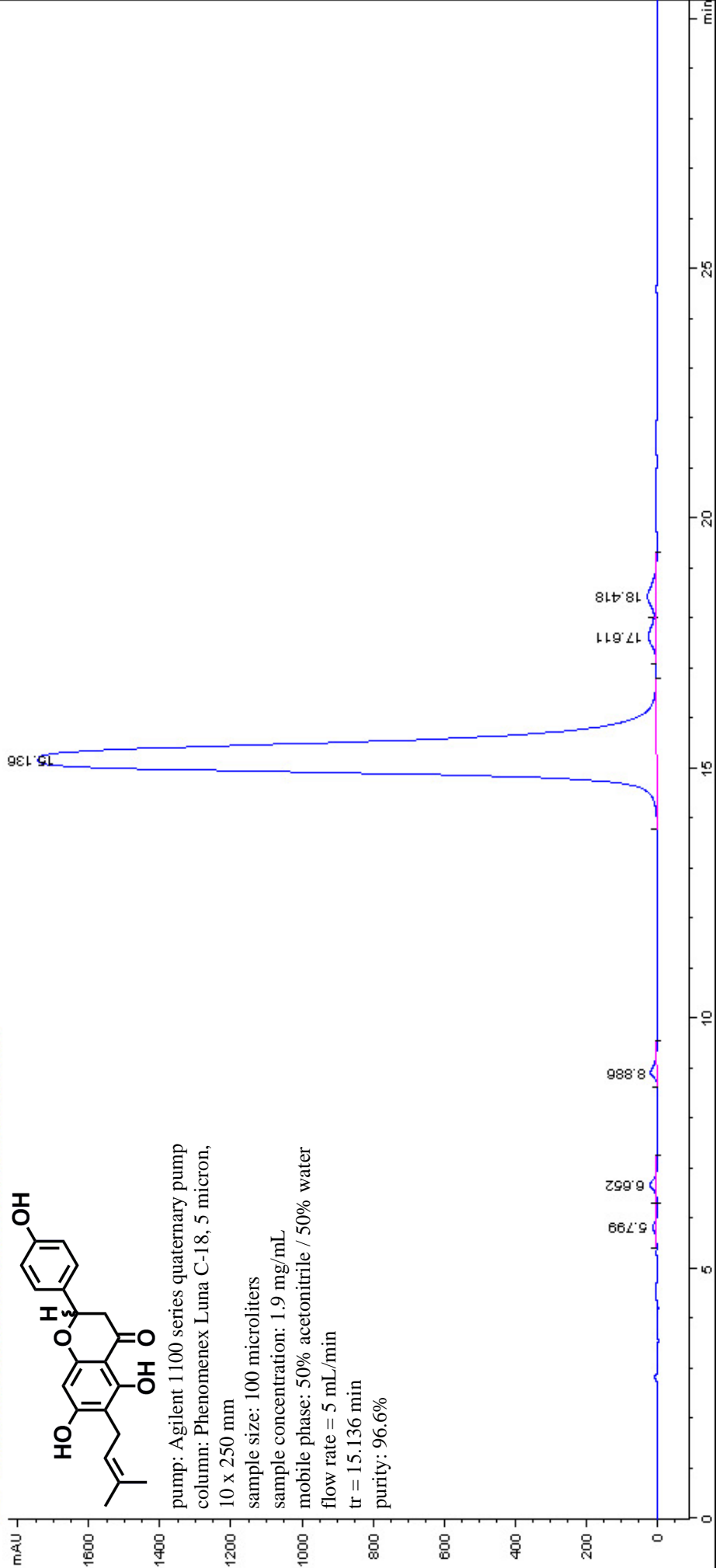
tr = 16.271 min

purity: 96.3%

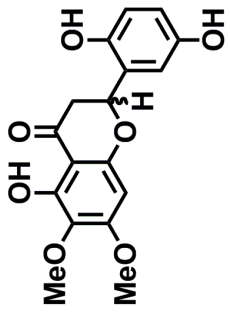
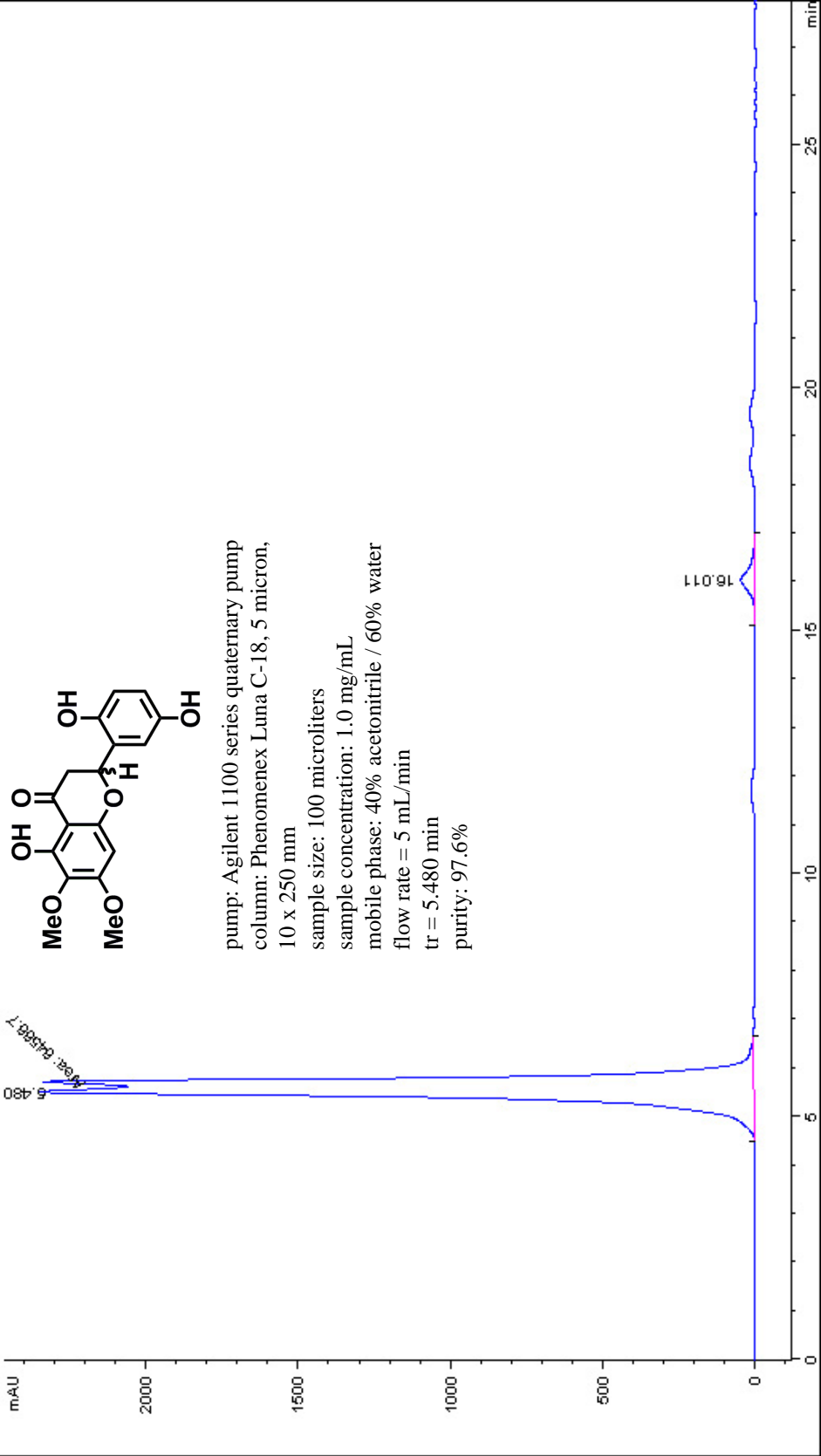




pump: Agilent 1100 series quaternary pump  
column: Phenomenex Luna C-18, 5 micron,  
10 x 250 mm  
sample size: 100 microliters  
sample concentration: 1.9 mg/mL  
mobile phase: 50% acetonitrile / 50% water  
flow rate = 5 mL/min  
tr = 15.136 min  
purity: 96.6%

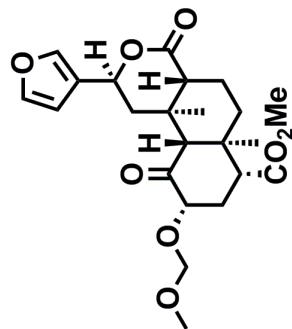


DAD1 A, Sig=209.4 Ref=360.100 (KARRIEN\MS-1-195000002.D)

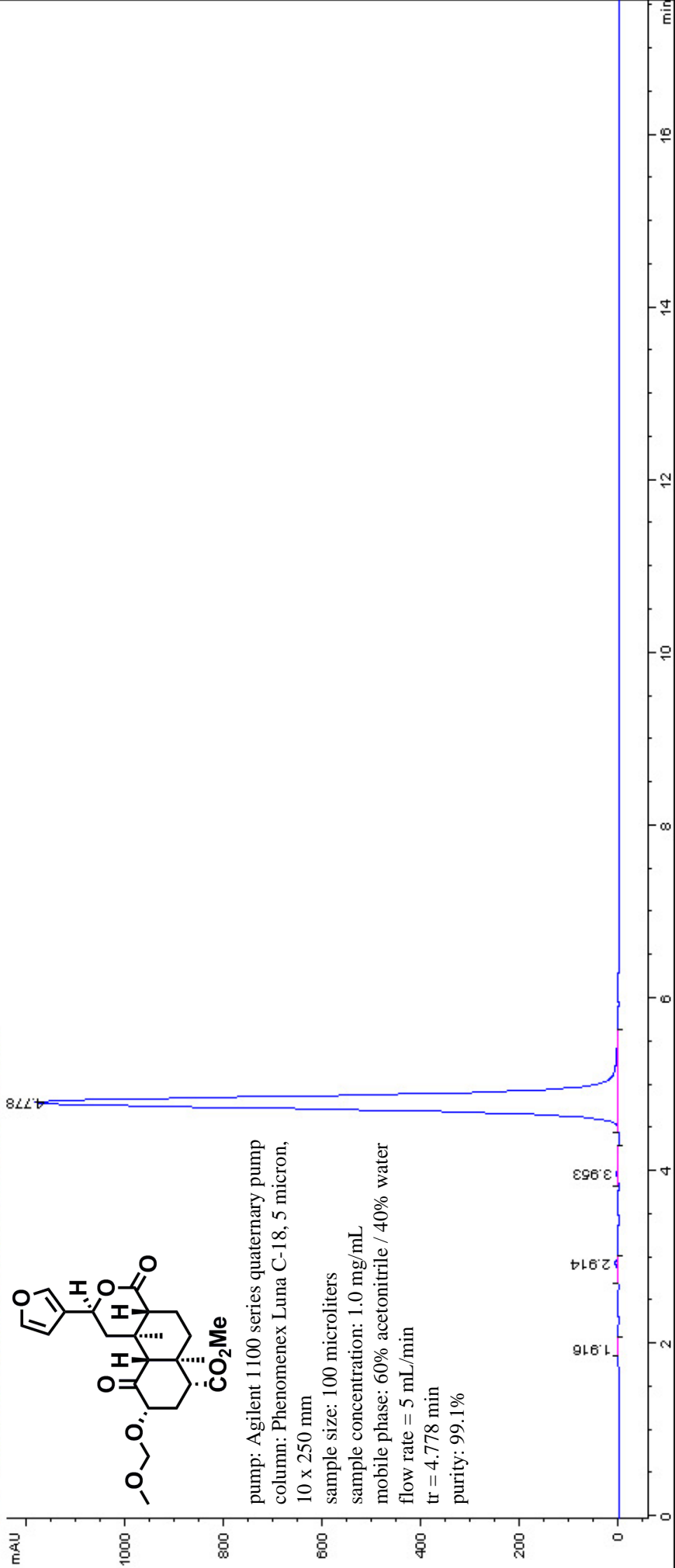


pump: Agilent 1100 series quaternary pump  
column: Phenomenex Luna C-18, 5 micron,  
10 x 250 mm  
sample size: 100 microliters  
sample concentration: 1.0 mg/mL  
mobile phase: 40% acetonitrile / 60% water  
flow rate = 5 mL/min  
tr = 5.480 min  
purity: 97.6%

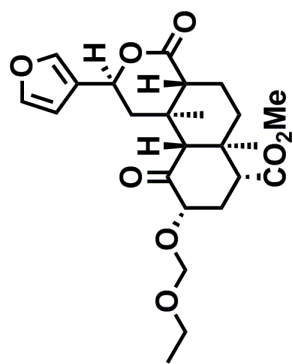
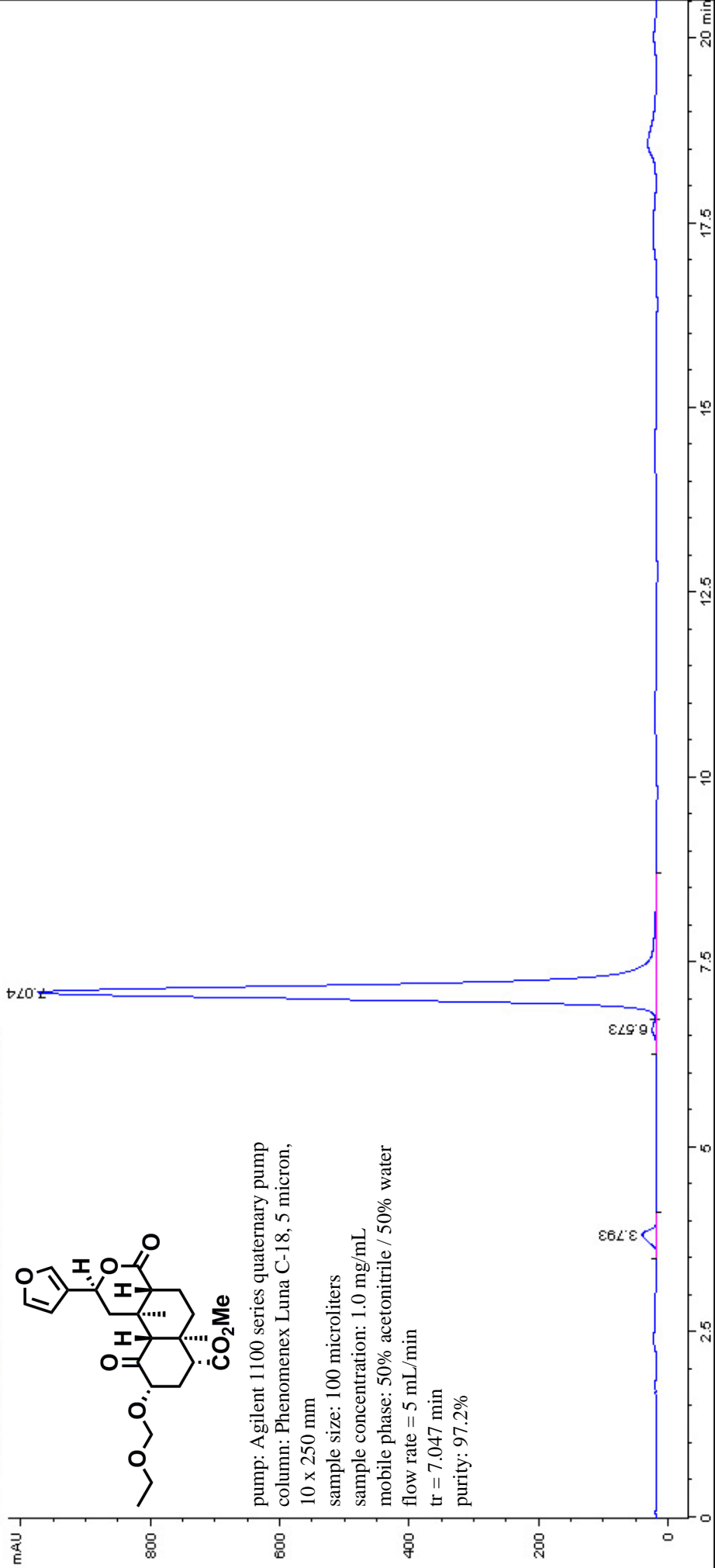
□ DAD1 A, Sig=209,4 Ref=360,100 (KARRIE\KMS-1-105000001.D)



pump: Agilent 1100 series quaternary pump  
column: Phenomenex Luna C-18, 5 micron,  
10 x 250 mm  
sample size: 100 microliters  
sample concentration: 1.0 mg/mL  
mobile phase: 60% acetonitrile / 40% water  
flow rate = 5 mL/min  
tr = 4.778 min  
purity: 99.1%



□ DAD1 A, Sig=209,4 Ref=360,100 (KARRIEKMS-1241000003.D)



pump: Agilent 1100 series quaternary pump

column: Phenomenex Luna C-18, 5 micron,  
10 x 250 mm

sample size: 100 microliters

sample concentration: 1.0 mg/mL

mobile phase: 50% acetonitrile / 50% water

flow rate = 5 mL/min

tr = 7.047 min

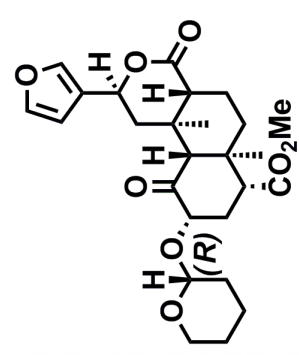
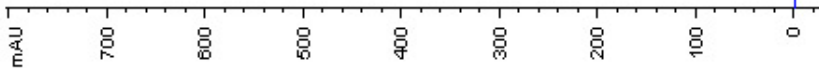
purity: 97.2%

□ DAD1 A, Sig=209,4 Ref=360,100 (KARRIE\KMS-1-129HS0001.D)

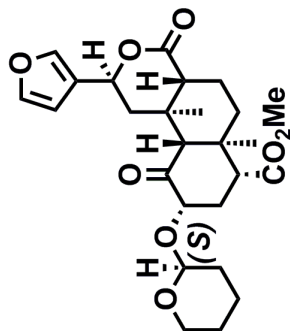
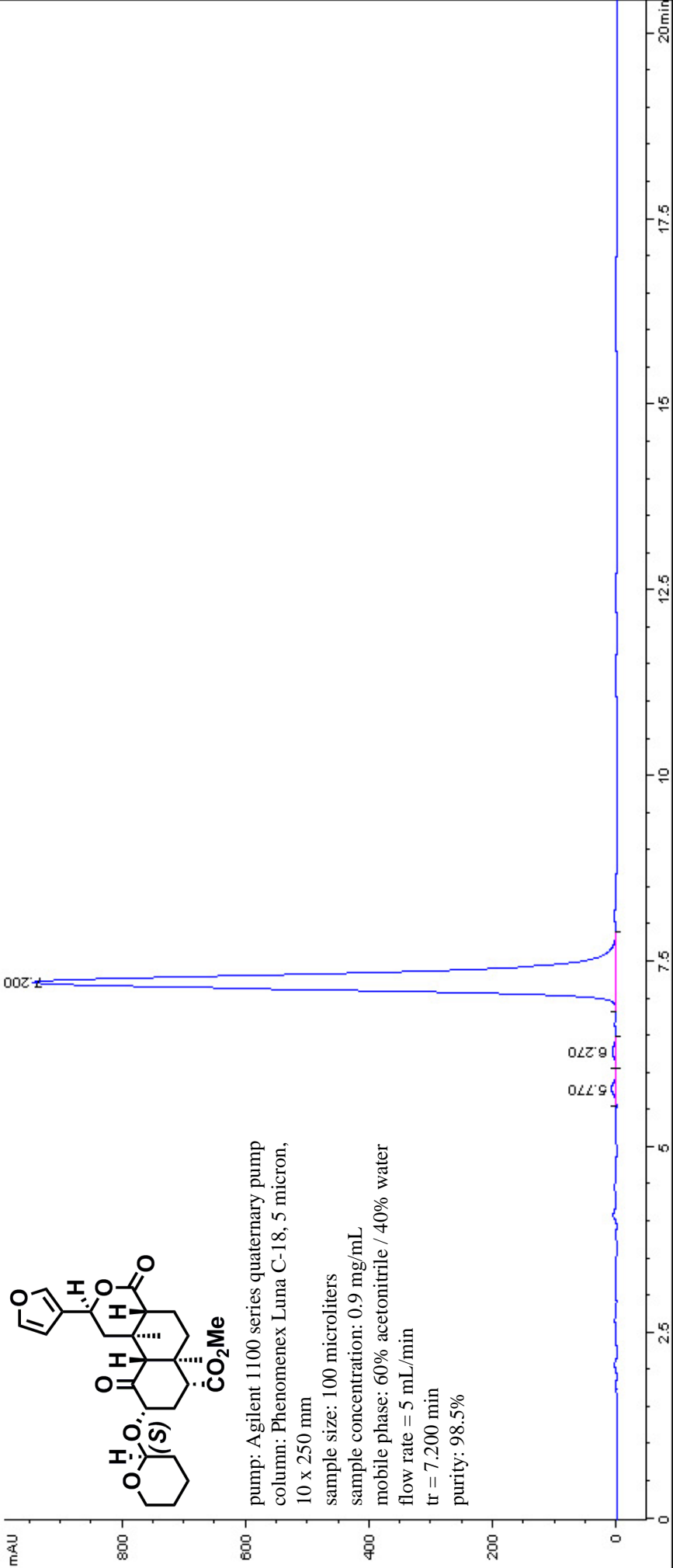
mAU

7.902

5.689

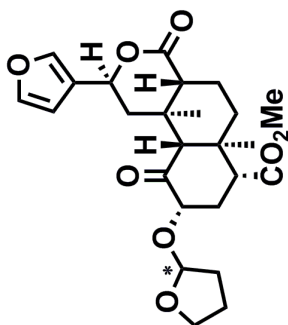
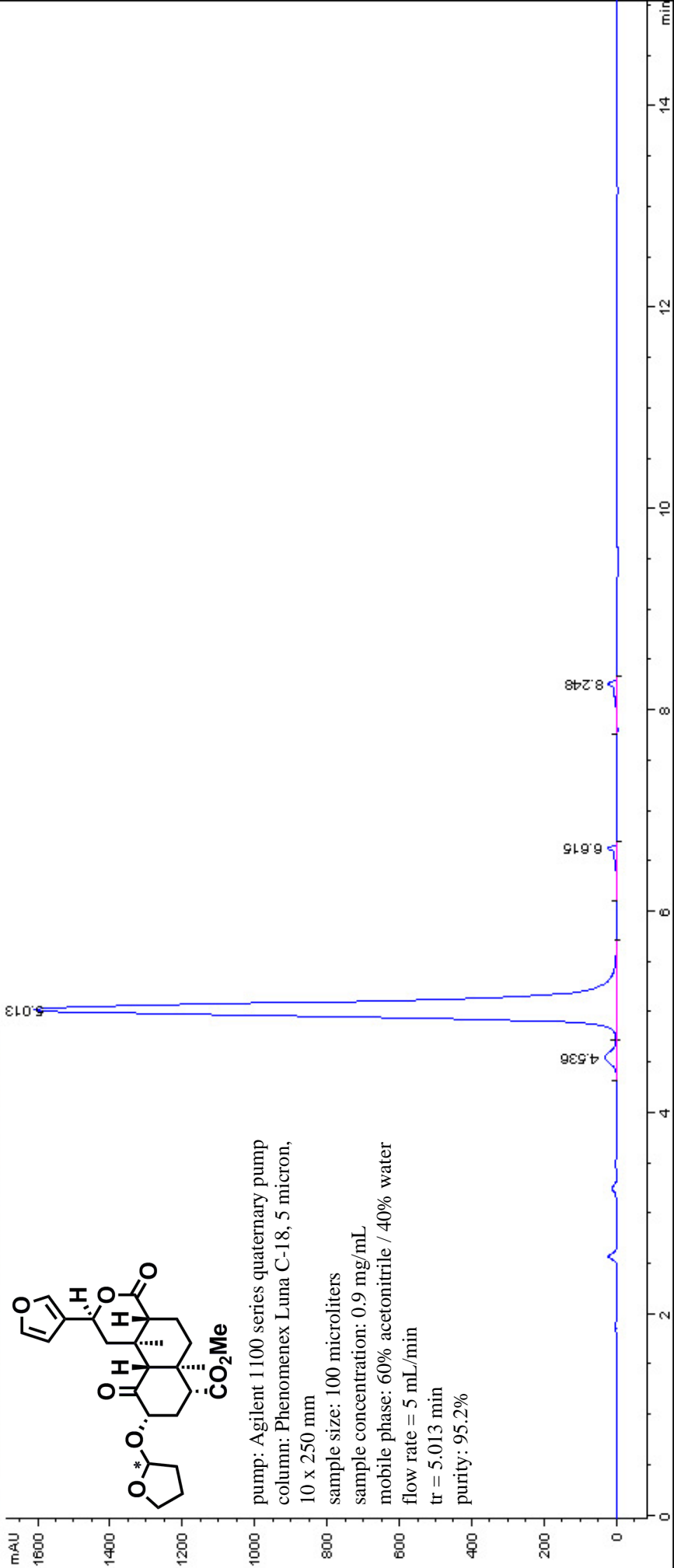


pump: Agilent 1100 series quaternary pump  
column: Phenomenex Luna C-18, 5 micron,  
10 x 250 mm  
sample size: 100 microliters  
sample concentration: 0.9 mg/mL  
mobile phase: 60% acetonitrile / 40% water  
flow rate = 5 mL/min  
tr = 7.902 min  
purity: 99.2%



pump: Agilent 1100 series quaternary pump  
column: Phenomenex Luna C-18, 5 micron,  
10 x 250 mm  
sample size: 100 microliters  
sample concentration: 0.9 mg/mL  
mobile phase: 60% acetonitrile / 40% water  
flow rate = 5 mL/min  
tr = 7.200 min  
purity: 98.5%

DAD1 A, Sig=209,4 Ref=360,100 (KARRIE\KMS-1-263-HS001.D)



pump: Agilent 1100 series quaternary pump  
column: Phenomenex Luna C-18, 5 micron,  
10 x 250 mm

sample size: 100 microliters

sample concentration: 0.9 mg/mL

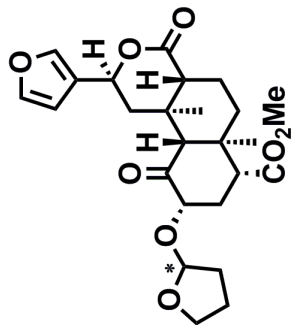
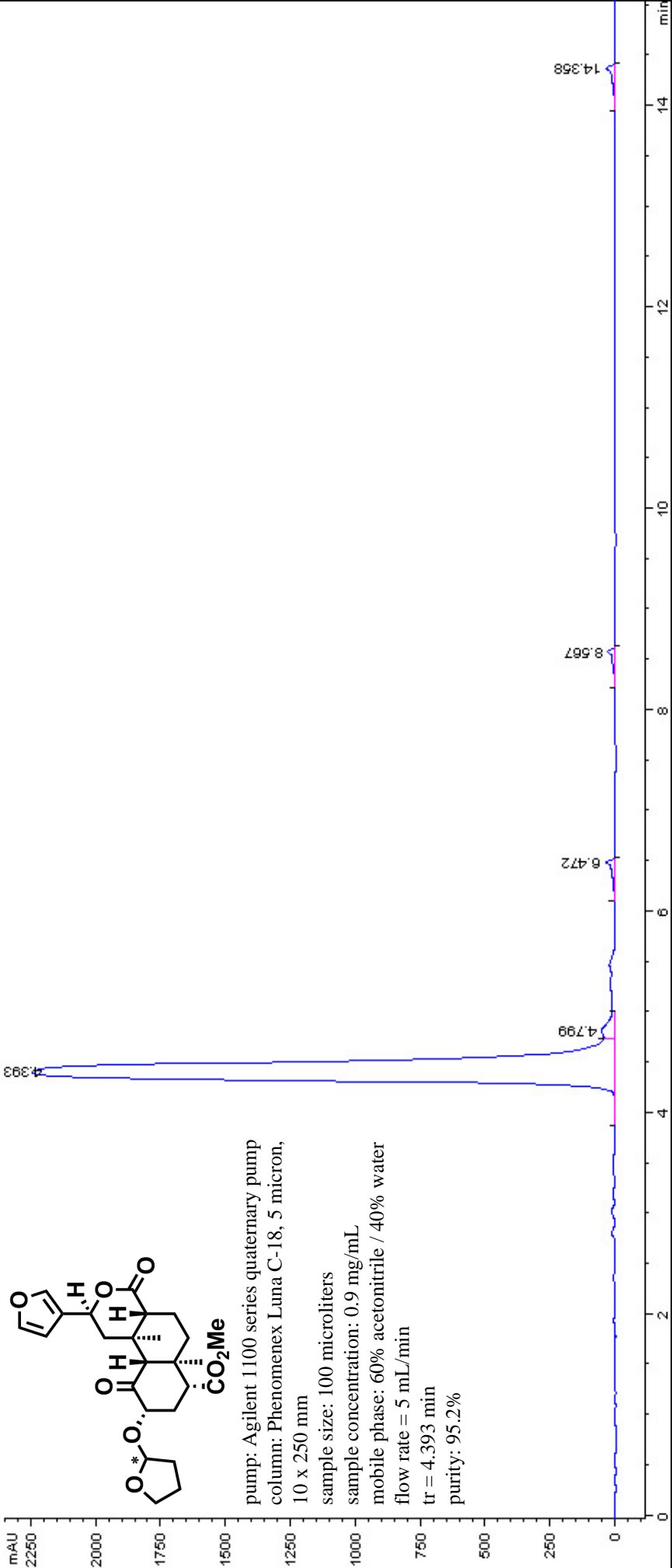
mobile phase: 60% acetonitrile / 40% water

flow rate = 5 mL/min

tr = 5.013 min

purity: 95.2%





pump: Agilent 1100 series quaternary pump

column: Phenomenex Luna C-18, 5 micron,

10 x 250 mm

sample size: 100 microliters

sample concentration: 0.9 mg/mL

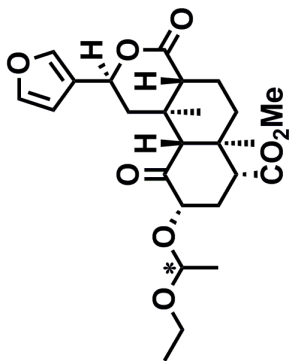
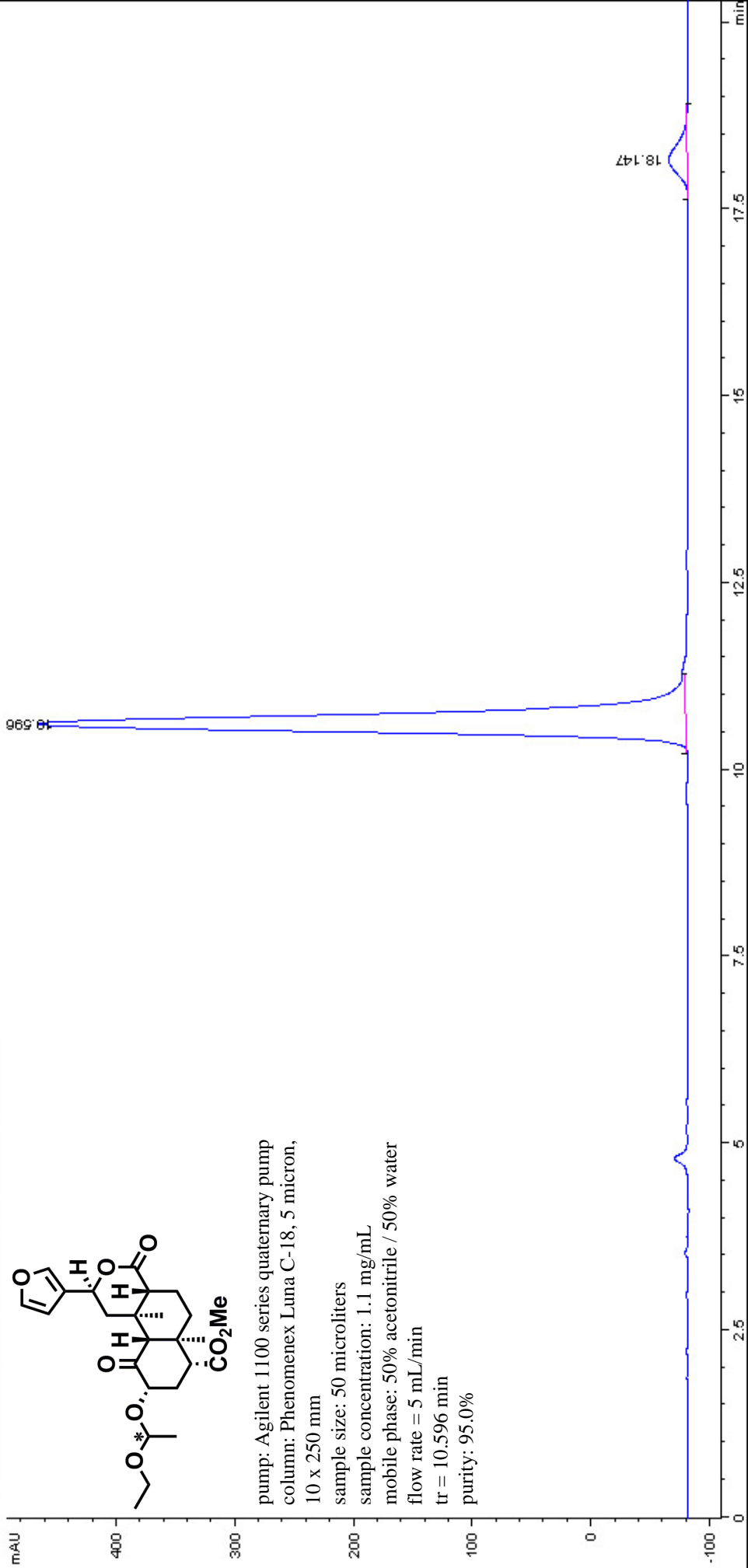
mobile phase: 60% acetonitrile / 40% water

flow rate = 5 mL/min

tr = 4.393 min

purity: 95.2%

□ DAD1 A, Sig=209,4 Ref=360,100 (KARRIEI\KMS-1-233-HS-22.D)



pump: Agilent 1100 series quaternary pump  
column: Phenomenex Luna C-18, 5 micron,  
10 x 250 mm

sample size: 50 microliters

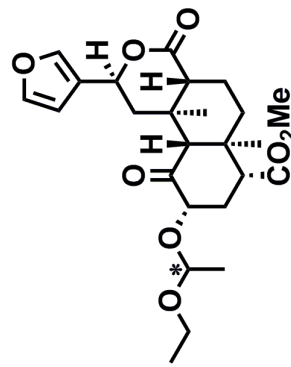
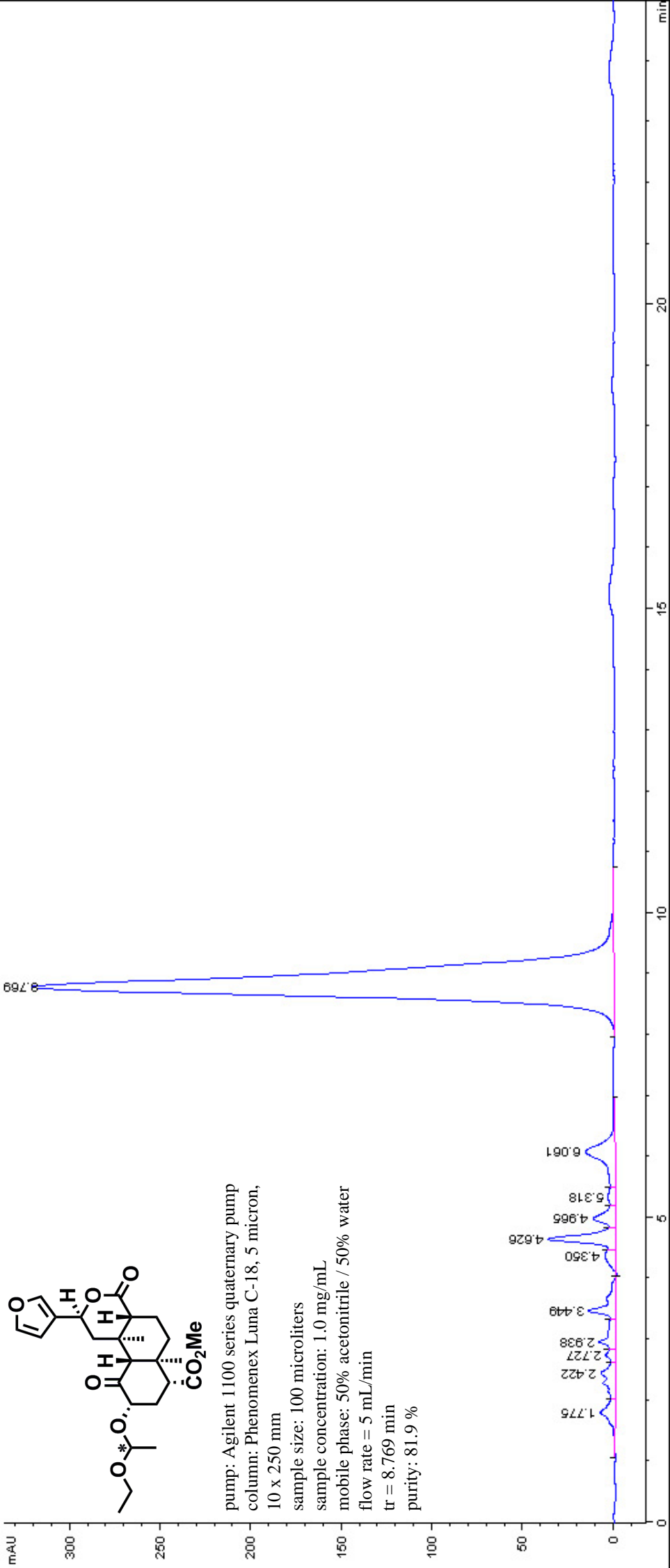
sample concentration: 1.1 mg/mL

mobile phase: 50% acetonitrile / 50% water

flow rate = 5 mL/min

tr = 10.596 min

purity: 95.0%



pump: Agilent 1100 series quaternary pump  
column: Phenomenex Luna C-18, 5 micron,  
10 x 250 mm

sample size: 100 microliters

sample concentration: 1.0 mg/mL

mobile phase: 50% acetonitrile / 50% water

flow rate = 5 mL/min

tr = 8.769 min

purity: 81.9 %

□ DAD1 A, Sig=209,4 Ref=360,100 (KARRIE\KMS-1-255-HSH01.D)

mAU

9.104

0

700

600

500

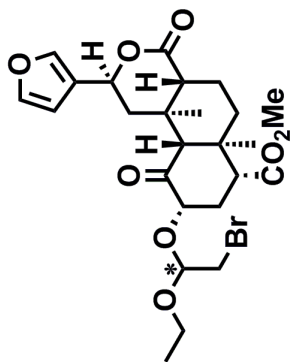
400

300

200

100

0



pump: Agilent 1100 series quaternary pump

column: Phenomenex Luna C-18, 5 micron,

10 x 250 mm

sample size: 100 microliters

sample concentration: 1.8 mg/mL

mobile phase: 60% acetonitrile / 40% water

flow rate = 5 mL/min

tr = 9.104 min

purity: 99.9%

0

7.5

10

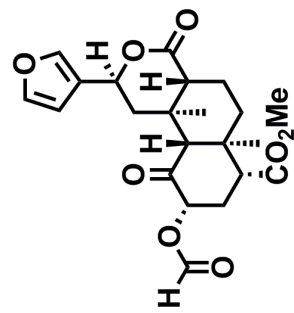
12.5

15

17.5

m





pump: Agilent 1100 series quaternary pump  
column: Phenomenex Luna C-18, 5 micron,  
10 x 250 mm

sample size: 50 microliters

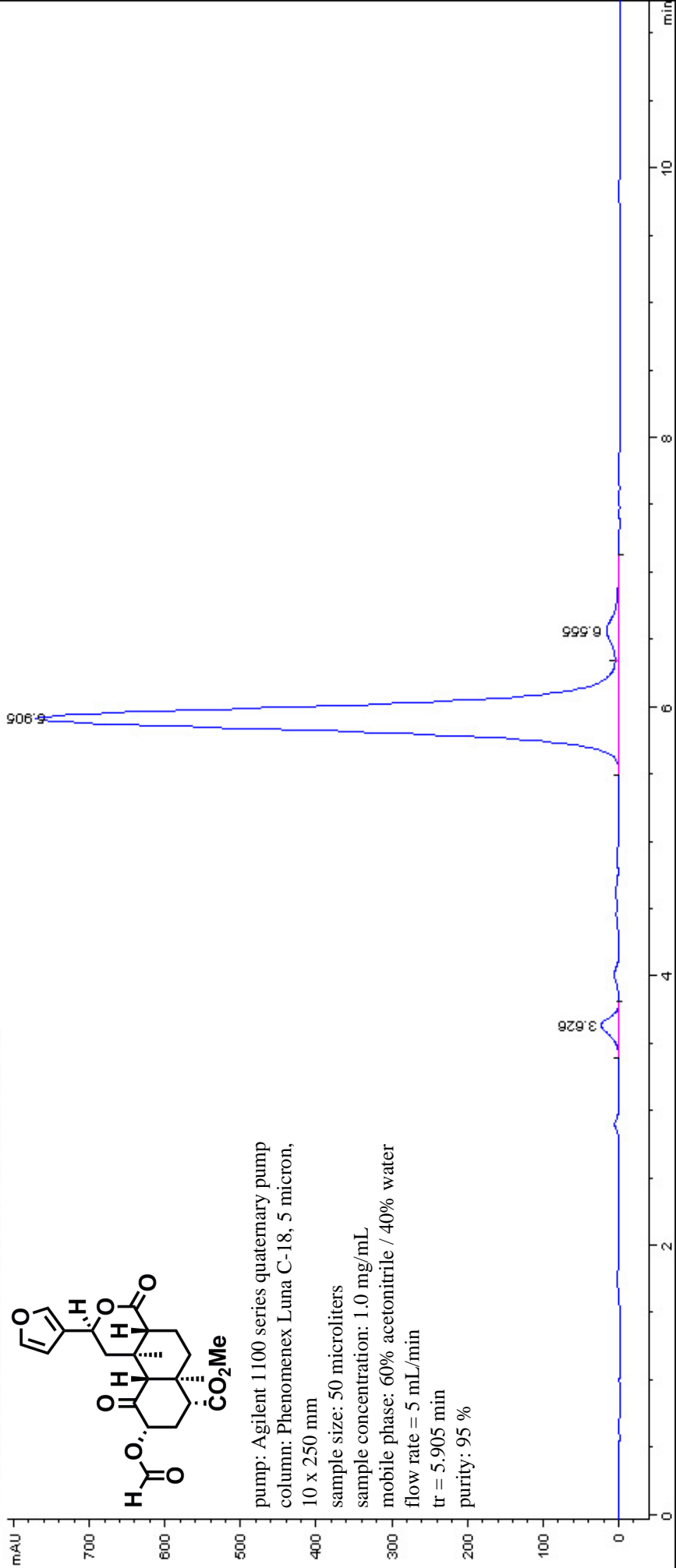
sample concentration: 1.0 mg/mL

mobile phase: 60% acetonitrile / 40% water

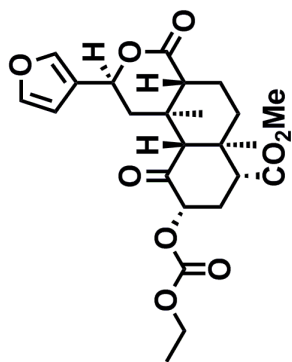
flow rate = 5 mL/min

tr = 5.905 min

purity: 95 %



□ DAD1 A, Sig=209,4 Ref=360,100 (KARRIE\KMS-1-275000002.D)



pump: Agilent 1100 series quaternary pump  
column: Phenomenex Luna C-18, 5 micron,  
10 x 250 mm

sample size: 100 microliters

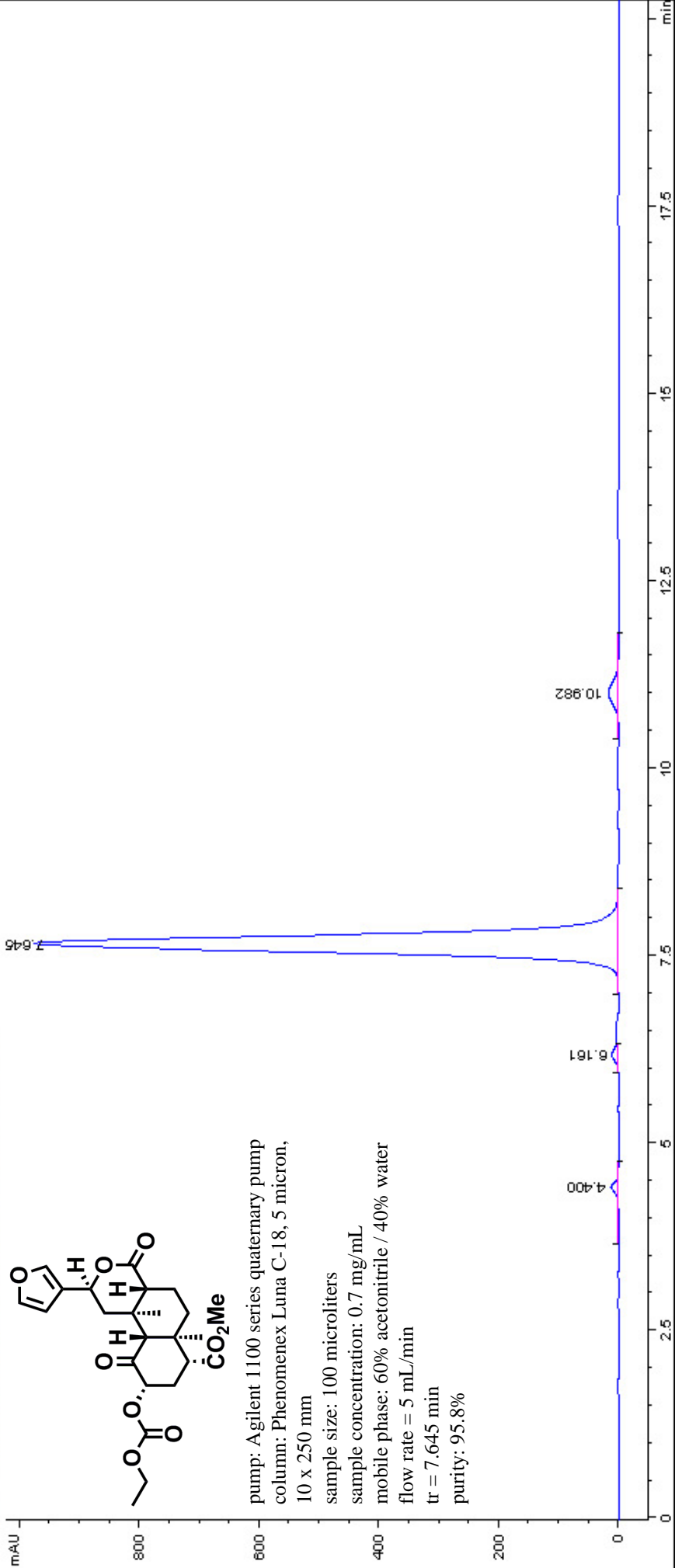
sample concentration: 0.7 mg/mL

mobile phase: 60% acetonitrile / 40% water

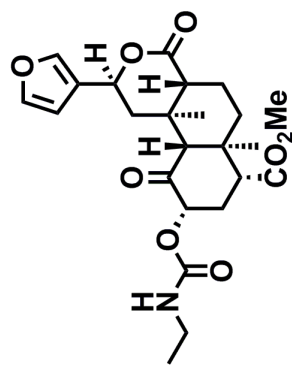
flow rate = 5 mL/min

tr = 7.645 min

purity: 95.8%



□ DAD1 A, Sig=209,4 Ref=360,100 (KARRIE\KMS-2-350000001.D)



pump: Agilent 1100 series quaternary pump  
column: Phenomenex Luna C-18, 5 micron,  
10 x 250 mm

sample size: 50 microliters

sample concentration: 1.3 mg/mL

mobile phase: 60% acetonitrile / 40% water

flow rate = 5 mL/min

tr = 5.074 min

purity: >99.9%

mAU

1200

1000

800

600

400

200

0

5.074

0

2

4

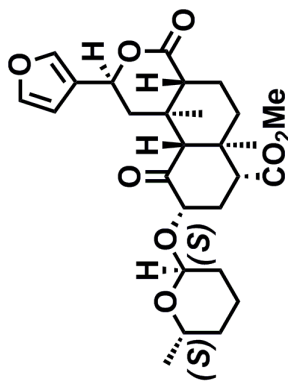
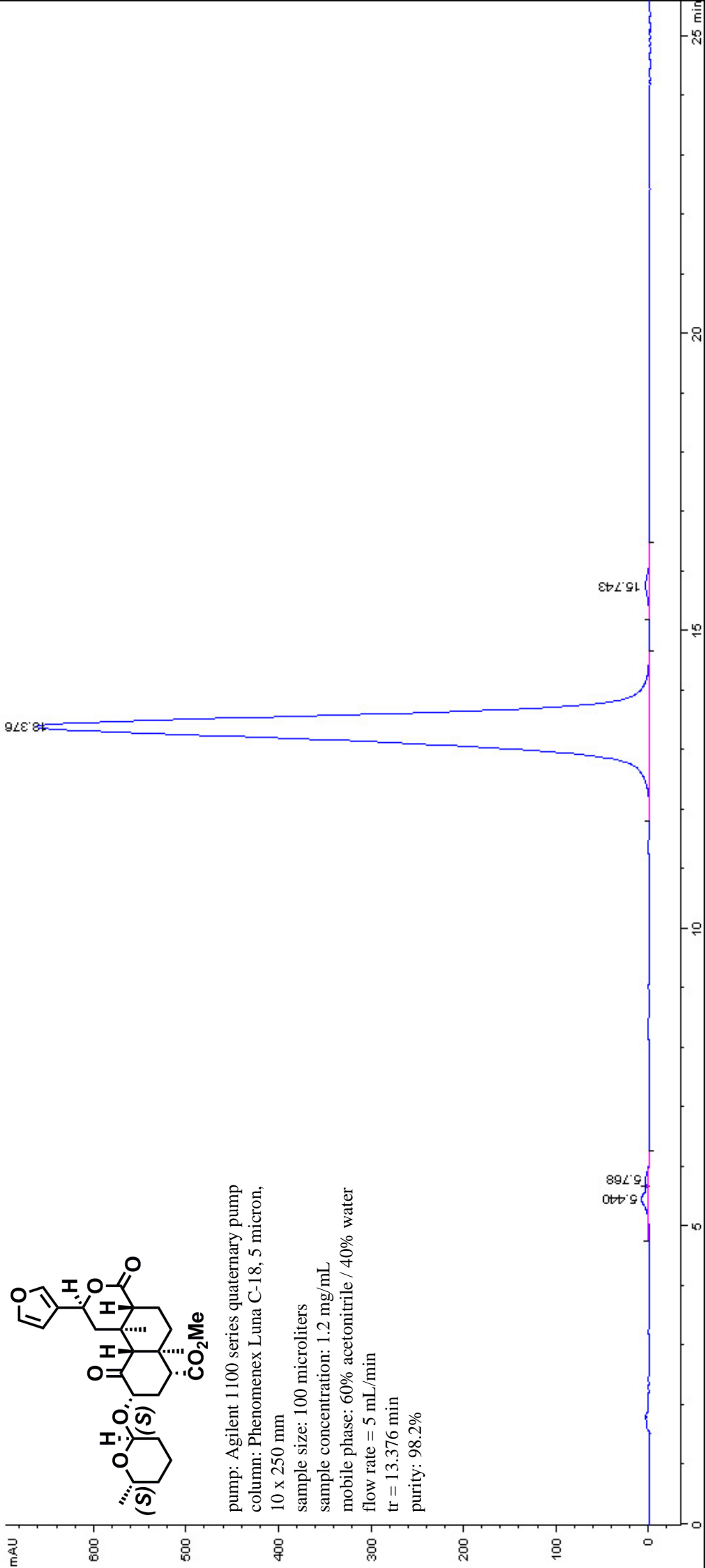
6

8

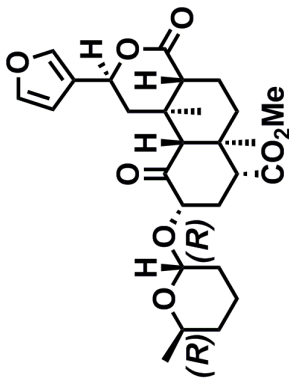
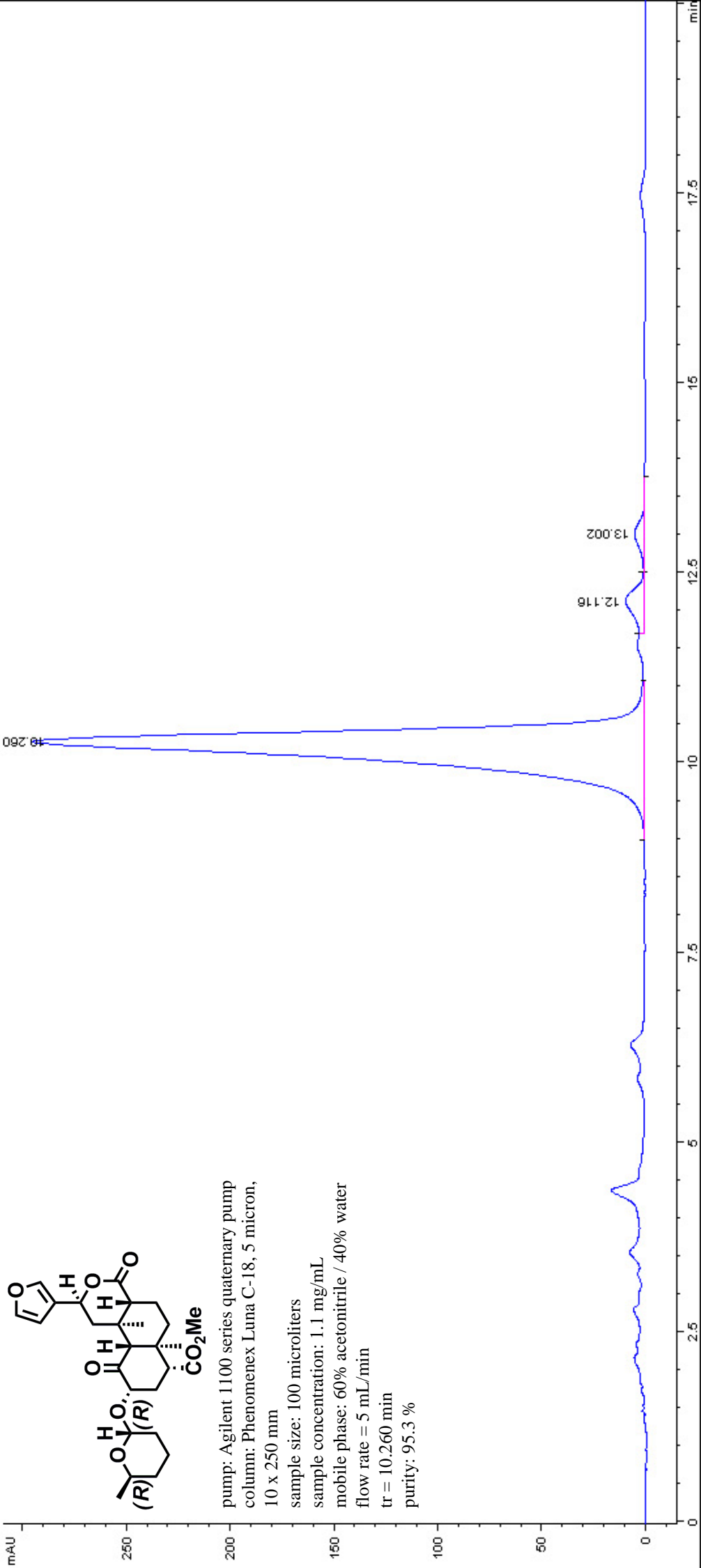
10

min

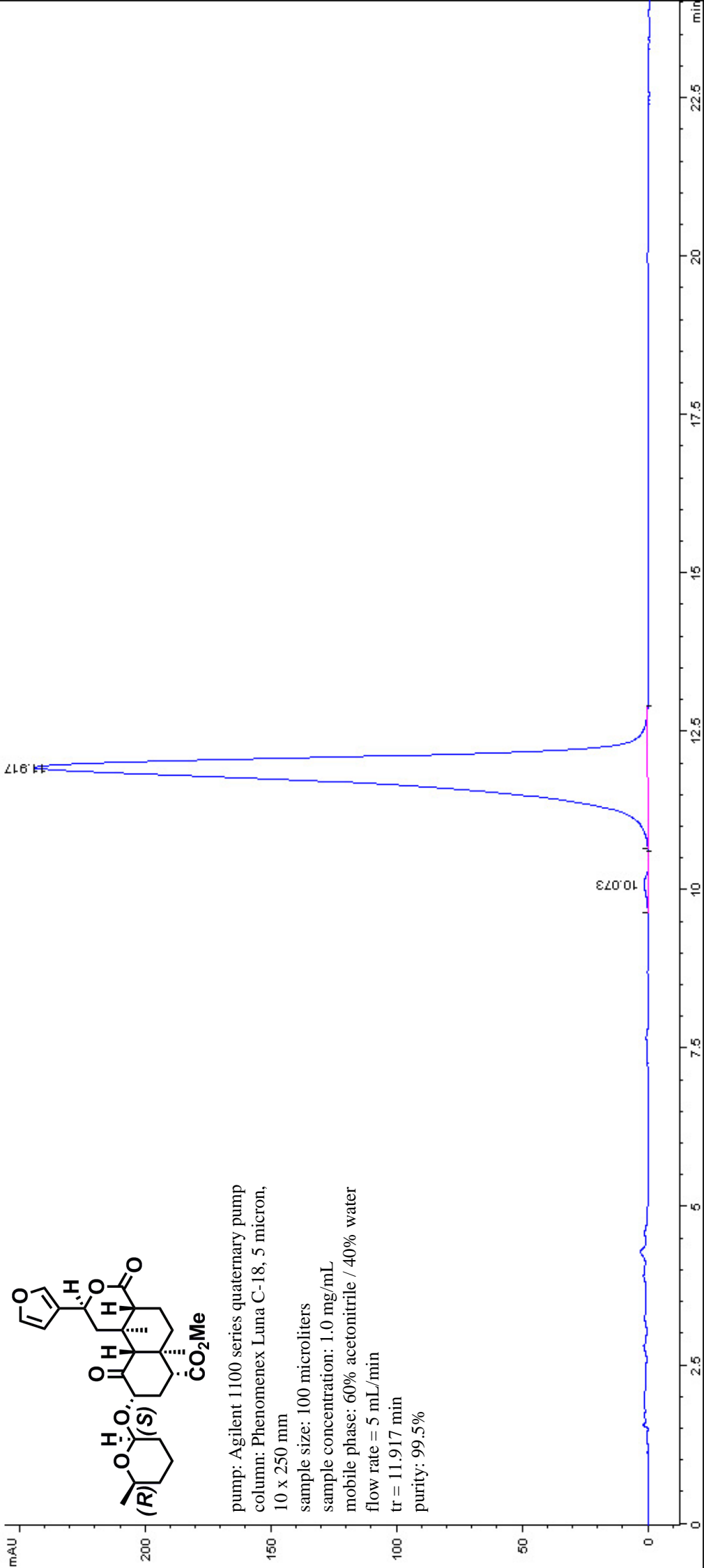




pump: Agilent 1100 series quaternary pump  
column: Phenomenex Luna C-18, 5 micron,  
10 x 250 mm  
sample size: 100 microliters  
sample concentration: 1.2 mg/mL  
mobile phase: 60% acetonitrile / 40% water  
flow rate = 5 mL/min  
tr = 13.376 min  
purity: 98.2%



pump: Agilent 1100 series quaternary pump  
column: Phenomenex Luna C-18, 5 micron,  
10 x 250 mm  
sample size: 100 microliters  
sample concentration: 1.1 mg/mL  
mobile phase: 60% acetonitrile / 40% water  
flow rate = 5 mL/min  
tr = 10.260 min  
purity: 95.3 %



mAU

200

150

100

50

0

11.917

10.073

0

2.5

5

7.5

10

12.5

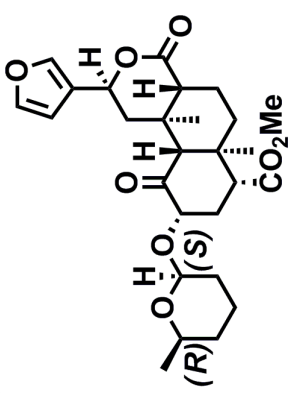
15

17.5

20

22.5

min



pump: Agilent 1100 series quaternary pump  
column: Phenomenex Luna C-18, 5 micron,  
10 x 250 mm  
sample size: 100 microliters  
sample concentration: 1.0 mg/mL  
mobile phase: 60% acetonitrile / 40% water  
flow rate = 5 mL/min  
tr = 11.917 min  
purity: 99.5%